Copyright

by

Glen Nelson Mackey, III

2009

Provenance of the South Texas Paleocene-Eocene Wilcox Group, Western Gulf of Mexico Basin: Insights from Sandstone Modal Compositions and Detrital Zircon Geochronology

by

Glen Nelson Mackey, III, B.A.

Thesis

Presented to the Faculty of the Graduate School of

The University of Texas at Austin

in Partial Fulfillment

of the Requirements

for the Degree of

Master of Science in Geological Sciences

The University of Texas at Austin

August 2009

The Thesis committee for Glen Nelson Mackey, III

Certifies that this is the approved version of the following thesis:

Provenance of the South Texas Paleocene-Eocene Wilcox Group, Western Gulf of Mexico Basin: Insights from Sandstone Modal Compositions and Detrital Zircon Geochronology

Approved by
Supervising Committee:

Kitty L. Milliken, Supervisor

Brian K. Horton

Ronald J. Steel

Acknowledgements

I would like to thank my supervisor, Kitty Milliken, and the members of my thesis committee, Brian Horton and Ron Steel, for help and guidance during my research and feedback that improved the quality of my thesis. A summer research assistanceship provided by Brian Horton to analyze detrital zircons for his project with Ecopetrol proved to be an invaluable learning experience and greatly improved the quality and speed of my analyses. I would also like thank James Donelly of the Core Research Center for assistance in accessing and sampling cores, Bill Galloway for providing access to the Gulf of Mexico Basin Depositional Synthesis project which was a great help in locating cores to sample, John Breyer for leading an excellent field trip to Bee Bluff, the Briscoe Ranch and Martin Marrietta Materials for permission to take samples from their property, James Connelly for teaching me zircon systematics, Todd Housh (deceased) for guidance on analyzing detrital zircons on the Isoprobe and assistance in data reduction. Discussions with Bill Galloway, Tim Lawton, and Bill Dickinson refined many of my thoughts and helped me identify some areas that I needed to rethink. Funding for this research was provided by the AAPG Grants-in-Aid program, the Geological Society of America Graduate Student Research Grants, the Jackson School of Geosciences and the Geology Foundation of the University of Texas at Austin.

July 28, 2009

Abstract

Provenance of the South Texas Paleocene-Eocene Wilcox Group, Western Gulf of Mexico Basin: Insights from Sandstone Modal Compositions and Detrital Zircon Geochronology

Glen Nelson Mackey, III, MSGeoSci

The University of Texas at Austin, 2009

Supervisor: Kitty L. Milliken

Sandstone modal compositions and detrital zircon U-Pb analysis of the Paleocene-Eocene Wilcox Group of the southern Gulf Coast of Texas indicate long-distance sediment transport primarily from volcanic and basement sources to the west, northwest and southwest.

The Wilcox Group of south Texas represents the earliest series of major post-Cretaceous pulses of sand deposition along the western margin of the Gulf of Mexico (GoM). Laramide basement uplifts have long been held to be the provenance of the Wilcox Group, implying that initiation of basement uplifts was the driving factor for this transition from carbonate sedimentation to clastic deposition. To determine the provenance of the Wilcox Group and test this conventional hypothesis, 40 thin sections were point-counted using the Gazzi-Dickinson method to determine sandstone

composition and 10 detrital zircon samples were analyzed by LA-ICP-MS to determine U-Pb age spectra for each of the sampled areas.

Modal data for sand grain populations suggest mixed sources including basement rocks, magmatic arc rocks and subordinate sedimentary rocks for the Wilcox Group. Zircon age spectra for these sandstones reveal a complex grain assemblage derived from older sediments and crystalline rocks ranging in age from Archean to Cenozoic. Sediment was primarily derived from Laramide uplifted crystalline blocks of the central and southern Rocky Mountains, the Cordilleran arc of western North America, and arc related extrusive and intrusive igneous rock of northern Mexico. Comparisons of Upper and Lower Wilcox zircon age spectra show that more arc related material was deposited in the Lower Wilcox, whereas more basement material was deposited in the Upper Wilcox.

Table of Contents

List of Tables

List of Figures

INTRODUCTION

Passive margins commonly draw sediment from a vast area. One only needs to consider the modern Mississippi river to observe the scale and diversity of sediment sources in a passive-margin drainage system/network. In the case of the Mississippi River, the detrital zircon age spectra of modern sediment taken from the river mouth match well the known geologic complexity of the river drainage (Iizuka et al., 2005), suggesting that detrital zircons from an ancient passive margin will be equally informative concerning the lithologies and geographic extent of sediment sources.

Understanding the provenance of sediment in basins far from areas of uplift can address several tectonic and sedimentological questions. If specific sources can be identified, then a paleogeographic picture of uplifts and drainages can be developed for the region, as well as a notion of how this picture changes through time if samples are available from several stratigraphic levels. On the other hand, if high-resolution uplift histories of the sources areas have already been determined, then it is possible to assess whether tectonics are responsible for pulses of sedimentary deposition, and if so, how much lag time there is between uplift and erosion in the source area and deposition in the basin (e.g., Crabaugh, 2001).

The Gulf of Mexico (GoM) sedimentary basin contains a prolonged record of North American denudation (Winker, 1982; Galloway, 2008). A key transition within this record is the shift from dominantly carbonate sedimentation to siliciclastic deposition that occurred along the western Gulf margin during the Late Cretaceous to Paleocene. The Paleocene-Eocene Wilcox Group of south Texas represents the earliest major pulse of sand deposition along this segment of the margin, though much of the previous thought on its provenance has been based solely on the tectonic history of North America

(Winker, 1982). There are several possible source areas for the Wilcox Group: 1) Laramide uplifts of the Rocky Mountains, 2) Appalachian uplifts, 3) volcanic rocks in northern Mexico, 4) magmatic rocks of the Cordilleran arc, and 5) strata of the mid-continent High Plains. The goal of this study is to test these possible source areas and determine the provenance of the Wilcox Group using sandstone petrography and detrital zircon geochronology.

Geological Setting

The Paleocene-Eocene (60.6-49.0 Ma (Crabaugh, 2001 and references therein)) Wilcox Group of the Texas Gulf Coast records the first major deliveries of Cenozoic clastic wedges to the northwest Gulf of Mexico in the form of large delta systems (Galloway, 2008), comparable in size to the modern Mississippi system (Fisher and McGowen, 1967), with accompanying coastal plain and fluvial systems. Overall southeastward progradation of the shelf edge and continental margin during this period was approximately 150-200 km beyond Cretaceous reef deposits that marked the earlier shelf edge (Galloway et al., 2000). Extensive petroleum and mineral resource exploration has led to a very complex stratigraphic nomenclature system for the Wilcox group (e.g., Hargis, 1985; Galloway and Williams, 1991; Xue and Galloway, 1993, 1995), so I will use the simplified lithostratigraphic nomenclature system of Hargis (1996) and divide the Wilcox group into three informal subunits, the Upper, Middle and Lower (Figure 1). High-resolution biostratigraphic calibration of the Wilcox group to the Cenozoic time scale by Crabaugh (2001) and Crabaugh and Elsik (2000) give the following ages for each subunit: Lower Wilcox, 60.6-57.5 Ma; Middle Wilcox, 57.5-54.8 Ma; and Upper Wilcox, 54.8-49.0 Ma. Based on accessed uncertainties in

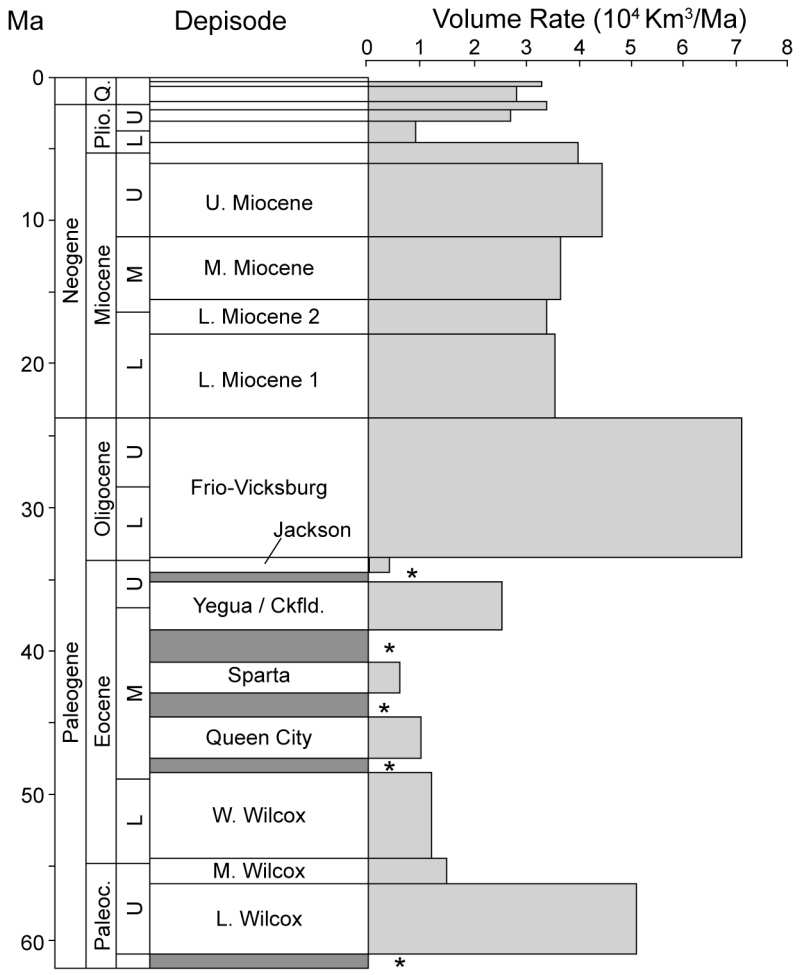

Figure 1. Chronology of Cenozoic Gulf of Mexico deposition after Galloway (2001). The right hand bar chart plots the volumetric rate of sediment accumulation in combined shore-zone and delta systems of each episode. * = extensive marine condensed section characterized by very low accumulation rates.

correlating biostratigraphic datums in the Wilcox Group to absolute biozone ages, Crabaugh and Elsik (2000) assigned ±0.5 Ma uncertainties to each of these ages. The upper Paleocene Lower Wilcox subunit, the most voluminous of the three subunits, which records the initial entry of Cenozoic sand into the basin (Galloway, 2001), is known in outcrop as the Indio Formation, Calvert Bluff Formation, Hooper Formation and Simsboro Formation, though the latter three names are restricted to northeast Texas (Thorkildsen and Price, 1991; Stoeser et al., 2005). The Middle Wilcox subunit, bounded above and below by transgressive shales, is sometimes included in the Lower Wilcox because it records mild regression in a period of overall waning sediment supply that followed the significant input of the Lower Wilcox and preceded the much larger Upper Wilcox (Galloway, 2005, 2008). The lower Eocene Upper Wilcox subunit, known as the Carrizo Formation in outcrop, is the result of a resurgence of sediment to the GOM following the volumetrically minor Middle Wilcox (Galloway, 2005). The regional-scale depositional architecture of the Wilcox Group shows changing depositional axes during the different pulses of sedimentation (Galloway, 1989). In broad terms the Lower and Middle Wilcox subunits were primarily deposited by the Rockdale Delta system in the Houston Embayment (Fisher and McGowen, 1967; Ayers and Lewis, 1985), while the Upper Wilcox subunit was primarily deposited by the Rosita Delta system in the Rio Grande Embayment to the south (Edwards, 1981) (Figure 1).

Deposition of the Wilcox group coincides with an active period of regional shortening and magmatism in the geologic history of western North America. Laramide tectonics were creating basement-cored uplands and adjacent basins in the region of the modern Rocky Mountains (Dickinson et al., 1988; Cather, 2004), while movement on the Sevier thrust belt farther west was waning, with the exception of the more northern sections of the belt (Miller et al., 1992). At the same time volcanism in the Cordilleran

arc was beginning to migrate inland toward the Laramide uplifts (Lipman, 1992; McDowell et al., 2001; Breyer et al., 2007; Befus et al., 2008), and previously active portions of the arc began to be uplifted (Miller et al., 1992). Deposition of the Wilcox Group preceded the voluminous mid-Tertiary ignimbrite flare-up of the southwestern U.S. and northern Mexico (McDowell and Keizer, 1977; Ferrari et al., 1999; Ferrari et al., 2002; Chapin et al., 2004), an event that buried older volcanic rocks in northern Mexico, making it difficult to determine their age and outcrop extent.

Previous Work

Various possibilities have been proposed for the provenance of the Wilcox Group. The most commonly accepted interpretation, based primarily on the timing of uplifts and magmatic events, is that Wilcox sediment is derived from Laramide uplifts of the central and southern Rocky Mountains (Winker, 1982; Galloway, 2005), a concept that dates to the middle of the last century (Storm, 1945; Murray, 1955). In the same vein, Crabaugh (2001) correlated details of the uplift history of the late-stage Sevier thrust belt in the Green River Basin area of Wyoming to the depositional history of the Wilcox group, implying a northern Rockies provenance. Based on the presence of kyanite and staurolite in Wilcox strata of the northeast portion of the Texas Gulf Coast, Todd and Folk (1957) suggested that Wilcox sediments were most likely derived from the southern Appalachian mountains, though Brewton (1970) also examined the kyanite and staurolite content of Wilcox rocks and interpreted a southern Laramide source. Looking farther southwest along the coast, McCarley (1981) examined the ratio of garnet + epidote to kyanite + staurolite for several Eocene sands and determined that the Upper Wilcox could have been derived from southern Laramide uplifts. Based on zircon morphology, Callender and Folk (1958) concluded that the upper Wilcox did not have a volcanic source.

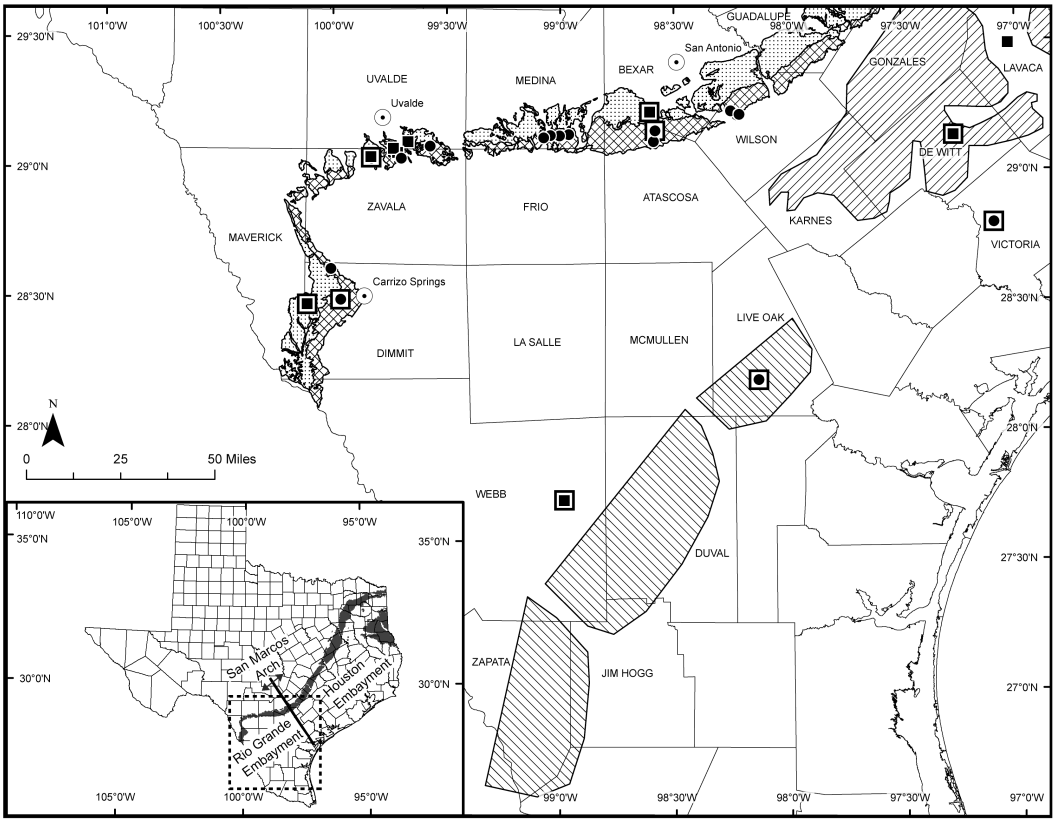

Figure 2. Map of sample area showing Upper Wilcox outcrop in cross-hatch pattern, Lower Wilcox outcrop in stipple pattern, Upper Wilcox deltas in down-to-the-right diagonal lines and Lower Wilcox deltas in down-to-the-left diagonal lines. Lower Wilcox sample locations are filled in squares and Upper Wilcox sample locations are filled in circles. Boxes around sample locations indicate a zircon sample. Empty circles with dots represent cities for geographic reference. County names are in all caps. Inset Texas State map shows regional geological features (i.e., the San Marcos Arch, the Houston Embayment, and the Rio Grande Embayment) and the sampling area as a dashed box. Wilcox outcrop from Stoeser et al. (2005). Upper and Lower Wilcox deltas after Edwards (1981).

METHODS

Samples from the Upper and Lower Wilcox were collected from 18 outcrop localities and 5 cores (Figure 2). Geologic maps produced by the Bureau of Economic Geology, University of Texas at Austin (1976, 1983), supplemented by the stratigraphic column of Bee Bluff by Breyer (1997), were used to determine outcrop sampling locations. Cores were sampled from wells and depths previously studied by Fisher (1982), Loucks et al. (1984, 1986), and Dickerson et al. (1995). Sandstone point counts (n=350 grains) were conducted on 40 thin sections using the Gazzi-Dickinson method (Ingersoll et al., 1984). Thin sections were impregnated with blue-dyed epoxy and stained for potassium feldspar and plagioclase using the techniques of Houghton (1980). Albitized and sericitized grains were counted as plagioclase. Raw point counts were recalculated using the parameters of Graham et al. (1976) (Table 1).

Geochronology samples were collected from both outcrop and core. Approximately 3-5 kg of material were collected from each sample locality. Core samples were collected from the sandiest parts of the core interval examined. A 1.5 m continuous section of core was sampled by cutting a 2.5 cm wide slice off of the back of the core. Prior to further processing, the pieces of core were washed and scrubbed with a wire brush to remove possible contamination from drilling mud. Samples were then crushed using a rock hammer and disc mill (Larsen and Poldervaart, 1957), and sorted by density using a Wilfley table and organic heavy liquids (bromoform (ρ=2.96 g/cm^3) and methylene iodide (ρ=3.32)). Prior to the heavy liquid mineral separation, a Frantz magnetic separator was used in freefall mode to remove metal shavings and strongly

Table 1. Point counting parameters.

Symbol	Definition
Qm	Monocrystalline quartz
Qpq	Polycrystalline quartz
Qc	Chert
Km	Microcline
Ko	Orthoclase
K	Potassium feldspar (= Km + Ko)
P	Plagioclase feldspar
Fu	Unknown feldspar
Lmf	Foliated quart-mica metamorphic grains
Lmp	Polygonal quartz-mica metamorphic grains
Lmqf	Quartzofeldspathic metamorphic grains
Lmu	Unknown metamorphic grains
Lss	Sedimentary lithic grains: siltstone, argillite, phosphatic grains
Lvf	Felsitic volcanic lithic grains
Lvl	Lathwork volcanic lithic grains
Lvm	Microlitic volcanic lithic grains
Lva	Altered volcanic lithic grains
Lvu	Unknown volcanic lithic grains
Lu	Unknown lithic grain
Qt	Total quartzose grains (= Qm + Qpc + Qc)
Qtc	Total quartzose grains excluding chert (= Qm + Qpc)
F	Total feldspar (= K + P + Fu)
Lm	Total metamorphic grains (= Lmf + Lmp + Lmqf + Lmu)
Lv	Total volcanic grains (= Lvf + Lvl + Lvm + Lva + Lvu)
Ls	Total sedimentary grains (= Lss)
L	Total unstable lithic grains (= Lm + Lv + Ls)
Qp	Total polycrystalline quartz (= Qpq + Qc)
Lt	Total lithic grains (= L + Qp)

Recalculated Parameters	
QtFL%Qt	=100Qt/(Qt + F + L)
QtFL%F	=100F/(Qt + F + L)
QtFL%L	=100L/(Qt + F + L)
QmFLt%Qm	=100Qm/(Qm + F + L)
QmFLt%F	=100F/(Qm + F + L)
QmFLt%Lt	=100Lt/(Qm + F + L)
LmLvLs%Lm	=100Lm/(Lm + Lv + Ls)
LmLvLs%Lv	=100Lv/(Lm + Lv + Ls)
LmLvLs%Ls	=100Ls/(Lm + Lv + Ls)
QmPK%Qm	=100Qm/(Qm + P + K)
QmPK%P	=100P/(Qm + P + K)
QmPK%K	=100K/(Qm + P + K)
QmQtc%Qm	=100Qm/(Qm + Qtc)
QtcF%F	=100F/(F + Qtc)
QtcF%Qtc	=100Qtc/(F + Qtc)
PK%P	=100P/(P + K)
KmKo%Km	=100Km/(Km + Ko)
QcQt%Qc	=100Qc/(Qc + Qt)
QcLt%Qc	=100Qc/(Qc + Lt)

magnetic minerals. Following the heavy liquid separation, samples were processed through a Frantz magnetic separator three times, once with all of the grains at 1.0 A, once with the non-magnetic fraction from the previous step at 1.8 A, and finally the magnetic fraction at 1.8 A to ensure that no non-magnetic grains had become entrained with the magnetic grains and improperly sorted. The mechanical parameters for each of these steps were set at 20˚ side slope and 20˚ front slope to minimize bias towards less paramagnetic age populations at the expense of increased discordance in the sample population (Sircombe and Stern, 2002). Zircon grains were visually picked under a binocular microscope, and then a random portion of the picked group was mounted on double stick tape in a 1mm x 1cm strip divided into 4 rows. Typically 250-350 grains were mounted per sample. Epoxy was poured around the grains to create a 1" diameter epoxy mount. The epoxy mount was ground using a 30 μm grit grinding disc to expose the grains, and then polished using 1 μm grit polishing paste. Cathodoluminescence (CL) images were produced for each grain to serve as a guide during ablation.

Zircon grains were analyzed on a GVI Isoprobe multicollector magnetic sector Laser Ablation-Inductively Coupled Plasma-Mass Spectrometer (LA-ICP-MS) with a Merchantek New Wave LUV213 sample introduction system, using a 213 nm Nd:YAG laser to ablate the grains. Faraday cups with 10^{11} Ω resistors were used to collect ^{238}U, ^{207}Pb, and ^{206}Pb, while a channeltron ion counter was used to collect ^{204}Pb in isobaric interference with ^{204}Hg. The laser was set at 52% power with a 30 μm spot size and 10 Hz laser cycle, resulting in approximately 70-80 J/cm^2 of energy delivered to ablate the zircon grain during each analysis. U concentrations for each grain were determined based on an analysis carried out on NIST SRM 610 glass (^{238}U concentration ~461.5 ppm) (Reed, 1992) at the beginning of each day. Prior to analysis, each grain was pre-ablated for 1-2 s with an expanded 410 μm laser beam, delivering 2-3 J/cm^2 of energy, in

order to remove any material that may have accumulated on the grain surfaces while the mount was exposed during transfer to the sample introduction system. Each analysis consisted of 30 s data collection prior to ablation to measure background counts, otherwise known as an on peak zero, 10 s warm-up time for the laser and 20 s analysis time, followed by 20-30 s to flush the ablation chamber before analyzing the next grain. Every effort was made to ablate only the most recent magmatic growth of each grain since this will indicate its crystallization age and can be linked to a basement provenance. CL images were used to identify recycled cores and metamorphic rims on grains so that they could be avoided during isotopic analysis (Connelly, 2001; Corfu et al., 2003). Analyses of the in-house standard S97-19 were conducted after every 15 unknown grains to characterize mass fractionation and elemental (U/Pb) bias during the course of the day. S97-19 has been characterized by ID-TIMS at The University of Texas at Austin. In addition, the Plešovice (PL) zircon standard (Sláma et al., 2008) was analyzed to monitor system behavior. Typically 135-150 grains were analyzed per sample, so that even after rejecting some analyses due to high discordance or error there should be approximately 120 acceptable ages for each sample. This meets the criteria of Vermeesch (2004), so it is possible to be certain, at the 95% confidence level, of not missing a fraction of the population comprising at least 5% of the total population. While many detrital zircon studies typically have approximately 100 grains per sample (Dickinson and Gehrels, 2003, 2008a, b, 2009; Dickinson et al., 2009), Andersen (2005) warns that interpretations of the relative proportions of inputs from different source areas even when 120 grains are analyzed must be looked at with caution. In his study, Andersen (2005) used Monte Carlo simulations to compare the age spectra of samples of 120 grains drawn from a total population of 2000 grains to the age spectra of the total population, and found that the sample populations were not quantitatively similar to the total population.

Data were downloaded and reduced off-line using in-house Excel software to remove unacceptable data points for each analysis that may be the product of common Pb on the surface of the epoxy mount, ablating into another zone of the grain or ablating all the way through the grain. Depth-dependent U/Pb fractionation was also corrected at this step by using regression of the U/Pb data points to determine the initial U/Pb ratio at time zero (Košler and Sylvester, 2003). A second step of data reduction was conducted to correct for mass fractionation, elemental bias, and initial Pb. An isobarically corrected $^{206}Pb/^{204}Pb$ ratio was determined using the method of Gehrels et al. (2006), and then used to correct for common Pb using the Stacey and Kramers (1975) model for Pb evolution. Following established lab procedure, no uncertainty was applied to the common Pb correction. Work by the University of Texas at Austin LA-ICP-MS lab has found that for moderately radiogenic zircons, the uncertainty on the grain age is dominated by uncertainty on the U/Pb ratios, while uncertainty on the common Pb correction typically makes up less than 1% of the final age uncertainty (Housh, 2009, personal communication). Finally, mass fractionation and elemental bias factors determined on the standard were applied to the unknowns to determine the corrected, radiogenic $^{206}Pb^*/^{238}U$ and $^{207}Pb^*/^{206}Pb^*$ ratios and ages. The $^{207}Pb^*/^{235}U$ ratio and age was determined using a $^{238}U/^{235}U$ ratio of 137.88 (Faure and Mensing, 2005). Measured errors as well as the errors associated with mass fractionation and the elemental (U/Pb) bias determined on the standard S97-19 were propagated to yield the final errors on $^{207}Pb^*/^{206}Pb^*$, $^{206}Pb^*/^{238}U$, and $^{207}Pb^*/^{235}U$ for the unknown grains; measured errors alone are reported for $^{206}Pb/^{204}Pb$. The best ages for each grain were identified based on the $^{206}Pb^*/^{238}U$ age for grains generally younger than 950 Ma and the $^{207}Pb^*/^{206}Pb^*$ age for grains generally older than 950 Ma; however, the precise cutoff was picked individually

for each sample to avoid splitting up clusters of grain ages. Discordance for each analysis was determined using the following equation:

$$Discordance = \left(\frac{^{207}Pb^{*}/^{235}U\ \ age - {}^{206}Pb^{*}/^{238}U\ age}{\left(^{207}Pb^{*}/^{235}U\ \ age + {}^{206}Pb^{*}/^{238}U\ age\right)/2} \right) \qquad (1.1)$$

Grains were filtered by discordance and error with the filter being set at -10% to 60% discordance for grains younger than 350 Ma, -10% to 30% discordance for grains 1000-350 Ma in age, and -5% to 10% discordance for grains older than 1000 Ma. Grains outside of those ranges or with 1σ error exceeding 10% on the best age were excluded from further analysis. All plots and analysis were conducted using Isoplot 3.2 and 3.7 (Ludwig, 2003, 2008) and Excel worksheets designed by the University of Arizona Laserchron center (available online at www.geo.arizona.edu/alc).

Table 2. Recalculated modal point-count data for the Wilcox Group.

Sample Name	Sample Type [a]	QtFL%			QmFLt%			LmLvLs%			QmPK%			QmQtc	QtcF%			PK%	KmKo%	QcQt%	QcLt%		Grain Size (μm)	IGV	Primary Porosity
		Qt	F	L	Qm	F	Lt	Lm	Lv	Ls	Qm	P	K	Qm	F	Qtc	P	Km	Qc	Qc				
Upper Wilcox Samples																									
GM-C-051408-1	o	87%	7%	6%	72%	7%	21%	75%	17%	8%	92%	4%	4%	88%	7%	93%	47%	75%	6%	23%	219.1	34%	18%		
GM-C-051408-2	o	91%	6%	2%	78%	6%	15%	50%	50%	0%	93%	1%	6%	90%	7%	93%	9%	40%	5%	29%	299.8	38%	27%		
GM-C-051408-3	o	95%	4%	2%	80%	4%	16%	0%	0%	100%	96%	1%	3%	92%	4%	96%	17%	0%	7%	43%	339.2	38%	26%		
GM-C-051408-5	o	92%	5%	4%	79%	5%	16%	0%	75%	25%	96%	0%	4%	90%	5%	95%	0%	13%	4%	20%	346.6	32%	z24%		
GM-C-051408-7	o	93%	3%	4%	79%	3%	18%	0%	71%	29%	97%	1%	3%	88%	3%	97%	20%	0%	3%	17%	349.2	41%	17%		
GM-C-051408-8	o	94%	1%	6%	83%	1%	16%	0%	0%	100%	99%	0%	1%	92%	1%	99%	0%	0%	4%	22%	302.4	42%	10%		
GM-C-051408-9	o	91%	7%	2%	81%	7%	12%	20%	20%	60%	92%	1%	7%	92%	7%	93%	13%	38%	3%	25%	408.5	37%	3%		
GM-C-051408-10	o	77%	16%	7%	60%	16%	24%	30%	60%	10%	79%	0%	21%	89%	19%	81%	0%	18%	12%	40%	310.9	47%	11%		
GM-C-051408-11	o	84%	6%	10%	71%	6%	23%	9%	9%	83%	93%	1%	6%	88%	7%	94%	15%	18%	3%	11%	421.8	30%	1%		
GM-C-051408-12	o	85%	9%	6%	68%	9%	23%	58%	25%	17%	88%	0%	12%	89%	11%	89%	0%	5%	10%	38%	172.4	36%	27%		
GM-C-051408-13	o	95%	3%	1%	82%	3%	14%	0%	33%	67%	96%	0%	4%	93%	4%	96%	0%	14%	7%	48%	228.1	35%	19%		
GM-C-051408-14	o	82%	12%	6%	74%	12%	15%	50%	25%	25%	86%	0%	14%	94%	13%	87%	0%	9%	4%	24%	244.2	37%	1%		
GM-C-051508-1	o	80%	11%	9%	71%	11%	18%	47%	47%	6%	86%	0%	14%	95%	13%	87%	0%	8%	6%	27%	162.2	34%	23%		
GM-C-051508-2	o	86%	7%	6%	62%	7%	31%	0%	18%	82%	90%	0%	10%	86%	9%	91%	0%	8%	17%	47%	249.6	46%	0%		
GM-C-051508-3	o	84%	6%	10%	53%	6%	41%	11%	50%	39%	90%	0%	10%	87%	8%	92%	0%	0%	27%	55%	393.6	33%	33%		
GM-C-051608-1	o	96%	3%	1%	83%	3%	14%	0%	0%	100%	96%	0%	4%	88%	3%	97%	0%	29%	1%	10%	449.9	36%	0%		
GM-C-051608-2	o	92%	6%	2%	78%	6%	16%	50%	0%	50%	93%	1%	6%	88%	6%	94%	17%	10%	4%	22%	260.4	36%	0%		
GM-C-051608-3	o	83%	8%	9%	66%	8%	26%	63%	31%	6%	89%	3%	7%	89%	10%	90%	29%	0%	12%	37%	217.8	35%	22%		
GM-C-051608-4	o	90%	5%	5%	80%	5%	16%	44%	56%	0%	95%	1%	4%	92%	5%	95%	11%	38%	4%	22%	204.4	30%	28%		
GM-C-051608-5	o	86%	5%	9%	73%	5%	22%	38%	38%	25%	94%	0%	6%	89%	5%	95%	0%	73%	4%	16%	291.7	28%	27%		
Bailey 1C-10474	c	81%	14%	5%	77%	14%	8%	91%	9%	0%	92%	6%	1%	97%	15%	85%	83%	0%	1%	13%	158.9	13%	10%		
Bailey 1C-10491	c	91%	4%	5%	84%	4%	12%	25%	50%	25%	96%	3%	1%	96%	5%	95%	75%	0%	3%	27%	121.3	23%	6%		
Urban1-13896	c	85%	11%	4%	81%	11%	7%	88%	13%	0%	95%	4%	1%	97%	12%	88%	73%	0%	1%	11%	80.6	20%	15%		
Urban1-14097	c	83%	13%	3%	77%	13%	9%	88%	13%	0%	94%	6%	0%	93%	14%	86%	100%	0%	0%	4%	106.8	20%	11%		
Mean		88%	7%	5%	75%	7%	18%	35%	30%	36%	93%	1%	6%	91%	8%	92%	21%	16%	6%	26%	264.1	33%	15%		
Std Dev [b]		5.4%	3.9%	2.9%	8.1%	3.9%	7.5%	31.4%	23.2%	35.4%	4.4%	1.9%	5.0%	3.2%	4.5%	4.5%	30.7%	21.9%	5.9%	13.4%	102.3	8.0%	10.7%		

Sample Name	Sample Type [a]	QtFL%			QmFLt%			LmLvLs%			QmPK%			QmQtc	QtcF%		PK%	KmKo%	QcQt%	QcLt%	Grain Size (μm)	IGV	Primary Porosity
		Qt	F	L	Qm	F	Lt	Lm	Lv	Ls	Qm	P	K	Qm	F	Qtc	P	Km	Qc	Qc			
Lower Wilcox Samples																							
GM-W-051408-1	o	80%	11%	9%	68%	11%	21%	56%	22%	22%	88%	1%	11%	91%	13%	87%	5%	44%	7%	26%	178.6	32%	24%
GM-W-051508-2	o	81%	7%	12%	55%	7%	38%	41%	55%	5%	89%	2%	9%	88%	10%	90%	20%	17%	22%	48%	167.5	38%	26%
GM-W-051508-3	o	83%	10%	7%	61%	10%	29%	31%	69%	0%	86%	0%	14%	90%	13%	87%	0%	20%	18%	52%	148.8	38%	21%
GM-W-051508-4	o	82%	9%	9%	69%	9%	22%	29%	57%	14%	89%	1%	11%	95%	11%	89%	6%	6%	11%	43%	82.3	40%	28%
GM-W-051608-1	o	80%	11%	8%	66%	11%	23%	25%	63%	13%	86%	1%	14%	92%	14%	86%	4%	23%	11%	40%	184.7	34%	19%
GM-W-051608-2	o	86%	4%	10%	53%	4%	42%	6%	82%	12%	92%	0%	8%	83%	7%	93%	0%	10%	25%	51%	199.0	32%	25%
GM-W-051608-3	o	80%	16%	4%	66%	16%	18%	71%	29%	0%	81%	0%	19%	88%	18%	82%	0%	15%	6%	27%	169.2	47%	0%
GM-W-051608-4	o	83%	8%	9%	71%	8%	21%	41%	59%	0%	90%	1%	9%	93%	9%	91%	13%	7%	8%	30%	115.6	37%	16%
Burns1-9241	c	75%	13%	12%	61%	13%	26%	25%	61%	14%	85%	4%	10%	95%	17%	83%	29%	35%	15%	42%	174.9	34%	6%
Burns1-9297	c	78%	9%	13%	64%	9%	27%	24%	59%	18%	92%	5%	3%	96%	11%	89%	59%	29%	14%	41%	207.1	16%	8%
Burns1-9334	c	80%	9%	11%	65%	9%	26%	13%	71%	16%	88%	4%	8%	92%	11%	89%	33%	19%	12%	36%	239.9	20%	9%
Burns1-9525	c	81%	14%	5%	74%	14%	12%	23%	77%	0%	86%	4%	10%	96%	15%	85%	28%	9%	5%	33%	223.9	25%	13%
Burns1-9614	c	85%	10%	5%	79%	10%	11%	90%	10%	0%	90%	4%	6%	97%	11%	89%	44%	14%	4%	32%	208.0	14%	9%
Paul1-9152	c	83%	11%	6%	78%	11%	12%	50%	44%	6%	91%	3%	6%	96%	11%	89%	35%	0%	3%	19%	127.8	20%	9%
Winch St. 4-9310	c	82%	12%	5%	80%	12%	8%	67%	22%	11%	92%	6%	2%	98%	13%	87%	72%	0%	1%	10%	73.6	17%	9%
Winch St. 4-9948	c	83%	13%	5%	72%	13%	15%	10%	80%	10%	91%	5%	5%	96%	14%	86%	50%	0%	8%	47%	105.4	35%	1%
Mean		81%	10%	8%	68%	10%	22%	38%	54%	9%	88%	3%	9%	93%	12%	88%	25%	15%	11%	36%	162.9	30%	14%
Std Dev [b]		2.7%	2.8%	3.0%	8.0%	2.8%	9.6%	23.8%	22.2%	7.4%	3.1%	2.0%	4.3%	4.0%	2.8%	2.8%	22.8%	12.8%	6.9%	11.8%	49.9	10.0%	9.0%

[a] Sample type c is from core and sample type o is from outcrop.

[b] Std Dev is one standard deviation for the mean.

RESULTS

Sandstone Petrography

The samples in this study are very-well to moderately-well sorted, very fine- to medium-grained, subarkose, sublitharenite, litharenite, feldspathic litharenite, and lithic arkose (Folk, 1980) (Table 2). Framework grains include monocrystalline quartz; polycrystalline quartz; chert; plagioclase and albitized plagioclase; orthoclase; microcline; volcanic rock fragments, primarily highly altered felsitic and lathwork grains; metamorphic rock fragments; and sedimentary rock fragments. Large mica crystals, both biotite and muscovite, and zircons are the primary accessory minerals.

Huminite reflectance of shallow (200-565 m burial depth) Wilcox lignite and coal from northeast Texas suggests that it has not been buried deeper than its current location (Mukhopadhyay, 1989), whereas structural projections of more deeply buried strata from Leon County, Texas indicate that the Wilcox may have experience up to 300 m of uplift (Galloway et al., 1994). McBride et al. (1991) suggested that as much as 762 m of Wilcox strata may have been eroded in Bastrop County, TX along the San Marcos Arch. If this uplift history is representative of the Wilcox in south Texas, then this would suggest that most up-dip Wilcox strata, not adjacent to the San Marcos Arch, have not experienced significant uplift. Despite the limited exposure to subsurface heating, outcrop samples show a significant diagenetic overprinting arising from processes within the meteoric regime of shallow burial, primarily dissolution of feldspar and lithic fragments. Approximately one-third of outcrop samples contain poikilotopic calcite cement; minor hematite or kaolinite cements are also common. In the case of calcite-cemented samples, intergranular volumes (IGV) in excess of 36% indicate an early

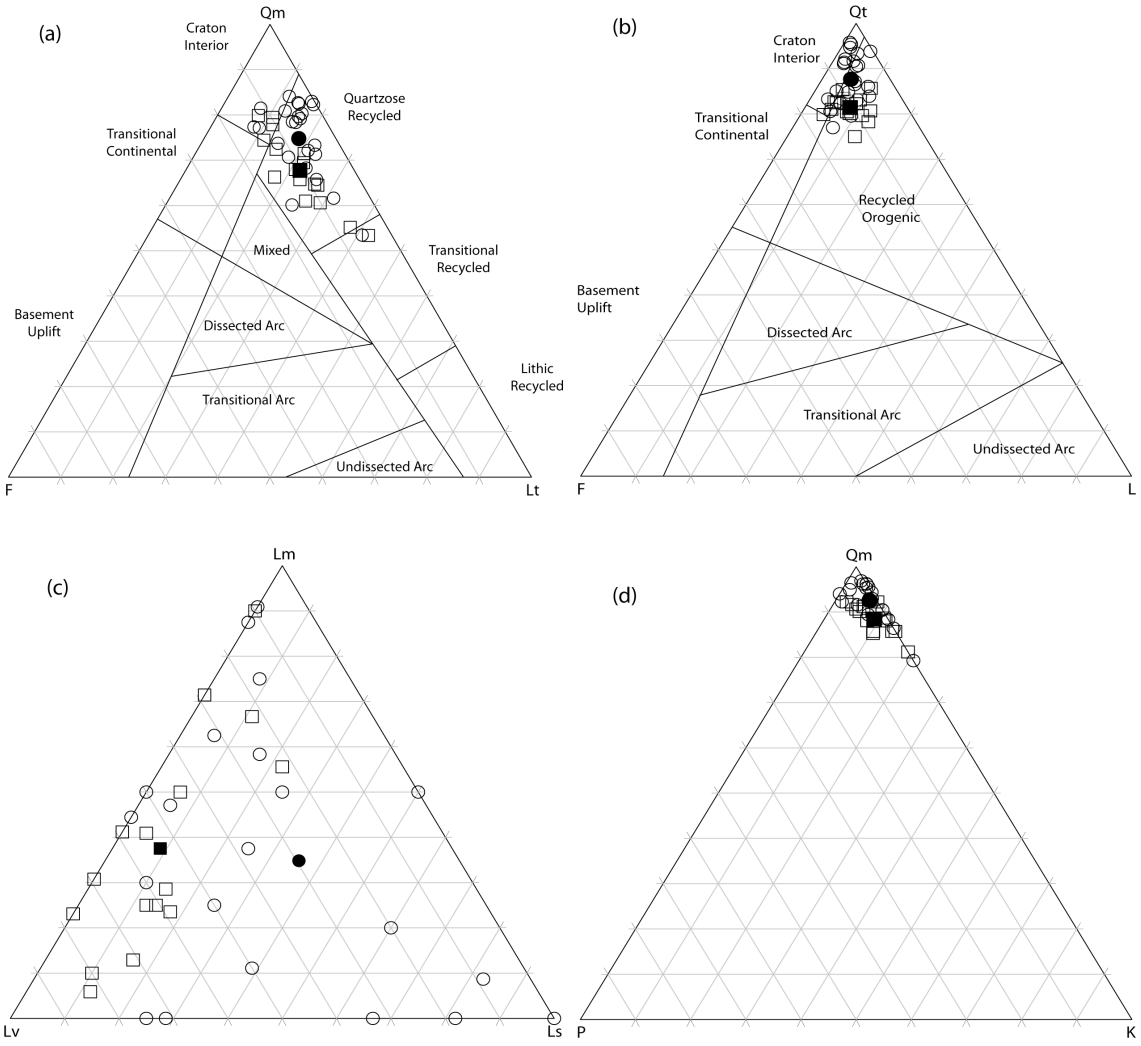

Figure 3. Detrital modes of Paleocene-Eocene Wilcox Group. Data are listed in Table 2. Provenance fields of QmFLt and QtFL ternary plots are from Dickinson (1985). Each axis is from 0% to 100%. Open squares represent Lower Wilcox samples. Open circles represent Upper Wilcox samples. Filled symbols are subunit mean values. (a) QmFLt. (b) QtFL. (c) LmLvLs. (d) QmPK.

Table 3. (a) χ^2 test of Upper and Lower Wilcox QmFLt data.[a] (b) χ^2 test of Upper and Lower Wilcox QtFL data. (c) Students-t test of all Upper and Lower Wilcox recalculated modal point-count data. [b]

(a)	Actual		Expected	
	UW	LW	UW	LW
Qm	3941	2535	3795	2681
F	379	384	447	316
Lt	938	795	1016	717
# of Samples	24	16	24	16

χ2 Distribution	52.948
Probability	3.181E-12

[a] The χ2 test compares the actual values of a two or more sets of measurements to their expected values calculated based on the null hypothesis that each of the data sets is the same, and returns a probability (P) that the differences between the two data sets are random. If P<0.05, then at a 95% confidence level the two data sets can be said to be different. If P≥0.05, then the two data sets are statistically the same. Tests where P≥0.05 are marked by bold text.

(b)	Actual		Expected	
	UW	LW	UW	LW
Qt	4601	3025	4469	3157
F	379	384	447	316
L	278	305	342	241
# of Samples	24	16	24	16

χ2 Distribution	63.143
Probability	1.944E-14

(c)	UW			LW				
	Mean	Std Dev	# of Samples	Mean	Std Dev	# of Samples	t -Distribution	Probability
QtFL%Qt	87.7%	5.4%	24	81.4%	2.7%	16	4.267	0.000
QtFL%F	7.1%	3.9%	24	10.4%	2.8%	16	2.872	0.007
QtFL%L	5.2%	2.9%	24	8.2%	3.0%	16	3.094	0.004
QmFLt%Qm	74.8%	8.1%	24	67.8%	8.0%	16	2.705	0.010
QmFLt%F	7.1%	3.9%	24	10.4%	2.8%	16	2.872	0.007
QmFLt%Lt	18.1%	7.5%	24	21.8%	9.6%	16	1.375	**0.177**
LmLvLs%Lm	34.8%	31.4%	24	37.5%	23.8%	16	0.294	**0.770**
LmLvLs%Lv	29.5%	23.2%	24	53.7%	22.2%	16	3.275	0.002
LmLvLs%Ls	35.7%	35.4%	24	8.8%	7.4%	16	2.976	0.005
QmPK%Qm	92.5%	4.4%	24	88.5%	3.1%	16	3.234	0.003
QmPK%P	1.3%	1.9%	24	2.5%	2.0%	16	1.882	**0.067**
QmPK%K	6.1%	5.0%	24	9.0%	4.3%	16	1.893	**0.066**
Qm/Qtc	90.8%	3.2%	24	92.9%	4.0%	16	1.786	**0.082**
QtcF%F	8.0%	4.5%	24	12.4%	2.8%	16	3.466	0.001
QtcF%Qtc	92.0%	4.5%	24	87.6%	2.8%	16	3.466	0.001
PK%P	21.2%	30.7%	24	24.9%	22.8%	16	0.408	**0.685**
KmKo%Km	16.5%	21.9%	24	15.5%	12.8%	16	0.162	**0.872**
QcQt%Qc	6.2%	5.9%	24	10.6%	6.9%	16	2.146	0.038
QcLt%Qc	26.3%	13.4%	24	36.0%	11.8%	16	2.354	0.024

[b] The Student's T-test compares the mean values for two sets of data, and returns a probability (P) that the differences between the two data sets are random. If $P<0.05$, then at a 95% confidence level the two data sets can be said to be different. If $P\geq0.05$, then the two data sets are statistically the same. Tests where $P\geq0.05$ are marked by bold text.

timing for complete calcite cementation (Paxton et al., 2002). Samples with IGVs in excess of 45%, even after correcting for obviously oversized patches of cement, most likely indicate fill of calcite cement into voids left by the dissolution of rock fragment and feldspar grains (Beard and Weyl, 1973; Pryor, 1973).

In comparison to outcrops samples, subsurface samples show less diagenetic alteration. All core samples but one (Winch St. 4-9948) contain quartz cement, typically 3%–5% but ranging up to 9%, with some samples also containing patchy kaolinite cement. Core samples also tend to display more variation in the content of rock fragments, especially in highly unstable volcanic rock fragments.

Wilcox samples plot mainly in the quartz recycled, transitional recycled and craton recycled fields in QmFLt space, and in the recycled orogenic and craton interior fields of the QtFL space (Dickinson and Suczek, 1979; Dickinson, 1985) (Figure 3). Although the compositional differences are not large, χ^2 tests of the QmFLt and QtFL values of the Upper and Lower Wilcox indicate that the differences are significant at the 95% confidence level (Folk, 1980) (Table 3). The Lower Wilcox is richer in lithic fragments, in particular chert and volcanic rock fragments, and feldspar, whereas the Upper Wilcox contains more sedimentary rock fragments. A possible cause of the differing proportions may relate primarily to the lack of volcanic rock fragments in the Upper Wilcox. While there are many differences between the Upper and Lower Wilcox samples, the percentage of metamorphic rock fragments and the ratio of plagioclase to total identifiable grains are fairly consistent.

Figure 4. Detrital zircon age probability distributions for all analyzed Wilcox samples. Numbers mark prominent age peaks. Horizontal bars labeled A–E indicate age populations described in text and table 5. N=number of samples, n= number of grains. (a) All grains from Wilcox Group. Subpopulations A1, A2, A3, and A4, of population A; B1, B2, and B3 of population B; and D1, D2, D3, D4, D5, and D6 of population D are indicated. Histogram bins equal 50 m.y. (b) Wilcox Grains younger than 350 Ma. Subpopulations E1, E2, E3, E4 and E5 of population E are indicated. Histogram bins equal 10 m.y.

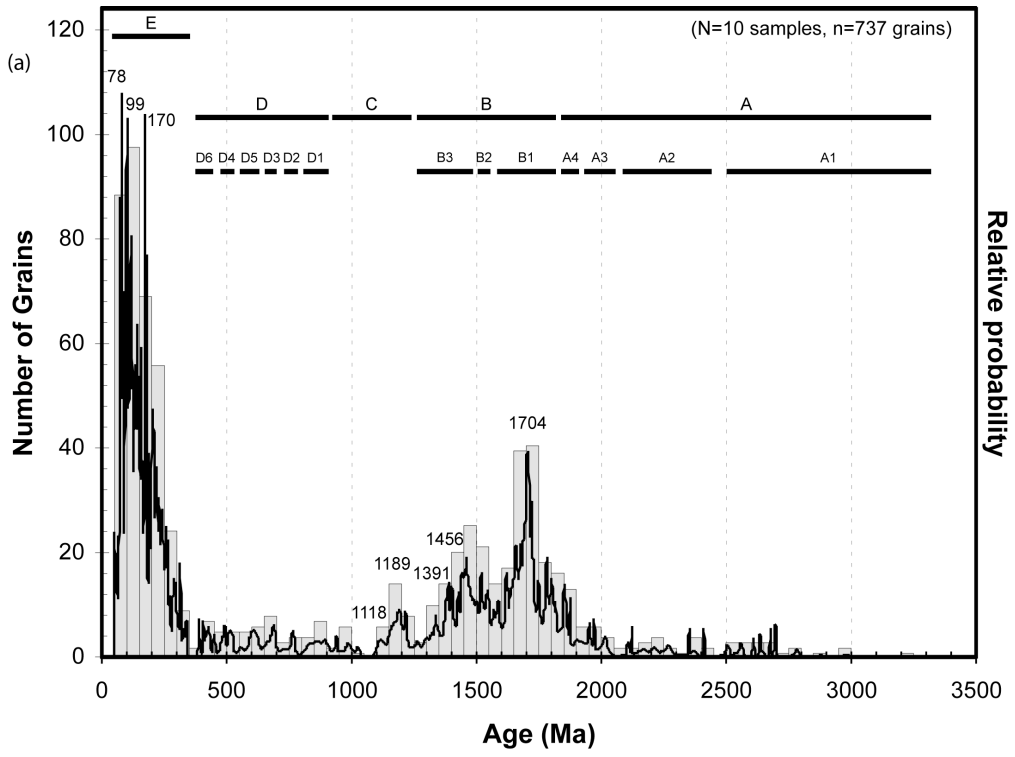
(a)
(N=10 samples, n=737 grains)
E
D
C
B
A
D6 D4 D5 D3 D2 D1
B3 B2 B1 A4 A3 A2 A1
78
99
170
1704
1456
1189
1391
1118
Number of Grains
Relative probability
Age (Ma)

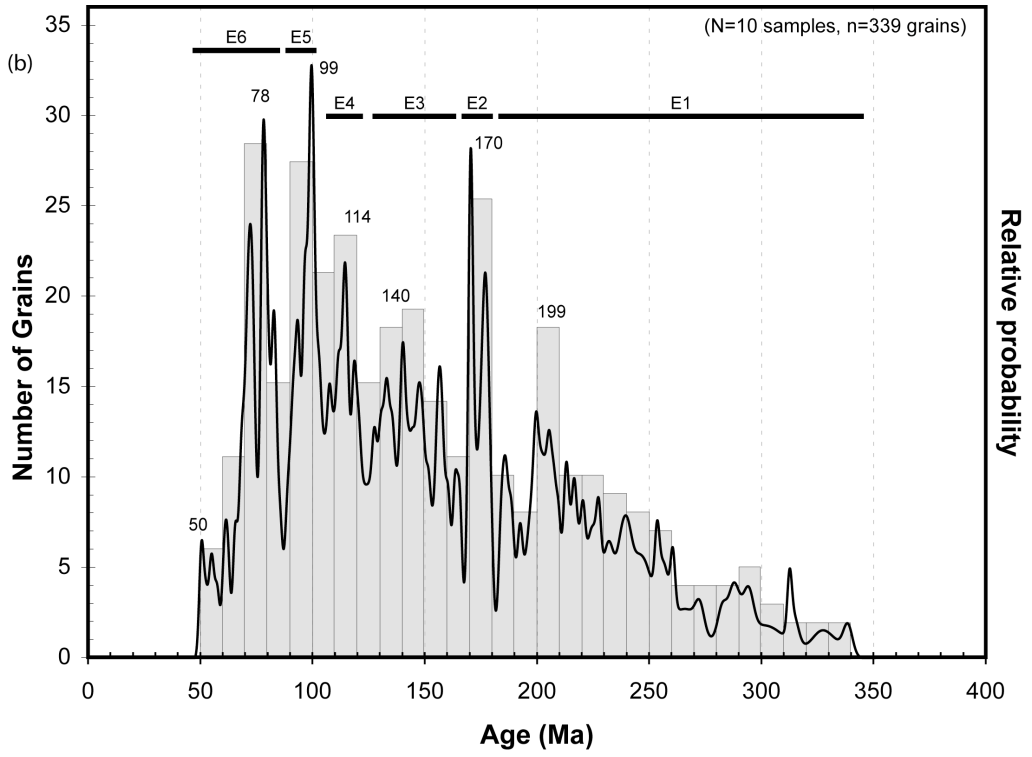
(b)
(N=10 samples, n=339 grains)
E6
E5
E4
E3
E2
E1
99
78
170
114
140
199
50
Number of Grains
Relative probability
Age (Ma)

Figure 5. Normalized age probability plots for all Wilcox Samples. Wilcox subunits are arranged in stratigraphic order. Samples within subunits are organized geographically from southwest at the bottom to northeast at the top.

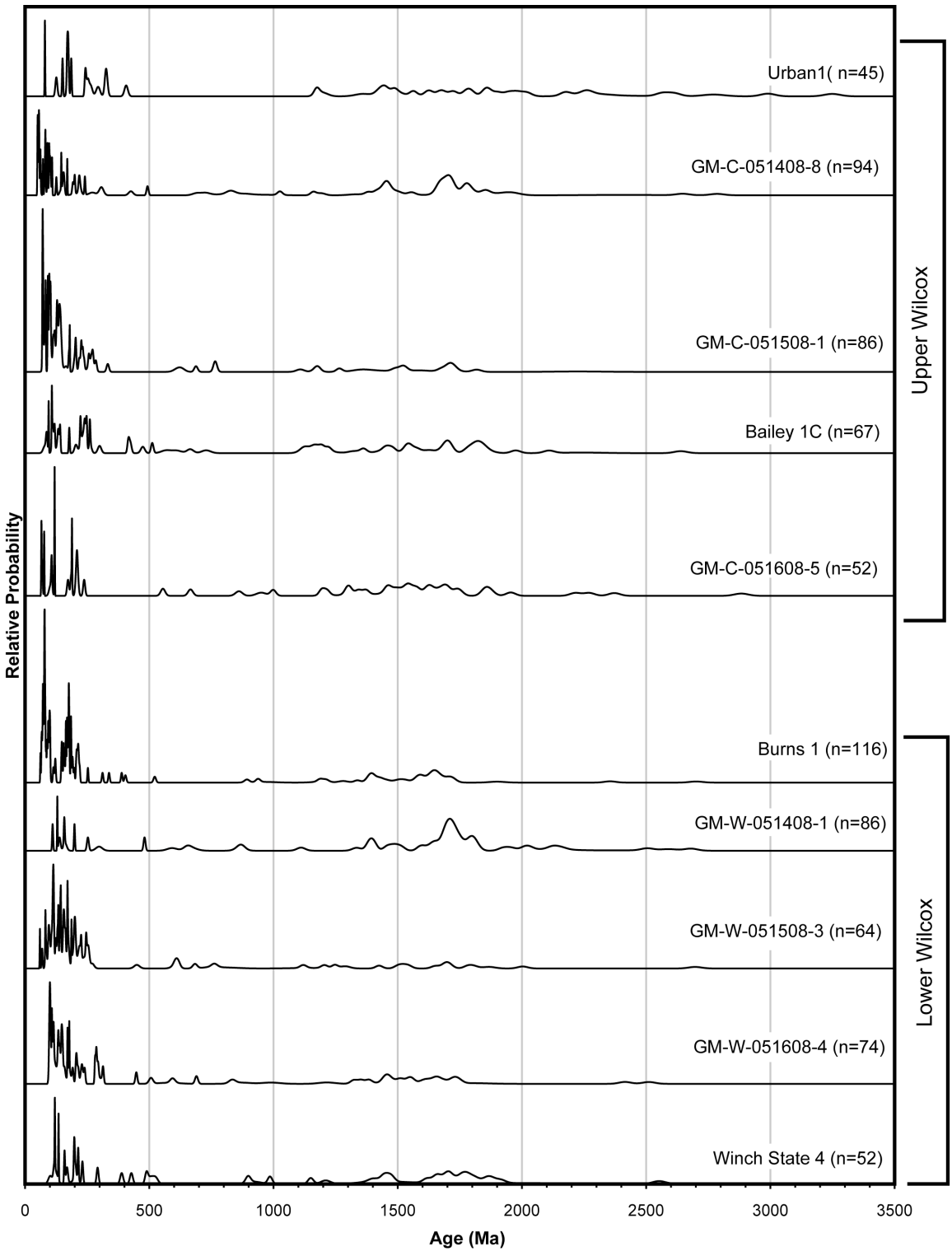
Urban1(n=45)
GM-C-051408-8 (n=94)
GM-C-051508-1 (n=86)
Bailey 1C (n=67)
GM-C-051608-5 (n=52)
Burns 1 (n=116)
GM-W-051408-1 (n=86)
GM-W-051508-3 (n=64)
GM-W-051608-4 (n=74)
Winch State 4 (n=52)
Upper Wilcox
Lower Wilcox
Relative Probability
0
500
1000
1500
2000
2500
3000
3500
Age (Ma)

Table 4. Correlation coefficients (R^2) between grain size and recalculated modal point-count data for all Wilcox Group samples.

	Outcrop Samples R^2	Core Samples R^2	All Samples R^2
QtFL%Qt	0.2812	0.1975	0.2362
QtFL%F	0.2069	0.0085	0.2778
QtFL%L	0.1532	0.3418	0.0344
QmFLt%Qm	0.1295	0.3412	0.0063
QmFLt%F	0.2069	0.0085	0.2778
QmFLt%Lt	0.0384	0.3699	0.0252
LmLvLs%Lm	0.2959	0.1364	0.2950
LmLvLs%Lv	0.1217	0.1734	0.0386
LmLvLs%Ls	0.4190	0.0060	0.4416
QmPK%Qm	0.2177	0.4424	0.0630
QmPK%P	0.0180	0.0099	0.2216
QmPK%K	0.1828	0.4368	0.0007
QmQtc%Qm	0.1038	0.0791	0.2953
QtcF%F	0.2356	0.0095	0.2654
QtcF%Qtc	0.2356	0.0095	0.2654
PK%P	9.05E-06	0.3710	0.2317
KmKo%Km	0.0029	0.4543	0.0579
QcQt%Qc	0.0728	0.3533	3.25E-06
QcLt%Lt	0.1586	0.3478	0.0041
Average Value	0.1621	0.2156	0.1599
Minimum Value	9.05E-06	0.0060	3.25E-06
Maximum Value	0.4190	0.4543	0.4416

Table 5. Zircon population ages with relative proportions of each population in the Wilcox Group, Upper Wilcox, and Lower Wilcox and most likely proximal source.

Age Group	Age Range (Ma)	Primary Age Peak (Ma)	Proportion of Wilcox Group	Proportion of Lower Wilcox	Proportion of Upper Wilcox	Most Likely Proximal Source [a b c]
E6	87-49	78	7.73%	7.14%	8.41%	Cordilleran Arc
E5	105-87	99	5.97%	5.87%	6.09%	Cordilleran Arc
E4	123-105	114	4.61%	5.36%	3.77%	Cordilleran Arc
E3	167-123	140	9.63%	11.73%	7.25%	Cordilleran Arc
E2	181-167	170	3.66%	4.85%	2.32%	Cordilleran Arc
E1	339-181	199	14.38%	14.80%	13.91%	East Mexico Arc, Older arcs in Mexico, Cordilleran Arc
D6	451-388	425	1.36%	1.53%	1.16%	Volcanic arc terranes of western NA
D5	526-473	491	1.22%	1.53%	0.87%	OK Aulacogen, Triassic strata of western NA
D4	630-554	607	1.49%	1.53%	1.45%	Unclear
D3	691-652	687	1.09%	1.02%	1.16%	Strata of the RMA
D2	785-726	764	0.95%	0.51%	1.45%	Strata from western NA
D1	923-815	894	1.63%	2.04%	1.16%	Unclear
C	1326-937	1189	5.97%	4.59%	7.54%	Mexican Grenville basement
B3	1500-1334	1456	8.68%	8.16%	9.28%	Southern Laramide basement
B2	1590-1500	1530	4.48%	3.83%	5.22%	Strata from western NA
B1	1819-1590	1704	17.50%	18.37%	16.52%	Southern Laramide basement
A4	1920-1829	1852	2.71%	1.53%	4.06%	Volcanic arc terranes of western NA, Strata of RMA
A3	2062-1920	1954	1.76%	1.53%	2.03%	Volcanic arc terranes of western NA, Strata of RMA
A2	2415-2090	2251	2.58%	1.79%	3.48%	Volcanic arc terranes of western NA, Strata of RMA
A1	3250-2503	2680	2.58%	2.30%	2.90%	Volcanic arc terranes of western NA, Strata of RMA
E	339-49	99	46.00%	49.74%	41.74%	Cordilleran Arc
D	923-388	no primary peak	7.73%	8.16%	7.25%	Numerous minor sources
C	1326-937	1189	5.97%	4.59%	7.54%	Mexican Grenville basement
B	1819-1334	1705	30.66%	30.36%	31.01%	Southern Laramide Basement
A	3250-1829	no primary peak	9.63%	7.14%	12.46%	Volcanic arc terranes of western NA, Strata of RMA

[a] NA=North America

[b] RMA=Roberts Mountain Allochthon

[c] OK=Oklahoma

Grain size is not a significant controlling factor in sandstone composition. Samples from core tend to have higher correlation coefficients (R^2) between grain size and compositional parameters than outcrop samples (Table 4), but when the data for all samples are examined, R^2 values are less than 0.3 for all recalculated ratios except LmLvLs%Ls. This indicates that while grain size has some control on composition, it typically does not account for more than 30% of the variation. The higher R^2 values for core samples may be due to better compositional sorting in a high-energy delta-front to shallow-marine environment.

Detrital Zircon Geochronology

U-Pb ages of detrital zircon grains from samples of the Wilcox Group range from 50 Ma to 3249 Ma (Figure 4, 5). Data tables and Concordia plots for each sample are available in Appendices C and D. Seven age populations can be discriminated based on the relative age probabilities (i.e., peaks and valleys) observed in the normalized age probability plot depicting all of the grains analyzed in this study (Table 5, Figure 4, Appendix F).

Population A represents a minor population composed of Archean and Paleoproterozoic grains (3250-1850 Ma). In contrast, the Paleoproterozoic to Mesoproterozoic (1819-1334 Ma) zircons of population B compose one of the two most prominent populations, making up 31% of the entire sample set, though there are wide variations in its prominence in individual samples, ranging from 12% to 58%. Population C is a relatively minor age population of Mesoproterozoic to Neoproterozoic (1326-937 Ma) grains. Population D is comprised of Neoproterozoic to Devonian (923-388 Ma) zircons that define a minor population composed of six low peaks. Mississippian to Paleocene (338-50 Ma) zircons of population E define a relatively major peak, made

Figure 6. Maps showing sample location and detrital zircon age probability distributions for each sample. Histogram bins equal 50 m.y., n=number of grains. Upper Wilcox outcrop in cross hatch pattern, Lower Wilcox outcrop in stipple pattern, Upper Wilcox deltas in down-to-the-right diagonal lines and Lower Wilcox deltas in down-to-the-left diagonal lines. Wilcox outcrop from Stoeser et al. (2005). Upper and Lower Wilcox deltas after Edwards (1981). (a) Lower Wilcox sample map. Lower Wilcox samples marked by squares. (b) Upper Wilcox Sample map. Upper Wilcox samples marked by circles.

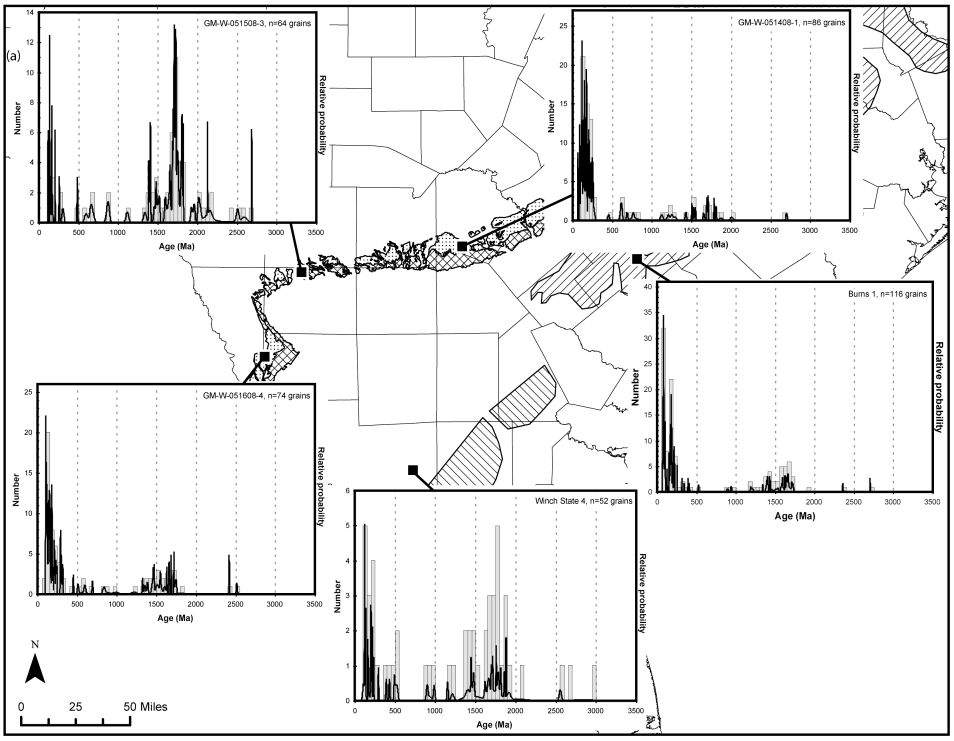
(a)
GM-W-051508-3, n=64 grains
GM-W-051408-1, n=86 grains
Burns 1, n=116 grains
GM-W-051608-4, n=74 grains
Winch State 4, n=52 grains
Number
Relative probability
Age (Ma)
N
0 25 50 Miles

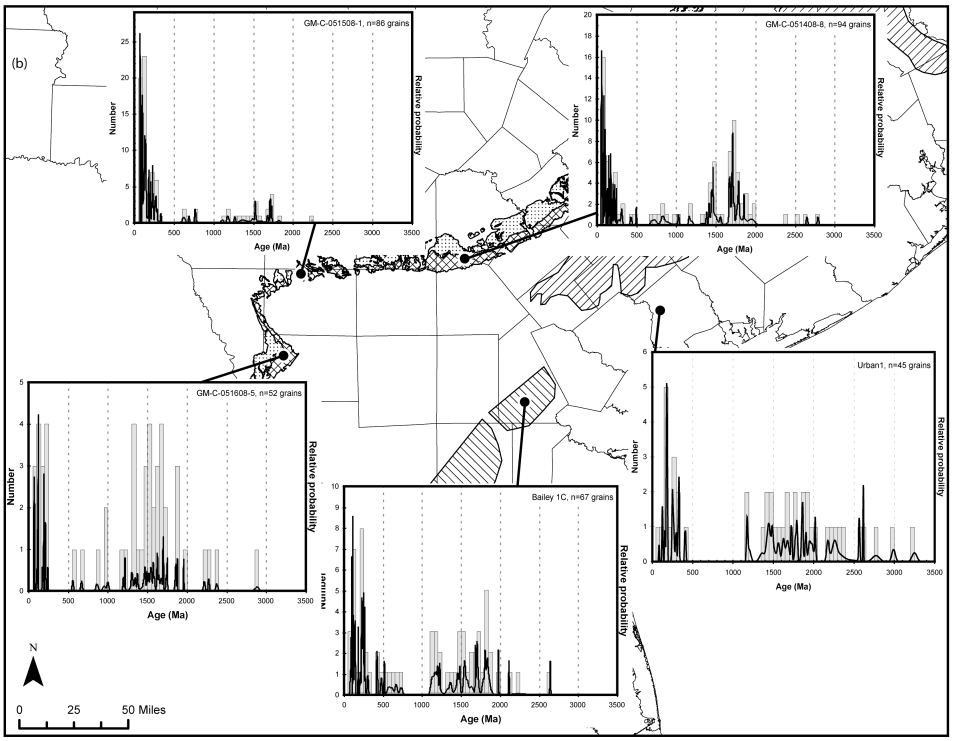
(b)
GM-C-051508-1, n=86 grains
GM-C-051408-8, n=94 grains
Urban1, n=45 grains
GM-C-051608-5, n=52 grains
Bailey 1C, n=67 grains
Number
Relative probability
Age (Ma)
N
0 25 50 Miles

Figure 7. Comparison of normalized age probability plots of the Upper and Lower Wilcox samples. Horizontal bars labeled A–E indicate age populations described in text and table 5. Upper Wilcox is in black, Lower Wilcox is in grey. N=number of samples, n=number of grains. Numbers mark prominent age probability peaks referenced in the text. (a) All grains in Upper and Lower Wilcox. Subpopulations A1, A2, A3, and A4, of population A; B1, B2, and B3 of population B; and D1, D2, D3, D4, D5, and D6 of population D are indicated. Plot is normalized so that the area under both curves is the same. (b) Upper and Lower Wilcox grains younger than 350 Ma. Subpopulations E1, E2, E3, E4 and E5 of population E are indicated. Plot is a rescaled version of figure 7A. It is not normalized to the number of grains younger than 350 Ma, but represents the fact that grains younger than 350 Ma make up a larger proportion of the Lower Wilcox than Upper Wilcox.

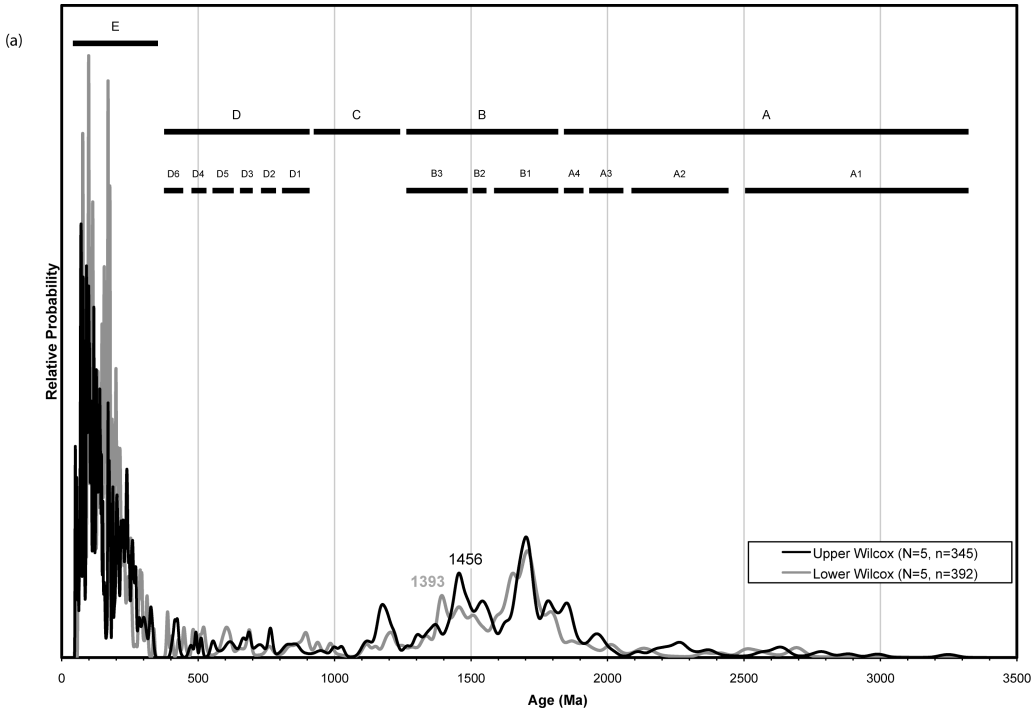
(a)
E
D
C
B
A
D6 D4 D5 D3 D2 D1
B3 B2 B1 A4 A3 A2 A1
Relative Probability
1456
1393
Upper Wilcox (N=5, n=345)
Lower Wilcox (N=5, n=392)
0 500 1000 1500 2000 2500 3000 3500
Age (Ma)

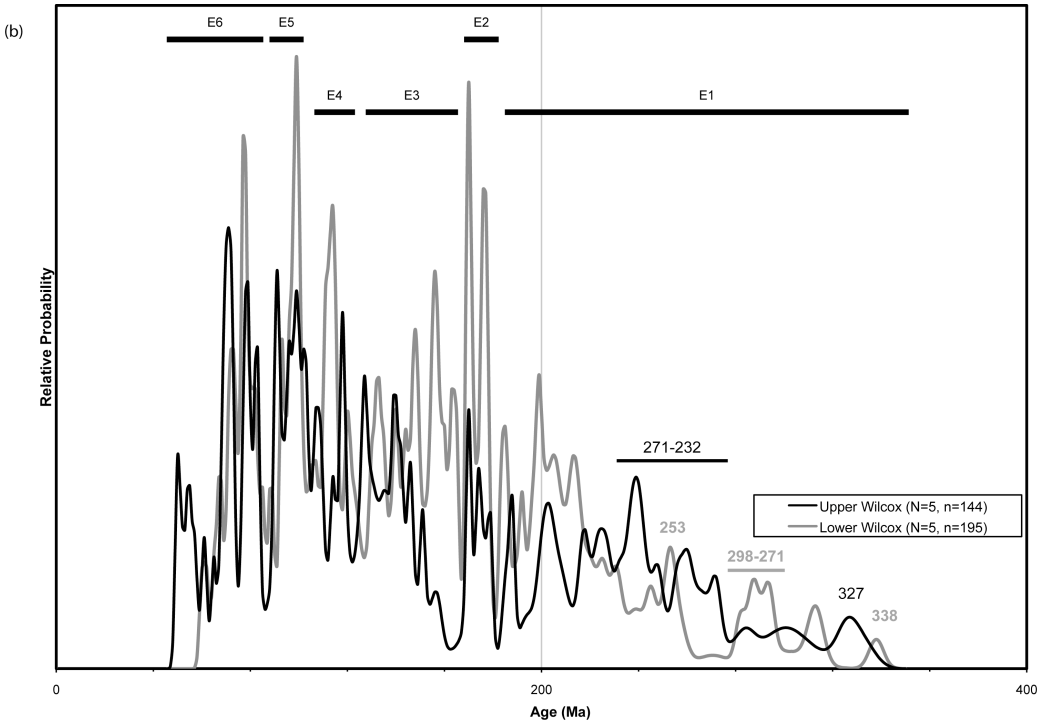
(b)
E6 E5 E2
E4 E3 E1
Relative Probability
271-232
253
298-271
327
338
Upper Wilcox (N=5, n=144)
Lower Wilcox (N=5, n=195)
0 200 400
Age (Ma)

Table 6. (a) K-S test results for all grains in the Wilcox Group, Upper Wilcox, Lower Wilcox and individual samples. [a] (b) K-S test results for grains younger than 350 Ma in the Wilcox Group, Upper Wilcox, Lower Wilcox and individual samples. (c) K-S test results for grains older than 350 Ma in the Wilcox Group, Upper Wilcox, Lower Wilcox and individual samples.

(a)	All Grains	LW	UW	Winch State 4[b]	GM-W-051608-4[b]	GM-W-051508-3[b]	GM-W-051408-1[b]	Burns 1[b]	GM-C-051608-5[c]	Bailey 1C[c]	GM-C-051508-1[c]	GM-C-051408-8[c]	Urban 1[c]
All Grains													
LW	**0.383**												
UW	**0.256**	0.008											
Winch St. 4[b]	0.027	0.005	**0.199**										
GM-W-051608-4[b]	**0.219**	**0.523**	0.038	0.004									
GM-W-051508-3[b]	0.000	0.002	0.000	0.000	**0.065**								
GM-W-051408-1[b]	0.000	0.000	0.000	**0.138**	0.000	0.000							
Burns 1[b]	0.000	0.006	0.000	0.000	0.013	0.030	0.000						
GM-C-051608-5[c]	0.010	0.001	**0.099**	**0.900**	0.001	0.000	0.008	0.000					
Bailey 1C[c]	0.017	0.001	**0.264**	**0.679**	0.015	0.000	0.001	0.000	**0.379**				
GM-C-051508-1[c]	0.000	0.001	0.000	0.000	**0.101**	**0.303**	0.000	**0.445**	0.000	0.000			
GM-C-051408-8[c]	**0.114**	0.016	**0.622**	**0.309**	0.010	0.000	0.014	0.000	**0.642**	**0.395**	0.000		
Urban 1[c]	0.005	0.001	0.025	**0.267**	0.001	0.000	**0.336**	0.000	**0.103**	0.046	0.000	0.045	

[a] The K-S test compares the age distribution of two detrital zircon samples and determines a probability (P) that the differences between the two samples are due to random chance. If P<0.05 then the two samples are considered to be different at the 95% confidence level. If P≥0.05 the two samples are considered to be statistically similar. Comparisons where P≥0.05 are marked by bold text.

[b] Lower Wilcox Samples

[c] Upper Wilcox Samples

(b)	All Grains	LW	UW	Winch State 4[b]	GM-W-051608-4[b]	GM-W-051508-3[b]	GM-W-051408-1[b]	Burns 1[b]	GM-C-051608-5[c]	Bailey 1C[c]	GM-C-051508-1[c]	GM-C-051408-8[c]	Urban 1[c]
All Grains													
LW	**0.985**												
UW	**0.914**	**0.421**											
Winch St. 4[b]	**0.362**	**0.524**	**0.215**										
GM-W-051608-4[b]	**0.082**	**0.245**	0.033	**0.937**									
GM-W-051508-3[b]	**0.310**	**0.732**	**0.122**	**0.891**	**0.719**								
GM-W-051408-1[b]	**0.464**	**0.638**	**0.301**	**0.999**	**0.944**	**0.929**							
Burns 1[b]	0.025	0.011	**0.085**	0.036	0.001	0.002	**0.081**						
GM-C-051608-5[c]	**0.994**	**0.974**	**0.906**	**0.563**	**0.713**	**0.798**	**0.471**	**0.604**					
Bailey 1C[c]	**0.102**	0.046	**0.349**	**0.543**	**0.408**	**0.152**	**0.912**	0.011	**0.189**				
GM-C-051508-1[c]	**0.123**	0.048	**0.600**	**0.181**	**0.068**	**0.094**	**0.229**	**0.354**	**0.691**	**0.196**			
GM-C-051408-8[c]	**0.074**	0.031	**0.312**	**0.023**	0.003	0.007	**0.056**	**0.221**	**0.526**	**0.043**	**0.185**		
Urban 1[c]	**0.059**	**0.079**	0.030	**0.311**	**0.160**	**0.123**	**0.532**	0.041	**0.187**	**0.452**	0.004	0.025	

(c)	All Grains	LW	UW	Winch State 4[b]	GM-W-051608-4[b]	GM-W-051508-3[b]	GM-W-051408-1[b]	Burns 1[b]	GM-C-051608-5[c]	Bailey 1C[c]	GM-C-051508-1[c]	GM-C-051408-8[c]	Urban 1[c]
All Grains													
LW	**0.996**												
UW	**0.997**	**0.706**											
Winch St. 4[b]	**0.939**	**0.748**	**0.949**										
GM-W-051608-4[b]	**0.206**	**0.380**	**0.144**	**0.197**									
GM-W-051508-3[b]	**0.105**	**0.126**	**0.124**	**0.364**	**0.540**								
GM-W-051408-1[b]	0.021	0.013	**0.052**	**0.561**	0.003	0.016							
Burns 1[b]	0.031	**0.096**	0.020	**0.066**	**0.888**	**0.180**	0.000						
GM-C-051608-5[c]	**0.927**	**0.982**	**0.832**	**0.786**	**0.890**	**0.163**	0.035	**0.534**					
Bailey 1C[c]	**0.615**	**0.684**	**0.640**	**0.813**	**0.606**	**0.892**	0.032	**0.350**	**0.599**				
GM-C-051508-1[c]	**0.463**	**0.530**	**0.311**	**0.235**	**1.000**	**0.990**	0.022	**0.781**	**0.754**	**0.677**			
GM-C-051408-8[c]	**0.472**	**0.307**	**0.813**	**0.984**	0.036	**0.091**	**0.581**	0.010	**0.294**	**0.383**	**0.248**		
Urban 1[c]	0.004	0.002	0.016	**0.100**	0.002	0.019	**0.074**	0.000	**0.023**	0.013	0.003	0.018	

up of a series of climbing peaks bounded by sharp lows, reaching its zenith at 99 Ma. Population E is present in all samples, and constitutes the second major peak of the Wilcox data set. Population E makes up 46% of the data set as a whole, but there is significant variability in its relative proportion within each sample (12%-70%).

Normalized age probability plots show that all of the samples are dominated by broad Mississippian to Eocene and Paleoproterozoic to Mesoproterozoic peaks (Figures 4, 5, 6 and 7), with all of the samples containing the same large scale populations though there are wide variations in the specific proportions of these populations between samples.

The Upper and Lower Wilcox have different U-Pb age distributions (Figure 7), as confirmed by the results of a Kolmogorov-Smirnov (K-S) statistical test to compare the two populations (Table 6a), conducted using Excel software provided by the University of Arizona Laserchron center (available online at www.geo.arizona.edu/alc). In particular the Upper Wilcox has more of populations B, specifically B1 and B3, and C, while the Lower Wilcox contains more of population E. If grains younger than 350 Ma are examined more closely (Figure 7b), differences in populations E1 and E3 are apparent. Population E1 is distinct because it appears that in this age band the source areas of the Upper and Lower Wilcox are mutually exclusive (i.e., peaks in the Upper Wilcox age probability plot correspond to valleys in the Lower Wilcox age probability plot).

Statistically, the Lower Wilcox shows little similarity between samples, with only two of the ten possible sample combinations passing the K-S test (Table 6a) with $P \geq 0.05$. Burns 1, GM-W-051508-3, and GM-W-051608-4 all contain higher proportions of population E, but less of populations A and B, though only GM-W-051508-3 and GM-W-051608-4 are statistically similar ($P=0.138$). Winch State 4 and GM-W-051408-1

contain higher proportions of populations A and B, but less of population E and are statistically similar (P = 0.065). This later case is worth noting because Winch State 4 and GM-W-051408-1 are approximately 170 km apart, with Winch State 4 being deposited off of the depositional axis and GM-W-051408-1 being near one of the southern most deltas of the Lower Wilcox (Figure 6a). It is also interesting that Burns 1, in much closer proximity to GM-W-051408-1 than GM-W-051608-4 and taken from within the same delta that GM-W-051408-1 is near to (Figure 6a), is distinctly different from GM-W-051408-1 (P<0.001).

In contrast, the Upper Wilcox samples are much more statistically similar, with four out of ten possible sample combinations yielding P values greater than 0.05 (Table 6a). Bailey 1C and GM-C-051608-5 are statistically similar (P=0.379), while GM-C-051408-8 and Urban 1 barely fail the K-S test (P=0.045). Each of the samples contains a higher proportion of populations A and B to population E than the Lower Wilcox samples, except GM-C-051508-1 which is similar in composition to the Lower Wilcox average values.

If a geographic trend is defined as two adjacent (either along strike or dip) samples that are statistically similar then several trends can be noted. The first is that Lower Wilcox samples in the southwestern portion of the study area are more similar to Upper Wilcox samples in the same area than is the case in the northeastern portion of the study area. Bailey 1C and Winch State 4, GM-W-051508-3 and GM-C-051508-1, GM-C-051608-5 and Winch State 4, and GM-C-051508-1 and GM-W-051608-4 are all Lower Wilcox-Upper Wilcox sample pairs from the southwestern portion of the study area that pass the K-S test, while only GM-W-051408-1 and Urban 1 and Burns 1 and GM-C-051508-1 are sample pairs from the northeastern portion of the study area that pass the test. Second, as previously noted, the Upper Wilcox is fairly uniform across its

geographic extent. Most Upper Wilcox samples, with the exception of GM-C-051508-1, have higher proportions of populations A and B to population E than is seen in the Lower Wilcox. Finally, in the Lower Wilcox, where GM-C-051508-1 and GM-C-051608-5 are the only adjacent samples that are statistically similar, there appears to be no coherent regional trend, with samples that differ greatly in age distribution being adjacent.

There are two important considerations when interpreting these results. The first is that interpretations of the relative proportions of different age populations may not be valid with the sample sizes used in this study (Andersen, 2005). With this in mind it is worth noting that all of the major age populations (i.e., B1, B3, C and E) are represented in each sample, though not each of the subcomponents of population E are present in every sample. This is typically the case in samples where population E makes up less than 30% of the sample population, except in the case of sample GM-C-051608-5. The second consideration is that the precise stratigraphic and temporal relationship between each of the samples is not known. Consequently it is difficult to determine if differences in the relative proportions of the age populations are the result of sampling deposits of multiple contemporaneous rivers systems draining different areas, or if there was a single river system and changes in relative proportions reflect changes in the drainage of that river system. It is unlikely that all of the samples are stratigraphically correlative, but this in itself does not preclude either of the options above. The depositional history of the Wilcox (Galloway, 2001) supports the presence of the multiple river systems, but this does not preclude an evolution of the drainage through time within in each subunit.

Two additional K-S tests were conducted to compare only the grains younger than 350 Ma or older than 350 Ma between the Upper and Lower Wilcox, as well as between the individual samples (Tables 6b and 6c). The results of these tests show that for the Upper and Lower Wilcox subunits and for most individual samples the populations of

grains younger than 350 Ma and older than 350 Ma are statistically similar. This suggests that the principal difference between the two subunits lies in the relative proportion of grains younger than 350 Ma and those older than 350 Ma. As will be shown later the grains younger than 350 Ma of population E likely come from related sources areas, but the same is not true for the grains older than 350 Ma grains of populations A, B, C and D. Regardless, there is a mild correlation (R^2=0.45) between the proportions of populations A and B, the two largest older than 350 Ma, if the data from the Urban-1 well is excluded on the basis of small sample size (there are only 45 acceptable grain ages for this sample).

The youngest grains in both the Upper and Lower Wilcox nearly approximate the age of deposition. The average age of the three youngest grains in the Lower Wilcox is 63 Ma while Lower Wilcox deposition ended at 57.5 Ma (Crabaugh, 2001). The time difference is even less in the case of the Upper Wilcox, where the average age of the three youngest grain is 51 Ma and deposition ceased at 49 Ma (Crabaugh, 2001).

DISCUSSION

Sandstone Petrography

The lithic fragments present in Wilcox sandstone samples suggest a variety of source rock types. Siltstone and sandstone lithic fragments, together with quartz grains with recycled overgrowths, indicate derivation from clastic sedimentary rocks, whereas chert grains could indicate either a carbonate or deepwater marine source (Mack, 1981). The presence of rip-up clasts similar in composition to the samples in the Upper Wilcox indicates some amount of local recycling of sediment. Volcanic lithic fragments are present in both the Lower Wilcox and Upper Wilcox subunits, indicating volcanogenic

input into both subunits. Metamorphic fragments, typically non-foliated and only containing small mica crystals, as well as polycrystalline quartz fragments that do not show signs of high-grade metamorphism (i.e., small crystals with undulose crystal boundaries and undulatory extinction) are indicators of low-grade metamorphic sources (Young, 1976; Garzanti and Vezzoli, 2003), whereas large mica crystals could be remnants of schistose metamorphic rock fragments that did not survive transport (Cameron and Blatt, 1971). The Gazzi-Dickinson point counting method does not count plutonic rock fragments due to their large crystal size (Ingersoll et al., 1984), but a tally was kept of framework grains that appear to be part of a plutonic rock fragment during point counting. The number of plutonic rock fragments is very low, typically only one or two per sample, but this is not unexpected given the grain size of the samples and the transport distances to potential plutonic sources.

As stated previously, χ^2 tests show that the Upper and Lower Wilcox are statistically different (Tables 3a and 3b). The Lower Wilcox contains more volcanic rock fragments, suggesting either enhanced input or greater proximity to volcanic provinces in northern Mexico and the Cordilleran magmatic arc. The chert to total quartz and chert to total lithics ratios are not statistically similar between the Upper and Lower Wilcox subunits (Table 3c). If the ratios were the same for both subunits this would suggest that most of the chert was derived during transport from local sources available to both units, such as Cretaceous limestone units covering much of central Texas (Galloway, 2008). That they are not implies that most of the chert was derived from external uplifts. This is supported by the lack of carbonate rock fragments in either subunit, which are unlikely to survive the long transport distances from external uplifts (Mack, 1984). The statistically significant greater proportion of chert in the Lower Wilcox implies that it drew more sediment from distant carbonate-rich sources (Mack, 1981), which could point to

derivation from sources in northern Mexico (McBride et al., 1974; McKee et al., 1990). This suggests that most of the chert was derived from external uplifts tapped only by the Lower Wilcox, instead of continuously exposed local sources, thus explaining why no carbonate rock fragments were recorded in either subunit. Metamorphic rock fragments are consistent with derivation from the southern Laramide province (McCarley, 1981). The percentage of metamorphic rock fragments is statistically consistent between the two units indicating relatively similar inputs, but as in the case of the other rock fragments, the raw counts vary greatly, suggesting that the source areas were not of uniform composition.

The compositional differences between the Upper and Lower Wilcox suggest contrasting source areas. The higher proportion of volcanic rock fragments and chert grains in the Lower Wilcox suggest derivation from volcanic and carbonate-rich sources, possibly in the Cordilleran arc or northern Mexico. The Upper Wilcox is more quartzose, and contains a higher proportion of sedimentary and metamorphic rock fragments suggesting derivation from basement and clastic sedimentary rich sources, pointing towards Laramide basement uplifts.

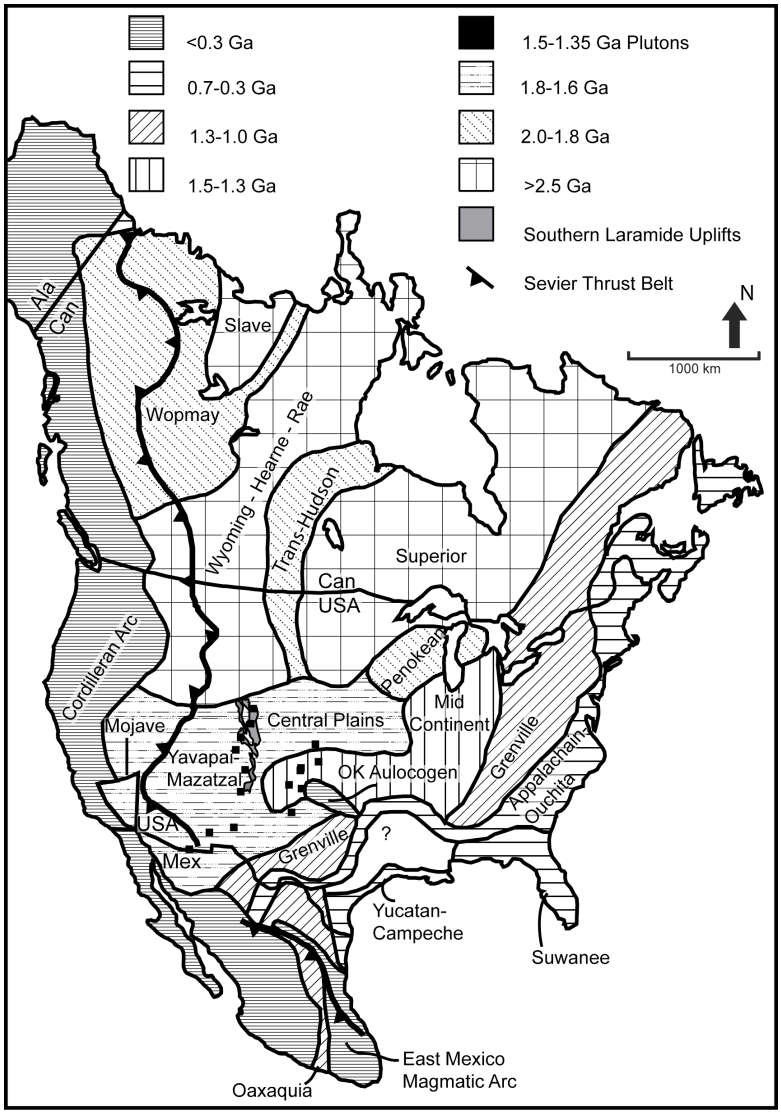

Figure 8. Map of basement rock ages of North America. Basement provinces and ages modified from Dickinson and Gehrels (2009), Sevier thrust belt modified from DeCelles (2004), central and southern Laramide uplifts modified from Dickinson and Gehrels (2008a), and 1.5-1.35 Ga plutons from Hoffman (1988).

Detrital Zircon Geochronology

Most of the U-Pb ages for detrital zircon grains can be attributed to basement sources in the central and southern Laramide uplifts and the Cordilleran magmatic arc of western North America, though some grains may have come from recycling of sedimentary rocks.

Major Sources

Population B (1819-1334 Ma) is most likely derived from the Laramide basement uplifts of the central and southern Rocky Mountains (Figure 8). Population B1 coincides in age with the 1800-1650 Ma basement rocks of the Yavapai and Mazatzal orogenies of New Mexico, Arizona and Colorado, which form the core of most of the Laramide uplifts (Condie, 1982; Grambling et al., 1988; Pedrick et al., 1998; Karlstrom et al., 2004). The distribution of grain ages (Figure 4) suggest that most grains were derived from the younger, more southerly Mazatzal orogenic belt (Karlstrom et al., 2004) instead of the older, northern Yavapai belt. Alternative sources for this age range include the Mojave basement (Barth et al., 2009) exposed by basement uplifts in southern California and western Arizona (Miller et al., 1992), though much of the sediment from these uplifts could have been trapped by the adjacent basins. Basement of this age is also exposed in Sonora, Mexico (Andersen and Silver, 1981), which would be difficult to distinguish from Yavapai-Mazatzal basement farther north. Population B3 is from the dominantly 1500-1350 Ma granitic intrusions in the southwestern U.S. (Anderson, 1983; Hoffman, 1988; Hoffman, 1989; Karlstrom et al., 1997; Karlstrom et al., 2004) and Sonora (Andersen and Silver, 1981). Work on the "zircon fertility" of various Precambrian plutons of North America suggest that the amount of sediment derived from ~1400 Ma plutons in the southwestern U.S. is most likely less than what is represented by their

proportion of the zircon age spectrum (Dickinson, 2008). One complicating factor is that grains of B1 and B3 age are found in Mesoproterozoic to Triassic strata of the western U.S. and northern Mexico (Gehrels and Dickinson, 1995; Gehrels et al., 1995; Gehrels and Stewart, 1998; Stewart et al., 2001), though these would most likely have been eroded off uplands that subsequently exposed basement. This does not change the provenance interpretation, though it does imply a different source rock type. Population B2 is more challenging to explain because the only documented basement rocks of this age are in the 1577-1576 Ma Laclede augen gneiss of the Priest River Complex in British Columbia (Doughty et al., 1998). Detrital zircons of this age, believed to have been ultimately derived from the Gawler craton of Australia, are found in strata ranging from Alaska's Alexander terrane to the Marathon basin of west Texas (Stewart et al., 2001; Gleason et al., 2007). In this case, population B2 represents recycling of sedimentary sources into the Wilcox Group.

Population E represents the Cordilleran magmatic arc and its predecessors. Continental magmatism in the Cordilleran arc began around 245 Ma in the Mojave Desert region (Barth and Wooden, 2006; Dickinson and Gehrels, 2009). Following its initiation in the early Triassic, arc magmatism was very continuous and widespread for most of its history (Stewart et al., 1986; Busby-Spera, 1988; McKee et al., 1990; Cowan and Bruhn, 1992; Miller et al., 1992; Saleeby and Busby-Spera, 1992; Gehrels and Stewart, 1998; Dickinson and Lawton, 2001; Kimbrough et al., 2001; Ortega-Rivera, 2003; Wetmore et al., 2003; Busby, 2004; Lawton et al., 2009). Because of this, it would be difficult to assign specific source areas for arc grains based on age alone, though it is interesting to note that the Wilcox age probability curve reaches its peak around 99 Ma (Figure 4b), a time at which the Peninsular Range Batholith and Sierra Nevada Batholith were peaking in magmatic output (Miller et al., 1992; Kimbrough et al., 2001; Ortega-

Rivera, 2003). Grains in population E1 older than 245 Ma could have come from several sources: 1) Mississippian ash-flow tuffs of the Tesnus Formation in the Marathon Basin (Imoto and McBride, 1990), 2) the 334 Ma El Aserradero Rhyolite of the Sierra Madre near Ciudad Victoria, Mexico (Stewart et al., 1999), 3) the 331 and 285 Ma plutons and 303 and 268 Ma volcanics of the Las Delicias Arc, Coahuila Terrane (Lopez, 1997; Stewart et al., 1999; Lopez et al., 2001), 4) the 284-232 Ma East Mexico Arc (Torres et al., 1999), or 5) the Lovelock and Luning assemblages of Nevada, where grains as old as 281 Ma have been reported (Manuszak et al., 2000). These suggest sources from northern and eastern Mexico as well as central Nevada, both of which are source regions corroborated by other age peaks. Near the end of the Cretaceous, arc magmatism for most of the western U.S. began to wane, while simultaneously migrating landward in northern Mexico and the western U.S. (Lipman, 1992). Grains younger than 80 Ma are most likely from igneous activity in northern Mexico (McDowell and Clabaugh, 1984; McDowell and Mauger, 1994), southern New Mexico (Chapin et al., 2004) and west Texas (Breyer et al., 2007; Befus et al., 2008), though activity in northern Mexico and southern New Mexico also overlaps temporally with activity farther west in the arc (McDowell et al., 2001; Chapin et al., 2004). Although there was voluminous magmatic activity in the Boulder, Pioneer and Idaho batholiths of Idaho and Montana after 100 Ma (Miller et al., 1992), the paucity of Archean age grains (Figure 4a) makes them unlikely sources because there is Archean basement in Sevier and Laramide uplifts in the same region (Ross et al., 1955; Armstrong and Hills, 1967; Doughty et al., 1998; Chamberlain et al., 2003).

Minor Sources

3250-2620 Ma grains could have come directly from the Archean Wyoming province (Chamberlain et al., 2003), but this is not supported by current theories (e.g. Dickinson et al., 1988; Lawton, 2008) of the internal drainage structure of the northern Laramide uplifts and ponded basins. Grains of the same wide range of ages as Population A are common in arc and coastal terranes of California and Oregon (i.e. the northern Sierra Terrane, Eastern Klamath Terrane, Yreka Terrane, Black Rock Terrane and Shoo Fly Complex) (Darby et al., 2000; Gehrels et al., 2000a; Gehrels and Miller, 2000; Harding et al., 2000; Spurlin et al., 2000; Wallin et al., 2000) which were accreted to the western Cordilleran margin by Late Jurassic time (Saleeby and Busby-Spera, 1992), as well as farther inland in the Roberts Mountain allochthon, Antler foreland basin, Golconda allochthon, and Triassic assemblages of western Nevada (Gehrels and Dickinson, 2000; Gehrels et al., 2000b; Manuszak et al., 2000; Riley et al., 2000). The paucity of 338-358 Ma grains in the Wilcox samples suggests against the Golconda allochthon being one of the sources. While this may seem overly complex, the data point toward two broad source areas: arc terranes of northern California/Oregon and allochthons and parautochthons of western Nevada. The Archean and Paleoproterozoic grains of these samples were probably derived from the same ultimate source, the Paleozoic Peace River Arch (Gehrels et al., 2000a), and have been recycled from older strata into younger ones in these arc terranes, allochthons and parautochthons. Some older basement maps (e.g., Hoffman, (1988)) indicate that the Mojave basement could have been the source of 2300-2100 Ma grains. More recent studies (Barth et al., 2000; Barth et al., 2001; Barth et al., 2009) indicate that the primary magmatic age of Mojave basement is 1800-1630 Ma, with 2300-2100 Ma ages existing only as cores. The negative

Figure 9. Comparison of normalized age probability plots of the Wilcox Group samples and Dickinson and Gehrels (2008a) samples. Wilcox Group is in black, Dickinson and Gehrels (2008a) is in grey. N=number of samples, n=number of grains. Numbers mark prominent age probability peaks referenced in the text. (a) All grains in Wilcox Group and Dickinson and Gehrels (2008a). Plot is normalized so that the area under both curves is the same. (b) Wilcox Group and Dickinson and Gehrels (2008a) grains younger than 350 Ma. Plot is a rescaled version of figure 9A. Plot is not normalized to the number of grains younger than 350 Ma, but represents the fact that grains younger than 350 Ma make up a larger proportion of the Wilcox Group than the sediments of the Cordilleran foreland basin.

(a)

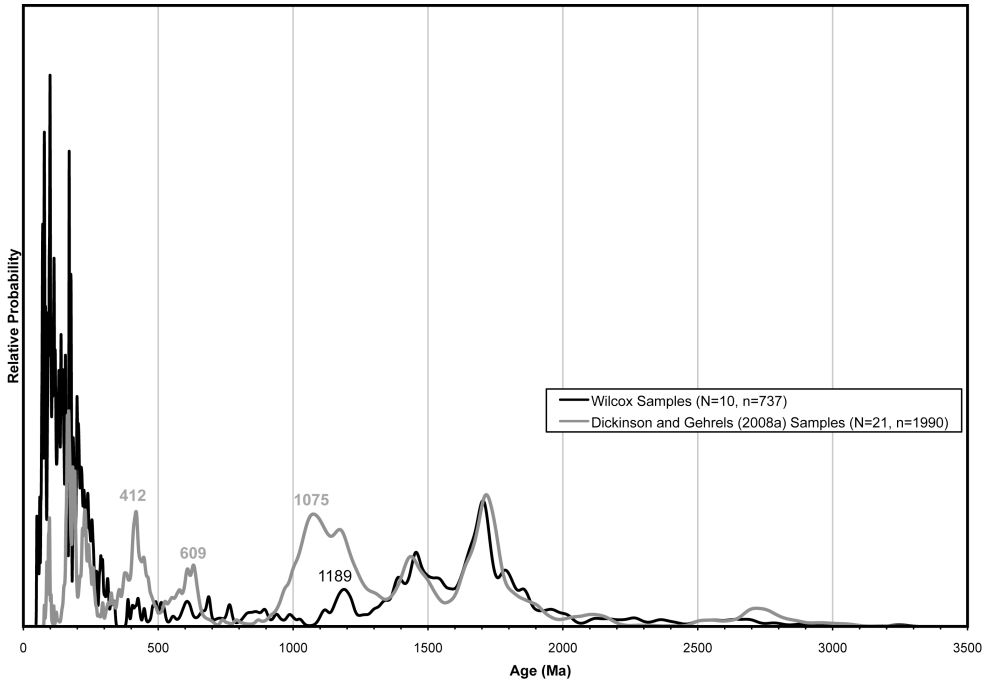
Relative Probability
Wilcox Samples (N=10, n=737)
Dickinson and Gehrels (2008a) Samples (N=21, n=1990)
412
609
1075
1189
0
500
1000
1500
2000
2500
3000
3500
Age (Ma)

(b)

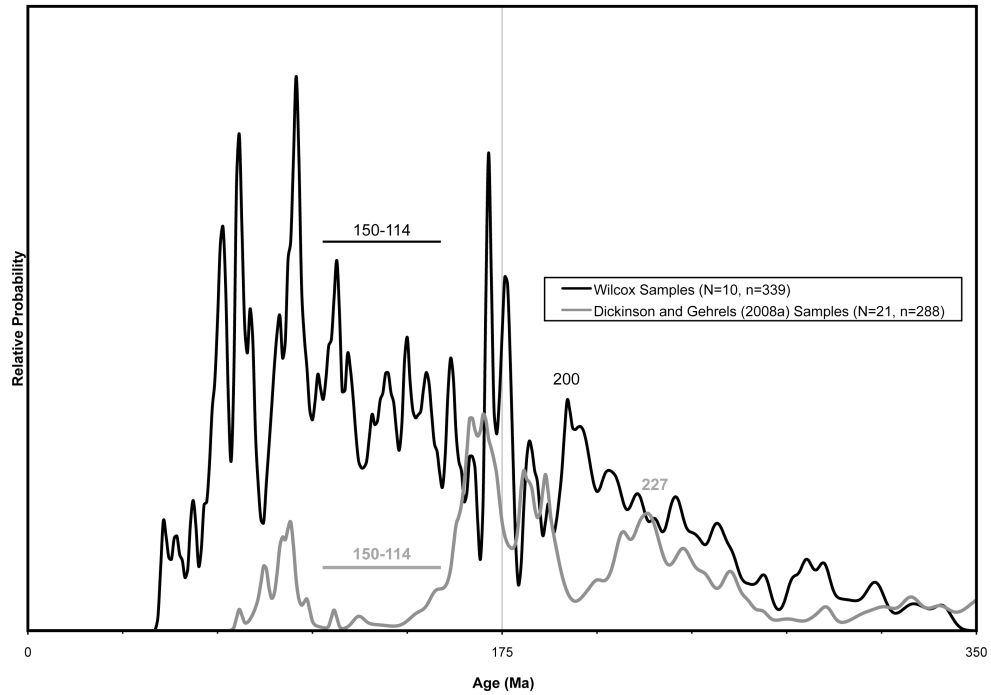
Relative Probability
Wilcox Samples (N=10, n=339)
Dickinson and Gehrels (2008a) Samples (N=21, n=288)
150-114
200
227
150-114
0
175
350
Age (Ma)

correlation between populations A and E (R^2=.64) suggest that the arc terranes of California and Oregon may not be as large of contributor. If the opposite were the case then a positive correlations would be expected due to proximity to the Cordilleran arc. This implies that much of population A may have originated from the allochthons of Nevada. Alternatively, the arc terranes in California and Oregon could have been sources if little arc material originated from that far north.

There are numerous possible sources for the Grenville-age grains of population C, though due to the high zircon content of Grenville plutons (Dickinson, 2008), the total sediment volume that these sources yield is almost certainly overestimated if based on zircon populations alone. Grenville-age grains are common in Cordilleran foreland basin sediments (Figure 9a) (Dickinson and Gehrels, 2008a) where they are believed to be derived from Jurassic and Permian eolianites (Dickinson and Gehrels, 2003, 2009) uplifted by the Sevier thrust belt. A statistical (K-S test, P<0.001) comparison of grains indicate that the Cordilleran foreland basin, and therefore the Sevier thrust belt, were not the likeliest sources of the Wilcox Group (Dickinson and Gehrels, 2008a). This is supported by differences in the character of the peaks at 412 Ma (D6) and 600 Ma (D4) between the Wilcox Group and Cordilleran foreland basin (Dickinson and Gehrels, 2008a) (Figure 9a), which Dickinson and Gehrels (2009) attribute to Taconic plutons in the case of the former and either Pan-African sources or pre-Iapetan rift plutons related to the break up of Rodinia in the case of the later. The Llano uplift of central Texas contains modern exposure of Grenville age basement in close proximity to the Texas Gulf Coast (Mosher, 1998). Though it is uncertain whether the Llano uplift was covered by Cretaceous carbonates during the Paleocene and Eocene (Ewing, 2005), it is not a likely source for the Wilcox Group because it differs significantly in its kyanite, staurolite, and green hornblende content (Todd and Folk, 1957). The southern and

central Appalachian Mountains are also an unlikely source because the major pulses of granitic intrusions are younger than the ages observed in the Wilcox samples (Aleinikoff et al., 2000; Eriksson et al., 2003). Other potential sources of Grenville-age grains include basement rocks of the Franklin Mountains in west Texas (Mosher, 1998), 1100 Ma intrusions in Sonora (Andersen and Silver, 1981), and the 1090 Ma Pikes Peak Batholith (Anderson, 1983; Smith et al., 1999), though none of these ages match precisely the age peaks in Population C. Therefore, the most likely source for population C is basement in Mexico (Dickinson and Lawton, 2001), particularly 1150-1230 Ma basement in the Oaxaquia microcontinent of eastern Mexico (Ortega-Gutierrez et al., 1995; Lawlor et al., 1999; Lopez et al., 2001; Cameron et al., 2004) and 1170-1220 Ma basement in the Coahuila terrane (Lopez, 1997) which seem to be good matches for the primary 1189 Ma and lesser 1118 Ma age peaks in the Wilcox samples (Figure 4).

Population D most likely represents a mix of sources from the arc terranes of California and Oregon with the sedimentary rocks of the western U.S. and northern Mexico. The ultimate source of D1 is enigmatic, though grains of this age are present in minor amounts in Jurassic eolianites of the southwestern U.S. (Dickinson and Gehrels, 2009) and the Haymond Formation of the Marathon Basin (Gleason et al., 2007). While this does not necessarily mean that sediments derived from the Marathon Basin or Jurassic eolianites were incorporated in the Wilcox, it does indicate that grains of that age were present in North America, even if the source is unknown. D2 grains are most likely from Pan-African terranes associated with the Appalachian orogen or from plutons related to the Neoproterozoic breakup of Rodinia, and are seen in Mesoproterozoic strata in Sonora and miogeoclinal strata of the western U.S., as well as being present as a minor population in the Marathon Basin (Stewart et al., 2001; Dickinson and Gehrels, 2003; Cather et al., 2006; Gleason et al., 2007). The Roberts Mountain Allochthon is the likely

proximal source for population D3, though the ultimate source is likely either Pan-African grains of the Appalachian orogen or an unknown source in the southwest U.S. (Gehrels et al., 2000a; Dickinson and Gehrels, 2003). There are several possible sources for population D4 which are difficult to differentiate: 1) Jurassic eolianites (Dickinson and Gehrels, 2003), 2) igneous rocks of the Trinity terrane (Gehrels et al., 2000a), 3) Cambrian-Ordovician intrusive rocks of the New Mexico aulacogen (McMillan and McLemore, 2004), or 4) gabbros of the Oklahoma aulacogen that have returned U-Pb zircon ages around 577 Ma (Keller and Baldridge, 1995; Hogan and Gilbert, 1998). The last option was probably not a significant source due to the lack of evidence of mafic material in the sandstone point counts. The most likely of these four sources, based primarily on which sources are deemed to be significant to the Wilcox, are the Trinity terrane and New Mexico aulacogen. The Oklahoma aulacogen is a much better age and source match for Population D5 (Keller and Baldridge, 1995; Hogan and Gilbert, 1997; Hogan and Gilbert, 1998). The Oklahoma aulacogen need not provide sediment directly to the Wilcox as it was uplifted as part of the Pennsylvanian-Permian Ancestral Rocky Mountains and zircons of this age are very prominent in Triassic strata from Texas to Utah (Dickinson and Gehrels, 2008b). Population D6 matches well, and is most likely derived from, igneous rocks of the northern California/Oregon arc terranes (Gehrels et al., 2000a), though detrital zircon grains (369-457 Ma) found in volcanic and metamorphic boulders in the Haymond Formation of the Marathon Basin (Denison et al., 1969) which Gleason et al. (2007) attribute to unknown sources in Mexico are also a good match. Taconic sources are unlikely as there are major differences in the Taconic ages peaks between the Wilcox and the most likely source of Taconic grains, the Sevier thrust belt (Dickinson and Gehrels, 2008b), is not a likely source for much of the sediment delivered to the Wilcox Group.

Summary

The detrital zircon age spectra suggest that the Wilcox Group had a large drainage area, with the primary sources being central and southern Laramide uplifts and the Cordilleran magmatic arc of western North America. The lack of a prominent Grenville age peak (Figure 9a) precludes the Cordilleran foreland basin or the Sevier thrust belt from being major contributors, and the distribution of ages for population C suggests that the Grenville grains were probably derived from basement in Mexico. Considering the regional tectonic history prior to and during Wilcox deposition, these source areas are reasonable because: 1) the Rocky Mountains were experiencing shortening-related uplift (Dickinson et al., 1988; Cather, 2004) but still had drainage outlets to the south (Lawton, 2008), 2) the Cordilleran arc was undergoing uplift as magma production began to wane (Miller et al., 1992; Ortega-Rivera, 2003), and 3) magmatism was migrating cratonward into Mexico and the southwestern U.S. (Lipman, 1992; McDowell et al., 2001; Chapin et al., 2004). Sediment from the Sevier thrust belt and northern Rocky Mountain province would have been trapped in the ponded and perimeter basins associated with the northern Laramide uplifts (Dickinson et al., 1988; Lawton, 2008), so its absence is not unexpected.

Arc sources in particular represent a wide geographic area, with likely sources as far north as the arc terranes and allochthons of California, Oregon and Nevada, and as far south as the East Mexico Arc of southern and central Mexico. Comparisons of the Wilcox data to the Cordilleran foreland basin data of Dickinson and Gehrels (2008a) and the Difunta Group data of Lawton et al. (2009) indicate that in the grain population younger than 350 Ma there are not any peaks present in the either of the other two data sets that are not also present in the Wilcox Group (Figures 9b and 10). In a rough sense, this correlation suggests that the Wilcox sediment was drawn from the same arc sources

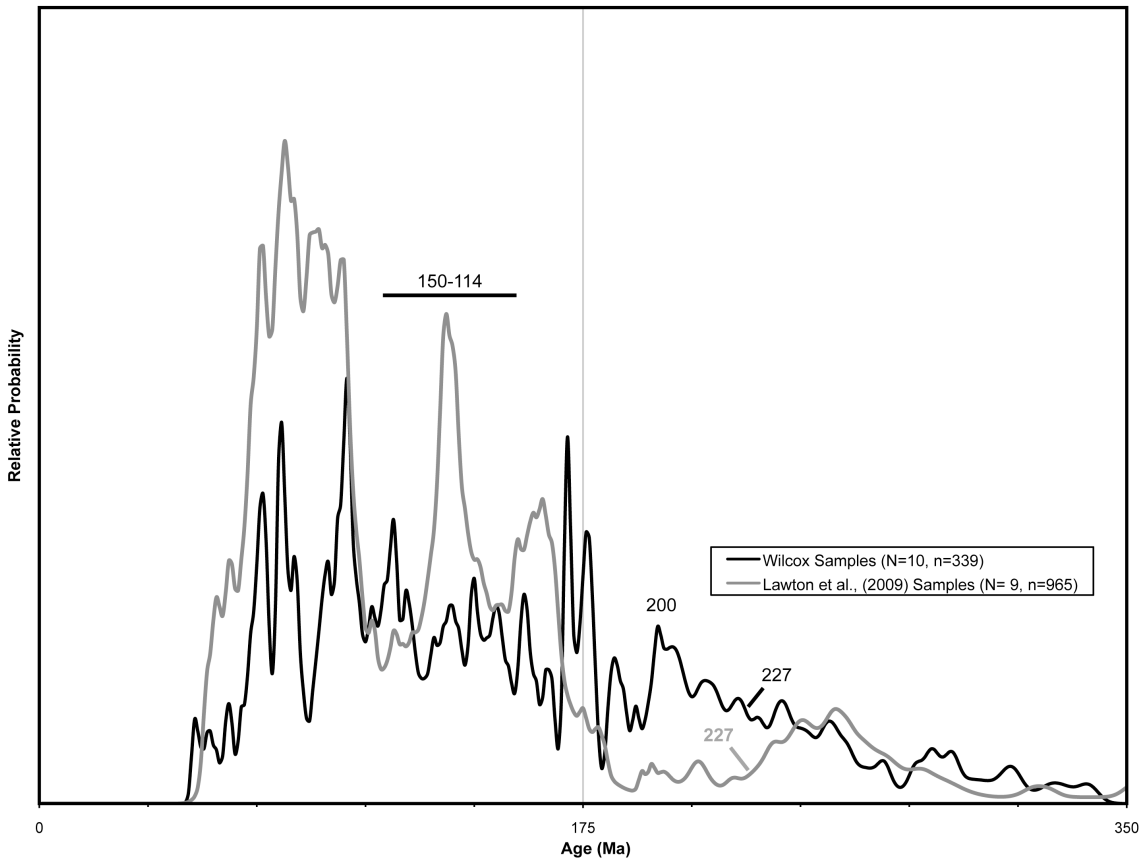

Figure 10. Comparison of normalized age probability plots of the Wilcox Group samples and Lawton et al. (2009) samples younger than 350 Ma. Wilcox Group is in black, Lawton et al. (2009) is in grey. N=number of samples, n=number of grains. Numbers mark prominent age probability peaks referenced in the text. Plot is a rescaled version of a normalized age probability plot of both samples. Plot is not normalized to the number of grains younger than 350 Ma, but represents the fact that grains younger than 350 Ma make up a smaller proportion of the Wilcox Group than the sediments of the Difunta Group.

that fed the other two, with the Cordilleran foreland basin data approximating the zircon signature of the northern arc sources and the Difunta group the zircon signature of the southern arc sources. This interpretation is substantiated by age peaks at 150-114 Ma, present in the Wilcox Group and Difunta Group only, and 227 Ma, present in the Wilcox Group and Cordilleran foreland basin only. While the provenance of the 227 Ma peak is hard to pin down because it is found in strata of the Luning, Lovelock and Pine Nut assemblages emplaced during the Sonoman Orogeny (Manuszak et al., 2000) as well as in granites and strata in Sonora (Gehrels and Stewart, 1998), the 150-114 Ma peak most likely corresponds to activity in the Peninsular Range Batholith and Alisitos Arc of southern California and the Baja Peninsula (Dickinson and Lawton, 2001; Kimbrough et al., 2001; Ortega-Rivera, 2003; Wetmore et al., 2003; Lawton et al., 2009) which would have been blocked from delivering sediment to the Cordilleran foreland basin by the Mogollon highlands (Cumella, 1983; Dickinson and Gehrels, 2008a). This, along with some striking similarities between the age probability curves of the Wilcox and the Cordilleran foreland basin, even though the latter did not provide sediment directly to the former, is a good indicator that the Wilcox depositional system incorporated sediment from both the northern and southern sections of the arc. A peak at 200 Ma in the Wilcox Group that is absent in both the Difunta Group and the Cordilleran foreland basin (Dickinson and Gehrels, 2008a; Lawton et al., 2009) (Figures 9b and 10) indicates that it also drew sediment from arc sources not available to the other two.

The cause of the distinct differences in the age signatures of population E1 in the Upper and Lower Wilcox from 340 Ma to 220 Ma is hard to explain (Figure 7b). The Upper Wilcox contains grains that correspond in age to the East Mexico Arc (284-232 Ma) (Torres et al., 1999), with a lesser peak at 327 Ma that could correspond to the Aserradero Rhyolite or the Las Delicias Arc (Lopez, 1997; Stewart et al., 1999; Lopez et

al., 2001). The Lower Wilcox contains age peaks at 298-272 Ma, 253 Ma, 313 Ma and 338 Ma. These ages overlap with know ages for the East Mexico Arc, as well as volcanic and plutonic activity seen further north in Mexico (Imoto and McBride, 1990; Lopez, 1997; Stewart et al., 1999; Torres et al., 1999; Lopez et al., 2001). That the possible source areas for the two subunits seem to geographically overlap yet yield age signatures that are distinctly different highlights the difficulty in precisely identifying source areas with detrital zircon data, and opens the possibility that an as yet unknown sources contributed sediment to the Wilcox Group. In this case all that can be said for sure is that two distinct sources areas preferentially contributed 340 Ma to 220 Ma sediment to the Upper and Lower Wilcox subunits, though it is difficult to resolve the details.

Figure 7b and table 5 show that the Upper and Lower Wilcox subunits received different enough proportions of sediment from the various source areas to be statistically distinct (Table 6). If the specific source areas mentioned above are applied to these differences, then the Lower Wilcox is enriched in sediment from the Cordilleran arc and northern Mexican volcanics, while the Upper Wilcox is enriched in sediment from Laramide basement uplifts of the central and southern Rockies and Mexico, volcanic arc terranes of western North America and the Roberts Mountain Allochthon. None of these source areas is absent from either the Upper or Lower Wilcox, so any changes in the source area were not large enough to exclude one of them. While the age spectra for populations A, B1, B2, C and D are visually similar between the two subunits, there are some differences in the age spectra for populations E and B3 (Figure 7b). As discussed in the previous paragraph, the Cordilleran arc and northern Mexican volcanics are the most likely sources for population E to both the Upper and Lower Wilcox, even though the temporal evolution of this source area is hard to resolve. Likewise, both the Lower Wilcox (1393 Ma) and Upper Wilcox (1456 Ma) B3 peaks (Figure 7a) correspond in age

to granitic intrusions in western North America (Andersen and Silver, 1981; Anderson, 1983; Hoffman, 1988; Hoffman, 1989; Karlstrom et al., 1997; Karlstrom et al., 2004), even though the difference in age peaks suggests derivation from different parts of this source. This indicates that even though there were some differences in how each sub unit received sediment corresponding to those age populations, the source regions they represent for each subunit are the same.

There is a contrast between the source areas suggested by the sandstone modal composition and the detrital zircons. While the Upper and Lower Wilcox plot primarily in the quartzose recycled and orogenic recycled fields on QmFLt and QtFL diagrams (Figure 3), the detrital zircon data suggest that there was a significant volcanic arc and basement input. The statistically significant increase in the plagioclase to total identifiable feldspar ratios between outcrop and core samples (student's t-test, $P<0.001$), implying albitization and destruction of potassium feldspar, suggest that some of the difference between the sources suggested by petrography and geochronology may be due to diagenetic effects. Still the core samples are still far more quartzose than the detrital zircon geochronology suggest. A significant body of literature (e.g., Potter, 1978; Suttner et al., 1981; Mack, 1984; Johnsson et al., 1988; Johnsson, 1990; Johnsson and Meade, 1990; Avigad et al., 2005) suggests this disparity could be the result of humid climate weathering during transport along the low relief coastal plane of the northern Gulf of Mexico, especially concerning the preferential loss of volcanic rock fragments (Smyth et al., 2008).

There has been some suggestion that sedimentation in the southwestern portion of the Lower Wilcox was the result of long-shore drift of sediment originating in the deltas to the northeast (Fisher and McGowen, 1967; Dickerson et al., 1995). The detrital zircon data shows however that Lower Wilcox sediment in the southwestern portion of the study

area is more related to the overlying Upper Wilcox sediment than it is to the Lower Wilcox sediment in the northeastern portion of the study area. This suggests that river systems of the Upper Wilcox in far south Texas were already active during deposition of the Lower Wilcox. The data from this study do not support the idea of significant long-shore drift derived strand plain sedimentation in the Lower Wilcox, though they do not definitively refute it either.

CONCLUSIONS

The broad, continent-scale derivation of the Wilcox Group is likely to be from three principal source areas: 1) central and southern Laramide uplifts south of the Archean-Proterozoic suture at the Wyoming Shear Zone (Condie, 1982), as represented in the consensus from previous studies, 2) the Cordilleran arc as Miller et al. (1992) suggested, and 3) the volcanics of northern Mexico. The Cordilleran foreland basin and the Sevier thrust belt were not major sources. Both the major grain populations and the detrital zircon data support a change in provenance from a source richer in volcanic rock fragments and young zircons in the Lower Wilcox, to a source richer in basement-derived zircons in the Upper Wilcox. Tentatively, humid climate weathering is implicated in the failure of major grain modal composition to more fully reveal the complex sources indicated by the zircons.

Appendix A : Sample Locations

Table A.1. Outcrop sample locations.

Sample Name	Easting[a, b]	Northing[a, b]	Latitude[c]	Longitude[c]	County	Road/River/Location
GM-C-51408-1[d, f]	572699	3233977	29.2341º N	98.2519º W	Wilson	Tx 181
GM-C-51408-2[d]	576379	3232455	29.2201º N	98.2142º W	Wilson	Abrego Lake Dr
GM-C-51408-3[d]	576379	3232455	29.2201º N	98.2142º W	WIlson	Abrego Lake Dr
GM-C-51408-5[d]	576379	3232455	29.2201º N	98.2142º W	Wilson	Abrego Lake Dr
GM-C-51408-7[d]	539817	3220767	29.1163º N	98.5908º W	Atascosa	TX 16
GM-C-51408-8[d]	540584	3225452	29.1586º N	98.5827º W	Atascosa	Martin Marietta Materials
GM-C-51408-9[d]	563638	3223805	29.1428º N	98.3458º W	Medina	TX 2200
GM-C-51408-10[d]	563638	3223805	29.1428º N	98.3458º W	Medina	TX 2201
GM-C-51408-11[d]	563638	3223805	29.1428º N	98.3458º W	Medina	TX 2202
GM-C-51408-12[d]	499783	3223275	29.1396º N	99.0022º W	Medina	TX 2200
GM-C-51408-13[d]	495843	3223350	29.1403º N	99.0427º W	Medina	Tx 2200
GM-C-51408-14[d]	492977	3222428	29.1319º N	99.0722º W	Medina	Tx 2200
GM-C-51508-1[d, f]	419317	3214290	29.0559º N	99.8288º W	Zavala	Bee Bluff, Nueces River
GM-C-51508-2[d]	419356	3213772	29.0513º N	99.8283º W	Zavala	Bee Bluff, Nueces River
GM-C-51508-3[d]	419356	3213772	29.0513º N	99.8283º W	Zavala	Bee Bluff, Nueces River
GM-C-51608-1[d]	444498	3218861	29.0985º N	99.5704º W	Uvalde	Tx 140
GM-C-51608-2[d]	444498	3218861	29.0985º N	99.5704º W	Uvalde	Tx 141
GM-C-51608-3[d]	432115	3213805	29.0523º N	99.6973º W	Zavala	Tx 117
GM-C-51608-4[d]	402085	3166681	28.6250º N	100.0016º W	Dimmit	Tx 277
GM-C-51608-5[d, f]	406281	3153583	28.5071º N	99.9577º W	Dimmit	Tx 2644
GM-W-51408-1[e, f]	538167	3233448	29.2308º N	98.6073º W	Bexar	TX 1604
GM-W-51508-2[e]	419170	3214409	29.0570º N	99.8303º W	Zavala	Bee Bluff, Nueces River
GM-W-51508-3[e, f]	419170	3214409	29.0570º N	99.8303º W	Zavala	Bee Bluff, Nueces River
GM-W-51508-4[e]	419170	3214409	29.0570º N	99.8303º W	Zavala	Bee Bluff, Nueces River
GM-W-51608-1[e]	434943	3220731	29.1150º N	99.6687º W	Uvalde	Tx 140
GM-W-51608-2[e]	430454	3216202	29.0738º N	99.7145º W	Zavala	TX 117
GM-W-51608-3[e]	428714	3217985	29.0898º N	99.7325º W	Uvalde	TX 117
GM-W-51608-4[e, f]	391918	3151762	28.4896º N	100.1042º W	Dimmit	Tx 2644

[a] UTM Zone 14R
[b] Datum is NAD27
[c] Measured in Decimal Degrees
[d] Upper Wilcox
[e] Lower Wilcox
[f] Zircon Sample

Table A.2. Core sample locations.

Sample Name	Operator	Well	API[a] Number	Latitude[b]	Longitude[b]	County	Depth[g]
Burns 1-9241[d]	Getty Oil	Burns #1	421233037500	29.1368º N	97.2747º W	Dewitt	9241
Burns 1-9297[d]	Getty Oil	Burns #1	421233037500	29.1368º N	97.2747º W	Dewitt	9297
Burns 1-9334[d]	Getty Oil	Burns #1	421233037500	29.1368º N	97.2747º W	Dewitt	9334
Burns 1-9525[d]	Getty Oil	Burns #1	421233037500	29.1368º N	97.2747º W	Dewitt	9525
Burns 1-9562[d]	Getty Oil	Burns #1	421233037500	29.1368º N	97.2747º W	Dewitt	9562
Burns 1-9614d	Getty Oil	Burns #1	421233037500	29.1368º N	97.2747º W	Dewitt	9614
Burns 1[d, e]	Getty Oil	Burns #1	421233037500	29.1368º N	97.2747º W	Dewitt	9266-9271
Paul 1-9152[d]	Hawkins & Co.	Paul #1	422853029300	29.4879º N	97.0297º W	Lavaca	9152
Urban 1-13896[c]	Sun	Urban #1	424690095100	28.7999º N	97.1012º W	Victoria	13896
Urban 1-14097[c]	Sun	Urban #1	424690095100	28.7999º N	97.1012º W	Victoria	14097
Urban 1[c, e]	Sun	Urban #1	424690095100	28.7999º N	97.1012º W	Victoria	13893-13902
Bailey 1C-10474[c]	Cities Service	Bailey #1 "C"	422973001900	28.1984º N	98.1345º W	Live Oak	10474
Bailey 1C-10491[c]	Cities Service	Bailey #1 "C"	422973001900	28.1984º N	98.1345º W	Live Oak	10491
Bailey 1C[c, e]	Cities Service	Bailey #1 "C"	422973001900	28.1984º N	98.1345º W	Live Oak	10470-10480
Winch St. 4-9310[d]	Forest Oil	Winch State No. 4	424793267000	27.7351º N	98.9826º W	Webb	9310
Winch St. 4-9948[d]	Forest Oil	Winch State No. 4	424793267000	27.7351º N	98.9826º W	Webb	9948
Winch St. 4[d, e]	Forest Oil	Winch State No. 4	424793267000	27.7351º N	98.9826º W	Webb	9309-9315

[a] American Petroleum Institute
[b] Measured in Decimal Degrees
[c] Upper Wilcox
[d] Lower Wilcox
[e] Zircon Sample
[f] Measured in Feet

Appendix B : Point Count Data Tables

Table B.1. Point count data table for GM-C-051408-1.

Sample Name:	GM-C-051408-1	Sub-unit:	Upper Wilcox
Sample Type:	Outcrop	Total Points Counted:	350

Category	Counts
Quartz	
Mono Crystalline:	158
Poly Crystalline:	23
Volcanic:	2
Sedimentary:	3
Total:	186
Feldspar	
Plagioclase:	3
Orthoclase:	2
Microcline:	5
Total	10
Sedimentary Rock Fragment (SRF)	
Argillaceous RF[a]:	1
Chert:	7
Siltstone RF:	
Sandstone RF:	
Argillaceous Chert:	4
Unknown SRF:	
Total:	12
Metamorphic Rock Fragment (MRF)	
Quartzofeldspathic:	6
Quartz-Rich	
foliated:	1
polygonal:	1
Mica-Rich	
foliated:	1
polygonal:	
Unknown MRF:	
Total:	9
Volcanic Rock Fragment (VRF)	
Microlitic:	
Lathwork:	1
Felsitic:	1
Altered VRF:	
Unknown VRF:	
Total:	2
Accessory Minerals	
Muscovite:	
Biotite:	
Tourmaline:	
Sphene:	
Zircon:	
Total:	0
Other	
Unknown RF:	
Total:	0
Matrix	
Clay Cutans:	56
Pore Filling:	
Total:	56

[a] Rock Fragment

Category	Counts
Porosity	
Intergranular:	64
Intragranular Plagioclase:	4
Intragranular Microcline:	1
Intragranular Potassium Feldspar:	
Intragranular Unknown Feldspar:	
Oversized:	4
Intragrannular VRF	
Intragrannular MRF	
Intragrannular SRF	
Intragranular Unknown RF:	2
Intragranular Unknown Grain:	
Total:	75
Cement/Overgrowth	
Quartz:	
Kaolinte:	
Fe-Oxide:	
Calcite	
intergranular:	
oversized:	
Total:	0
Grain Replacement	
Kaolinite	
Orthoclase:	
Microcline:	
Plagioclase:	
Unknown Feldspar:	
SRF:	
VRF:	
MRF:	
Mica:	
Unknown RF:	
Unknown Grain:	
Calcite	
Orthoclase:	
Microcline:	
Plagioclase:	
Unknown Feldspar:	
SRF:	
VRF:	
MRF:	
Mica:	
Unknown RF:	
Unknown Grain:	
Fe-O	
Orthoclase:	
Microcline:	
Plagioclase:	
Unknown Feldspar:	
SRF:	
VRF:	
MRF:	
Mica:	
Unknown RF:	
Unknown Grain:	
Total:	0

Table B.2. Point count data table for GM-C-051408-2.

Sample Name:	GM-C-051408-2	Sub-unit:	Upper Wilcox
Sample Type:	Outcrop	Total Points Counted:	350

Category	Counts
Quartz	
Mono Crystalline:	138
Poly Crystalline:	16
Volcanic:	5
Sedimentary:	3
Total:	162
Feldspar	
Plagioclase:	1
Orthoclase:	5
Microcline:	4
Total	10
Sedimentary Rock Fragment (SRF)	
Argillaceous RF[a]:	
Chert:	5
Siltstone RF:	
Sandstone RF:	
Argillaceous Chert:	3
Unknown SRF:	
Total:	8
Metamorphic Rock Fragment (MRF)	
Quartzofeldspathic:	2
Quartz-Rich	
foliated:	
polygonal:	
Mica-Rich	
foliated:	
polygonal:	
Unknown MRF:	
Total:	2
Volcanic Rock Fragment (VRF)	
Microlitic:	
Lathwork:	
Felsitic:	
Altered VRF:	1
Unknown VRF:	
Total:	1
Accessory Minerals	
Muscovite:	
Biotite:	
Tourmaline:	
Sphene:	
Zircon:	
Total:	0
Other	
Unknown RF:	
Total:	0
Matrix	
Clay Cutans:	40
Pore Filling:	
Total:	40

[a] Rock Fragment

Category	Counts
Porosity	
Intergranular:	93
Intragranular Plagioclase:	
Intragranular Microcline:	
Intragranular Potassium Feldspar:	1
Intragranular Unknown Feldspar:	1
Oversized:	30
Intragrannular VRF	
Altered VRF:	1
Intragrannular MRF	
Intragrannular SRF	
Intragranular Unknown RF:	
Intragranular Unknown Grain:	
Total:	126
Cement/Overgrowth	
Quartz:	
Kaolinte:	
Fe-Oxide:	
Calcite	
intergranular:	
oversized:	
Total:	0
Grain Replacement	
Kaolinite	
Orthoclase:	
Microcline:	
Plagioclase:	
Unknown Feldspar:	
SRF:	
VRF:	
MRF:	
Mica:	1
Unknown RF:	
Unknown Grain:	
Calcite	
Orthoclase:	
Microcline:	
Plagioclase:	
Unknown Feldspar:	
SRF:	
VRF:	
MRF:	
Mica:	
Unknown RF:	
Unknown Grain:	
Fe-O	
Orthoclase:	
Microcline:	
Plagioclase:	
Unknown Feldspar:	
SRF:	
VRF:	
MRF:	
Mica:	
Unknown RF:	
Unknown Grain:	
Total:	1

Table B.3. Point count data table for GM-C-051408-3.

Sample Name:	GM-C-051408-3	Sub-unit:	Upper Wilcox
Sample Type:	Outcrop	Total Points Counted:	349

Category	Counts
Quartz	
Mono Crystalline:	150
Poly Crystalline:	14
Volcanic:	
Sedimentary:	1
Total:	165
Feldspar	
Plagioclase:	1
Orthoclase:	3
Microcline:	
Total	4
Sedimentary Rock Fragment (SRF)	
Argillaceous RF[a]:	1
Chert:	8
Siltstone RF:	1
Sandstone RF:	
Argillaceous Chert:	4
Unknown SRF:	1
Total:	15
Metamorphic Rock Fragment (MRF)	
Quartzofeldspathic:	
Quartz-Rich	
foliated:	
polygonal:	
Mica-Rich	
foliated:	
polygonal:	
Unknown MRF:	
Total:	0
Volcanic Rock Fragment (VRF)	
Microlitic:	
Lathwork:	
Felsitic:	
Altered VRF:	
Unknown VRF:	
Total:	0
Accessory Minerals	
Muscovite:	
Biotite:	
Tourmaline:	1
Sphene:	
Zircon:	1
Total:	2
Other	
Unknown RF:	
Total:	0
Matrix	
Clay Cutans:	27
Pore Filling:	15
Total:	42

[a] Rock Fragment

Category	Counts
Porosity	
Intergranular:	90
Intragranular Plagioclase:	
Intragranular Microcline:	
Intragranular Potassium Feldspar:	2
Intragranular Unknown Feldspar:	1
Oversized:	26
Intragrannular VRF	
Intragrannular MRF	
Intragrannular SRF	
Chert:	1
Intragranular Unknown RF:	
Intragranular Unknown Grain:	1
Total:	121
Cement/Overgrowth	
Quartz:	
Kaolinte:	
Fe-Oxide:	
Calcite	
intergranular:	
oversized:	
Total:	0
Grain Replacement	
Kaolinite	
Orthoclase:	
Microcline:	
Plagioclase:	
Unknown Feldspar:	
SRF:	
VRF:	
MRF:	
Mica:	
Unknown RF:	
Unknown Grain:	
Calcite	
Orthoclase:	
Microcline:	
Plagioclase:	
Unknown Feldspar:	
SRF:	
VRF:	
MRF:	
Mica:	
Unknown RF:	
Unknown Grain:	
Fe-O	
Orthoclase:	
Microcline:	
Plagioclase:	
Unknown Feldspar:	
SRF:	
VRF:	
MRF:	
Mica:	
Unknown RF:	
Unknown Grain:	
Total:	0

Table B.4. Point count data table for GM-C-051408-5.

Sample Name:	GM-C-051408-5	Sub-unit:	Upper Wilcox
Sample Type:	Outcrop	Total Points Counted:	352

Category	Counts
Quartz	
Mono Crystalline:	171
Poly Crystalline:	20
Volcanic:	
Sedimentary:	
Total:	191
Feldspar	
Plagioclase:	
Orthoclase:	7
Microcline:	1
Unknown Feldspar:	1
Total	9
Sedimentary Rock Fragment (SRF)	
Argillaceous RF[a]:	2
Chert:	3
Siltstone RF:	
Sandstone RF:	
Argillaceous Chert:	4
Unknown SRF:	
Total:	9
Metamorphic Rock Fragment (MRF)	
Quartzofeldspathic:	
Quartz-Rich	
foliated:	
polygonal:	
Mica-Rich	
foliated:	
polygonal:	
Unknown MRF:	
Total:	0
Volcanic Rock Fragment (VRF)	
Microlitic:	
Lathwork:	1
Felsitic:	3
Altered VRF:	1
Unknown VRF:	
Total:	5
Accessory Minerals	
Muscovite:	
Biotite:	
Tourmaline:	
Sphene:	
Zircon:	
Total:	0
Other	
Unknown RF:	
Unknown Highly Dissolved Grain:	3
Total:	3
Matrix	
Clay Cutans:	28
Pore Filling:	
Total:	28

[a] Rock Fragment

Category	Counts
Porosity	
Intergranular:	84
Intragranular Plagioclase:	
Intragranular Microcline:	
Intragranular Potassium Feldspar:	
Intragranular Unknown Feldspar:	1
Oversized:	21
Intragrannular VRF	
Altered VRF:	1
Intragrannular MRF	
Intragrannular SRF	
Intragranular Unknown RF:	
Intragranular Unknown Grain:	
Total:	107
Cement/Overgrowth	
Quartz:	
Kaolinte:	
Fe-Oxide:	
Calcite	
intergranular:	
oversized:	
Total:	0
Grain Replacement	
Kaolinite	
Orthoclase:	
Microcline:	
Plagioclase:	
Unknown Feldspar:	
SRF:	
VRF:	
MRF:	
Mica:	
Unknown RF:	
Unknown Grain:	
Calcite	
Orthoclase:	
Microcline:	
Plagioclase:	
Unknown Feldspar:	
SRF:	
VRF:	
MRF:	
Mica:	
Unknown RF:	
Unknown Grain:	
Fe-O	
Orthoclase:	
Microcline:	
Plagioclase:	
Unknown Feldspar:	
SRF:	
VRF:	
MRF:	
Mica:	
Unknown RF:	
Unknown Grain:	
Total:	0

Table B.5. Point count data table for GM-C-051408-7.

Sample Name:	GM-C-051408-7	Sub-unit:	Upper Wilcox
Sample Type:	Outcrop	Total Points Counted:	350

Category	Counts
Quartz	
Mono Crystalline:	142
Poly Crystalline:	22
Volcanic:	12
Sedimentary:	1
Total:	177
Feldspar	
Plagioclase:	1
Orthoclase:	3
Microcline:	
Total	4
Sedimentary Rock Fragment (SRF)	
Argillaceous RF[a]:	
Chert:	2
Siltstone RF:	1
Sandstone RF:	
Argillaceous Chert:	4
Unknown SRF:	
Total:	7
Metamorphic Rock Fragment (MRF)	
Quartzofeldspathic:	
Quartz-Rich	
foliated:	
polygonal:	
Mica-Rich	
foliated:	
polygonal:	
Unknown MRF:	
Total:	0
Volcanic Rock Fragment (VRF)	
Microlitic:	
Lathwork:	
Felsitic:	1
Altered VRF:	1
Unknown VRF:	
Total:	2
Accessory Minerals	
Muscovite:	
Biotite:	
Tourmaline:	
Sphene:	
Zircon:	
Total:	0
Other	
Unknown RF:	
Total:	0
Matrix	
Clay Cutans:	67
Pore Filling:	16
Total:	83

[a] Rock Fragment

Category	Counts
Porosity	
Intergranular:	59
Intragranular Plagioclase:	
Intragranular Microcline:	
Intragranular Potassium Feldspar:	1
Intragranular Unknown Feldspar:	1
Oversized:	12
Intragrannular VRF	
Unknown VRF:	3
Intragrannular MRF	
Intragrannular SRF	
Siltstone RF:	1
Intragranular Unknown RF:	
Intragranular Unknown Grain:	
Total:	77
Cement/Overgrowth	
Quartz:	
Kaolinte:	
Fe-Oxide:	
Calcite	
intergranular:	
oversized:	
Total:	0
Grain Replacement	
Kaolinite	
Orthoclase:	
Microcline:	
Plagioclase:	
Unknown Feldspar:	
SRF:	
VRF:	
MRF:	
Mica:	
Unknown RF:	
Unknown Grain:	
Calcite	
Orthoclase:	
Microcline:	
Plagioclase:	
Unknown Feldspar:	
SRF:	
VRF:	
MRF:	
Mica:	
Unknown RF:	
Unknown Grain:	
Fe-O	
Orthoclase:	
Microcline:	
Plagioclase:	
Unknown Feldspar:	
SRF:	
VRF:	
MRF:	
Mica:	
Unknown RF:	
Unknown Grain:	
Total:	0

Table B.6. Point count data table for GM-C-051408-8.

Sample Name:	GM-C-051408-8	Sub-unit:	Upper Wilcox
Sample Type:	Outcrop	Total Points Counted:	348

Category	Counts
Quartz	
Mono Crystalline:	160
Poly Crystalline:	14
Volcanic:	1
Sedimentary:	
Total:	175
Feldspar	
Plagioclase:	
Orthoclase:	1
Microcline:	
Total	1
Sedimentary Rock Fragment (SRF)	
Argillaceous RF[a]:	
Chert:	7
Siltstone RF:	
Sandstone RF:	
Argillaceous Chert:	
Unknown SRF:	
Local Siltstone RF:	9
Local Argillaceous RF:	2
Total:	18
Metamorphic Rock Fragment (MRF)	
Quartzofeldspathic:	
Quartz-Rich	
foliated:	
polygonal:	
Mica-Rich	
foliated:	
polygonal:	
Unknown MRF:	
Total:	0
Volcanic Rock Fragment (VRF)	
Microlitic:	
Lathwork:	
Felsitic:	
Altered VRF:	
Unknown VRF:	
Total:	0
Accessory Minerals	
Muscovite:	
Biotite:	
Tourmaline:	
Sphene:	
Zircon:	
Total:	0
Other	
Unknown RF:	
Total:	0
Matrix	
Clay Cutans:	31
Pore Filling:	79
Total:	110

[a] Rock Fragment

Category	Counts
Porosity	
Intergranular:	36
Intragranular Plagioclase:	
Intragranular Microcline:	
Intragranular Potassium Feldspar:	
Intragranular Unknown Feldspar:	
Oversized:	8
Intragrannular VRF	
Intragrannular MRF	
Intragrannular SRF	
Intragranular Unknown RF:	
Intragranular Unknown Grain:	
Total:	44
Cement/Overgrowth	
Quartz:	
Kaolinte:	
Fe-Oxide:	
Calcite	
intergranular:	
oversized:	
Total:	0
Grain Replacement	
Kaolinite	
Orthoclase:	
Microcline:	
Plagioclase:	
Unknown Feldspar:	
SRF:	
VRF:	
MRF:	
Mica:	
Unknown RF:	
Unknown Grain:	
Calcite	
Orthoclase:	
Microcline:	
Plagioclase:	
Unknown Feldspar:	
SRF:	
VRF:	
MRF:	
Mica:	
Unknown RF:	
Unknown Grain:	
Fe-O	
Orthoclase:	
Microcline:	
Plagioclase:	
Unknown Feldspar:	
SRF:	
VRF:	
MRF:	
Mica:	
Unknown RF:	
Unknown Grain:	
Total:	0

Table B.7. Point count data table for GM-C-051408-9.

Sample Name:	GM-C-051408-9	Sub-unit:	Upper Wilcox
Sample Type:	Outcrop	Total Points Counted:	360

Category	Counts
Quartz	
Mono Crystalline:	163
Poly Crystalline:	16
Volcanic:	16
Sedimentary:	3
Total:	198
Feldspar	
Plagioclase:	1
Orthoclase:	8
Microcline:	4
Total	13
Sedimentary Rock Fragment (SRF)	
Argillaceous RF[a]:	2
Chert:	7
Siltstone RF:	1
Sandstone RF:	
Argillaceous Chert:	
Unknown SRF:	
Total:	10
Metamorphic Rock Fragment (MRF)	
Quartzofeldspathic:	
Quartz-Rich	
foliated:	1
polygonal:	
Mica-Rich	
foliated:	
polygonal:	
Unknown MRF:	
Total:	1
Volcanic Rock Fragment (VRF)	
Microlitic:	
Lathwork:	
Felsitic:	1
Altered VRF:	
Unknown VRF:	
Total:	1
Accessory Minerals	
Muscovite:	1
Biotite:	
Tourmaline:	
Sphene:	
Zircon:	
Total:	1
Other	
Unknown RF:	
Total:	0
Matrix	
Clay Cutans:	
Pore Filling:	
Total:	0

[a] Rock Fragment

Category	Counts
Porosity	
Intergranular:	9
Intragranular Plagioclase:	1
Intragranular Microcline:	1
Intragranular Potassium Feldspar:	
Intragranular Unknown Feldspar:	
Oversized:	
Intragrannular VRF	
Intragrannular MRF	
Intragrannular SRF	
Intragranular Unknown RF:	
Intragranular Unknown Grain:	
Total:	11
Cement/Overgrowth	
Quartz:	
Kaolinte:	2
Fe-Oxide:	
Calcite	
intergranular:	123
oversized:	
Total:	125
Grain Replacement	
Kaolinite	
Orthoclase:	
Microcline:	
Plagioclase:	
Unknown Feldspar:	
SRF:	
VRF:	
MRF:	
Mica:	
Unknown RF:	
Unknown Grain:	
Calcite	
Orthoclase:	
Microcline:	
Plagioclase:	
Unknown Feldspar:	
SRF:	
VRF:	
MRF:	
Mica:	
Unknown RF:	
Unknown Grain:	
Fe-O	
Orthoclase:	
Microcline:	
Plagioclase:	
Unknown Feldspar:	
SRF:	
VRF:	
MRF:	
Mica:	
Unknown RF:	
Unknown Grain:	
Total:	0

Table B.8. Point count data table for GM-C-051408-10.

Sample Name:	GM-C-051408-10	Sub-unit:	Upper Wilcox
Sample Type:	Outcrop	Total Points Counted:	350

Category	Counts
Quartz	
Mono Crystalline:	94
Poly Crystalline:	13
Volcanic:	11
Sedimentary:	2
Total:	120
Feldspar	
Plagioclase:	
Orthoclase:	19
Microcline:	4
Total	23
Sedimentary Rock Fragment (SRF)	
Argillaceous RF[a]:	
Chert:	8
Siltstone RF:	1
Sandstone RF:	
Argillaceous Chert:	5
Unknown SRF:	
Total:	14
Metamorphic Rock Fragment (MRF)	
Quartzofeldspathic:	
Quartz-Rich	
foliated:	1
polygonal:	
Mica-Rich	
foliated:	
polygonal:	
Unknown MRF:	
Total:	1
Volcanic Rock Fragment (VRF)	
Microlitic:	
Lathwork:	
Felsitic:	5
Altered VRF:	
Unknown VRF:	
Total:	5
Accessory Minerals	
Muscovite:	
Biotite:	
Tourmaline:	
Sphene:	
Zircon:	
Total:	0
Other	
Unknown RF:	3
Unknown Highly Dissolved Grain:	4
Total:	7
Matrix	
Clay Cutans:	
Pore Filling:	
Total:	0

[a] Rock Fragment

Category	Counts
Porosity	
Intergranular:	38
Intragranular Plagioclase:	
Intragranular Microcline:	1
Intragranular Potassium Feldspar:	
Intragranular Unknown Feldspar:	
Oversized:	2
Intragrannular VRF	
Unknown VRF:	1
Intragrannular MRF	
Quartz-Rich, Foliated:	2
Intragrannular SRF	
Chert:	4
Intragranular Unknown RF:	
Intragranular Unknown Grain:	
Total:	48
Cement/Overgrowth	
Quartz:	
Kaolinte:	3
Fe-Oxide:	
Calcite	
intergranular:	122
oversized:	3
Total:	128
Grain Replacement	
Kaolinite	
Orthoclase:	
Microcline:	
Plagioclase:	
Unknown Feldspar:	
SRF:	
VRF:	
MRF:	
Mica:	
Unknown RF:	
Unknown Grain:	
Calcite	
Orthoclase:	4
Microcline:	
Plagioclase:	
Unknown Feldspar:	
SRF:	
VRF:	
MRF:	
Mica:	
Unknown RF:	
Unknown Grain:	
Fe-O	
Orthoclase:	
Microcline:	
Plagioclase:	
Unknown Feldspar:	
SRF:	
VRF:	
MRF:	
Mica:	
Unknown RF:	
Unknown Grain:	
Total:	4

Table B.9. Point count data table for GM-C-051408-11.

Sample Name:	GM-C-051408-11	Sub-unit:	Upper Wilcox
Sample Type:	Outcrop	Total Points Counted:	351

Category	Counts
Quartz	
Mono Crystalline:	154
Poly Crystalline:	23
Volcanic:	8
Sedimentary:	2
Total:	187
Feldspar	
Plagioclase:	2
Orthoclase:	7
Microcline:	1
Total	10
Sedimentary Rock Fragment (SRF)	
Argillaceous RF[a]:	3
Chert:	3
Siltstone RF:	10
Sandstone RF:	
Argillaceous Chert:	3
Unknown SRF:	
Total:	19
Metamorphic Rock Fragment (MRF)	
Quartzofeldspathic:	
Quartz-Rich	
foliated:	1
polygonal:	1
Mica-Rich	
foliated:	
polygonal:	
Unknown MRF:	
Total:	2
Volcanic Rock Fragment (VRF)	
Microlitic:	
Lathwork:	
Felsitic:	
Altered VRF:	
Unknown VRF:	2
Total:	2
Accessory Minerals	
Muscovite:	
Biotite:	
Tourmaline:	
Sphene:	
Zircon:	
Total:	0
Other	
Unknown RF:	
Total:	0
Matrix	
Clay Cutans:	
Pore Filling:	
Total:	0

[a] Rock Fragment

Category	Counts
Porosity	
Intergranular:	2
Intragranular Plagioclase:	
Intragranular Microcline:	
Intragranular Potassium Feldspar:	
Intragranular Unknown Feldspar:	
Oversized:	7
Intragrannular VRF	
Intragrannular MRF	
Intragrannular SRF	
Siltstone RF:	4
Sandstone RF:	1
Argillaceous RF:	1
Intragranular Unknown RF:	1
Intragranular Unknown Grain:	
Total:	16
Cement/Overgrowth	
Quartz:	
Kaolinte:	
Fe-Oxide:	
Calcite	
intergranular:	104
oversized:	8
Total:	112
Grain Replacement	
Kaolinite	
Orthoclase:	
Microcline:	
Plagioclase:	
Unknown Feldspar:	
SRF:	
VRF:	
MRF:	
Mica:	
Unknown RF:	
Unknown Grain:	
Calcite	
Orthoclase:	2
Microcline:	1
Plagioclase:	
Unknown Feldspar:	
SRF:	
VRF:	
MRF:	
Mica:	
Unknown RF:	
Unknown Grain:	
Fe-O	
Orthoclase:	
Microcline:	
Plagioclase:	
Unknown Feldspar:	
SRF:	
VRF:	
MRF:	
Mica:	
Unknown RF:	
Unknown Grain:	
Total:	3

Table B.10. Point count data table for GM-C-051408-12.

Sample Name:	GM-C-051408-12	Sub-unit:	Upper Wilcox
Sample Type:	Outcrop	Total Points Counted:	350

Category	Counts
Quartz	
Mono Crystalline:	134
Poly Crystalline:	17
Volcanic:	5
Sedimentary:	5
Total:	161
Feldspar	
Plagioclase:	
Orthoclase:	11
Microcline:	
Total	11
Sedimentary Rock Fragment (SRF)	
Argillaceous RF[a]:	1
Chert:	11
Siltstone RF:	
Sandstone RF:	
Argillaceous Chert:	7
Unknown SRF:	
Total:	19
Metamorphic Rock Fragment (MRF)	
Quartzofeldspathic:	
Quartz-Rich	
foliated:	2
polygonal:	3
Mica-Rich	
foliated:	
polygonal:	1
Unknown MRF:	
Total:	6
Volcanic Rock Fragment (VRF)	
Microlitic:	
Lathwork:	
Felsitic:	
Altered VRF:	1
Unknown VRF:	
Total:	1
Accessory Minerals	
Muscovite:	
Biotite:	
Tourmaline:	
Sphene:	
Zircon:	
Total:	0
Other	
Unknown RF:	
Total:	0
Matrix	
Clay Cutans:	
Pore Filling:	
Total:	0

[a] Rock Fragment

Category	Counts
Porosity	
Intergranular:	95
Intragranular Plagioclase:	
Intragranular Microcline:	1
Intragranular Potassium Feldspar:	6
Intragranular Unknown Feldspar:	
Oversized:	5
Intragrannular VRF	
Unknown VRF:	2
Intragrannular MRF	
Intragrannular SRF	
Intragranular Unknown RF:	
Intragranular Unknown Grain:	
Total:	109
Cement/Overgrowth	
Quartz:	
Kaolinte:	3
Fe-Oxide:	
Calcite	
intergranular:	27
oversized:	
Total:	30
Grain Replacement	
Kaolinite	
Orthoclase:	
Microcline:	
Plagioclase:	
Unknown Feldspar:	
SRF:	
VRF:	
MRF:	
Mica:	1
Unknown RF:	
Unknown Grain:	2
Calcite	
Orthoclase:	1
Microcline:	
Plagioclase:	
Unknown Feldspar:	
SRF:	1
VRF:	
MRF:	1
Mica:	
Unknown RF:	1
Unknown Grain:	6
Fe-O	
Orthoclase:	
Microcline:	
Plagioclase:	
Unknown Feldspar:	
SRF:	
VRF:	
MRF:	
Mica:	
Unknown RF:	
Unknown Grain:	
Total:	13

Table B.11. Point count data table for GM-C-051408-13.

Sample Name:	GM-C-051408-13	Sub-unit:	Upper Wilcox
Sample Type:	Outcrop	Total Points Counted:	350

Category	Counts
Quartz	
Mono Crystalline:	160
Poly Crystalline:	13
Volcanic:	15
Sedimentary:	4
Total:	192
Feldspar	
Plagioclase:	
Orthoclase:	5
Microcline:	1
Total	6
Sedimentary Rock Fragment (SRF)	
Argillaceous RF[a]:	
Chert:	9
Siltstone RF:	2
Sandstone RF:	
Argillaceous Chert:	4
Unknown SRF:	
Total:	15
Metamorphic Rock Fragment (MRF)	
Quartzofeldspathic:	
Quartz-Rich	
foliated:	
polygonal:	
Mica-Rich	
foliated:	
polygonal:	
Unknown MRF:	
Total:	0
Volcanic Rock Fragment (VRF)	
Microlitic:	
Lathwork:	
Felsitic:	
Altered VRF:	
Unknown VRF:	
Total:	0
Accessory Minerals	
Muscovite:	
Biotite:	
Tourmaline:	
Sphene:	
Zircon:	
Total:	0
Other	
Unknown RF:	
Total:	0
Matrix	
Clay Cutans:	30
Pore Filling:	21
Total:	51

[a] Rock Fragment

Category	Counts
Porosity	
Intergranular:	65
Intragranular Plagioclase:	
Intragranular Microcline:	
Intragranular Potassium Feldspar:	1
Intragranular Unknown Feldspar:	
Oversized:	12
Intragrannular VRF	
Unknown VRF:	1
Intragrannular MRF	
Intragrannular SRF	
Chert:	2
Intragranular Unknown RF:	
Intragranular Unknown Grain:	
Total:	81
Cement/Overgrowth	
Quartz:	
Kaolinte:	5
Fe-Oxide:	
Calcite	
intergranular:	
oversized:	
Total:	5
Grain Replacement	
Kaolinite	
Orthoclase:	
Microcline:	
Plagioclase:	
Unknown Feldspar:	
SRF:	
VRF:	
MRF:	
Mica:	
Unknown RF:	
Unknown Grain:	
Calcite	
Orthoclase:	
Microcline:	
Plagioclase:	
Unknown Feldspar:	
SRF:	
VRF:	
MRF:	
Mica:	
Unknown RF:	
Unknown Grain:	
Fe-O	
Orthoclase:	
Microcline:	
Plagioclase:	
Unknown Feldspar:	
SRF:	
VRF:	
MRF:	
Mica:	
Unknown RF:	
Unknown Grain:	
Total:	0

Table B.12. Point count data table for GM-C-051408-14.

Sample Name:	GM-C-051408-14	Sub-unit:	Upper Wilcox
Sample Type:	Outcrop	Total Points Counted:	350

Category	Counts
Quartz	
Mono Crystalline:	130
Poly Crystalline:	10
Volcanic:	10
Sedimentary:	6
Total:	156
Feldspar	
Plagioclase:	
Orthoclase:	21
Microcline:	2
Total	23
Sedimentary Rock Fragment (SRF)	
Argillaceous RF[a]:	3
Chert:	5
Siltstone RF:	
Sandstone RF:	
Argillaceous Chert:	2
Unknown SRF:	
Total:	10
Metamorphic Rock Fragment (MRF)	
Quartzofeldspathic:	
Quartz-Rich	
foliated:	1
polygonal:	4
Mica-Rich	
foliated:	
polygonal:	1
Unknown MRF:	
Total:	6
Volcanic Rock Fragment (VRF)	
Microlitic:	
Lathwork:	
Felsitic:	3
Altered VRF:	
Unknown VRF:	
Total:	3
Accessory Minerals	
Muscovite:	
Biotite:	
Tourmaline:	
Sphene:	
Zircon:	
Total:	0
Other	
Unknown RF:	
Total:	0
Matrix	
Clay Cutans:	
Pore Filling:	
Total:	0

[a] Rock Fragment

Category	Counts
Porosity	
Intergranular:	2
Intragranular Plagioclase:	
Intragranular Microcline:	
Intragranular Potassium Feldspar:	
Intragranular Unknown Feldspar:	
Oversized:	
Intragrannular VRF	
Intragrannular MRF	
Intragrannular SRF	
Intragranular Unknown RF:	
Intragranular Unknown Grain:	
Total:	2
Cement/Overgrowth	
Quartz:	
Kaolinte:	
Fe-Oxide:	1
Calcite	
intergranular:	127
oversized:	20
Total:	148
Grain Replacement	
Kaolinite	
Orthoclase:	
Microcline:	
Plagioclase:	
Unknown Feldspar:	
SRF:	
VRF:	
MRF:	
Mica:	
Unknown RF:	
Unknown Grain:	2
Calcite	
Orthoclase:	
Microcline:	
Plagioclase:	
Unknown Feldspar:	
SRF:	
VRF:	
MRF:	
Mica:	
Unknown RF:	
Unknown Grain:	
Fe-O	
Orthoclase:	
Microcline:	
Plagioclase:	
Unknown Feldspar:	
SRF:	
VRF:	
MRF:	
Mica:	
Unknown RF:	
Unknown Grain:	
Total:	2

Table B.13. Point count data table for GM-C-051508-1.

Sample Name:	GM-C-051508-1	Sub-unit:	Upper Wilcox
Sample Type:	Outcrop	Total Points Counted:	350

Category	Counts
Quartz	
Mono Crystalline:	150
Poly Crystalline:	9
Volcanic:	6
Sedimentary:	3
Total:	168
Feldspar	
Plagioclase:	
Orthoclase:	19
Microcline:	1
Total	20
Sedimentary Rock Fragment (SRF)	
Argillaceous RF[a]:	
Chert:	5
Siltstone RF:	1
Sandstone RF:	
Argillaceous Chert:	5
Unknown SRF:	
Total:	11
Metamorphic Rock Fragment (MRF)	
Quartzofeldspathic:	
Quartz-Rich	
foliated:	2
polygonal:	4
Mica-Rich	
foliated:	1
polygonal:	
Unknown MRF:	
Total:	7
Volcanic Rock Fragment (VRF)	
Microlitic:	
Lathwork:	
Felsitic:	1
Altered VRF:	5
Unknown VRF:	
Total:	6
Accessory Minerals	
Muscovite:	
Biotite:	
Tourmaline:	
Sphene:	
Zircon:	
Total:	0
Other	
Unknown RF:	1
Unknown Highly Dissolved Grain:	1
Total:	2
Matrix	
Clay Cutans:	
Pore Filling:	31
Total:	31

[a] Rock Fragment

Category	Counts
Porosity	
Intergranular:	80
Intragranular Plagioclase:	
Intragranular Microcline:	1
Intragranular Potassium Feldspar:	4
Intragranular Unknown Feldspar:	
Oversized:	4
Intragrannular VRF	
Altered VRF:	2
Intragrannular MRF	
Quartz-Rich, Polygonal:	1
Intragrannular SRF	
Chert:	1
Intragranular Unknown RF:	3
Intragranular Unknown Grain:	
Total:	96
Cement/Overgrowth	
Quartz:	
Kaolinte:	2
Fe-Oxide:	7
Calcite	
intergranular:	
oversized:	
Total:	9
Grain Replacement	
Kaolinite	
Orthoclase:	
Microcline:	
Plagioclase:	
Unknown Feldspar:	
SRF:	
VRF:	
MRF:	
Mica:	
Unknown RF:	
Unknown Grain:	
Calcite	
Orthoclase:	
Microcline:	
Plagioclase:	
Unknown Feldspar:	
SRF:	
VRF:	
MRF:	
Mica:	
Unknown RF:	
Unknown Grain:	
Fe-O	
Orthoclase:	
Microcline:	
Plagioclase:	
Unknown Feldspar:	
SRF:	
VRF:	
MRF:	
Mica:	
Unknown RF:	
Unknown Grain:	
Total:	0

Table B.14. Point count data table for GM-C-051508-2.

Sample Name:	GM-C-051508-2	Sub-unit:	Upper Wilcox
Sample Type:	Outcrop	Total Points Counted:	349

Category	Counts
Quartz	
Mono Crystalline:	105
Poly Crystalline:	19
Volcanic:	6
Sedimentary:	3
Total:	133
Feldspar	
Plagioclase:	
Orthoclase:	11
Microcline:	1
Total	12
Sedimentary Rock Fragment (SRF)	
Argillaceous RF[a]:	2
Chert:	12
Siltstone RF:	2
Sandstone RF:	
Argillaceous Chert:	15
Unknown SRF:	1
Total:	32
Metamorphic Rock Fragment (MRF)	
Quartzofeldspathic:	
Quartz-Rich	
foliated:	
polygonal:	
Mica-Rich	
foliated:	
polygonal:	
Unknown MRF:	
Total:	0
Volcanic Rock Fragment (VRF)	
Microlitic:	
Lathwork:	
Felsitic:	2
Altered VRF:	
Unknown VRF:	
Total:	2
Accessory Minerals	
Muscovite:	
Biotite:	
Tourmaline:	
Sphene:	
Zircon:	
Total:	0
Other	
Unknown RF:	
Total:	0
Matrix	
Clay Cutans:	
Pore Filling:	
Total:	0

[a] Rock Fragment

Category	Counts
Porosity	
Intergranular:	1
Intragranular Plagioclase:	
Intragranular Microcline:	
Intragranular Potassium Feldspar:	
Intragranular Unknown Feldspar:	1
Oversized:	
Intragrannular VRF	
Intragrannular MRF	
Siltstone RF:	2
Intragrannular SRF	
Intragranular Unknown RF:	1
Intragranular Unknown Grain:	
Total:	5
Cement/Overgrowth	
Quartz:	
Kaolinte:	
Fe-Oxide:	
Calcite	
intergranular:	154
oversized:	7
Total:	161
Grain Replacement	
Kaolinite	
Orthoclase:	
Microcline:	
Plagioclase:	
Unknown Feldspar:	
SRF:	
VRF:	
MRF:	
Mica:	
Unknown RF:	
Unknown Grain:	
Calcite	
Orthoclase:	
Microcline:	
Plagioclase:	
Unknown Feldspar:	
SRF:	2
VRF:	
MRF:	
Mica:	
Unknown RF:	
Unknown Grain:	2
Fe-O	
Orthoclase:	
Microcline:	
Plagioclase:	
Unknown Feldspar:	
SRF:	
VRF:	
MRF:	
Mica:	
Unknown RF:	
Unknown Grain:	
Total:	4

Table B.15. Point count data table for GM-C-051508-3.

Sample Name:	GM-C-051508-3	Sub-unit:	Upper Wilcox
Sample Type:	Outcrop	Total Points Counted:	350

Category	Counts
Quartz	
Mono Crystalline:	104
Poly Crystalline:	18
Volcanic:	17
Sedimentary:	2
Total:	141
Feldspar	
Plagioclase:	
Orthoclase:	9
Microcline:	
Total	9
Sedimentary Rock Fragment (SRF)	
Argillaceous RF[a]:	1
Chert:	41
Siltstone RF:	3
Sandstone RF:	1
Argillaceous Chert:	10
Unknown SRF:	
Evaporitic Quartz with Chalcedony Overgrowth:	1
Total:	57
Metamorphic Rock Fragment (MRF)	
Quartzofeldspathic:	
Quartz-Rich	
foliated:	1
polygonal:	1
Mica-Rich	
foliated:	
polygonal:	
Unknown MRF:	
Total:	2
Volcanic Rock Fragment (VRF)	
Microlitic:	
Lathwork:	
Felsitic:	3
Altered VRF:	5
Unknown VRF:	
Total:	8
Accessory Minerals	
Muscovite:	
Biotite:	
Tourmaline:	
Sphene:	
Zircon:	
Total:	0
Other	
Unknown RF:	
Unknown Highly Dissolved Grain:	6
Total:	6
Matrix	
Clay Cutans:	
Pore Filling:	
Total:	0

[a] Rock Fragment

Category	Counts
Porosity	
Intergranular:	114
Intragranular Plagioclase:	
Intragranular Microcline:	
Intragranular Potassium Feldspar:	4
Intragranular Unknown Feldspar:	
Oversized:	3
Intragrannular VRF	
Lathwork:	1
Intragrannular MRF	
Intragrannular SRF	
Chert:	1
Siltstone RF:	1
Intragranular Unknown RF:	
Intragranular Unknown Grain:	
Total:	124
Cement/Overgrowth	
Quartz:	
Kaolinte:	3
Fe-Oxide:	
Calcite	
intergranular:	
oversized:	
Total:	3
Grain Replacement	
Kaolinite	
Orthoclase:	
Microcline:	
Plagioclase:	
Unknown Feldspar:	
SRF:	
VRF:	
MRF:	
Mica:	
Unknown RF:	
Unknown Grain:	
Calcite	
Orthoclase:	
Microcline:	
Plagioclase:	
Unknown Feldspar:	
SRF:	
VRF:	
MRF:	
Mica:	
Unknown RF:	
Unknown Grain:	
Fe-O	
Orthoclase:	
Microcline:	
Plagioclase:	
Unknown Feldspar:	
SRF:	
VRF:	
MRF:	
Mica:	
Unknown RF:	
Unknown Grain:	
Total:	0

Table B.16. Point count data table for GM-C-051608-1.

Sample Name:	GM-C-051608-1	Sub-unit:	Upper Wilcox
Sample Type:	Outcrop	Total Points Counted:	348

Category	Counts
Quartz	
Mono Crystalline:	155
Poly Crystalline:	25
Volcanic:	19
Sedimentary:	3
Total:	202
Feldspar	
Plagioclase:	
Orthoclase:	4
Microcline:	2
Total	6
Sedimentary Rock Fragment (SRF)	
Argillaceous RF[a]:	
Chert:	1
Siltstone RF:	2
Sandstone RF:	
Argillaceous Chert:	2
Unknown SRF:	
Total:	5
Metamorphic Rock Fragment (MRF)	
Quartzofeldspathic:	
Quartz-Rich	
foliated:	
polygonal:	
Mica-Rich	
foliated:	
polygonal:	
Unknown MRF:	
Total:	0
Volcanic Rock Fragment (VRF)	
Microlitic:	
Lathwork:	
Felsitic:	
Altered VRF:	
Unknown VRF:	
Total:	0
Accessory Minerals	
Muscovite:	
Biotite:	
Tourmaline:	
Sphene:	
Zircon:	
Total:	0
Other	
Unknown RF:	
Total:	0
Matrix	
Clay Cutans:	
Pore Filling:	
Total:	0

[a] Rock Fragment

Category	Counts
Porosity	
Intergranular:	
Intragranular Plagioclase:	
Intragranular Microcline:	
Intragranular Potassium Feldspar:	
Intragranular Unknown Feldspar:	
Oversized:	1
Intragrannular VRF	
Intragrannular MRF	
Intragrannular SRF	
Intragranular Unknown RF:	
Intragranular Unknown Grain:	
Total:	1
Cement/Overgrowth	
Quartz:	
Kaolinte:	1
Fe-Oxide:	1
Oversized Fe-O:	3
Calcite	
intergranular:	124
oversized:	4
Total:	133
Grain Replacement	
Kaolinite:	
Orthoclase:	
Microcline:	
Plagioclase:	
Unknown Feldspar:	
SRF:	
VRF:	
MRF:	
Mica:	
Unknown RF:	
Unknown Grain:	
Calcite	
Orthoclase:	1
Microcline:	
Plagioclase:	
Unknown Feldspar:	
SRF:	
VRF:	
MRF:	
Mica:	
Unknown RF:	
Unknown Grain:	
Fe-O	
Orthoclase:	
Microcline:	
Plagioclase:	
Unknown Feldspar:	
SRF:	
VRF:	
MRF:	
Mica:	
Unknown RF:	
Unknown Grain:	
Total:	1

Table B.17. Point count data table for GM-C-051608-2.

Sample Name:	GM-C-051608-2	Sub-unit:	Upper Wilcox
Sample Type:	Outcrop	Total Points Counted:	362

Category	Counts
Quartz	
Mono Crystalline:	148
Poly Crystalline:	21
Volcanic:	3
Sedimentary:	8
Total:	180
Feldspar	
Plagioclase:	2
Orthoclase:	7
Microcline:	1
Total	10
Sedimentary Rock Fragment (SRF)	
Argillaceous RF[a]:	1
Chert:	4
Siltstone RF:	1
Sandstone RF:	
Argillaceous Chert:	3
Unknown SRF:	
Total:	9
Metamorphic Rock Fragment (MRF)	
Quartzofeldspathic:	
Quartz-Rich	
foliated:	1
polygonal:	
Mica-Rich	
foliated:	
polygonal:	
Unknown MRF:	
Total:	1
Volcanic Rock Fragment (VRF)	
Microlitic:	
Lathwork:	
Felsitic:	
Altered VRF:	
Unknown VRF:	
Total:	0
Accessory Minerals	
Muscovite:	
Biotite:	
Tourmaline:	
Sphene:	
Zircon:	
Total:	0
Other	
Unknown RF:	
Total:	0
Matrix	
Clay Cutans:	
Pore Filling:	
Total:	0

[a] Rock Fragment

Category	Counts
Porosity	
Intergranular:	
Intragranular Plagioclase:	
Intragranular Microcline:	
Intragranular Potassium Feldspar:	
Intragranular Unknown Feldspar:	
Oversized:	
Intragrannular VRF	
Intragrannular MRF	
Unknown MRF:	1
Intragrannular SRF	
Intragranular Unknown RF:	
Intragranular Unknown Grain:	
Total:	1
Cement/Overgrowth	
Quartz:	
Kaolinte:	
Fe-Oxide:	
Calcite	
intergranular:	131
oversized:	28
Total:	159
Grain Replacement	
Kaolinite	
Orthoclase:	
Microcline:	
Plagioclase:	
Unknown Feldspar:	
SRF:	
VRF:	
MRF:	
Mica:	
Unknown RF:	
Unknown Grain:	
Calcite	
Orthoclase:	2
Microcline:	
Plagioclase:	
Unknown Feldspar:	
SRF:	
VRF:	
MRF:	
Mica:	
Unknown RF:	
Unknown Grain:	
Fe-O	
Orthoclase:	
Microcline:	
Plagioclase:	
Unknown Feldspar:	
SRF:	
VRF:	
MRF:	
Mica:	
Unknown RF:	
Unknown Grain:	
Total:	2

Table B.18. Point count data table for GM-C-051608-3.

Sample Name:	GM-C-051608-3	Sub-unit:	Upper Wilcox
Sample Type:	Outcrop	Total Points Counted:	350

Category	Counts
Quartz	
Mono Crystalline:	140
Poly Crystalline:	17
Volcanic:	2
Sedimentary:	2
Total:	161
Feldspar	
Plagioclase:	3
Orthoclase:	11
Microcline:	
Unknown Feldspar:	1
Total	15
Sedimentary Rock Fragment (SRF)	
Argillaceous RF[a]:	
Chert:	13
Siltstone RF:	1
Sandstone RF:	
Argillaceous Chert:	6
Unknown SRF:	
Total:	20
Metamorphic Rock Fragment (MRF)	
Quartzofeldspathic:	
Quartz-Rich	
foliated:	3
polygonal:	3
Mica-Rich	
foliated:	
polygonal:	
Unknown MRF:	
Total:	6
Volcanic Rock Fragment (VRF)	
Microlitic:	
Lathwork:	
Felsitic:	1
Altered VRF:	2
Unknown VRF:	1
Total:	4
Accessory Minerals	
Muscovite:	
Biotite:	
Tourmaline:	
Sphene:	
Zircon:	
Total:	0
Other	
Unknown RF:	
Total:	0
Matrix	
Clay Cutans:	
Pore Filling:	45
Total:	45

[a] Rock Fragment

Category	Counts
Porosity	
Intergranular:	78
Intragranular Plagioclase:	2
Intragranular Microcline:	
Intragranular Potassium Feldspar:	1
Intragranular Unknown Feldspar:	
Oversized:	4
Intragrannular VRF	
Altered VRF:	1
Intragrannular MRF	
Quartzofeldspathic:	2
Quartz-Rich, Foliated	2
Intragrannular SRF	
Chert	2
Intragranular Unknown RF:	2
Intragranular Unknown Grain:	
Total:	94
Cement/Overgrowth	
Quartz:	
Kaolinte:	1
Fe-Oxide:	
Calcite	
intergranular:	
oversized:	
Total:	1
Grain Replacement	
Kaolinite	
Orthoclase:	
Microcline:	
Plagioclase:	
Unknown Feldspar:	
SRF:	
VRF:	
MRF:	
Mica:	1
Unknown RF:	1
Unknown Grain:	2
Calcite	
Orthoclase:	
Microcline:	
Plagioclase:	
Unknown Feldspar:	
SRF:	
VRF:	
MRF:	
Mica:	
Unknown RF:	
Unknown Grain:	
Fe-O	
Orthoclase:	
Microcline:	
Plagioclase:	
Unknown Feldspar:	
SRF:	
VRF:	
MRF:	
Mica:	
Unknown RF:	
Unknown Grain:	
Total:	4

Table B.19. Point count data table for GM-C-051608-4.

Sample Name:	GM-C-051608-4	Sub-unit:	Upper Wilcox
Sample Type:	Outcrop	Total Points Counted:	349

Category	Counts
Quartz	
Mono Crystalline:	176
Poly Crystalline:	17
Volcanic:	2
Sedimentary:	6
Total:	201
Feldspar	
Plagioclase:	1
Orthoclase:	4
Microcline:	3
Total	8
Sedimentary Rock Fragment (SRF)	
Argillaceous RF[a]:	
Chert:	2
Siltstone RF:	
Sandstone RF:	
Argillaceous Chert:	4
Unknown SRF:	
Total:	6
Metamorphic Rock Fragment (MRF)	
Quartzofeldspathic:	
Quartz-Rich	
foliated:	1
polygonal:	2
Mica-Rich	
foliated:	
polygonal:	
Unknown MRF:	
Total:	3
Volcanic Rock Fragment (VRF)	
Microlitic:	
Lathwork:	
Felsitic:	4
Altered VRF:	
Unknown VRF:	
Total:	4
Accessory Minerals	
Muscovite:	
Biotite:	
Tourmaline:	
Sphene:	
Zircon:	
Total:	0
Other	
Unknown RF:	
Total:	0
Matrix	
Clay Cutans:	
Pore Filling:	2
Total:	2

[a] Rock Fragment

Category	Counts
Porosity	
Intergranular:	97
Intragranular Plagioclase:	
Intragranular Microcline:	
Intragranular Potassium Feldspar:	1
Intragranular Unknown Feldspar:	2
Oversized:	8
Intragrannular VRF	
Altered VRF:	1
Intragrannular MRF	
Quartz-Rich, Polygonal:	1
Intragrannular SRF	
Chert:	2
Intragranular Unknown RF:	2
Intragranular Unknown Grain:	
Total:	114
Cement/Overgrowth	
Quartz:	
Kaolinte:	3
Fe-Oxide:	2
Calcite	
intergranular:	
oversized:	
Total:	5
Grain Replacement	
Kaolinite	
Orthoclase:	
Microcline:	
Plagioclase:	
Unknown Feldspar:	
SRF:	
VRF:	
MRF:	
Mica:	1
Unknown RF:	
Unknown Grain:	2
Calcite	
Orthoclase:	
Microcline:	
Plagioclase:	
Unknown Feldspar:	
SRF:	
VRF:	
MRF:	
Mica:	
Unknown RF:	
Unknown Grain:	
Fe-O	
Orthoclase:	
Microcline:	
Plagioclase:	
Unknown Feldspar:	
SRF:	
VRF:	
MRF:	
Mica:	
Unknown RF:	
Unknown Grain:	3
Total:	6

Table B.20. Point count data table for GM-C-051608-5.

Sample Name:	GM-C-051608-5	Sub-unit:	Upper Wilcox
Sample Type:	Outcrop	Total Points Counted:	350

Category	Counts
Quartz	
Mono Crystalline:	179
Poly Crystalline:	23
Volcanic:	2
Sedimentary:	3
Total:	207
Feldspar	
Plagioclase:	
Orthoclase:	3
Microcline:	7
Total	10
Sedimentary Rock Fragment (SRF)	
Argillaceous RF[a]:	
Chert:	7
Siltstone RF:	2
Sandstone RF:	
Argillaceous Chert:	1
Unknown SRF:	
Lengthslow Chalcedony:	1
Total:	11
Metamorphic Rock Fragment (MRF)	
Quartzofeldspathic:	
Quartz-Rich	
foliated:	
polygonal:	6
Mica-Rich	
foliated:	
polygonal:	
Unknown MRF:	
Total:	6
Volcanic Rock Fragment (VRF)	
Microlitic:	
Lathwork:	
Felsitic:	2
Altered VRF:	2
Unknown VRF:	2
Total:	6
Accessory Minerals	
Muscovite:	
Biotite:	
Tourmaline:	
Sphene:	
Zircon:	
Total:	0
Other	
Unknown RF:	
Unknown Highly Dissolved Grain:	6
Total:	6
Matrix	
Clay Cutans:	
Pore Filling:	
Total:	0

[a] Rock Fragment

Category	Counts
Porosity	
Intergranular:	96
Intragranular Plagioclase:	
Intragranular Microcline:	1
Intragranular Potassium Feldspar:	
Intragranular Unknown Feldspar:	1
Oversized:	
Intragrannular VRF	
Intragrannular MRF	
Intragrannular SRF	
Chert:	1
Unknown SRF:	1
Intragranular Unknown RF:	1
Intragranular Unknown Grain:	
Total:	101
Cement/Overgrowth	
Quartz:	
Kaolinte:	3
Fe-Oxide:	
Calcite	
intergranular:	
oversized:	
Total:	3
Grain Replacement	
Kaolinite	
Orthoclase:	
Microcline:	
Plagioclase:	
Unknown Feldspar:	
SRF:	
VRF:	
MRF:	
Mica:	
Unknown RF:	
Unknown Grain:	
Calcite	
Orthoclase:	
Microcline:	
Plagioclase:	
Unknown Feldspar:	
SRF:	
VRF:	
MRF:	
Mica:	
Unknown RF:	
Unknown Grain:	
Fe-O	
Orthoclase:	
Microcline:	
Plagioclase:	
Unknown Feldspar:	
SRF:	
VRF:	
MRF:	
Mica:	
Unknown RF:	
Unknown Grain:	
Total:	0

Table B.21. Point count data table for Bailey 1C-10474.

Sample Name:	Bailey1C-10474	Sub-unit:	Upper Wilcox
Sample Type:		Total Points Counted:	345

Category	Counts
Quartz	
Mono Crystalline:	215
Poly Crystalline:	6
Volcanic:	
Sedimentary:	
Total:	221
Feldspar	
Plagioclase:	14
Orthoclase:	2
Microcline:	
Total	16
Sedimentary Rock Fragment (SRF)	
Argillaceous RF[a]:	
Chert:	3
Siltstone RF:	
Sandstone RF:	
Argillaceous Chert:	
Unknown SRF:	
Total:	3
Metamorphic Rock Fragment (MRF)	
Quartzofeldspathic:	
Quartz-Rich	
foliated:	5
polygonal:	3
Mica-Rich	
foliated:	1
polygonal:	
Unknown MRF:	
Total:	9
Volcanic Rock Fragment (VRF)	
Microlitic:	
Lathwork:	
Felsitic:	
Altered VRF:	
Unknown VRF:	
Total:	0
Accessory Minerals	
Muscovite:	1
Biotite:	
Tourmaline:	1
Sphene:	
Zircon:	
Total:	2
Other	
Unknown RF:	
Total:	0
Matrix	
Clay Cutans:	
Pore Filling:	
Total:	0

[a] Rock Fragment

Category	Counts
Porosity	
Intergranular:	33
Intragranular Plagioclase:	1
Intragranular Microcline:	
Intragranular Potassium Feldspar:	1
Intragranular Unknown Feldspar:	6
Oversized:	19
Intragrannular VRF	
Felsitic:	1
Intragrannular MRF	
Quartzofeldspathic:	1
Intragrannular SRF	
Intragranular Unknown RF:	3
Intragranular Unknown Grain:	
Total:	65
Cement/Overgrowth	
Quartz:	6
Kaolinte:	5
Fe-Oxide:	2
Calcite	
intergranular:	
oversized:	
Total:	13
Grain Replacement	
Kaolinite	
Orthoclase:	
Microcline:	
Plagioclase:	
Unknown Feldspar:	7
SRF:	
VRF:	
MRF:	
Mica:	
Unknown RF:	
Unknown Grain:	
Calcite	
Orthoclase:	
Microcline:	
Plagioclase:	
Unknown Feldspar:	9
SRF:	
VRF:	
MRF:	
Mica:	
Unknown RF:	
Unknown Grain:	
Fe-O	
Orthoclase:	
Microcline:	
Plagioclase:	
Unknown Feldspar:	
SRF:	
VRF:	
MRF:	
Mica:	
Unknown RF:	
Unknown Grain:	
Total:	16

Table B.22. Point count data table for Bailey 1C-10491.

Sample Name:	Bailey1C-10491	Sub-unit:	Upper Wilcox
Sample Type:	Core	Total Points Counted:	350

Category	Counts
Quartz	
Mono Crystalline:	214
Poly Crystalline:	9
Volcanic:	3
Sedimentary:	
Total:	226
Feldspar	
Plagioclase:	6
Orthoclase:	2
Microcline:	
Unknown Feldspar	1
Total	9
Sedimentary Rock Fragment (SRF)	
Argillaceous RF[a]:	3
Chert:	5
Siltstone RF:	
Sandstone RF:	
Argillaceous Chert:	2
Unknown SRF:	
Total:	10
Metamorphic Rock Fragment (MRF)	
Quartzofeldspathic:	
Quartz-Rich	
foliated:	
polygonal:	2
Mica-Rich	
foliated:	
polygonal:	
Unknown MRF:	1
Total:	3
Volcanic Rock Fragment (VRF)	
Microlitic:	
Lathwork:	1
Felsitic:	4
Altered VRF:	1
Unknown VRF:	
Total:	6
Accessory Minerals	
Muscovite:	1
Biotite:	
Tourmaline:	
Sphene:	
Zircon:	1
Total:	2
Other	
Unknown RF:	1
Total:	1
Matrix	
Clay Cutans:	
Pore Filling:	9
Total:	9

[a] Rock Fragment

Category	Counts
Porosity	
Intergranular:	21
Intragranular Plagioclase:	
Intragranular Microcline:	
Intragranular Potassium Feldspar:	
Intragranular Unknown Feldspar:	1
Oversized:	4
Intragrannular VRF	
Intragrannular MRF	
Intragrannular SRF	
Chert:	1
Intragranular Unknown RF:	
Intragranular Unknown Grain:	3
Total:	30
Cement/Overgrowth	
Quartz:	25
Kaolinte:	2
Fe-Oxide:	1
Calcite	
intergranular:	17
oversized:	5
Total:	50
Grain Replacement / Intragranular Cement	
Kaolinite	
Orthoclase:	
Microcline:	
Plagioclase:	
Unknown Feldspar:	
SRF:	
VRF:	
MRF:	
Mica:	
Unknown RF:	
Unknown Grain:	
Calcite	
Orthoclase:	
Microcline:	
Plagioclase:	
Unknown Feldspar:	1
SRF:	
VRF:	
MRF:	
Mica:	
Unknown RF:	
Unknown Grain:	3
Fe-O	
Orthoclase:	
Microcline:	
Plagioclase:	
Unknown Feldspar:	
SRF:	
VRF:	
MRF:	
Mica:	
Unknown RF:	
Unknown Grain:	
Total:	4

Table B.23. Point count data table for Urban 1-13896.

Sample Name:	Urban1-13896	Sub-unit:	Upper Wilcox
Sample Type:	Core	Total Points Counted:	344

Category	Counts
Quartz	
Mono Crystalline:	206
Poly Crystalline:	7
Volcanic:	1
Sedimentary:	
Total:	214
Feldspar	
Plagioclase:	8
Orthoclase:	2
Microcline:	
Total	10
Sedimentary Rock Fragment (SRF)	
Argillaceous RF[a]:	
Chert:	2
Siltstone RF:	
Sandstone RF:	
Argillaceous Chert:	
Unknown SRF:	
Total:	2
Metamorphic Rock Fragment (MRF)	
Quartzofeldspathic:	
Quartz-Rich	
foliated:	1
polygonal:	4
Mica-Rich	
foliated:	2
polygonal:	
Unknown MRF:	
Total:	7
Volcanic Rock Fragment (VRF)	
Microlitic:	
Lathwork:	
Felsitic:	1
Altered VRF:	
Unknown VRF:	
Total:	1
Accessory Minerals	
Muscovite:	2
Biotite:	1
Tourmaline:	
Sphene:	
Zircon:	
Total:	3
Other	
Unknown RF:	1
Total:	1
Matrix	
Clay Cutans:	
Pore Filling:	6
Total:	6

[a] Rock Fragment

Category	Counts
Porosity	
Intergranular:	52
Intragranular Plagioclase:	
Intragranular Microcline:	
Intragranular Potassium Feldspar:	1
Intragranular Unknown Feldspar:	7
Oversized:	3
Intragrannular VRF	
Intragrannular MRF	
Intragrannular SRF	
Intragranular Unknown RF:	1
Intragranular Unknown Grain:	2
Total:	66
Cement/Overgrowth	
Quartz:	7
Kaolinte:	
Fe-Oxide:	5
Calcite	
intergranular:	
oversized:	7
Total:	19
Grain Replacement	
Kaolinite	
Orthoclase:	
Microcline:	
Plagioclase:	
Unknown Feldspar:	
SRF:	
VRF:	
MRF:	
Mica:	
Unknown RF:	
Unknown Grain:	
Calcite	
Orthoclase:	
Microcline:	
Plagioclase:	
Unknown Feldspar:	10
SRF:	
VRF:	
MRF:	
Mica:	
Unknown RF:	
Unknown Grain:	5
Fe-O	
Orthoclase:	
Microcline:	
Plagioclase:	
Unknown Feldspar:	
SRF:	
VRF:	
MRF:	
Mica:	
Unknown RF:	
Unknown Grain:	
Total:	15

Table B.24. Point count data table for Urban 1-14097.

Sample Name:	Urban1-14097	Sub-unit:	Upper Wilcox
Sample Type:	Core	Total Points Counted:	348

Category	Counts
Quartz	
Mono Crystalline:	184
Poly Crystalline:	14
Volcanic:	5
Sedimentary:	
Total:	203
Feldspar	
Plagioclase:	8
Orthoclase:	
Microcline:	
Total	8
Sedimentary Rock Fragment (SRF)	
Argillaceous RF[a]:	
Chert:	1
Siltstone RF:	
Sandstone RF:	
Argillaceous Chert:	
Unknown SRF:	
Total:	1
Metamorphic Rock Fragment (MRF)	
Quartzofeldspathic:	
Quartz-Rich	
foliated:	2
polygonal:	4
Mica-Rich	
foliated:	1
polygonal:	
Unknown MRF:	
Total:	7
Volcanic Rock Fragment (VRF)	
Microlitic:	
Lathwork:	
Felsitic:	
Altered VRF:	
Unknown VRF:	
Total:	0
Accessory Minerals	
Muscovite:	3
Biotite:	1
Tourmaline:	
Sphene:	
Zircon:	1
Total:	5
Other	
Unknown RF:	
Total:	0
Matrix	
Clay Cutans:	
Pore Filling:	
Total:	0

[a] Rock Fragment

Category	Counts
Porosity	
Intergranular:	35
Intragranular Plagioclase:	3
Intragranular Microcline:	
Intragranular Potassium Feldspar:	
Intragranular Unknown Feldspar:	7
Oversized:	27
Intragrannular VRF	
Lathwork:	1
Intragrannular MRF	
Intragrannular SRF	
Intragranular Unknown RF:	
Intragranular Unknown Grain:	1
Intragranular Calcite replacing Feldspar	2
Mica:	2
Total:	78
Cement/Overgrowth	
Quartz:	13
Kaolinte:	
Fe-Oxide:	1
Calcite	
intergranular:	19
oversized:	
Total:	33
Grain Replacement	
Kaolinite	
Orthoclase:	
Microcline:	
Plagioclase:	
Unknown Feldspar:	
SRF:	
VRF:	
MRF:	
Mica:	
Unknown RF:	
Unknown Grain:	
Calcite	
Orthoclase:	
Microcline:	
Plagioclase:	1
Unknown Feldspar:	12
SRF:	
VRF:	
MRF:	
Mica:	
Unknown RF:	
Unknown Grain:	
Fe-O	
Orthoclase:	
Microcline:	
Plagioclase:	
Unknown Feldspar:	
SRF:	
VRF:	
MRF:	
Mica:	
Unknown RF:	
Unknown Grain:	
Total:	13

Table B.25. Point count data table for GM-W-051408-1.

Sample Name:	GM-W-051408-1	Sub-unit:	Lower Wilcox
Sample Type:	Outcrop	Total Points Counted:	351

Category	Counts
Quartz	
Mono Crystalline:	123
Poly Crystalline:	14
Volcanic:	16
Sedimentary:	1
Total:	154
Feldspar	
Plagioclase:	1
Orthoclase:	9
Microcline:	7
Unknown Feldspar:	1
Total	18
Sedimentary Rock Fragment (SRF)	
Argillaceous RF[a]:	
Chert:	6
Siltstone RF:	2
Sandstone RF:	
Argillaceous Chert:	3
Unknown SRF:	
Evaporitic Quartz with Chalcedony Overgrowth:	1
Total:	12
Metamorphic Rock Fragment (MRF)	
Quartzofeldspathic:	
Quartz-Rich	
foliated:	
polygonal:	7
Mica-Rich	
foliated:	1
polygonal:	1
Unknown MRF:	
Total:	9
Volcanic Rock Fragment (VRF)	
Microlitic:	
Lathwork:	
Felsitic:	2
Altered VRF:	1
Unknown VRF:	
Total:	3
Accessory Minerals	
Muscovite:	
Biotite:	
Tourmaline:	
Sphene:	
Zircon:	
Total:	0
Other	
Unknown RF:	
Unknown Highly Dissolved Grain:	8
Total:	8
Matrix	
Clay Cutans:	
Pore Filling:	
Total:	0

Category	Counts
Porosity	
Intergranular:	84
Intragranular Plagioclase:	
Intragranular Microcline:	1
Intragranular Potassium Feldspar:	1
Intragranular Unknown Feldspar:	1
Oversized:	7
Intragrannular VRF	
Altered VRF:	1
Intragrannular MRF	
Intragrannular SRF	
Argillaceous Chert:	2
Siltstone RF:	1
Intragranular Unknown RF:	
Intragranular Unknown Grain:	
Total:	98
Cement/Overgrowth	
Quartz:	
Kaolinte:	
Fe-Oxide:	
Calcite	
intergranular:	29
oversized:	
Total:	29
Grain Replacement	
Kaolinite	
Orthoclase:	
Microcline:	
Plagioclase:	
Unknown Feldspar:	
SRF:	
VRF:	
MRF:	
Mica:	6
Unknown RF:	
Unknown Grain:	
Siderite:	
Orthoclase:	
Microcline:	
Plagioclase:	
Unknown Feldspar:	2
SRF:	
VRF:	
MRF:	1
Mica:	
Unknown RF:	
Unknown Grain:	11
Fe-O	
Orthoclase:	
Microcline:	
Plagioclase:	
Unknown Feldspar:	
SRF:	
VRF:	
MRF:	
Mica:	
Unknown RF:	
Unknown Grain:	
Total:	20

Table B.26. Point count data table for GM-W-051508-2.

Sample Name:	GM-W-051508-2	Sub-unit:	Lower Wilcox
Sample Type:	Outcrop	Total Points Counted:	350

Category	Counts
Quartz	
Mono Crystalline:	116
Poly Crystalline:	16
Volcanic:	1
Sedimentary:	
Total:	133
Feldspar	
Plagioclase:	1
Orthoclase:	10
Microcline:	2
Total	13
Sedimentary Rock Fragment (SRF)	
Argillaceous RF[a]:	1
Chert:	21
Siltstone RF:	
Sandstone RF:	
Argillaceous Chert:	14
Unknown SRF:	
Total:	36
Metamorphic Rock Fragment (MRF)	
Quartzofeldspathic:	2
Quartz-Rich	
foliated:	1
polygonal:	4
Mica-Rich	
foliated:	2
polygonal:	
Unknown MRF:	
Total:	9
Volcanic Rock Fragment (VRF)	
Microlitic:	
Lathwork:	
Felsitic:	
Altered VRF:	6
Unknown VRF:	
Total:	6
Accessory Minerals	
Muscovite:	
Biotite:	
Tourmaline:	
Sphene:	
Zircon:	
Total:	0
Other	
Unknown RF:	
Total:	0
Matrix	
Clay Cutans:	
Pore Filling:	25
Total:	25

[a] Rock Fragment

Category	Counts
Porosity	
Intergranular:	90
Intragranular Plagioclase:	2
Intragranular Microcline:	
Intragranular Potassium Feldspar:	
Intragranular Unknown Feldspar:	
Oversized:	3
Intragrannular VRF	
Unknown VRF:	3
Altered VRF:	3
Intragrannular MRF	
Intragrannular SRF	
Chert:	3
Intragranular Unknown RF:	3
Intragranular Unknown Grain:	
Total:	107
Cement/Overgrowth	
Quartz:	
Kaolinte:	6
Fe-Oxide:	13
Calcite	
intergranular:	
oversized:	
Total:	19
Grain Replacement	
Kaolinite	
Orthoclase:	
Microcline:	
Plagioclase:	
Unknown Feldspar:	
SRF:	
VRF:	
MRF:	
Mica:	1
Unknown RF:	1
Unknown Grain:	
Calcite	
Orthoclase:	
Microcline:	
Plagioclase:	
Unknown Feldspar:	
SRF:	
VRF:	
MRF:	
Mica:	
Unknown RF:	
Unknown Grain:	
Fe-O	
Orthoclase:	
Microcline:	
Plagioclase:	
Unknown Feldspar:	
SRF:	
VRF:	
MRF:	
Mica:	
Unknown RF:	
Unknown Grain:	
Total:	2

Table B.27. Point count data table for GM-W-051508-3.

Sample Name:	GM-W-051508-3	Sub-unit:	Lower Wilcox
Sample Type:	Outcrop	Total Points Counted:	350

Category	Counts
Quartz	
Mono Crystalline:	115
Poly Crystalline:	14
Volcanic:	3
Sedimentary:	2
Total:	134
Feldspar	
Plagioclase:	
Orthoclase:	15
Microcline:	4
Total	19
Sedimentary Rock Fragment (SRF)	
Argillaceous RF[a]:	
Chert:	16
Siltstone RF:	
Sandstone RF:	
Argillaceous Chert:	6
Unknown SRF:	
Total:	22
Metamorphic Rock Fragment (MRF)	
Quartzofeldspathic:	
Quartz-Rich	
foliated:	1
polygonal:	2
Mica-Rich	
foliated:	
polygonal:	
Unknown MRF:	
Total:	3
Volcanic Rock Fragment (VRF)	
Microlitic:	
Lathwork:	
Felsitic:	
Altered VRF:	5
Unknown VRF:	
Total:	5
Accessory Minerals	
Muscovite:	
Biotite:	
Tourmaline:	
Sphene:	
Zircon:	
Total:	0
Other	
Unknown RF:	
Total:	0
Matrix	
Clay Cutans:	11
Pore Filling:	8
Total:	19

[a] Rock Fragment

Category	Counts
Porosity	
Intergranular:	75
Intragranular Plagioclase:	
Intragranular Microcline:	
Intragranular Potassium Feldspar:	1
Intragranular Unknown Feldspar:	
Oversized:	13
Intragrannular VRF	
Altered VRF:	3
Intragrannular MRF	
Quartz-Rich, Polygonal:	1
Intragrannular SRF	
Chert:	5
Argillaceous Chert:	3
Intragranular Unknown RF:	1
Intragranular Unknown Grain:	
Total:	102
Cement/Overgrowth	
Quartz:	
Kaolinte:	4
Fe-Oxide:	36
Calcite	
intergranular:	
oversized:	
Total:	40
Grain Replacement	
Kaolinite	
Orthoclase:	
Microcline:	
Plagioclase:	
Unknown Feldspar:	
SRF:	
VRF:	
MRF:	
Mica:	2
Unknown RF:	
Unknown Grain:	2
Calcite	
Orthoclase:	
Microcline:	
Plagioclase:	
Unknown Feldspar:	
SRF:	
VRF:	
MRF:	
Mica:	
Unknown RF:	
Unknown Grain:	
Fe-O	
Orthoclase:	
Microcline:	
Plagioclase:	
Unknown Feldspar:	
SRF:	
VRF:	1
MRF:	
Mica:	
Unknown RF:	
Unknown Grain:	1
Total:	6

Table B.28. Point count data table for GM-W-051508-4.

Sample Name:	GM-W-051508-4	Sub-unit:	Lower Wilcox
Sample Type:	Outcrop	Total Points Counted:	350

Category	Counts
Quartz	
Mono Crystalline:	140
Poly Crystalline:	7
Volcanic:	1
Sedimentary:	
Total:	148
Feldspar	
Plagioclase:	1
Orthoclase:	7
Microcline:	1
Total	9
Sedimentary Rock Fragment (SRF)	
Argillaceous RF[a]:	1
Chert:	13
Siltstone RF:	1
Sandstone RF:	
Argillaceous Chert:	2
Unknown SRF:	
Total:	17
Metamorphic Rock Fragment (MRF)	
Quartzofeldspathic:	
Quartz-Rich	
foliated:	1
polygonal:	2
Mica-Rich	
foliated:	
polygonal:	
Unknown MRF:	
Total:	3
Volcanic Rock Fragment (VRF)	
Microlitic:	
Lathwork:	
Felsitic:	1
Altered VRF:	5
Unknown VRF:	
Total:	6
Accessory Minerals	
Muscovite:	
Biotite:	
Tourmaline:	
Sphene:	
Zircon:	
Total:	0
Other	
Unknown RF:	1
Total:	1
Matrix	
Clay Cutans:	
Pore Filling:	36
Total:	36

[a] Rock Fragment

Category	Counts
Porosity	
Intergranular:	97
Intragranular Plagioclase:	
Intragranular Microcline:	
Intragranular Potassium Feldspar:	9
Intragranular Unknown Feldspar:	
Oversized:	4
Intragrannular VRF	
Unknown VRF:	2
Intragrannular MRF	
Quartz-Rich, Foliated:	1
Intragrannular SRF	
Chert:	4
Intragranular Unknown RF:	3
Intragranular Unknown Grain:	1
Total:	121
Cement/Overgrowth	
Quartz:	
Kaolinte:	2
Fe-Oxide:	4
Calcite	
intergranular:	
oversized:	
Total:	6
Grain Replacement	
Kaolinite	
Orthoclase:	
Microcline:	
Plagioclase:	
Unknown Feldspar:	
SRF:	
VRF:	
MRF:	
Mica:	
Unknown RF:	
Unknown Grain:	
Calcite	
Orthoclase:	
Microcline:	
Plagioclase:	
Unknown Feldspar:	
SRF:	
VRF:	
MRF:	
Mica:	
Unknown RF:	
Unknown Grain:	
Fe-O	
Orthoclase:	
Microcline:	
Plagioclase:	
Unknown Feldspar:	
SRF:	
VRF:	
MRF:	
Mica:	
Unknown RF:	
Unknown Grain:	3
Total:	3

Table B.29. Point count data table for GM-W-051608-1.

Sample Name:	GM-W-051608-1	Sub-unit:	Lower Wilcox
Sample Type:	Outcrop	Total Points Counted:	350

Category	Counts
Quartz	
Mono Crystalline:	129
Poly Crystalline:	12
Volcanic:	5
Sedimentary:	4
Total:	150
Feldspar	
Plagioclase:	1
Orthoclase:	13
Microcline:	5
Total	19
Sedimentary Rock Fragment (SRF)	
Argillaceous RF[a]:	1
Chert:	11
Siltstone RF:	
Sandstone RF:	
Argillaceous Chert:	7
Unknown SRF:	
Total:	19
Metamorphic Rock Fragment (MRF)	
Quartzofeldspathic:	
Quartz-Rich	
foliated:	1
polygonal:	2
Mica-Rich	
foliated:	
polygonal:	
Unknown MRF:	
Total:	3
Volcanic Rock Fragment (VRF)	
Microlitic:	
Lathwork:	
Felsitic:	1
Altered VRF:	5
Unknown VRF:	
Total:	6
Accessory Minerals	
Muscovite:	2
Biotite:	1
Tourmaline:	
Sphene:	
Zircon:	
Total:	3
Other	
Unknown RF:	
Unknown Highly Dissolved Grain:	3
Total:	3
Matrix	
Clay Cutans:	
Pore Filling:	47
Total:	47

[a] Rock Fragment

Category	Counts
Porosity	
Intergranular:	67
Intragranular Plagioclase:	
Intragranular Microcline:	
Intragranular Potassium Feldspar:	4
Intragranular Unknown Feldspar:	1
Oversized:	7
Intragrannular VRF	
Altered VRF:	1
Unknown VRF:	3
Intragrannular MRF	
Mica Rich, Foliated:	1
Intragrannular SRF	
Chert	1
Siltstone RF	1
Intragranular Unknown RF:	1
Intragranular Unknown Grain:	6
Total:	93
Cement/Overgrowth	
Quartz:	
Kaolinte:	4
Fe-Oxide:	
Calcite	
intergranular:	
oversized:	
Total:	4
Grain Replacement	
Kaolinite	
Orthoclase:	
Microcline:	
Plagioclase:	
Unknown Feldspar:	
SRF:	
VRF:	
MRF:	
Mica:	1
Unknown RF:	
Unknown Grain:	1
Calcite	
Orthoclase:	
Microcline:	
Plagioclase:	
Unknown Feldspar:	
SRF:	
VRF:	
MRF:	
Mica:	
Unknown RF:	
Unknown Grain:	
Fe-O	
Orthoclase:	
Microcline:	
Plagioclase:	
Unknown Feldspar:	
SRF:	
VRF:	
MRF:	
Mica:	1
Unknown RF:	
Unknown Grain:	
Total:	3

Table B.30. Point count data table for GM-W-051608-2.

Sample Name:	GM-W-051608-2	Sub-unit:	Lower Wilcox
Sample Type:	Outcrop	Total Points Counted:	350

Category	Counts
Quartz	
Mono Crystalline:	113
Poly Crystalline:	25
Volcanic:	4
Sedimentary:	2
Total:	144
Feldspar	
Plagioclase:	
Orthoclase:	7
Microcline:	
Total	7
Sedimentary Rock Fragment (SRF)	
Argillaceous RF[a]:	
Chert:	30
Siltstone RF:	
Sandstone RF:	
Argillaceous Chert:	13
Unknown SRF:	
Total:	43
Metamorphic Rock Fragment (MRF)	
Quartzofeldspathic:	
Quartz-Rich	
foliated:	
polygonal:	
Mica-Rich	
foliated:	
polygonal:	
Unknown MRF:	
Total:	0
Volcanic Rock Fragment (VRF)	
Microlitic:	
Lathwork:	
Felsitic:	
Altered VRF:	2
Unknown VRF:	6
Total:	8
Accessory Minerals	
Muscovite:	
Biotite:	
Tourmaline:	
Sphene:	
Zircon:	
Total:	0
Other	
Unknown RF:	
Unknown Highly Dissolved Grain:	4
Total:	4
Matrix	
Clay Cutans:	3
Pore Filling:	17
Total:	20

[a] Rock Fragment

Category	Counts
Porosity	
Intergranular:	89
Intragranular Plagioclase:	
Intragranular Microcline:	1
Intragranular Potassium Feldspar:	2
Intragranular Unknown Feldspar:	
Oversized:	10
Intragrannular VRF	
Unknown VRF:	6
Intragrannular MRF	
Quartzofeldspathic:	1
Intragrannular SRF	
Chert:	5
Argillaceous Chert:	2
Intragranular Unknown RF:	5
Intragranular Unknown Grain:	1
Total:	122
Cement/Overgrowth	
Quartz:	
Kaolinte:	1
Fe-Oxide:	1
Calcite	
intergranular:	
oversized:	
Total:	2
Grain Replacement	
Kaolinite	
Orthoclase:	
Microcline:	
Plagioclase:	
Unknown Feldspar:	
SRF:	
VRF:	
MRF:	
Mica:	
Unknown RF:	
Unknown Grain:	
Calcite	
Orthoclase:	
Microcline:	
Plagioclase:	
Unknown Feldspar:	
SRF:	
VRF:	
MRF:	
Mica:	
Unknown RF:	
Unknown Grain:	
Fe-O	
Orthoclase:	
Microcline:	
Plagioclase:	
Unknown Feldspar:	
SRF:	
VRF:	
MRF:	
Mica:	
Unknown RF:	
Unknown Grain:	
Total:	0

Table B.31. Point count data table for GM-W-051608-3.

Sample Name:	GM-W-051608-3	Sub-unit:	Lower Wilcox
Sample Type:	Outcrop	Total Points Counted:	350

Category	Counts
Quartz	
Mono Crystalline:	110
Poly Crystalline:	15
Volcanic:	2
Sedimentary:	
Total:	127
Feldspar	
Plagioclase:	
Orthoclase:	20
Microcline:	4
Total	24
Sedimentary Rock Fragment (SRF)	
Argillaceous RF[a]:	
Chert:	7
Siltstone RF:	
Sandstone RF:	
Argillaceous Chert:	1
Unknown SRF:	
Total:	8
Metamorphic Rock Fragment (MRF)	
Quartzofeldspathic:	
Quartz-Rich	
foliated:	1
polygonal:	3
Mica-Rich	
foliated:	1
polygonal:	
Unknown MRF:	
Total:	5
Volcanic Rock Fragment (VRF)	
Microlitic:	
Lathwork:	
Felsitic:	1
Altered VRF:	1
Unknown VRF:	
Total:	2
Accessory Minerals	
Muscovite:	3
Biotite:	
Tourmaline:	
Sphene:	1
Zircon:	
Total:	4
Other	
Unknown RF:	
Total:	0
Matrix	
Clay Cutans:	
Pore Filling:	
Total:	0

[a] Rock Fragment

Category	Counts
Porosity	
Intergranular:	
Intragranular Plagioclase:	
Intragranular Microcline:	
Intragranular Potassium Feldspar:	
Intragranular Unknown Feldspar:	1
Oversized:	
Intragrannular VRF	
Intragrannular MRF	
Intragrannular SRF	
Intragranular Unknown RF:	
Intragranular Unknown Grain:	
Total:	1
Cement/Overgrowth	
Quartz:	
Kaolinte:	
Fe-Oxide:	27
Calcite	
intergranular:	136
oversized:	8
Total:	171
Grain Replacement	
Kaolinite	
Orthoclase:	
Microcline:	
Plagioclase:	
Unknown Feldspar:	
SRF:	
VRF:	
MRF:	
Mica:	6
Unknown RF:	
Unknown Grain:	
Calcite	
Orthoclase:	2
Microcline:	
Plagioclase:	
Unknown Feldspar:	
SRF:	
VRF:	
MRF:	
Mica:	
Unknown RF:	
Unknown Grain:	
Fe-O	
Orthoclase:	
Microcline:	
Plagioclase:	
Unknown Feldspar:	
SRF:	
VRF:	
MRF:	
Mica:	
Unknown RF:	
Unknown Grain:	
Total:	8

Table B.32. Point count data table for GM-W-051608-4.

Sample Name:	GM-W-051608-4	Sub-unit:	Lower Wilcox
Sample Type:	Outcrop	Total Points Counted:	349

Category	Counts
Quartz	
Mono Crystalline:	143
Poly Crystalline:	11
Volcanic:	4
Sedimentary:	1
Total:	159
Feldspar	
Plagioclase:	2
Orthoclase:	12
Microcline:	1
Total	15
Sedimentary Rock Fragment (SRF)	
Argillaceous RF[a]:	
Chert:	9
Siltstone RF:	
Sandstone RF:	
Argillaceous Chert:	4
Unknown SRF:	
Total:	13
Metamorphic Rock Fragment (MRF)	
Quartzofeldspathic:	
Quartz-Rich	
foliated:	2
polygonal:	4
Mica-Rich	
foliated:	
polygonal:	
Unknown MRF:	
Total:	6
Volcanic Rock Fragment (VRF)	
Microlitic:	
Lathwork:	
Felsitic:	1
Altered VRF:	3
Unknown VRF:	
Total:	4
Accessory Minerals	
Muscovite:	3
Biotite:	1
Tourmaline:	
Sphene:	
Zircon:	
Total:	4
Other	
Unknown RF:	2
Total:	2
Matrix	
Clay Cutans:	6
Pore Filling:	
Total:	6

[a] Rock Fragment

Category	Counts
Porosity	
Intergranular:	56
Intragranular Plagioclase:	
Intragranular Microcline:	
Intragranular Potassium Feldspar:	
Intragranular Unknown Feldspar:	
Oversized:	2
Intragrannular VRF	
Unknown VRF:	3
Felsitic:	3
Intragrannular MRF	
Quartzofeldspathic:	1
Intragrannular SRF	
Intragranular Unknown RF:	
Intragranular Unknown Grain:	2
Intragranular Mica:	1
Total:	68
Cement/Overgrowth	
Quartz:	
Kaolinte:	1
Fe-Oxide:	66
Calcite	
intergranular:	
oversized:	
Total:	67
Grain Replacement	
Kaolinite	
Orthoclase:	
Microcline:	
Plagioclase:	
Unknown Feldspar:	
SRF:	
VRF:	
MRF:	
Mica:	
Unknown RF:	
Unknown Grain:	1
Calcite	
Orthoclase:	
Microcline:	
Plagioclase:	
Unknown Feldspar:	
SRF:	
VRF:	
MRF:	
Mica:	
Unknown RF:	
Unknown Grain:	
Fe-O	
Orthoclase:	1
Microcline:	
Plagioclase:	
Unknown Feldspar:	
SRF:	
VRF:	
MRF:	
Mica:	
Unknown RF:	
Unknown Grain:	3
Total:	5

Table B.33. Point count data table for Burns 1-9241.

Sample Name:	Burns1-9241	Sub-unit:	Lower Wilcox
Sample Type:	Core	Total Points Counted:	351

Category	Counts
Quartz	
Mono Crystalline:	135
Poly Crystalline:	7
Volcanic:	4
Sedimentary:	
Total:	146
Feldspar	
Plagioclase:	7
Orthoclase:	11
Microcline:	6
Total	24
Sedimentary Rock Fragment (SRF)	
Argillaceous RF[a]:	3
Chert:	15
Siltstone RF:	1
Sandstone RF:	
Argillaceous Chert:	10
Unknown SRF:	
Total:	29
Metamorphic Rock Fragment (MRF)	
Quartzofeldspathic:	2
Quartz-Rich	
foliated:	
polygonal:	2
Mica-Rich	
foliated:	
polygonal:	
Unknown MRF:	1
Metamorphosed Chert:	2
Total:	7
Volcanic Rock Fragment (VRF)	
Microlitic:	
Lathwork:	6
Felsitic:	6
Altered VRF:	1
Unknown VRF:	
Total:	13
Accessory Minerals	
Muscovite:	
Biotite:	
Tourmaline:	
Sphene:	
Zircon:	
Total:	0
Other	
Unknown RF:	
Total:	0
Matrix	
Clay Cutans:	
Pore Filling:	55
Total:	55

[a] Rock Fragment

Category	Counts
Porosity	
Intergranular:	22
Intragranular Plagioclase:	
Intragranular Microcline:	
Intragranular Potassium Feldspar:	
Intragranular Unknown Feldspar:	3
Oversized:	
Intragrannular VRF	
Lathwork:	4
Intragrannular MRF	
Intragrannular SRF	
Intragranular Unknown RF:	
Intragranular Unknown Grain:	3
Total:	32
Cement/Overgrowth	
Quartz:	6
Kaolinte:	36
Fe-Oxide:	1
Calcite	
intergranular:	
oversized:	
Total:	43
Grain Replacement	
Kaolinite	
Orthoclase:	
Microcline:	
Plagioclase:	
Unknown Feldspar:	2
SRF:	
VRF:	
MRF:	
Mica:	
Unknown RF:	
Unknown Grain:	
Calcite	
Orthoclase:	
Microcline:	
Plagioclase:	
Unknown Feldspar:	
SRF:	
VRF:	
MRF:	
Mica:	
Unknown RF:	
Unknown Grain:	
Fe-O	
Orthoclase:	
Microcline:	
Plagioclase:	
Unknown Feldspar:	
SRF:	
VRF:	
MRF:	
Mica:	
Unknown RF:	
Unknown Grain:	
Total:	2

Table B.34. Point count data table for Burns 1-9297.

Sample Name:	Burns1-9297	Sub-unit:	Lower Wilcox
Sample Type:	Core	Total Points Counted:	350

Category	Counts
Quartz	
Mono Crystalline:	182
Poly Crystalline:	8
Volcanic:	4
Sedimentary:	1
B	
Total:	195
Feldspar	
Plagioclase:	9
Orthoclase:	1
Microcline:	1
Unknown Feldspar	1
Total	12
Sedimentary Rock Fragment (SRF)	
Argillaceous RF[a]:	4
Chert:	27
Siltstone RF:	1
Sandstone RF:	
Argillaceous Chert:	5
Unknown SRF:	
Total:	37
Metamorphic Rock Fragment (MRF)	
Quartzofeldspathic:	5
Quartz-Rich	
foliated:	
polygonal:	
Mica-Rich	
foliated:	1
polygonal:	
Unknown MRF:	
Total:	6
Volcanic Rock Fragment (VRF)	
Microlitic:	
Lathwork:	2
Felsitic:	5
Altered VRF:	2
Unknown VRF:	
Total:	9
Accessory Minerals	
Muscovite:	
Biotite:	
Tourmaline:	
Sphene:	
Zircon:	
Total:	0
Other	
Unknown RF:	
Glauconite	1
Total:	1
Matrix	
Clay Cutans:	
Pore Filling:	
Total:	0

[a] Rock Fragment

Category	Counts
Porosity	
Intergranular:	28
Intragranular Plagioclase:	1
Intragranular Microcline:	1
Intragranular Potassium Feldspar:	4
Intragranular Unknown Feldspar:	7
Oversized:	
Intragrannular VRF	
Lathwork:	6
Felsitic:	3
Unknown VRF:	2
Intragrannular MRF	
Quartzofeldspathic:	2
Intragrannular SRF	
Argillaceous RF:	1
Intragranular Unknown RF:	4
Intragranular Unknown Grain:	3
Total:	62
Cement/Overgrowth	
Quartz:	20
Kaolinte:	3
Fe-Oxide:	4
Calcite	
intergranular:	
oversized:	
Total:	27
Grain Replacement	
Kaolinite	
Orthoclase:	
Microcline:	
Plagioclase:	
Unknown Feldspar:	
SRF:	
VRF:	
MRF:	
Mica:	
Unknown RF:	
Unknown Grain:	1
Calcite	
Orthoclase:	
Microcline:	
Plagioclase:	
Unknown Feldspar:	
SRF:	
VRF:	
MRF:	
Mica:	
Unknown RF:	
Unknown Grain:	
Fe-O	
Orthoclase:	
Microcline:	
Plagioclase:	
Unknown Feldspar:	
SRF:	
VRF:	
MRF:	
Mica:	
Unknown RF:	
Unknown Grain:	
Total:	1

Table B.35. Point count data table for Burns 1-9334.

Sample Name:	Burns1-9334	Sub-unit:	Lower Wilcox
Sample Type:	Core	Total Points Counted:	350

Category	Counts
Quartz	
Mono Crystalline:	173
Poly Crystalline:	15
Volcanic:	5
Sedimentary:	
Total:	193
Feldspar	
Plagioclase:	7
Orthoclase:	8
Microcline:	3
Total	18
Sedimentary Rock Fragment (SRF)	
Argillaceous RF[a]:	3
Chert:	14
Siltstone RF:	2
Sandstone RF:	
Argillaceous Chert:	9
Unknown SRF:	
Total:	28
Metamorphic Rock Fragment (MRF)	
Quartzofeldspathic:	
Quartz-Rich	
foliated:	1
polygonal:	3
Mica-Rich	
foliated:	
polygonal:	
Unknown MRF:	
Total:	4
Volcanic Rock Fragment (VRF)	
Microlitic:	
Lathwork:	7
Felsitic:	7
Altered VRF:	3
Unknown VRF:	
Devitrified Glass:	1
Total:	18
Accessory Minerals	
Muscovite:	
Biotite:	
Tourmaline:	
Sphene:	
Zircon:	
Total:	0
Other	
Unknown RF:	
Total:	0
Matrix	
Clay Cutans:	
Pore Filling:	
Total:	0

[a] Rock Fragment

Category	Counts
Porosity	
Intergranular:	33
Intragranular Plagioclase:	1
Intragranular Microcline:	
Intragranular Potassium Feldspar:	5
Intragranular Unknown Feldspar:	
Oversized:	5
Intragrannular VRF	
Altered VRF:	1
Lathwortk:	2
Felsitic:	1
Intragrannular MRF	
Intragrannular SRF	
Chert:	3
Intragranular Unknown RF:	
Intragranular Unknown Grain:	1
Total:	52
Cement/Overgrowth	
Quartz:	33
Kaolinte:	
Fe-Oxide:	
Calcite	
intergranular:	
oversized:	3
Total:	36
Grain Replacement	
Kaolinite	
Orthoclase:	
Microcline:	
Plagioclase:	
Unknown Feldspar:	
SRF:	
VRF:	
MRF:	
Mica:	
Unknown RF:	
Unknown Grain:	
Calcite	
Orthoclase:	
Microcline:	
Plagioclase:	
Unknown Feldspar:	1
SRF:	
VRF:	
MRF:	
Mica:	
Unknown RF:	
Unknown Grain:	
Fe-O	
Orthoclase:	
Microcline:	
Plagioclase:	
Unknown Feldspar:	
SRF:	
VRF:	
MRF:	
Mica:	
Unknown RF:	
Unknown Grain:	
Total:	1

Table B.36. Point count data table for Burns 1-9525.

Sample Name:	Burns 1-9525	Sub-unit:	Lower Wilcox
Sample Type:	Core	Total Points Counted:	350

Category	Counts
Quartz	
Mono Crystalline:	191
Poly Crystalline:	7
Volcanic:	1
Sedimentary:	
Total:	199
Feldspar	
Plagioclase:	8
Orthoclase:	14
Microcline:	2
Altered Feldspar:	2
Total	26
Sedimentary Rock Fragment (SRF)	
Argillaceous RF[a]:	
Chert:	4
Siltstone RF:	
Sandstone RF:	
Argillaceous Chert:	1
Unknown SRF:	
Total:	5
Metamorphic Rock Fragment (MRF)	
Quartzofeldspathic:	
Quartz-Rich	
foliated:	
polygonal:	2
Mica-Rich	
foliated:	1
polygonal:	
Unknown MRF:	
Total:	3
Volcanic Rock Fragment (VRF)	
Microlitic:	
Lathwork:	1
Felsitic:	3
Altered VRF:	1
Unknown VRF:	
Total:	5
Accessory Minerals	
Muscovite:	
Biotite:	
Tourmaline:	
Sphene:	
Zircon:	
Total:	0
Other	
Unknown RF:	
Total:	0
Matrix	
Clay Cutans:	
Pore Filling:	3
Total:	3

[a] Rock Fragment

Category	Counts
Porosity	
Intergranular:	44
Intragranular Plagioclase:	1
Intragranular Microcline:	
Intragranular Potassium Feldspar:	7
Intragranular Unknown Feldspar:	2
Oversized:	5
Intragrannular VRF	
Felsitic:	3
Lathwork:	1
Altered VRF:	1
Intragrannular MRF	
Intragrannular SRF	
Chert:	4
Argillaceous Chert:	1
Intragranular Unknown RF:	
Intragranular Unknown Grain:	
Total:	69
Cement/Overgrowth	
Quartz:	27
Kaolinte:	12
Fe-Oxide:	1
Calcite	
intergranular:	
oversized:	
Total:	40
Grain Replacement	
Kaolinite	
Orthoclase:	
Microcline:	
Plagioclase:	
Unknown Feldspar:	
SRF:	
VRF:	
MRF:	
Mica:	
Unknown RF:	
Unknown Grain:	
Calcite	
Orthoclase:	
Microcline:	
Plagioclase:	
Unknown Feldspar:	
SRF:	
VRF:	
MRF:	
Mica:	
Unknown RF:	
Unknown Grain:	
Fe-O	
Orthoclase:	
Microcline:	
Plagioclase:	
Unknown Feldspar:	
SRF:	
VRF:	
MRF:	
Mica:	
Unknown RF:	
Unknown Grain:	
Total:	0

Table B.37. Point count data table for Burns 1-9614.

Sample Name:	Burns 1-9614	Sub-unit:	Lower Wilcox
Sample Type:	Core	Total Points Counted:	348

Category	Counts
Quartz	
Mono Crystalline:	225
Poly Crystalline:	7
Volcanic:	3
Sedimentary:	
Total:	235
Feldspar	
Plagioclase:	9
Orthoclase:	7
Microcline:	2
Unknown Feldspar:	1
Total	19
Sedimentary Rock Fragment (SRF)	
Argillaceous RF[a]:	
Chert:	8
Siltstone RF:	
Sandstone RF:	
Argillaceous Chert:	
Unknown SRF:	
Total:	8
Metamorphic Rock Fragment (MRF)	
Quartzofeldspathic:	
Quartz-Rich	
foliated:	1
polygonal:	6
Mica-Rich	
foliated:	
polygonal:	2
Unknown MRF:	
Total:	9
Volcanic Rock Fragment (VRF)	
Microlitic:	
Lathwork:	
Felsitic:	1
Altered VRF:	
Unknown VRF:	
Total:	1
Accessory Minerals	
Muscovite:	1
Biotite:	1
Tourmaline:	
Sphene:	
Zircon:	
Total:	2
Other	
Unknown RF:	1
Total:	1
Matrix	
Clay Cutans:	
Pore Filling:	
Total:	0

[a] Rock Fragment

Category	Counts
Porosity	
Intergranular:	30
Intragranular Plagioclase:	2
Intragranular Microcline:	
Intragranular Potassium Feldspar:	5
Intragranular Unknown Feldspar:	2
Oversized:	
Intragrannular VRF	
Intragrannular MRF	
Intragrannular SRF	
Chert:	2
Intragranular Unknown RF:	3
Intragranular Unknown Grain:	6
Total:	50
Cement/Overgrowth	
Quartz:	15
Kaolinte:	
Fe-Oxide:	1
Calcite	
intergranular:	1
oversized:	6
Total:	23
Grain Replacement	
Kaolinite	
Orthoclase:	
Microcline:	
Plagioclase:	
Unknown Feldspar:	
SRF:	
VRF:	
MRF:	
Mica:	
Unknown RF:	
Unknown Grain:	
Calcite	
Orthoclase:	
Microcline:	
Plagioclase:	
Unknown Feldspar:	
SRF:	
VRF:	
MRF:	
Mica:	
Unknown RF:	
Unknown Grain:	
Fe-O	
Orthoclase:	
Microcline:	
Plagioclase:	
Unknown Feldspar:	
SRF:	
VRF:	
MRF:	
Mica:	
Unknown RF:	
Unknown Grain:	
Total:	0

Table B.38. Point count data table for Paul 1-9152.

Sample Name:	Paul 1-9152	Sub-unit:	Lower Wilcox
Sample Type:	Core	Total Points Counted:	347

Category	Counts
Quartz	
Mono Crystalline:	207
Poly Crystalline:	9
Volcanic:	
Sedimentary:	
Total:	216
Feldspar	
Plagioclase:	7
Orthoclase:	9
Microcline:	
Total	16
Sedimentary Rock Fragment (SRF)	
Argillaceous RF[a]:	
Chert:	4
Siltstone RF:	
Sandstone RF:	1
Argillaceous Chert:	2
Unknown SRF:	
Total:	7
Metamorphic Rock Fragment (MRF)	
Quartzofeldspathic:	
Quartz-Rich	
foliated:	1
polygonal:	
Mica-Rich	
foliated:	3
polygonal:	3
Unknown MRF:	1
Total:	8
Volcanic Rock Fragment (VRF)	
Microlitic:	
Lathwork:	
Felsitic:	3
Altered VRF:	1
Unknown VRF:	
Total:	4
Accessory Minerals	
Muscovite:	2
Biotite:	
Tourmaline:	
Sphene:	
Zircon:	
Total:	2
Other	
Unknown RF:	
Glauconite:	1
Total:	1
Matrix	
Clay Cutans:	
Pore Filling:	14
Total:	14

[a] Rock Fragment

Category	Counts
Porosity	
Intergranular:	32
Intragranular Plagioclase:	
Intragranular Microcline:	
Intragranular Potassium Feldspar:	4
Intragranular Unknown Feldspar:	5
Oversized:	3
Intragrannular VRF	
Lathwork:	2
Felsitic:	1
Intragrannular MRF	
Intragrannular SRF	
Intragranular Unknown RF:	
Intragranular Unknown Grain:	2
Intragranular Calcite replacing Feldspar	1
Total:	50
Cement/Overgrowth	
Quartz:	12
Kaolinte:	
Fe-Oxide:	10
Calcite	
intergranular:	3
oversized:	
Total:	25
Grain Replacement	
Kaolinite	
Orthoclase:	
Microcline:	
Plagioclase:	
Unknown Feldspar:	
SRF:	
VRF:	
MRF:	
Mica:	
Unknown RF:	
Unknown Grain:	
Calcite	
Orthoclase:	
Microcline:	
Plagioclase:	
Unknown Feldspar:	2
SRF:	
VRF:	
MRF:	
Mica:	
Unknown RF:	
Unknown Grain:	
Fe-O	
Orthoclase:	
Microcline:	
Plagioclase:	
Unknown Feldspar:	
SRF:	
VRF:	
MRF:	
Mica:	1
Unknown RF:	
Unknown Grain:	1
Total:	4

Table B.39. Point count data table for Winch St. 4-9310.

Sample Name:	Winch St. 4- 9310	Sub-unit:	Lower Wilcox
Sample Type:	Core	Total Points Counted:	350

Category	Counts
Quartz	
Mono Crystalline:	208
Poly Crystalline:	5
Volcanic:	6
Sedimentary:	
Total:	219
Feldspar	
Plagioclase:	13
Orthoclase:	3
Microcline:	
Total	16
Sedimentary Rock Fragment (SRF)	
Argillaceous RF[a]:	1
Chert:	2
Siltstone RF:	
Sandstone RF:	
Argillaceous Chert:	
Unknown SRF:	
Total:	3
Metamorphic Rock Fragment (MRF)	
Quartzofeldspathic:	
Quartz-Rich	
foliated:	3
polygonal:	2
Mica-Rich	
foliated:	1
polygonal:	
Unknown MRF:	
Total:	6
Volcanic Rock Fragment (VRF)	
Microlitic:	
Lathwork:	1
Felsitic:	
Altered VRF:	
Unknown VRF:	
Total:	1
Accessory Minerals	
Muscovite:	3
Biotite:	1
Tourmaline:	1
Sphene:	
Zircon:	1
Total:	6
Other	
Unknown RF:	1
Total:	1
Matrix	
Clay Cutans:	
Pore Filling:	
Total:	0

[a] Rock Fragment

Category	Counts
Porosity	
Intergranular:	33
Intragranular Plagioclase:	
Intragranular Microcline:	
Intragranular Potassium Feldspar:	1
Intragranular Unknown Feldspar:	5
Oversized:	7
Intragrannular VRF	
Felsitic:	1
Intragrannular MRF	
Intragrannular SRF	
Intragranular Unknown RF:	4
Intragranular Unknown Grain:	5
Total:	56
Cement/Overgrowth	
Quartz:	10
Kaolinte:	
Fe-Oxide:	2
Calcite	
intergranular:	13
oversized:	2
Total:	27
Grain Replacement	
Kaolinite	
Orthoclase:	
Microcline:	
Plagioclase:	
Unknown Feldspar:	
SRF:	
VRF:	
MRF:	
Mica:	
Unknown RF:	
Unknown Grain:	
Calcite	
Orthoclase:	1
Microcline:	
Plagioclase:	
Unknown Feldspar:	10
SRF:	
VRF:	
MRF:	
Mica:	
Unknown RF:	
Unknown Grain:	3
Fe-O	
Orthoclase:	
Microcline:	
Plagioclase:	
Unknown Feldspar:	
SRF:	
VRF:	
MRF:	
Mica:	
Unknown RF:	
Unknown Grain:	1
Total:	15

Table B.40. Point count data table for Winch St 4-9948.

Sample Name:	Winch St. 4.-9948	Sub-unit:	Upper Wilcox
Sample Type:	Core	Total Points Counted:	350

Category	Counts
Quartz	
Mono Crystalline:	149
Poly Crystalline:	7
Volcanic:	4
Sedimentary:	2
Total:	162
Feldspar	
Plagioclase:	8
Orthoclase:	7
Microcline:	
Unknown Feldspar:	4
Total	19
Sedimentary Rock Fragment (SRF)	
Argillaceous RF[a]:	1
Chert:	13
Siltstone RF:	
Sandstone RF:	
Argillaceous Chert:	2
Unknown SRF:	
Total:	16
Metamorphic Rock Fragment (MRF)	
Quartzofeldspathic:	1
Quartz-Rich	
foliated:	
polygonal:	
Mica-Rich	
foliated:	
polygonal:	
Unknown MRF:	
Total:	1
Volcanic Rock Fragment (VRF)	
Microlitic:	
Lathwork:	2
Felsitic:	1
Altered VRF:	4
Unknown VRF:	
Total:	7
Accessory Minerals	
Muscovite:	
Biotite:	
Tourmaline:	
Sphene:	
Zircon:	
Total:	0
Other	
Unknown RF:	
Unknown Grain:	1
Total:	1
Matrix	
Clay Cutans:	
Pore Filling:	
Total:	0

[a] Rock Fragment

Category	Counts
Porosity	
Intergranular:	2
Intragranular Plagioclase:	
Intragranular Microcline:	
Intragranular Potassium Feldspar:	
Intragranular Unknown Feldspar:	6
Oversized:	
Intragrannular VRF	
Lathwork:	1
Intragrannular MRF	
Intragrannular SRF	
Intragranular Unknown RF:	
Intragranular Unknown Grain:	6
Total:	15
Cement/Overgrowth	
Quartz:	
Kaolinte:	
Fe-Oxide:	
Calcite	
intergranular:	120
oversized:	6
Total:	126
Grain Replacement	
Kaolinite	
Orthoclase:	
Microcline:	
Plagioclase:	
Unknown Feldspar:	
SRF:	
VRF:	
MRF:	
Mica:	
Unknown RF:	
Unknown Grain:	
Calcite	
Orthoclase:	1
Microcline:	
Plagioclase:	
Unknown Feldspar:	1
SRF:	
VRF:	
MRF:	
Mica:	
Unknown RF:	
Unknown Grain:	1
Fe-O	
Orthoclase:	
Microcline:	
Plagioclase:	
Unknown Feldspar:	
SRF:	
VRF:	
MRF:	
Mica:	
Unknown RF:	
Unknown Grain:	
Total:	3

Appendix C : Detrital Zircon Data Tables

Table C.1. Detrital zircon data table for Bailey 1C.

	Sample Name:	Bailey 1C				Isotopic Ratios					Apparent Ages (Ma)							
	Analysis	U	^{206}Pb	$^{207}Pb^*$	± 2 σ	$^{207}Pb^*$	± 2 σ	$^{206}Pb^*$	± 2 σ	Rho	$^{207}Pb^*$	± 1 σ	$^{207}Pb^*$	± 1 σ	$^{206}Pb^*$	± 1 σ	Best	± 1 σ
		ppm	^{204}Pb	$^{206}Pb^*$	abs	^{235}U	abs	^{238}U	abs		$^{206}Pb^*$	abs	^{235}U	abs	^{238}U	abs	Age	abs
1	Bailey-1C 72	287	66	0.0851	±0.0265	0.1458	±0.0519	0.0124	±0.0021	0.4846	1319	±301.6	138	±23.0	80	±6.8	80	±6.8
2	Bailey-1C 14	184	60	0.0850	±0.0169	0.1601	±0.0334	0.0137	±0.0008	0.2978	1316	±193.2	151	±14.6	87	±2.7	87	±2.7
3	Bailey-1C 69	817	236	0.0517	±0.0024	0.1056	±0.0052	0.0148	±0.0002	0.2827	274	±53.7	102	±2.4	95	±0.6	95	±0.6
4	Bailey-1C 124	469	172	0.0608	±0.0037	0.1414	±0.0090	0.0169	±0.0003	0.3104	632	±65.0	134	±4.0	108	±1.1	108	±1.1
5	Bailey-1C 25	278	76	0.0884	±0.0116	0.2114	±0.0319	0.0174	±0.0013	0.4926	1390	±126.2	195	±13.4	111	±4.1	111	±4.1
6	Bailey-1C 108	166	67	0.0844	±0.0189	0.2033	±0.0469	0.0175	±0.0010	0.2443	1303	±217.5	188	±19.8	112	±3.1	112	±3.1
7	Bailey-1C 22	419	111	0.0771	±0.0067	0.1973	±0.0185	0.0186	±0.0007	0.3770	1123	±86.7	183	±7.9	119	±2.1	119	±2.1
8	Bailey-1C 111	179	53	0.0820	±0.0202	0.2314	±0.0604	0.0205	±0.0018	0.3368	1246	±240.7	211	±24.9	131	±5.7	131	±5.7
9	Bailey-1C 19	216	89	0.0730	±0.0069	0.2118	±0.0215	0.0210	±0.0008	0.3808	1015	±95.1	195	±9.0	134	±2.6	134	±2.6
10	Bailey-1C 45	386	162	0.0656	±0.0046	0.1992	±0.0151	0.0220	±0.0006	0.3657	792	±73.9	184	±6.4	141	±1.9	141	±1.9
11	Bailey-1C 128	163	74	0.0884	±0.0091	0.3410	±0.0363	0.0280	±0.0007	0.2516	1391	±98.9	298	±13.7	178	±2.4	178	±2.4
12	Bailey-1C 50	412	269	0.0616	±0.0026	0.2739	±0.0189	0.0323	±0.0018	0.7947	659	±45.0	246	±7.5	205	±5.5	205	±5.5
13	Bailey-1C 59	216	81	0.0857	±0.0093	0.4166	±0.0458	0.0353	±0.0007	0.1882	1331	±104.5	354	±16.4	223	±2.3	223	±2.3
14	Bailey-1C 36	573	339	0.0536	±0.0020	0.2628	±0.0164	0.0356	±0.0018	0.8016	355	±42.1	237	±6.6	225	±5.5	225	±5.5
15	Bailey-1C 70	261	117	0.0866	±0.0051	0.4364	±0.0347	0.0365	±0.0019	0.6661	1352	±57.2	368	±12.3	231	±6.0	231	±6.0
16	Bailey-1C 5	361	189	0.0615	±0.0031	0.3168	±0.0189	0.0374	±0.0012	0.5335	655	±54.1	279	±7.3	237	±3.7	237	±3.7
17	Bailey-1C 80	396	165	0.0650	±0.0034	0.3411	±0.0203	0.0381	±0.0011	0.4764	774	±54.9	298	±7.7	241	±3.3	241	±3.3
18	Bailey-1C 94	442	211	0.0678	±0.0051	0.3621	±0.0304	0.0388	±0.0014	0.4442	861	±78.1	314	±11.3	245	±4.5	245	±4.5
19	Bailey-1C 106	391	200	0.0634	±0.0032	0.3438	±0.0182	0.0393	±0.0007	0.3296	723	±53.1	300	±6.9	248	±2.1	248	±2.1
20	Bailey-1C 51	235	143	0.0672	±0.0046	0.3826	±0.0266	0.0413	±0.0006	0.2054	844	±70.7	329	±9.8	261	±1.8	261	±1.8
21	Bailey-1C 27	145	115	0.0665	±0.0066	0.3808	±0.0420	0.0416	±0.0019	0.4229	821	±104.3	328	±15.4	262	±6.0	262	±6.0
22	Bailey-1C 47	91	61	0.0822	±0.0140	0.5398	±0.0959	0.0476	±0.0024	0.2792	1251	±167.0	438	±31.6	300	±7.3	300	±7.3
23	Bailey-1C 123	184	214	0.0605	±0.0037	0.5558	±0.0363	0.0666	±0.0014	0.3242	623	±66.7	449	±11.9	416	±4.3	416	±4.3
24	Bailey-1C 62	195	227	0.0638	±0.0037	0.5983	±0.0379	0.0681	±0.0016	0.3700	734	±62.2	476	±12.0	424	±4.8	424	±4.8
25	Bailey-1C 31	101	172	0.0694	±0.0037	0.7300	±0.0473	0.0763	±0.0028	0.5646	910	±55.1	557	±13.9	474	±8.4	474	±8.4
26	Bailey-1C 11	249	241	0.0788	±0.0039	0.8975	±0.0464	0.0826	±0.0014	0.3238	1166	±48.5	650	±12.4	512	±4.1	512	±4.1
27	Bailey-1C 21	302	361	0.0595	±0.0020	0.7540	±0.0577	0.0920	±0.0063	0.8987	584	±36.4	571	±16.7	567	±18.7	567	±18.7
28	Bailey-1C 135	168	268	0.0800	±0.0077	1.0937	±0.1301	0.0992	±0.0069	0.5877	1196	±94.9	750	±31.5	610	±20.3	610	±20.3
29	Bailey-1C 87	296	528	0.0645	±0.0028	0.9655	±0.0587	0.1086	±0.0046	0.7025	757	±45.6	686	±15.2	665	±13.5	665	±13.5
30	Bailey-1C 122	231	341	0.0711	±0.0040	1.1728	±0.0896	0.1197	±0.0063	0.6839	959	±56.9	788	±20.9	729	±18.0	729	±18.0
31	Bailey-1C 64	264	874	0.0771	±0.0013	1.9098	±0.0474	0.1797	±0.0034	0.7530	1123	±16.3	1084	±8.3	1066	±9.2	1123	±16.3
32	Bailey-1C 73	156	560	0.0774	±0.0019	2.2390	±0.0629	0.2098	±0.0028	0.4837	1131	±24.5	1193	±9.9	1228	±7.6	1131	±24.5
33	Bailey-1C 100	204	587	0.0781	±0.0023	2.0116	±0.0849	0.1868	±0.0057	0.7267	1149	±28.8	1119	±14.3	1104	±15.6	1149	±28.8
34	Bailey-1C 77	185	846	0.0788	±0.0012	2.0599	±0.0503	0.1895	±0.0036	0.7882	1168	±14.9	1136	±8.4	1119	±9.9	1168	±14.9
35	Bailey-1C 82	494	1,284	0.0790	±0.0015	1.9533	±0.0848	0.1794	±0.0070	0.8981	1171	±18.9	1100	±14.6	1064	±19.1	1171	±18.9
36	Bailey-1C 99	728	898	0.0799	±0.0006	2.2205	±0.0798	0.2015	±0.0071	0.9796	1195	±7.1	1188	±12.6	1183	±19.0	1195	±7.1
37	Bailey-1C 28	422	1,510	0.0810	±0.0004	2.5670	±0.0674	0.2299	±0.0059	0.9830	1221	±4.7	1291	±9.6	1334	±15.6	1221	±4.7
38	Bailey-1C 81	83	221	0.0811	±0.0024	1.8352	±0.0774	0.1642	±0.0049	0.7006	1223	±29.6	1058	±13.9	980	±13.4	1223	±29.6
39	Bailey-1C 30	144	506	0.0854	±0.0021	2.1970	±0.0721	0.1865	±0.0040	0.6492	1326	±24.2	1180	±11.4	1102	±10.8	1326	±24.2
40	Bailey-1C 26	494	858	0.0871	±0.0012	2.6026	±0.1651	0.2167	±0.0134	0.9753	1363	±13.5	1301	±23.3	1264	±35.5	1363	±13.5
41	Bailey-1C 132	116	380	0.0905	±0.0033	2.9022	±0.1639	0.2325	±0.0100	0.7616	1436	±34.9	1382	±21.3	1348	±26.2	1436	±34.9
42	Bailey-1C 114	265	1,133	0.0913	±0.0010	3.4663	±0.1157	0.2754	±0.0087	0.9478	1453	±10.1	1520	±13.2	1568	±22.0	1453	±10.1
43	Bailey-1C 104	114	336	0.0916	±0.0026	2.7507	±0.1831	0.2178	±0.0132	0.9078	1459	±26.5	1342	±24.8	1270	±34.8	1459	±26.5
44	Bailey-1C 9	159	764	0.0926	±0.0006	3.5171	±0.0966	0.2755	±0.0074	0.9727	1479	±6.0	1531	±10.9	1569	±18.6	1479	±6.0
45	Bailey-1C 32	107	630	0.0952	±0.0010	3.8300	±0.1087	0.2919	±0.0077	0.9256	1531	±10.1	1599	±11.4	1651	±19.1	1531	±10.1
46	Bailey-1C 34	250	785	0.0958	±0.0009	2.8678	±0.1382	0.2171	±0.0103	0.9798	1544	±9.1	1373	±18.1	1267	±27.1	1544	±9.1
47	Bailey-1C 49	136	576	0.0960	±0.0012	3.1303	±0.1319	0.2364	±0.0095	0.9532	1548	±12.0	1440	±16.2	1368	±24.7	1548	±12.0
48	Bailey-1C 107	239	719	0.0974	±0.0013	3.6113	±0.1120	0.2688	±0.0075	0.9046	1576	±12.4	1552	±12.3	1535	±19.2	1576	±12.4
49	Bailey-1C 4	147	551	0.0987	±0.0040	4.1795	±0.1860	0.3071	±0.0060	0.4364	1600	±37.4	1670	±18.2	1726	±14.7	1600	±37.4
50	Bailey-1C 76	785	1,610	0.1004	±0.0026	3.2539	±0.1205	0.2350	±0.0063	0.7269	1632	±23.6	1470	±14.4	1361	±16.5	1632	±23.6
51	Bailey-1C 18	422	1,730	0.1030	±0.0004	4.2276	±0.1337	0.2977	±0.0094	0.9942	1679	±3.1	1679	±13.0	1680	±23.2	1679	±3.1
52	Bailey-1C 74	97	394	0.1041	±0.0012	4.5713	±0.1572	0.3183	±0.0103	0.9446	1699	±10.4	1744	±14.3	1782	±25.3	1699	±10.4
53	Bailey-1C 46	632	1,902	0.1042	±0.0006	4.4728	±0.0978	0.3114	±0.0066	0.9619	1700	±5.5	1726	±9.1	1748	±16.1	1700	±5.5
54	Bailey-1C 15	258	996	0.1045	±0.0013	3.8657	±0.1850	0.2683	±0.0124	0.9679	1706	±11.1	1607	±19.3	1532	±31.6	1706	±11.1
55	Bailey-1C 10	72	333	0.1048	±0.0021	4.2514	±0.2149	0.2942	±0.0137	0.9183	1711	±18.4	1684	±20.8	1663	±34.0	1711	±18.4
56	Bailey-1C 84	414	892	0.1088	±0.0017	4.5514	±0.1516	0.3033	±0.0090	0.8904	1780	±13.8	1740	±13.9	1708	±22.3	1780	±13.8
57	Bailey-1C 78	305	1,516	0.1101	±0.0028	5.3515	±0.2192	0.3525	±0.0112	0.7756	1801	±23.5	1877	±17.5	1947	±26.7	1801	±23.5
58	Bailey-1C 23	387	940	0.1103	±0.0007	4.3074	±0.2064	0.2833	±0.0135	0.9921	1804	±5.5	1695	±19.7	1608	±33.8	1804	±5.5
59	Bailey-1C 133	181	427	0.1110	±0.0022	3.9641	±0.1900	0.2590	±0.0113	0.9124	1816	±17.8	1627	±19.4	1485	±29.0	1816	±17.8
60	Bailey-1C 134	125	556	0.1118	±0.0021	5.5519	±0.1598	0.3601	±0.0078	0.7536	1829	±17.1	1909	±12.4	1983	±18.5	1829	±17.1
61	Bailey-1C 24	131	551	0.1120	±0.0011	5.6039	±0.2174	0.3628	±0.0136	0.9663	1833	±9.0	1917	±16.7	1995	±32.2	1833	±9.0
62	Bailey-1C 118	265	836	0.1133	±0.0020	5.6972	±0.2552	0.3649	±0.0150	0.9150	1852	±16.3	1931	±19.3	2005	±35.3	1852	±16.3
63	Bailey-1C 119	64	171	0.1140	±0.0034	5.5617	±0.2344	0.3537	±0.0107	0.7167	1865	±26.5	1910	±18.1	1952	±25.4	1865	±26.5
64	Bailey-1C 67	909	3,041	0.1212	±0.0004	5.7354	±0.3547	0.3431	±0.0212	0.9987	1975	±2.8	1937	±26.7	1901	±50.9	1975	±2.8
65	Bailey-1C 53	124	1,516	0.1308	±0.0007	7.1401	±0.1077	0.3958	±0.0056	0.9431	2109	±4.4	2129	±6.7	2150	±13.0	2109	±4.4
66	Bailey-1C 54	125	217	0.1410	±0.0148	6.6139	±0.7720	0.3402	±0.0173	0.4360	2239	±90.8	2061	±51.5	1888	±41.6	2239	±90.8
67	Bailey-1C 37	79	852	0.1785	±0.0008	12.9040	±0.2586	0.5243	±0.0103	0.9757	2639	±3.6	2673	±9.4	2717	±21.7	2639	±3.6

Table C.2. Detrital zircon data table for Burns 1.

Sample Name: Burns 1

	Analysis	U ppm	$^{206}Pb/^{204}Pb$	$^{207}Pb^*/^{206}Pb^*$	± 2 σ abs	$^{207}Pb^*/^{235}U$	± 2 σ abs	$^{206}Pb^*/^{238}U$	± 2 σ abs	Rho	$^{207}Pb^*/^{206}Pb^*$	± 1 σ abs	$^{207}Pb^*/^{235}U$	± 1 σ abs	$^{206}Pb^*/^{238}U$	± 1 σ abs	Best Age	± 1 σ abs
			Isotopic Ratios								Apparent Ages (Ma)							
1	Burns-1 11	721	146	0.0538	±0.0045	0.0721	±0.0062	0.0097	±0.0002	0.2068	363	±94.2	71	±2.9	62	±0.5	62	±0.5
2	Burns-1 79	1389	475	0.0490	±0.0023	0.0695	±0.0033	0.0103	±0.0001	0.2118	149	±54.8	68	±1.6	66	±0.3	66	±0.3
3	Burns-1 26	449	112	0.0467	±0.0083	0.0679	±0.0122	0.0105	±0.0003	0.1515	35	±212.2	67	±5.8	68	±0.9	68	±0.9
4	Burns-1 55	118	34	0.0717	±0.0218	0.1054	±0.0325	0.0107	±0.0006	0.1736	978	±309.6	102	±14.9	68	±1.8	68	±1.8
5	Burns-1 18	232	75	0.0530	±0.0088	0.0814	±0.0138	0.0111	±0.0004	0.2287	331	±187.6	79	±6.5	71	±1.4	71	±1.4
6	Burns-1 25	203	62	0.0546	±0.0134	0.0842	±0.0210	0.0112	±0.0005	0.1739	394	±275.3	82	±9.8	72	±1.5	72	±1.5
7	Burns-1 88	1702	721	0.0468	±0.0015	0.0727	±0.0025	0.0113	±0.0001	0.3196	40	±38.2	71	±1.2	72	±0.4	72	±0.4
8	Burns-1 120	456	200	0.0782	±0.0139	0.1230	±0.0226	0.0114	±0.0005	0.2416	1152	±176.9	118	±10.2	73	±1.6	73	±1.6
9	Burns-1 119	795	176	0.0740	±0.0061	0.1170	±0.0100	0.0115	±0.0003	0.3011	1042	±82.5	112	±4.6	73	±0.9	73	±0.9
10	Burns-1 110	213	80	0.0577	±0.0119	0.0922	±0.0191	0.0116	±0.0003	0.1302	519	±225.7	90	±8.9	74	±1.0	74	±1.0
11	Burns-1 124	290	116	0.0502	±0.0103	0.0817	±0.0169	0.0118	±0.0003	0.1105	206	±238.6	80	±7.9	76	±0.9	76	±0.9
12	Burns-1 133	478	220	0.0442	±0.0048	0.0735	±0.0081	0.0121	±0.0002	0.1811	0	-±0.0	72	±3.8	77	±0.8	77	±0.8
13	Burns-1 9	186	52	0.0748	±0.0151	0.1251	±0.0256	0.0121	±0.0004	0.1745	1063	±202.8	120	±11.6	78	±1.4	78	±1.4
14	Burns-1 3	344	85	0.0665	±0.0027	0.1113	±0.0052	0.0121	±0.0003	0.5139	822	±41.8	107	±2.4	78	±0.9	78	±0.9
15	Burns-1 33	372	179	0.0519	±0.0074	0.0871	±0.0125	0.0122	±0.0002	0.1160	281	±163.6	85	±5.9	78	±0.6	78	±0.6
16	Burns-1 4	1194	338	0.0501	±0.0019	0.0849	±0.0036	0.0123	±0.0002	0.3946	199	±45.0	83	±1.7	79	±0.7	79	±0.7
17	Burns-1 48	374	120	0.0625	±0.0080	0.1060	±0.0137	0.0123	±0.0003	0.1811	690	±136.0	102	±6.3	79	±0.9	79	±0.9
18	Burns-1 128	249	85	0.0542	±0.0128	0.0921	±0.0218	0.0123	±0.0003	0.1051	379	±265.1	89	±10.1	79	±1.0	79	±1.0
19	Burns-1 92	520	165	0.0583	±0.0053	0.1008	±0.0093	0.0125	±0.0002	0.1547	542	±100.1	98	±4.3	80	±0.6	80	±0.6
20	Burns-1 63	478	206	0.0529	±0.0031	0.0921	±0.0054	0.0126	±0.0002	0.2173	324	±65.5	89	±2.5	81	±0.5	81	±0.5
21	Burns-1 42	177	55	0.0895	±0.0230	0.1573	±0.0416	0.0128	±0.0008	0.2325	1415	±246.1	148	±18.3	82	±2.5	82	±2.5
22	Burns-1 16	709	332	0.0491	±0.0030	0.0872	±0.0054	0.0129	±0.0002	0.1960	154	±71.4	85	±2.5	82	±0.5	82	±0.5
23	Burns-1 57	593	265	0.0455	±0.0035	0.0837	±0.0065	0.0133	±0.0002	0.1584	0	±0.0	82	±3.0	85	±0.5	85	±0.5
24	Burns-1 20	255	90	0.0775	±0.0135	0.1477	±0.0261	0.0138	±0.0004	0.1567	1135	±173.6	140	±11.5	88	±1.2	88	±1.2
25	Burns-1 101	1098	495	0.0482	±0.0025	0.0935	±0.0051	0.0141	±0.0002	0.2884	112	±61.2	91	±2.4	90	±0.7	90	±0.7
26	Burns-1 104	132	58	0.0523	±0.0208	0.1031	±0.0415	0.0143	±0.0009	0.1478	299	±454.0	100	±19.1	92	±2.7	92	±2.7
27	Burns-1 54	918	421	0.0516	±0.0032	0.1037	±0.0067	0.0146	±0.0002	0.2579	267	±71.6	100	±3.1	93	±0.8	93	±0.8
28	Burns-1 52	601	198	0.0455	±0.0041	0.0918	±0.0083	0.0146	±0.0002	0.1394	0	-±0.0	89	±3.9	94	±0.6	94	±0.6
29	Burns-1 114	305	135	0.0597	±0.0091	0.1244	±0.0190	0.0151	±0.0003	0.1149	592	±164.9	119	±8.6	97	±0.8	97	±0.8
30	Burns-1 8	838	259	0.0609	±0.0034	0.1274	±0.0116	0.0152	±0.0011	0.7962	635	±59.5	122	±5.2	97	±3.5	97	±3.5
31	Burns-1 44	678	390	0.0479	±0.0035	0.1018	±0.0076	0.0154	±0.0003	0.2713	94	±85.4	98	±3.5	99	±1.0	99	±1.0
32	Burns-1 90	132	62	0.0557	±0.0153	0.1195	±0.0331	0.0155	±0.0006	0.1446	442	±305.2	115	±15.0	99	±2.0	99	±2.0
33	Burns-1 72	133	76	0.0574	±0.0193	0.1235	±0.0417	0.0156	±0.0005	0.0981	508	±369.7	118	±18.9	100	±1.6	100	±1.6
34	Burns-1 70	1072	433	0.0512	±0.0018	0.1112	±0.0044	0.0157	±0.0003	0.4539	251	±40.2	107	±2.0	101	±0.9	101	±0.9
35	Burns-1 122	207	85	0.0724	±0.0090	0.1774	±0.0234	0.0178	±0.0008	0.3230	998	±126.6	166	±10.1	114	±2.4	114	±2.4
36	Burns-1 113	365	123	0.0774	±0.0075	0.2020	±0.0216	0.0189	±0.0009	0.4363	1131	±95.9	187	±9.1	121	±2.8	121	±2.8
37	Burns-1 75	942	592	0.0517	±0.0019	0.1368	±0.0068	0.0192	±0.0006	0.6644	274	±42.8	130	±3.1	122	±2.0	122	±2.0
38	Burns-1 13	148	101	0.0562	±0.0116	0.1787	±0.0373	0.0231	±0.0006	0.1228	459	±229.9	167	±16.1	147	±1.9	147	±1.9
39	Burns-1 82	140	94	0.0514	±0.0105	0.1650	±0.0339	0.0233	±0.0006	0.1212	258	±234.6	155	±14.8	148	±1.8	148	±1.8
40	Burns-1 102	242	184	0.0504	±0.0049	0.1626	±0.0161	0.0234	±0.0005	0.2137	212	±111.9	153	±7.0	149	±1.6	149	±1.6
41	Burns-1 103	250	176	0.0498	±0.0073	0.1672	±0.0245	0.0244	±0.0003	0.0928	184	±170.2	157	±10.7	155	±1.0	155	±1.0
42	Burns-1 21	110	105	0.0621	±0.0111	0.2102	±0.0385	0.0245	±0.0010	0.2309	678	±190.3	194	±16.1	156	±3.3	156	±3.3
43	Burns-1 56	236	171	0.0533	±0.0057	0.1849	±0.0202	0.0251	±0.0006	0.2149	343	±121.0	172	±8.7	160	±1.9	160	±1.9
44	Burns-1 129	352	266	0.0579	±0.0038	0.2053	±0.0138	0.0257	±0.0004	0.2558	524	±71.4	190	±5.8	164	±1.4	164	±1.4
45	Burns-1 30	416	321	0.0541	±0.0036	0.1940	±0.0131	0.0260	±0.0003	0.1807	376	±74.9	180	±5.6	165	±1.0	165	±1.0
46	Burns-1 132	456	384	0.0563	±0.0043	0.2026	±0.0160	0.0261	±0.0006	0.2751	466	±84.3	187	±6.8	166	±1.8	166	±1.8
47	Burns-1 64	206	170	0.0570	±0.0056	0.2091	±0.0209	0.0266	±0.0003	0.1286	491	±109.2	193	±8.8	169	±1.1	169	±1.1
48	Burns-1 35	196	156	0.0537	±0.0049	0.1980	±0.0184	0.0267	±0.0005	0.1910	359	±102.9	183	±7.8	170	±1.5	170	±1.5
49	Burns-1 22	262	150	0.0683	±0.0112	0.2519	±0.0415	0.0267	±0.0006	0.1257	879	±169.2	228	±16.8	170	±1.7	170	±1.7
50	Burns-1 77	297	274	0.0552	±0.0031	0.2068	±0.0121	0.0272	±0.0004	0.2738	420	±62.6	191	±5.1	173	±1.4	173	±1.4
51	Burns-1 83	489	449	0.0525	±0.0016	0.1999	±0.0067	0.0276	±0.0004	0.4696	307	±33.8	185	±2.8	176	±1.4	176	±1.4
52	Burns-1 47	385	231	0.0701	±0.0040	0.2680	±0.0158	0.0277	±0.0004	0.2664	930	±58.3	241	±6.3	176	±1.4	176	±1.4
53	Burns-1 40	253	242	0.0527	±0.0049	0.2016	±0.0192	0.0277	±0.0005	0.1831	316	±106.4	186	±8.1	176	±1.5	176	±1.5
54	Burns-1 19	300	273	0.0542	±0.0043	0.2085	±0.0171	0.0279	±0.0006	0.2583	379	±89.2	192	±7.2	177	±1.9	177	±1.9
55	Burns-1 53	115	81	0.0505	±0.0099	0.1946	±0.0387	0.0280	±0.0008	0.1478	216	±227.6	181	±16.4	178	±2.6	178	±2.6
56	Burns-1 127	198	209	0.0509	±0.0042	0.1966	±0.0167	0.0280	±0.0005	0.1948	237	±96.1	182	±7.1	178	±1.5	178	±1.5
57	Burns-1 94	378	285	0.0576	±0.0027	0.2293	±0.0115	0.0289	±0.0005	0.3179	514	±52.2	210	±4.7	184	±1.4	184	±1.4
58	Burns-1 59	267	227	0.0541	±0.0041	0.2168	±0.0164	0.0290	±0.0004	0.1615	376	±84.2	199	±6.9	185	±1.1	185	±1.1
59	Burns-1 66	426	328	0.0563	±0.0027	0.2270	±0.0113	0.0293	±0.0004	0.2773	464	±53.2	208	±4.7	186	±1.3	186	±1.3
60	Burns-1 91	376	235	0.0578	±0.0035	0.2381	±0.0152	0.0299	±0.0007	0.3450	522	±65.5	217	±6.2	190	±2.1	190	±2.1
61	Burns-1 68	290	276	0.0580	±0.0054	0.2418	±0.0229	0.0303	±0.0005	0.1688	528	±102.2	220	±9.4	192	±1.5	192	±1.5
62	Burns-1 100	277	314	0.0516	±0.0035	0.2216	±0.0157	0.0311	±0.0007	0.3114	267	±77.2	203	±6.5	198	±2.1	198	±2.1
63	Burns-1 37	397	348	0.0499	±0.0030	0.2234	±0.0141	0.0325	±0.0006	0.2746	191	±70.5	205	±5.9	206	±1.8	206	±1.8
64	Burns-1 27	834	700	0.0521	±0.0012	0.2351	±0.0061	0.0328	±0.0004	0.4522	288	±26.5	214	±2.5	208	±1.2	208	±1.2
65	Burns-1 31	344	360	0.0457	±0.0041	0.2082	±0.0189	0.0331	±0.0004	0.1423	0	-±0.0	192	±7.9	210	±1.3	210	±1.3
66	Burns-1 130	279	296	0.0508	±0.0038	0.2353	±0.0178	0.0336	±0.0005	0.1947	233	±85.5	215	±7.3	213	±1.5	213	±1.5
67	Burns-1 126	851	918	0.0485	±0.0013	0.2257	±0.0065	0.0337	±0.0004	0.4122	125	±30.8	207	±2.7	214	±1.2	214	±1.2
68	Burns-1 135	259	266	0.0540	±0.0028	0.2539	±0.0134	0.0341	±0.0004	0.2008	371	±58.3	230	±5.4	216	±1.1	216	±1.1
69	Burns-1 58	315	383	0.0518	±0.0039	0.2484	±0.0188	0.0348	±0.0005	0.1825	277	±85.2	225	±7.6	220	±1.5	220	±1.5
70	Burns-1 85	169	276	0.0562	±0.0050	0.3104	±0.0280	0.0401	±0.0005	0.1268	460	±99.0	275	±10.8	253	±1.4	253	±1.4
71	Burns-1 71	262	333	0.0556	±0.0026	0.3806	±0.0184	0.0496	±0.0006	0.2569	438	±51.9	327	±6.8	312	±1.9	312	±1.9
72	Burns-1 74	99	176	0.0668	±0.0081	0.4962	±0.0610	0.0539	±0.0009	0.1368	832	±126.9	409	±20.7	338	±2.8	338	±2.8
73	Burns-1 117	263	496	0.0556	±0.0030	0.4767	±0.0262	0.0621	±0.0008	0.2265	438	±59.5	396	±9.0	389	±2.3	389	±2.3
74	Burns-1 10	931	1,324	0.0565	±0.0012	0.5045	±0.0124	0.0647	±0.0009	0.5451	474	±22.9	415	±4.2	404	±2.6	404	±2.6
75	Burns-1 80	244	550	0.0608	±0.0013	0.7069	±0.0189	0.0843	±0.0014	0.6405	634	±22.1	543	±5.6	522	±4.3	522	±4.3
76	Burns-1 99	1032	1,746	0.0891	±0.0025	1.8237	±0.0672	0.1485	±0.0036	0.6536	1406	±26.7	1054	±12.1	893	±10.0	893	±10.0
77	Burns-1 12	191	1,132	0.0718	±0.0012	1.5508	±0.0303	0.1566	±0.0017	0.5700	981	±16.4	951	±6.0	938	±4.9	938	±4.9
78	Burns-1 34	72	398	0.0713	±0.0030	1.6349	±0.0712	0.1663	±0.0019	0.2679	966	±42.8	984	±13.7	992	±5.4	966	±42.8
79	Burns-1 89	354	2,131	0.0796	±0.0005	2.2984	±0.0451	0.2094	±0.0039	0.9515	1187	±6.0	1212	±6.9	1226	±10.4	1187	±6.0
80	Burns-1 81	95	693	0.0797	±0.0028	1.8109	±0.0726	0.1648	±0.0032	0.4779	1190	±34.8	1049	±13.1	983	±8.7	1190	±34.8
81	Burns-1 41	156	936	0.0806	±0.0008	2.1963	±0.0304	0.1977	±0.0019	0.6993	1211	±9.7	1180	±4.8	1163	±5.2	1211	±9.7
82	Burns-1 73	109	750	0.0835	±0.0016	2.5546	±0.1024	0.2219	±0.0078	0.8806	1281	±18.5	1288	±14.6	1292	±20.7	1281	±18.5
83	Burns-1 116	291	2,343	0.0860	±0.0003	2.6012	±0.0269	0.2194	±0.0021	0.9329	1338	±3.6	1301	±3.8	1279	±5.6	1338	±3.6
84	Burns-1 111	232	1,489	0.0879	±0.0009	2.7890	±0.0491	0.2302	±0.0033	0.8262	1379	±9.5	1353	±6.6	1336	±8.8	1379	±9.5
85	Burns-1 131	275	1,904	0.0884	±0.0005	2.4254	±0.0545	0.1990	±0.0044	0.9734	1391	±4.9	1250	±8.1	1170	±11.7	1391	±4.9
86	Burns-1 32	251	1,458	0.0885	±0.0007	2.9025	±0.0470	0.2379	±0.0033	0.8645	1393	±7.8	1383	±6.1	1376	±8.7	1393	±7.8
87	Burns-1 1	574	1,857	0.0888	±0.0004	2.7442	±0.0511	0.2240	±0.0041	0.9700	1401	±4.3	1341	±6.9	1303	±10.7	1401	±4.3
88	Burns-1 39	250	1,440	0.0889	±0.0006	3.1289	±0.0720	0.2553	±0.0056	0.9563	1402	±6.4	1440	±8.9	1466	±14.4	1402	±6.4
89	Burns-1 87	865	2,886	0.0901	±0.0003	3.0691	±0.0434	0.2471	±0.0034	0.9661	1427	±3.5	1425	±5.4	1424	±8.7	1427	±3.5
90	Burns-1 69	535	3,525	0.0902	±0.0004	3.1558	±0.0406	0.2538	±0.0031	0.9353	1429	±4.3	1446	±5.0	1458	±7.9	1429	±4.3
91	Burns-1 105	71	522	0.0914	±0.0010	3.3284	±0.0911	0.2642	±0.0066	0.9106	1454	±10.8	1488	±10.7	1511	±16.8	1454	±10.8
92	Burns-1 50	211	1,014	0.0930	±0.0018	3.2552	±0.0730	0.2538	±0.0027	0.4711	1488	±18.7	1470	±8.7	1458	±6.9	1488	±18.7
93	Burns-1 38	117	613	0.0941	±0.0013	2.7755	±0.0686	0.2140	±0.0043	0.8198	1510	±13.4	1349	±9.2	1250	±11.5	1510	±13.4
94	Burns-1 97	186	1,321	0.0952	±0.0008	3.1685	±0.0585	0.2413	±0.0040	0.8978	1533	±7.7	1450	±7.1	1393	±10.4	1533	±7.7
95	Burns-1 67	1436	8,214	0.0973	±0.0006	3.5320	±0.0555	0.2633	±0.0038	0.9185	1573	±5.8	1534	±6.2	1507	±9.7	1573	±5.8

Sample Name: Burns 1

	Analysis	U ppm	$^{206}Pb/^{204}Pb$	$^{207}Pb^*/^{206}Pb^*$	± 2 σ abs	$^{207}Pb^*/^{235}U$	± 2 σ abs	$^{206}Pb^*/^{238}U$	± 2 σ abs	Rho	Isotopic Ratios: $^{207}Pb^*/^{206}Pb^*$	± 1 σ abs	Apparent Ages (Ma): $^{207}Pb^*/^{235}U$	± 1 σ abs	$^{206}Pb^*/^{238}U$	± 1 σ abs	Best Age	± 1 σ abs
96	Burns-1 108	1021	4,168	0.0980	±0.0006	3.0470	±0.1430	0.2254	±0.0105	0.9913	1587	±5.8	1419	±17.9	1311	±27.6	1587	±5.8
97	Burns-1 112	253	2,104	0.0981	±0.0004	3.5226	±0.0361	0.2603	±0.0024	0.9002	1589	±4.2	1532	±4.1	1492	±6.1	1589	±4.2
98	Burns-1 96	85	560	0.0983	±0.0041	3.1114	±0.1386	0.2295	±0.0033	0.3238	1593	±39.4	1436	±17.1	1332	±8.7	1593	±39.4
99	Burns-1 123	160	1,523	0.0987	±0.0011	3.5044	±0.0852	0.2576	±0.0056	0.8901	1599	±10.3	1528	±9.6	1477	±14.3	1599	±10.3
100	Burns-1 45	845	6,311	0.0998	±0.0003	3.3697	±0.0538	0.2448	±0.0039	0.9859	1621	±2.5	1497	±6.3	1412	±10.0	1621	±2.5
101	Burns-1 134	392	2,161	0.1007	±0.0006	3.7117	±0.0836	0.2673	±0.0058	0.9690	1637	±5.2	1574	±9.0	1527	±14.8	1637	±5.2
102	Burns-1 61	139	1,058	0.1007	±0.0009	3.9313	±0.0596	0.2830	±0.0034	0.7984	1638	±8.5	1620	±6.1	1606	±8.6	1638	±8.5
103	Burns-1 95	144	1,419	0.1010	±0.0008	4.0103	±0.0553	0.2880	±0.0033	0.8356	1643	±7.0	1636	±5.6	1631	±8.3	1643	±7.0
104	Burns-1 2	186	1,318	0.1010	±0.0040	4.0636	±0.1685	0.2917	±0.0031	0.2593	1643	±37.2	1647	±16.9	1650	±7.8	1643	±37.2
105	Burns-1 93	169	2,022	0.1015	±0.0008	3.8764	±0.0541	0.2770	±0.0032	0.8205	1652	±7.4	1609	±5.6	1576	±8.0	1652	±7.4
106	Burns-1 7	50	423	0.1017	±0.0022	4.0999	±0.1034	0.2923	±0.0037	0.4959	1656	±20.3	1654	±10.3	1653	±9.1	1656	±20.3
107	Burns-1 78	452	3,888	0.1019	±0.0004	3.9870	±0.0512	0.2838	±0.0035	0.9635	1659	±3.2	1632	±5.2	1610	±8.8	1659	±3.2
108	Burns-1 115	213	2,106	0.1022	±0.0006	3.8857	±0.0417	0.2757	±0.0025	0.8576	1665	±5.1	1611	±4.3	1569	±6.4	1665	±5.1
109	Burns-1 107	33	341	0.1032	±0.0041	3.8152	±0.1660	0.2681	±0.0049	0.4184	1683	±36.5	1596	±17.5	1531	±12.4	1683	±36.5
110	Burns-1 29	77	548	0.1034	±0.0014	4.0331	±0.0867	0.2828	±0.0047	0.7672	1686	±12.7	1641	±8.7	1606	±11.7	1686	±12.7
111	Burns-1 51	383	3,173	0.1046	±0.0004	4.3209	±0.0555	0.2997	±0.0037	0.9503	1706	±3.7	1697	±5.3	1690	±9.1	1706	±3.7
112	Burns-1 62	121	1,238	0.1052	±0.0013	4.4736	±0.0754	0.3085	±0.0034	0.6538	1717	±11.7	1726	±7.0	1733	±8.4	1717	±11.7
113	Burns-1 15	147	1,391	0.1054	±0.0006	4.1287	±0.0528	0.2842	±0.0032	0.8855	1721	±5.5	1660	±5.2	1612	±8.1	1721	±5.5
114	Burns-1 24	48	259	0.1163	±0.0042	5.1896	±0.2173	0.3236	±0.0071	0.5222	1900	±32.1	1851	±17.8	1807	±17.2	1900	±32.1
115	Burns-1 17	472	5,284	0.1508	±0.0005	8.2570	±0.0902	0.3970	±0.0041	0.9503	2355	±2.9	2260	±4.9	2155	±9.5	2355	±2.9
116	Burns-1 65	122	1,935	0.1853	±0.0005	14.2230	±0.1443	0.5566	±0.0054	0.9563	2701	±2.4	2765	±4.8	2853	±11.2	2701	±2.4

Table C.3. Detrital zircon data table for GM-C-051408-8.

Sample Name: GM-C-051408-8 — Isotopic Ratios — Apparent Ages (Ma)

	Analysis	U ppm	$^{206}Pb/^{204}Pb$	$^{207}Pb^*/^{206}Pb^*$	± 2 σ abs	$^{207}Pb^*/^{235}U$	± 2 σ abs	$^{206}Pb^*/^{238}U$	± 2 σ abs	Rho	$^{207}Pb^*/^{206}Pb^*$	± 1 σ abs	$^{207}Pb^*/^{235}U$	± 1 σ abs	$^{206}Pb^*/^{238}U$	± 1 σ abs	Best Age	± 1 σ abs
1	C-051408-8 77	697	146	0.0645	±0.0088	0.0696	±0.0095	0.0078	±0.0001	0.1209	759	±143.6	68	±4.5	50	±0.4	50	±0.4
2	C-051408-8 70	319	97	0.0536	±0.0105	0.0586	±0.0117	0.0079	±0.0003	0.1725	354	±222.0	58	±5.6	51	±0.9	51	±0.9
3	C-051408-8 52	2469	498	0.0574	±0.0031	0.0644	±0.0042	0.0081	±0.0003	0.5640	508	±59.9	63	±2.0	52	±1.0	52	±1.0
4	C-051408-8 10	2116	562	0.0541	±0.0012	0.0635	±0.0018	0.0085	±0.0001	0.6030	375	±25.1	63	±0.8	55	±0.5	55	±0.5
5	C-051408-8 97	152	45	0.0599	±0.0185	0.0719	±0.0224	0.0087	±0.0004	0.1352	600	±334.0	71	±10.6	56	±1.2	56	±1.2
6	C-051408-8 65	150	125	0.0568	±0.0122	0.0697	±0.0153	0.0089	±0.0004	0.1946	484	±237.6	68	±7.3	57	±1.2	57	±1.2
7	C-051408-8 86	286	97	0.0533	±0.0158	0.0693	±0.0219	0.0094	±0.0010	0.3524	344	±334.1	68	±10.4	60	±3.3	60	±3.3
8	C-051408-8 26	325	123	0.0519	±0.0079	0.0687	±0.0105	0.0096	±0.0002	0.1399	283	±173.4	67	±5.0	62	±0.7	62	±0.7
9	C-051408-8 45	151	86	0.0715	±0.0204	0.1113	±0.0320	0.0113	±0.0003	0.1016	971	±291.5	107	±14.6	72	±1.1	72	±1.1
10	C-051408-8 47	191	115	0.0655	±0.0116	0.1124	±0.0212	0.0124	±0.0008	0.3329	792	±186.2	108	±9.7	80	±2.5	80	±2.5
11	C-051408-8 106	236	82	0.0761	±0.0163	0.1343	±0.0295	0.0128	±0.0006	0.2253	1098	±214.5	128	±13.2	82	±2.0	82	±2.0
12	C-051408-8 111	584	213	0.0528	±0.0044	0.0933	±0.0081	0.0128	±0.0004	0.3160	318	±93.9	91	±3.8	82	±1.1	82	±1.1
13	C-051408-8 100	164	76	0.0605	±0.0136	0.1178	±0.0267	0.0141	±0.0005	0.1442	622	±242.2	113	±12.1	90	±1.5	90	±1.5
14	C-051408-8 57	276	150	0.0672	±0.0256	0.1323	±0.0507	0.0143	±0.0007	0.1218	844	±395.6	126	±22.7	91	±2.1	91	±2.1
15	C-051408-8 7	704	306	0.0689	±0.0033	0.1436	±0.0079	0.0151	±0.0004	0.4874	895	±49.6	136	±3.5	97	±1.3	97	±1.3
16	C-051408-8 92	695	289	0.0556	±0.0033	0.1188	±0.0080	0.0155	±0.0005	0.4982	438	±65.1	114	±3.6	99	±1.7	99	±1.7
17	C-051408-8 53	147	82	0.0520	±0.0114	0.1127	±0.0252	0.0157	±0.0007	0.1913	285	±251.4	108	±11.5	101	±2.1	101	±2.1
18	C-051408-8 60	NA	49,159	0.0485	±0.0419	0.1081	±0.0936	0.0162	±0.0010	0.0743	125	±1016.1	104	±42.9	103	±3.3	103	±3.3
19	C-051408-8 39	605	347	0.0687	±0.0053	0.1620	±0.0128	0.0171	±0.0003	0.2119	890	±79.8	152	±5.6	109	±0.9	109	±0.9
20	C-051408-8 25	244	162	0.0660	±0.0060	0.1803	±0.0179	0.0198	±0.0008	0.3903	806	±95.8	168	±7.7	126	±2.4	126	±2.4
21	C-051408-8 139	87	63	0.0877	±0.0148	0.2767	±0.0528	0.0229	±0.0020	0.4693	1376	±162.1	248	±21.0	146	±6.5	146	±6.5
22	C-051408-8 143	400	264	0.0558	±0.0029	0.1767	±0.0096	0.0230	±0.0003	0.2674	445	±58.3	165	±4.2	146	±1.1	146	±1.1
23	C-051408-8 85	456	338	0.0500	±0.0023	0.1663	±0.0104	0.0241	±0.0011	0.6934	194	±52.6	156	±4.5	154	±3.3	154	±3.3
24	C-051408-8 43	390	408	0.0503	±0.0031	0.1717	±0.0123	0.0247	±0.0009	0.5317	211	±70.3	161	±5.3	157	±3.0	157	±3.0
25	C-051408-8 91	372	350	0.0499	±0.0028	0.1840	±0.0107	0.0267	±0.0004	0.2765	189	±64.9	171	±4.6	170	±1.3	170	±1.3
26	C-051408-8 90	300	343	0.0541	±0.0029	0.2272	±0.0146	0.0304	±0.0011	0.5623	376	±59.8	208	±6.0	193	±3.4	193	±3.4
27	C-051408-8 110	130	122	0.0538	±0.0088	0.2338	±0.0386	0.0315	±0.0008	0.1470	361	±184.2	213	±15.9	200	±2.4	200	±2.4
28	C-051408-8 124	767	884	0.0904	±0.0010	0.4154	±0.0778	0.0333	±0.0062	0.9984	1435	±10.1	353	±27.9	211	±19.4	211	±19.4
29	C-051408-8 19	323	365	0.0869	±0.0025	0.4132	±0.0161	0.0345	±0.0009	0.6718	1359	±27.9	351	±5.8	218	±2.8	218	±2.8
30	C-051408-8 132	286	223	0.0603	±0.0041	0.2894	±0.0240	0.0348	±0.0016	0.5620	615	±74.1	258	±9.5	221	±5.1	221	±5.1
31	C-051408-8 80	1922	677	0.0880	±0.0051	0.4615	±0.0285	0.0381	±0.0008	0.3284	1382	±56.1	385	±9.9	241	±2.4	241	±2.4
32	C-051408-8 128	101	139	0.0655	±0.0099	0.3877	±0.0693	0.0429	±0.0041	0.5337	791	±158.7	333	±25.4	271	±12.7	271	±12.7
33	C-051408-8 116	250	322	0.0673	±0.0032	0.4506	±0.0362	0.0486	±0.0032	0.8107	846	±49.0	378	±12.7	306	±9.7	306	±9.7
34	C-051408-8 31	285	349	0.0597	±0.0018	0.4033	±0.0249	0.0490	±0.0026	0.8710	592	±32.9	344	±9.0	308	±8.1	308	±8.1
35	C-051408-8 35	490	1,316	0.0616	±0.0021	0.5809	±0.0310	0.0684	±0.0028	0.7738	661	±36.2	465	±9.9	426	±8.5	426	±8.5
36	C-051408-8 122	161	358	0.0605	±0.0031	0.6623	±0.0356	0.0795	±0.0012	0.2778	620	±55.7	516	±10.9	493	±3.5	493	±3.5
37	C-051408-8 147	57	263	0.0723	±0.0049	1.1273	±0.0974	0.1131	±0.0060	0.6174	994	±69.1	766	±23.2	691	±17.5	691	±17.5
38	C-051408-8 82	333	707	0.0944	±0.0023	1.5537	±0.0869	0.1193	±0.0060	0.9008	1517	±22.9	952	±17.3	727	±17.3	727	±17.3
39	C-051408-8 78	138	521	0.0739	±0.0015	1.3187	±0.1453	0.1293	±0.0140	0.9826	1040	±20.7	854	±31.8	784	±40.0	784	±40.0
40	C-051408-8 131	1161	4,113	0.0862	±0.0006	1.6215	±0.0724	0.1364	±0.0060	0.9880	1343	±6.7	979	±14.0	824	±17.1	824	±17.1
41	C-051408-8 121	1362	4,095	0.0760	±0.0004	1.4475	±0.0694	0.1381	±0.0066	0.9953	1096	±4.6	909	±14.4	834	±18.7	834	±18.7
42	C-051408-8 142	94	458	0.0666	±0.0713	1.3473	±1.4455	0.1467	±0.0101	0.0639	826	±1117.1	866	±312.6	882	±28.3	882	±28.3
43	C-051408-8 84	45	263	0.0710	±0.0044	1.5826	±0.1056	0.1616	±0.0040	0.3705	958	±63.3	963	±20.8	966	±11.1	958	±63.3
44	C-051408-8 20	351	2,222	0.0735	±0.0005	1.6674	±0.0278	0.1646	±0.0025	0.9021	1026	±7.3	996	±5.3	983	±6.9	1026	±7.3
45	C-051408-8 79	192	1,223	0.0785	±0.0007	1.8484	±0.0232	0.1707	±0.0015	0.7223	1160	±8.6	1063	±4.1	1016	±4.3	1160	±8.6
46	C-051408-8 42	165	1,284	0.0798	±0.0014	2.1969	±0.1382	0.1997	±0.0121	0.9621	1191	±16.9	1180	±22.0	1174	±32.5	1191	±16.9
47	C-051408-8 50	45	397	0.0860	±0.0031	2.7509	±0.1243	0.2320	±0.0064	0.6093	1338	±34.6	1342	±16.8	1345	±16.7	1338	±34.6
48	C-051408-8 71	275	2,194	0.0879	±0.0005	2.5829	±0.0404	0.2130	±0.0031	0.9166	1381	±6.0	1296	±5.7	1245	±8.1	1381	±6.0
49	C-051408-8 55	536	2,924	0.0893	±0.0004	3.1914	±0.1824	0.2591	±0.0148	0.9967	1411	±4.4	1455	±22.1	1485	±37.8	1411	±4.4
50	C-051408-8 24	84	806	0.0899	±0.0011	2.9463	±0.0453	0.2376	±0.0023	0.6434	1424	±11.2	1394	±5.8	1374	±6.1	1424	±11.2
51	C-051408-8 40	557	7,155	0.0908	±0.0003	3.0559	±0.0367	0.2442	±0.0028	0.9485	1442	±3.6	1422	±4.6	1409	±7.2	1442	±3.6
52	C-051408-8 94	146	1,069	0.0911	±0.0007	2.9073	±0.0658	0.2316	±0.0049	0.9370	1448	±7.5	1384	±8.6	1343	±12.9	1448	±7.5
53	C-051408-8 99	161	1,304	0.0914	±0.0007	2.9407	±0.0561	0.2334	±0.0041	0.9127	1454	±7.4	1392	±7.2	1352	±10.6	1454	±7.4
54	C-051408-8 9	159	1,120	0.0917	±0.0017	3.1614	±0.1576	0.2502	±0.0115	0.9240	1460	±18.1	1448	±19.2	1439	±29.7	1460	±18.1
55	C-051408-8 41	1283	14,859	0.0917	±0.0002	3.1546	±0.0375	0.2495	±0.0029	0.9817	1461	±2.1	1446	±4.6	1436	±7.5	1461	±2.1
56	C-051408-8 15	105	939	0.0917	±0.0012	2.9393	±0.0475	0.2324	±0.0021	0.5470	1462	±12.9	1392	±6.1	1347	±5.4	1462	±12.9
57	C-051408-8 140	193	1,474	0.0929	±0.0022	3.0122	±0.0957	0.2351	±0.0049	0.6526	1487	±22.8	1411	±12.1	1361	±12.7	1487	±22.8
58	C-051408-8 96	57	519	0.0935	±0.0018	2.8328	±0.0606	0.2197	±0.0022	0.4613	1498	±17.9	1364	±8.0	1280	±5.7	1498	±17.9
59	C-051408-8 21	240	2,668	0.0947	±0.0049	3.0545	±0.1692	0.2339	±0.0046	0.3562	1522	±48.8	1421	±21.2	1355	±12.1	1522	±48.8
60	C-051408-8 54	245	2,034	0.0964	±0.0010	3.1909	±0.0558	0.2400	±0.0034	0.8148	1556	±9.5	1455	±6.8	1387	±8.9	1556	±9.5
61	C-051408-8 118	274	2,588	0.1021	±0.0003	3.9054	±0.0576	0.2774	±0.0040	0.9748	1663	±3.0	1615	±6.0	1578	±10.1	1663	±3.0
62	C-051408-8 134	156	1,415	0.1022	±0.0007	4.2489	±0.1093	0.3014	±0.0075	0.9626	1665	±6.4	1684	±10.6	1698	±18.5	1665	±6.4
63	C-051408-8 64	47	119	0.1025	±0.0030	4.5808	±0.2996	0.3243	±0.0189	0.8904	1669	±27.5	1746	±27.3	1810	±46.0	1669	±27.5
64	C-051408-8 89	125	766	0.1025	±0.0006	3.9158	±0.1296	0.2770	±0.0090	0.9853	1671	±5.2	1617	±13.4	1576	±22.8	1671	±5.2
65	C-051408-8 13	297	2,643	0.1028	±0.0004	4.0468	±0.0504	0.2854	±0.0034	0.9601	1676	±3.2	1644	±5.1	1618	±8.6	1676	±3.2
66	C-051408-8 75	302	2,499	0.1031	±0.0011	4.1607	±0.0863	0.2927	±0.0051	0.8476	1681	±10.2	1666	±8.5	1655	±12.8	1681	±10.2
67	C-051408-8 18	NA	9,095	0.1038	±0.0010	3.4632	±0.1167	0.2419	±0.0078	0.9587	1694	±8.8	1519	±13.3	1397	±20.3	1694	±8.8
68	C-051408-8 49	498	4,198	0.1042	±0.0003	3.5785	±0.0505	0.2492	±0.0034	0.9756	1700	±2.9	1545	±5.6	1434	±8.8	1700	±2.9
69	C-051408-8 4	73	705	0.1043	±0.0030	3.9624	±0.2965	0.2756	±0.0190	0.9220	1702	±26.7	1627	±30.3	1569	±48.0	1702	±26.7
70	C-051408-8 67	170	1,883	0.1045	±0.0005	4.3635	±0.0900	0.3027	±0.0061	0.9779	1706	±4.0	1705	±8.5	1705	±15.1	1706	±4.0
71	C-051408-8 129	218	1,765	0.1046	±0.0005	4.1524	±0.0532	0.2878	±0.0035	0.9365	1708	±4.1	1665	±5.2	1631	±8.6	1708	±4.1
72	C-051408-8 117	725	6,995	0.1048	±0.0003	4.0952	±0.0495	0.2835	±0.0033	0.9761	1710	±2.4	1653	±4.9	1609	±8.4	1710	±2.4
73	C-051408-8 87	66	555	0.1048	±0.0014	3.9752	±0.1903	0.2751	±0.0126	0.9593	1711	±12.4	1629	±19.4	1567	±31.9	1711	±12.4
74	C-051408-8 145	664	3,717	0.1048	±0.0005	3.6005	±0.0697	0.2491	±0.0047	0.9661	1711	±4.6	1550	±7.7	1434	±12.0	1711	±4.6
75	C-051408-8 102	455	2,801	0.1053	±0.0003	4.0448	±0.0804	0.2787	±0.0055	0.9859	1719	±3.1	1643	±8.1	1585	±13.8	1719	±3.1
76	C-051408-8 63	79	259	0.1057	±0.0114	4.7329	±1.4552	0.3247	±0.0934	0.9359	1727	±99.4	1773	±128.9	1813	±227.4	1727	±99.4
77	C-051408-8 44	277	4,408	0.1059	±0.0004	4.9474	±0.1417	0.3388	±0.0096	0.9899	1730	±3.7	1810	±12.1	1881	±23.1	1730	±3.7
78	C-051408-8 51	68	754	0.1082	±0.0014	4.2629	±0.0965	0.2857	±0.0052	0.8108	1769	±12.1	1686	±9.3	1620	±13.1	1769	±12.1
79	C-051408-8 123	67	677	0.1083	±0.0016	4.5580	±0.0892	0.3052	±0.0038	0.6392	1771	±13.7	1742	±8.1	1717	±9.4	1771	±13.7
80	C-051408-8 133	41	374	0.1085	±0.0018	4.7008	±0.2920	0.3143	±0.0189	0.9656	1774	±14.7	1767	±26.0	1762	±46.2	1774	±14.7
81	C-051408-8 2	107	713	0.1089	±0.0007	4.8883	±0.1571	0.3255	±0.0103	0.9814	1782	±5.6	1800	±13.5	1816	±25.0	1782	±5.6
82	C-051408-8 148	204	1,729	0.1092	±0.0005	3.9296	±0.0659	0.2610	±0.0042	0.9655	1786	±4.0	1620	±6.8	1495	±10.8	1786	±4.0
83	C-051408-8 76	153	48,401	0.1101	±0.0026	4.2112	±0.1145	0.2775	±0.0037	0.4943	1800	±21.5	1676	±11.2	1579	±9.4	1800	±21.5
84	C-051408-8 88	NA	48,296	0.1101	±0.0041	4.5720	±0.3560	0.3012	±0.0205	0.8754	1801	±34.2	1744	±32.4	1697	±50.8	1801	±34.2
85	C-051408-8 69	187	2,033	0.1133	±0.0004	4.5511	±0.0975	0.2914	±0.0062	0.9869	1852	±3.1	1740	±8.9	1649	±15.4	1852	±3.1
86	C-051408-8 101	289	1,323	0.1134	±0.0022	4.6341	±0.1359	0.2964	±0.0064	0.7418	1855	±17.8	1755	±12.2	1673	±16.0	1855	±17.8
87	C-051408-8 14	18	254	0.1156	±0.0057	5.3208	±0.2771	0.3338	±0.0059	0.3404	1889	±44.1	1872	±22.3	1857	±14.3	1889	±44.1
88	C-051408-8 104	119	751	0.1175	±0.0053	5.2405	±0.3237	0.3234	±0.0138	0.6902	1919	±40.1	1859	±26.3	1806	±33.6	1919	±40.1
89	C-051408-8 28	22	331	0.1202	±0.0042	5.8594	±0.2195	0.3537	±0.0051	0.3814	1959	±30.9	1955	±16.2	1952	±12.0	1959	±30.9
90	C-051408-8 8	68	319	0.1203	±0.0049	6.0344	±0.2565	0.3639	±0.0046	0.2992	1960	±36.2	1981	±18.5	2001	±10.9	1960	±36.2
91	C-051408-8 141	5	57	0.1526	±0.0254	8.7070	±1.8113	0.4138	±0.0515	0.5982	2375	±142.1	2308	±94.7	2232	±117.4	2375	±142.1
92	C-051408-8 1	3	39	0.1673	±0.0432	10.6692	±3.0049	0.4624	±0.0521	0.3999	2531	±216.6	2495	±130.7	2450	±114.8	2531	±216.6
93	C-051408-8 119	213	2,413	0.1793	±0.0018	11.9934	±0.2165	0.4850	±0.0072	0.8206	2647	±8.6	2604	±8.5	2549	±15.6	2647	±8.6
94	C-051408-8 72	26	481	0.1952	±0.0021	15.7502	±0.4496	0.5853	±0.0155	0.9294	2786	±8.6	2862	±13.6	2971	±31.6	2786	±8.6

Table C.4. Detrital zircon data table for GM-C-051508-1.

	Sample Name:	GM-C-051508-1	Isotopic Ratios								Apparent Ages (Ma)							
	Analysis	U	$^{206}Pb/^{204}Pb$	$^{207}Pb^*/^{206}Pb^*$	± 2 σ	$^{207}Pb^*/^{235}U$	± 2 σ	$^{206}Pb^*/^{238}U$	± 2 σ	Rho	$^{207}Pb^*/^{206}Pb^*$	± 1 σ	$^{207}Pb^*/^{235}U$	± 1 σ	$^{206}Pb^*/^{238}U$	± 1 σ	Best Age	± 1 σ
		ppm			abs		abs		abs			abs		abs		abs		abs
1	C-051508-1 27	515	205	0.0586	±0.0048	0.0881	±0.0078	0.0109	±0.0004	0.3810	551	±89.7	86	±3.7	70	±1.2	70	±1.2
2	C-051508-1 84	318	144	0.0694	±0.0100	0.1059	±0.0160	0.0111	±0.0005	0.2841	909	±149.2	102	±7.3	71	±1.5	71	±1.5
3	C-051508-1 148	481	248	0.0614	±0.0050	0.0937	±0.0083	0.0111	±0.0004	0.3635	653	±88.0	91	±3.8	71	±1.1	71	±1.1
4	C-051508-1 65	776	340	0.0513	±0.0022	0.0785	±0.0042	0.0111	±0.0004	0.5921	253	±49.6	77	±2.0	71	±1.1	71	±1.1
5	C-051508-1 54	220	64	0.0700	±0.0091	0.1084	±0.0160	0.0112	±0.0008	0.4726	929	±133.2	105	±7.3	72	±2.5	72	±2.5
6	C-051508-1 30	158	62	0.0504	±0.0131	0.0788	±0.0206	0.0114	±0.0004	0.1437	211	±300.3	77	±9.7	73	±1.4	73	±1.4
7	C-051508-1 50	236	82	0.0457	±0.0070	0.0722	±0.0117	0.0115	±0.0006	0.3361	0	±0.0	71	±5.5	73	±2.0	73	±2.0
8	C-051508-1 34	117	51	0.0640	±0.0119	0.1045	±0.0236	0.0118	±0.0015	0.5662	741	±196.6	101	±10.8	76	±4.8	76	±4.8
9	C-051508-1 78	294	164	0.0612	±0.0074	0.1034	±0.0135	0.0123	±0.0006	0.3619	646	±130.8	100	±6.2	79	±1.8	79	±1.8
10	C-051508-1 125	127	78	0.0531	±0.0106	0.0912	±0.0186	0.0124	±0.0005	0.2032	334	±226.8	89	±8.7	80	±1.6	80	±1.6
11	C-051508-1 4	232	78	0.0454	±0.0062	0.0813	±0.0114	0.0130	±0.0004	0.2398	0	±0.0	79	±5.4	83	±1.4	83	±1.4
12	C-051508-1 10	260	63	0.0539	±0.0048	0.0965	±0.0092	0.0130	±0.0004	0.3559	366	±100.7	93	±4.3	83	±1.4	83	±1.4
13	C-051508-1 15	321	184	0.0479	±0.0036	0.0941	±0.0074	0.0143	±0.0003	0.3064	93	±89.0	91	±3.4	91	±1.1	91	±1.1
14	C-051508-1 128	383	271	0.0533	±0.0038	0.1054	±0.0078	0.0143	±0.0002	0.2145	341	±81.7	102	±3.6	92	±0.7	92	±0.7
15	C-051508-1 103	175	93	0.0547	±0.0075	0.1094	±0.0154	0.0145	±0.0005	0.2239	398	±153.8	105	±7.0	93	±1.5	93	±1.5
16	C-051508-1 141	151	107	0.0674	±0.0107	0.1374	±0.0226	0.0148	±0.0007	0.2691	852	±165.0	131	±10.1	95	±2.1	95	±2.1
17	C-051508-1 122	239	178	0.0494	±0.0061	0.1032	±0.0129	0.0151	±0.0003	0.1763	167	±143.8	100	±5.9	97	±1.1	97	±1.1
18	C-051508-1 2	312	98	0.0580	±0.0039	0.1227	±0.0088	0.0154	±0.0004	0.3356	528	±74.1	118	±4.0	98	±1.2	98	±1.2
19	C-051508-1 121	210	133	0.0621	±0.0119	0.1321	±0.0264	0.0154	±0.0009	0.2975	679	±204.3	126	±11.9	99	±2.9	99	±2.9
20	C-051508-1 100	275	108	0.0884	±0.0159	0.1887	±0.0364	0.0155	±0.0011	0.3581	1390	±172.7	176	±15.5	99	±3.4	99	±3.4
21	C-051508-1 127	460	318	0.0543	±0.0025	0.1180	±0.0063	0.0158	±0.0004	0.5321	384	±50.7	113	±2.9	101	±1.4	101	±1.4
22	C-051508-1 91	164	112	0.0523	±0.0065	0.1152	±0.0149	0.0160	±0.0005	0.2569	299	±142.5	111	±6.8	102	±1.7	102	±1.7
23	C-051508-1 88	400	202	0.0795	±0.0063	0.1766	±0.0148	0.0161	±0.0005	0.3366	1185	±78.0	165	±6.4	103	±1.4	103	±1.4
24	C-051508-1 1	647	185	0.0507	±0.0016	0.1147	±0.0059	0.0164	±0.0007	0.7837	229	±37.0	110	±2.7	105	±2.1	105	±2.1
25	C-051508-1 147	87	61	0.0766	±0.0167	0.1829	±0.0412	0.0173	±0.0010	0.2476	1110	±217.9	171	±17.7	111	±3.1	111	±3.1
26	C-051508-1 115	354	229	0.0571	±0.0062	0.1409	±0.0159	0.0179	±0.0005	0.2610	497	±119.8	134	±7.1	114	±1.7	114	±1.7
27	C-051508-1 71	83	68	0.0682	±0.0133	0.1720	±0.0343	0.0183	±0.0008	0.2232	874	±201.3	161	±14.9	117	±2.6	117	±2.6
28	C-051508-1 45	250	97	0.0625	±0.0044	0.1610	±0.0130	0.0187	±0.0007	0.4943	691	±74.8	152	±5.7	119	±2.4	119	±2.4
29	C-051508-1 21	430	166	0.0891	±0.0145	0.2338	±0.0400	0.0190	±0.0010	0.3124	1406	±155.6	213	±16.5	122	±3.2	122	±3.2
30	C-051508-1 106	157	126	0.0524	±0.0053	0.1443	±0.0152	0.0200	±0.0006	0.2639	301	±115.8	137	±6.7	128	±1.8	128	±1.8
31	C-051508-1 29	272	186	0.0514	±0.0035	0.1418	±0.0117	0.0200	±0.0010	0.5810	259	±77.2	135	±5.2	128	±3.0	128	±3.0
32	C-051508-1 136	30	30	0.0647	±0.0439	0.1799	±0.1230	0.0202	±0.0018	0.1284	764	±714.6	168	±52.9	129	±5.6	129	±5.6
33	C-051508-1 140	210	191	0.0638	±0.0047	0.1784	±0.0144	0.0203	±0.0007	0.4145	736	±77.8	167	±6.2	129	±2.1	129	±2.1
34	C-051508-1 113	268	220	0.0602	±0.0086	0.1716	±0.0254	0.0207	±0.0007	0.2375	612	±155.1	161	±11.0	132	±2.3	132	±2.3
35	C-051508-1 57	72	49	0.0848	±0.0173	0.2419	±0.0516	0.0207	±0.0013	0.2895	1311	±198.3	220	±21.1	132	±4.0	132	±4.0
36	C-051508-1 137	44	46	0.0639	±0.0244	0.1890	±0.0724	0.0214	±0.0008	0.0936	739	±403.4	176	±30.9	137	±2.4	137	±2.4
37	C-051508-1 46	310	223	0.0563	±0.0048	0.1673	±0.0157	0.0215	±0.0009	0.4312	464	±94.1	157	±6.8	137	±2.8	137	±2.8
38	C-051508-1 105	353	176	0.0590	±0.0052	0.1779	±0.0161	0.0219	±0.0005	0.2545	569	±95.4	166	±7.0	139	±1.6	139	±1.6
39	C-051508-1 58	78	56	0.0784	±0.0081	0.2413	±0.0259	0.0223	±0.0006	0.2580	1158	±102.9	219	±10.6	142	±1.9	142	±1.9
40	C-051508-1 39	45	31	0.0817	±0.0172	0.2533	±0.0547	0.0225	±0.0011	0.2200	1238	±206.5	229	±22.2	143	±3.4	143	±3.4
41	C-051508-1 108	78	77	0.0550	±0.0120	0.1704	±0.0395	0.0225	±0.0017	0.3241	411	±244.8	160	±17.1	143	±5.3	143	±5.3
42	C-051508-1 149	67	77	0.0793	±0.0116	0.2497	±0.0382	0.0228	±0.0010	0.2976	1180	±144.4	226	±15.5	146	±3.3	146	±3.3
43	C-051508-1 126	145	146	0.0505	±0.0065	0.1593	±0.0245	0.0229	±0.0019	0.5389	218	±149.9	150	±10.7	146	±6.0	146	±6.0
44	C-051508-1 44	84	75	0.0510	±0.0173	0.1820	±0.0635	0.0259	±0.0021	0.2293	240	±391.5	170	±27.3	165	±6.5	165	±6.5
45	C-051508-1 73	353	344	0.0627	±0.0017	0.2401	±0.0092	0.0278	±0.0007	0.7015	699	±29.2	219	±3.8	177	±2.3	177	±2.3
46	C-051508-1 131	NA	107	0.0802	±0.0015	0.3127	±0.0067	0.0283	±0.0003	0.4372	1201	±18.9	276	±2.6	180	±0.8	180	±0.8
47	C-051508-1 22	94	102	0.0558	±0.0048	0.2410	±0.0233	0.0313	±0.0013	0.4443	443	±96.4	219	±9.5	199	±4.2	199	±4.2
48	C-051508-1 7	160	94	0.0679	±0.0030	0.3006	±0.0149	0.0321	±0.0007	0.4696	866	±45.5	267	±5.8	204	±2.3	204	±2.3
49	C-051508-1 32	339	407	0.0505	±0.0015	0.2241	±0.0107	0.0322	±0.0012	0.7715	219	±35.1	205	±4.4	204	±3.7	204	±3.7
50	C-051508-1 40	251	280	0.0572	±0.0028	0.2710	±0.0147	0.0344	±0.0008	0.4350	499	±53.7	244	±5.9	218	±2.5	218	±2.5
51	C-051508-1 33	190	224	0.0520	±0.0029	0.2552	±0.0160	0.0356	±0.0011	0.4761	286	±63.1	231	±6.5	225	±3.3	225	±3.3
52	C-051508-1 51	188	273	0.0553	±0.0026	0.2735	±0.0132	0.0359	±0.0004	0.2168	423	±52.6	246	±5.3	227	±1.2	227	±1.2
53	C-051508-1 19	143	150	0.0594	±0.0033	0.3001	±0.0174	0.0367	±0.0007	0.3070	581	±59.8	266	±6.8	232	±2.0	232	±2.0
54	C-051508-1 102	331	425	0.0560	±0.0030	0.2895	±0.0172	0.0375	±0.0010	0.4287	453	±59.7	258	±6.8	237	±3.0	237	±3.0
55	C-051508-1 116	27	44	0.1054	±0.0159	0.5875	±0.1042	0.0404	±0.0038	0.5265	1721	±138.5	469	±33.3	256	±11.7	256	±11.7
56	C-051508-1 66	137	147	0.0584	±0.0067	0.3268	±0.0379	0.0406	±0.0008	0.1787	544	±124.8	287	±14.5	257	±2.6	257	±2.6
57	C-051508-1 99	84	135	0.0718	±0.0057	0.4188	±0.0355	0.0423	±0.0013	0.3694	981	±80.1	355	±12.7	267	±4.1	267	±4.1
58	C-051508-1 62	30	38	0.0990	±0.0161	0.5855	±0.1049	0.0429	±0.0032	0.4137	1605	±152.0	468	±33.6	271	±9.8	271	±9.8
59	C-051508-1 64	253	338	0.0554	±0.0014	0.3302	±0.0105	0.0432	±0.0009	0.6315	428	±27.5	290	±4.0	273	±2.7	273	±2.7
60	C-051508-1 3	44	38	0.0626	±0.0090	0.3900	±0.0573	0.0452	±0.0014	0.2056	694	±153.3	334	±20.9	285	±4.2	285	±4.2
61	C-051508-1 120	80	186	0.0652	±0.0086	0.4771	±0.0645	0.0530	±0.0018	0.2454	782	±137.8	396	±22.2	333	±5.4	333	±5.4
62	C-051508-1 82	265	736	0.0637	±0.0012	0.8748	±0.0471	0.0995	±0.0050	0.9398	733	±19.5	638	±12.8	612	±14.8	612	±14.8
63	C-051508-1 52	89	264	0.0780	±0.0026	1.1032	±0.0637	0.1026	±0.0048	0.8096	1146	±33.7	755	±15.4	630	±14.0	630	±14.0
64	C-051508-1 17	58	206	0.0646	±0.0045	1.0028	±0.0732	0.1126	±0.0024	0.2872	762	±73.7	705	±18.6	688	±6.8	688	±6.8
65	C-051508-1 89	55	220	0.0629	±0.0035	1.0938	±0.0629	0.1260	±0.0020	0.2828	706	±58.7	750	±15.2	765	±5.9	765	±5.9
66	C-051508-1 135	32	176	0.0673	±0.0038	1.1699	±0.0709	0.1261	±0.0028	0.3702	846	±58.6	787	±16.6	766	±8.1	766	±8.1
67	C-051508-1 9	57	175	0.0765	±0.0012	2.2135	±0.0524	0.2098	±0.0036	0.7254	1108	±16.3	1185	±8.3	1228	±9.6	1108	±16.3
68	C-051508-1 92	399	1,496	0.0790	±0.0012	1.9121	±0.0887	0.1756	±0.0077	0.9430	1172	±15.3	1085	±15.5	1043	±21.1	1172	±15.3
69	C-051508-1 20	112	547	0.0792	±0.0009	1.8801	±0.0798	0.1721	±0.0070	0.9595	1178	±11.8	1074	±14.1	1024	±19.3	1178	±11.8
70	C-051508-1 13	192	853	0.0828	±0.0007	2.4018	±0.1483	0.2103	±0.0129	0.9918	1265	±7.7	1243	±22.1	1230	±34.3	1265	±7.7
71	C-051508-1 93	50	464	0.0865	±0.0029	2.7727	±0.1469	0.2326	±0.0094	0.7664	1349	±32.9	1348	±19.8	1348	±24.7	1349	±32.9
72	C-051508-1 124	64	562	0.0879	±0.0040	2.4680	±0.1528	0.2036	±0.0084	0.6692	1380	±44.2	1263	±22.4	1195	±22.6	1380	±44.2
73	C-051508-1 130	11	122	0.0894	±0.0071	2.7291	±0.2447	0.2214	±0.0092	0.4620	1413	±76.1	1336	±33.3	1289	±24.2	1413	±76.1
74	C-051508-1 72	95	801	0.0931	±0.0014	3.4394	±0.3008	0.2679	±0.0231	0.9842	1490	±14.6	1513	±34.4	1530	±58.6	1490	±14.6
75	C-051508-1 28	26	172	0.0938	±0.0071	3.4569	±0.2989	0.2672	±0.0111	0.4806	1505	±71.6	1517	±34.0	1526	±28.2	1505	±71.6
76	C-051508-1 80	603	2,558	0.0946	±0.0003	3.5767	±0.1175	0.2742	±0.0090	0.9964	1520	±2.6	1544	±13.0	1562	±22.7	1520	±2.6
77	C-051508-1 47	759	347	0.0949	±0.0007	2.8743	±0.0619	0.2197	±0.0044	0.9373	1526	±7.1	1375	±8.1	1280	±11.7	1526	±7.1
78	C-051508-1 144	213	1,465	0.0982	±0.0038	3.7032	±0.1753	0.2736	±0.0076	0.5827	1589	±35.9	1572	±18.9	1559	±19.1	1589	±35.9
79	C-051508-1 49	135	1,077	0.1029	±0.0008	3.8379	±0.3316	0.2706	±0.0233	0.9964	1676	±6.8	1601	±34.8	1544	±59.1	1676	±6.8
80	C-051508-1 53	120	650	0.1041	±0.0061	3.9201	±0.2453	0.2732	±0.0063	0.3681	1698	±53.6	1618	±25.3	1557	±15.9	1698	±53.6
81	C-051508-1 75	219	2,909	0.1045	±0.0003	4.1063	±0.0412	0.2851	±0.0027	0.9505	1705	±2.9	1656	±4.1	1617	±6.8	1705	±2.9
82	C-051508-1 36	461	2,993	0.1049	±0.0004	4.0246	±0.5303	0.2784	±0.0367	0.9996	1712	±3.3	1639	±53.6	1583	±92.4	1712	±3.3
83	C-051508-1 81	106	1,056	0.1049	±0.0009	3.4795	±0.0588	0.2405	±0.0034	0.8456	1713	±8.3	1523	±6.7	1389	±8.9	1713	±8.3
84	C-051508-1 95	213	2,439	0.1059	±0.0004	5.0346	±0.1390	0.3447	±0.0094	0.9922	1730	±3.2	1825	±11.7	1909	±22.6	1730	±3.2
85	C-051508-1 110	103	495	0.1112	±0.0022	4.9680	±0.3537	0.3242	±0.0222	0.9618	1818	±17.7	1814	±30.1	1810	±54.0	1818	±17.7
86	C-051508-1 94	35	214	0.1398	±0.0166	6.6214	±1.6535	0.3434	±0.0754	0.8797	2225	±102.8	2062	±110.1	1903	±181.0	2225	±102.8

Table C.5. Detrital zircon data table for GM-C-051608-5.

	Sample Name:	GM-C-051608-5				Isotopic Ratios						Apparent Ages (Ma)							
	Analysis	U	^{206}Pb	$^{207}Pb^{*}$	± 2 σ	$^{207}Pb^{*}$	± 2 σ	$^{206}Pb^{*}$	± 2 σ	Rho	$^{207}Pb^{*}$	± 1 σ	$^{207}Pb^{*}$	± 1 σ	$^{206}Pb^{*}$	± 1 σ	Best	± 1 σ
		ppm	^{204}Pb	$^{206}Pb^{*}$	abs	^{235}U	abs	^{238}U	abs		$^{206}Pb^{*}$	abs	^{235}U	abs	^{238}U	abs	Age	abs
1	C-051608-5 37	6806	229	0.0709	±0.0115	0.1005	±0.0186	0.0103	±0.0003	0.3397	955	±165.9	97	±8.6	66	±1.1	66	±1.1
2	C-051608-5 125	954	58,581	0.0830	±0.0096	0.1223	±0.0154	0.0107	±0.0005	0.3923	1269	±113.3	117	±7.0	69	±1.7	69	±1.7
3	C-051608-5 132	1297	62,148	0.0613	±0.0035	0.1020	±0.0067	0.0121	±0.0004	0.5094	650	±60.8	99	±3.1	77	±1.3	77	±1.3
4	C-051608-5 21	2103	196	0.0631	±0.0053	0.1407	±0.0196	0.0162	±0.0018	0.7972	711	±89.4	134	±8.7	103	±5.7	103	±5.7
5	C-051608-5 81	1342	41,999	0.0850	±0.0031	0.1963	±0.0117	0.0167	±0.0008	0.7909	1315	±35.3	182	±5.0	107	±2.5	107	±2.5
6	C-051608-5 128	905	59,841	0.0551	±0.0040	0.1411	±0.0108	0.0186	±0.0004	0.3098	414	±81.3	134	±4.8	119	±1.4	119	±1.4
7	C-051608-5 124	5665	1,304	0.0857	±0.0012	0.2197	±0.0043	0.0186	±0.0002	0.7069	1331	±13.1	202	±1.8	119	±0.7	119	±0.7
8	C-051608-5 18	2052	212	0.0855	±0.0034	0.3200	±0.0201	0.0271	±0.0013	0.7694	1328	±38.8	282	±7.7	173	±4.1	173	±4.1
9	C-051608-5 67	986	52,229	0.0751	±0.0020	0.3040	±0.0122	0.0293	±0.0009	0.7518	1072	±26.5	270	±4.7	186	±2.8	186	±2.8
10	C-051608-5 120	571	60,934	0.0543	±0.0026	0.2223	±0.0112	0.0297	±0.0004	0.2473	383	±54.6	204	±4.6	189	±1.1	189	±1.1
11	C-051608-5 57	485	56,414	0.0646	±0.0106	0.2886	±0.0489	0.0324	±0.0014	0.2542	762	±172.8	257	±19.3	206	±4.3	206	±4.3
12	C-051608-5 140	628	66,763	0.0562	±0.0018	0.2554	±0.0116	0.0329	±0.0011	0.7091	461	±35.5	231	±4.7	209	±3.3	209	±3.3
13	C-051608-5 71	860	49,306	0.0842	±0.0043	0.3889	±0.0251	0.0335	±0.0013	0.6192	1297	±49.2	334	±9.2	212	±4.2	212	±4.2
14	C-051608-5 84	706	41,998	0.0667	±0.0056	0.3461	±0.0314	0.0377	±0.0013	0.3862	827	±87.4	302	±11.9	238	±4.1	238	±4.1
15	C-051608-5 92	501	41,993	0.0577	±0.0014	0.7145	±0.0293	0.0899	±0.0029	0.7932	517	±27.4	547	±8.7	555	±8.6	555	±8.6
16	C-051608-5 82	652	41,999	0.0816	±0.0006	1.2240	±0.0414	0.1088	±0.0036	0.9760	1235	±7.2	812	±9.4	666	±10.4	666	±10.4
17	C-051608-5 80	5445	5,162	0.0918	±0.0003	1.8088	±0.0648	0.1429	±0.0050	0.9966	1463	±2.8	1049	±11.7	861	±14.0	861	±14.0
18	C-051608-5 83	153	41,998	0.0708	±0.0014	1.9822	±0.0743	0.2031	±0.0065	0.8563	951	±19.8	1109	±12.6	1192	±17.4	951	±19.8
19	C-051608-5 34	307	1,177	0.0655	±0.0013	1.5141	±0.0530	0.1677	±0.0040	0.8124	790	±21.1	936	±10.7	999	±11.1	999	±11.1
20	C-051608-5 90	3006	19,393	0.0799	±0.0005	2.1058	±0.0816	0.1912	±0.0072	0.9854	1194	±6.5	1151	±13.3	1128	±19.6	1194	±6.5
21	C-051608-5 134	639	63,302	0.0807	±0.0003	2.5453	±0.0441	0.2286	±0.0039	0.9810	1215	±3.3	1285	±6.3	1327	±10.2	1215	±3.3
22	C-051608-5 69	647	50,768	0.0843	±0.0008	2.5039	±0.0546	0.2153	±0.0042	0.8996	1300	±9.2	1273	±7.9	1257	±11.2	1300	±9.2
23	C-051608-5 32	760	1,051	0.0845	±0.0012	2.1920	±0.1366	0.1882	±0.0098	0.9716	1304	±14.1	1178	±21.7	1111	±26.7	1304	±14.1
24	C-051608-5 47	319	4,162	0.0849	±0.0064	2.0983	±0.2010	0.1793	±0.0102	0.6161	1313	±72.9	1148	±32.9	1063	±27.8	1313	±72.9
25	C-051608-5 27	1070	4,440	0.0862	±0.0007	2.8241	±0.1280	0.2377	±0.0102	0.9838	1342	±7.8	1362	±17.0	1375	±26.6	1342	±7.8
26	C-051608-5 40	985	35,371	0.0875	±0.0005	3.0983	±0.1240	0.2567	±0.0101	0.9881	1372	±5.9	1432	±15.4	1473	±25.9	1372	±5.9
27	C-051608-5 94	81	41,991	0.0904	±0.0034	3.0476	±0.1313	0.2445	±0.0049	0.4642	1434	±36.4	1420	±16.5	1410	±12.6	1434	±36.4
28	C-051608-5 127	366	59,264	0.0915	±0.0011	2.4333	±0.1590	0.1929	±0.0124	0.9833	1456	±11.3	1253	±23.5	1137	±33.4	1456	±11.3
29	C-051608-5 131	209	61,571	0.0919	±0.0006	3.2978	±0.1407	0.2602	±0.0109	0.9887	1466	±6.1	1481	±16.6	1491	±28.0	1466	±6.1
30	C-051608-5 73	521	47,845	0.0931	±0.0005	3.3502	±0.0902	0.2610	±0.0069	0.9835	1490	±4.6	1493	±10.5	1495	±17.6	1490	±4.6
31	C-051608-5 91	244	41,993	0.0940	±0.0006	3.5427	±0.0699	0.2733	±0.0051	0.9439	1509	±6.2	1537	±7.8	1557	±12.8	1509	±6.2
32	C-051608-5 136	401	64,456	0.0954	±0.0010	3.7578	±0.1310	0.2858	±0.0094	0.9489	1535	±10.3	1584	±14.0	1620	±23.6	1535	±10.3
33	C-051608-5 70	4913	1,380	0.0957	±0.0021	2.9304	±0.1219	0.2221	±0.0071	0.8479	1542	±20.5	1390	±15.7	1293	±18.7	1542	±20.5
34	C-051608-5 72	352	48,576	0.0959	±0.0008	3.0395	±0.0511	0.2298	±0.0033	0.8592	1546	±8.1	1418	±6.4	1333	±8.7	1546	±8.1
35	C-051608-5 130	497	60,994	0.0971	±0.0005	2.8177	±0.0943	0.2104	±0.0070	0.9900	1570	±4.4	1360	±12.5	1231	±18.5	1570	±4.4
36	C-051608-5 117	156	62,346	0.0978	±0.0008	3.8371	±0.0824	0.2844	±0.0057	0.9331	1583	±7.2	1601	±8.6	1614	±14.3	1583	±7.2
37	C-051608-5 121	635	60,463	0.0998	±0.0008	3.2648	±0.1274	0.2373	±0.0090	0.9790	1620	±7.4	1473	±15.2	1373	±23.6	1620	±7.4
38	C-051608-5 45	1017	16,469	0.0999	±0.0004	3.1448	±0.1938	0.2283	±0.0139	0.9979	1622	±3.7	1444	±23.7	1326	±36.5	1622	±3.7
39	C-051608-5 89	323	41,994	0.1009	±0.0007	3.5112	±0.3466	0.2523	±0.0248	0.9972	1641	±6.9	1530	±39.0	1450	±63.7	1641	±6.9
40	C-051608-5 137	463	65,033	0.1025	±0.0011	3.9626	±0.0976	0.2804	±0.0062	0.9069	1670	±9.6	1627	±10.0	1594	±15.7	1670	±9.6
41	C-051608-5 9	566	224	0.1028	±0.0032	3.9950	±0.1755	0.2817	±0.0087	0.7013	1676	±28.9	1633	±17.8	1600	±21.8	1676	±28.9
42	C-051608-5 44	2611	13,687	0.1038	±0.0003	3.3335	±0.1147	0.2328	±0.0079	0.9958	1694	±2.9	1489	±13.4	1349	±20.7	1694	±2.9
43	C-051608-5 68	530	51,498	0.1041	±0.0004	4.0384	±0.1097	0.2814	±0.0076	0.9909	1698	±3.4	1642	±11.1	1598	±19.0	1698	±3.4
44	C-051608-5 110	722	4,082	0.1062	±0.0007	4.2094	±0.1683	0.2875	±0.0110	0.9879	1735	±5.7	1676	±16.4	1629	±27.6	1735	±5.7
45	C-051608-5 46	2300	16,260	0.1070	±0.0003	3.8839	±0.4591	0.2633	±0.0309	0.9996	1749	±2.9	1610	±47.7	1507	±78.8	1749	±2.9
46	C-051608-5 96	192	2,342	0.1131	±0.0012	5.1516	±0.1237	0.3303	±0.0067	0.8912	1850	±9.8	1845	±10.2	1840	±16.3	1850	±9.8
47	C-051608-5 122	279	59,993	0.1135	±0.0006	4.1222	±0.0611	0.2634	±0.0037	0.9396	1857	±4.6	1659	±6.1	1507	±9.3	1857	±4.6
48	C-051608-5 106	873	58,249	0.1147	±0.0004	4.9917	±0.0765	0.3155	±0.0047	0.9747	1876	±3.1	1818	±6.5	1768	±11.5	1876	±3.1
49	C-051608-5 108	398	61,206	0.1199	±0.0004	6.2069	±0.1015	0.3755	±0.0060	0.9762	1955	±3.2	2005	±7.1	2055	±14.0	1955	±3.2
50	C-051608-5 98	107	8,915	0.1390	±0.0016	7.5792	±0.2102	0.3955	±0.0099	0.9152	2215	±9.7	2182	±12.4	2148	±22.9	2215	±9.7
51	C-051608-5 99	573	1,385	0.1436	±0.0014	7.6909	±0.2193	0.3883	±0.0098	0.9392	2271	±8.4	2196	±12.8	2115	±22.7	2271	±8.4
52	C-051608-5 93	39	41,992	0.1524	±0.0023	8.9932	±0.5365	0.4281	±0.0247	0.9675	2372	±12.9	2337	±27.3	2297	±55.7	2372	±12.9
53	C-051608-5 10	205	173	0.2071	±0.0061	16.4275	±0.6409	0.5753	±0.0146	0.6495	2883	±24.1	2902	±18.7	2929	±29.8	2883	±24.1

Table C.6. Detrital zircon data table for GM-W-051408-1.

	Sample Name:	GM-W-051408-1				Isotopic Ratios						Apparent Ages (Ma)							
	Analysis	U	^{206}Pb	$^{207}Pb^{*}$	± 2 σ	$^{207}Pb^{*}$	± 2 σ	$^{206}Pb^{*}$	± 2 σ	Rho	$^{207}Pb^{*}$	± 1 σ	$^{207}Pb^{*}$	± 1 σ	$^{206}Pb^{*}$	± 1 σ	Best	± 1 σ
		ppm	^{204}Pb	$^{206}Pb^{*}$	abs	^{235}U	abs	^{238}U	abs		$^{206}Pb^{*}$	abs	^{235}U	abs	^{238}U	abs	Age	abs
1	W-051408-8 69	721	52,053	0.0756	±0.0054	0.1817	±0.0145	0.0174	±0.0006	0.4245	1086	±72.2	170	±6.2	111	±1.9	111	±1.9
2	W-051408-8 132	1687	51,928	0.0528	±0.0013	0.1487	±0.0049	0.0204	±0.0004	0.6634	318	±28.1	141	±2.2	130	±1.4	130	±1.4
3	W-051408-8 104	408	51,186	0.0945	±0.0049	0.2834	±0.0219	0.0218	±0.0012	0.7394	1518	±49.0	253	±8.7	139	±3.9	139	±3.9
4	W-051408-8 101	1161	51,181	0.0500	±0.0008	0.1707	±0.0049	0.0247	±0.0006	0.8068	197	±19.6	160	±2.1	158	±1.8	158	±1.8
5	W-051408-8 14	1702	866	0.0754	±0.0041	0.2624	±0.0306	0.0253	±0.0021	0.8762	1078	±55.1	237	±12.3	161	±6.7	161	±6.7
6	W-051408-8 24	863	55,264	0.0603	±0.0016	0.2611	±0.0083	0.0314	±0.0005	0.5110	614	±29.4	236	±3.3	199	±1.6	199	±1.6
7	W-051408-8 43	282	51,244	0.0625	±0.0041	0.3449	±0.0258	0.0400	±0.0014	0.4861	693	±69.8	301	±9.8	253	±4.5	253	±4.5
8	W-051408-8 68	330	52,145	0.0901	±0.0035	0.5875	±0.0586	0.0473	±0.0043	0.9195	1428	±37.4	469	±18.8	298	±13.3	298	±13.3
9	W-051408-8 90	366	51,191	0.0757	±0.0013	0.8078	±0.0200	0.0774	±0.0014	0.7384	1087	±16.7	601	±5.6	481	±4.2	481	±4.2
10	W-051408-8 39	576	9,638	0.0825	±0.0052	1.0947	±0.1058	0.0962	±0.0069	0.7520	1258	±62.2	751	±25.6	592	±20.2	592	±20.2
11	W-051408-8 73	393	51,686	0.0650	±0.0012	0.9554	±0.0508	0.1066	±0.0053	0.9428	775	±18.6	681	±13.2	653	±15.5	653	±15.5
12	W-051408-8 63	184	399	0.0645	±0.0011	0.9777	±0.1089	0.1100	±0.0077	0.9868	757	±18.2	692	±27.9	673	±22.5	673	±22.5
13	W-051408-8 49	1175	11,715	0.0731	±0.0003	1.4470	±0.0741	0.1436	±0.0072	0.9973	1016	±3.8	909	±15.4	865	±20.3	865	±20.3
14	W-051408-8 40	1634	51,998	0.0869	±0.0003	1.7317	±0.0651	0.1445	±0.0054	0.9969	1358	±2.9	1020	±12.1	870	±15.2	870	±15.2
15	W-051408-8 71	310	51,869	0.0766	±0.0013	1.7187	±0.0620	0.1627	±0.0052	0.8875	1111	±16.6	1016	±11.6	972	±14.4	1111	±16.6
16	W-051408-8 107	147	50,805	0.0858	±0.0016	3.0696	±0.1667	0.2593	±0.0132	0.9414	1335	±17.7	1425	±20.8	1487	±33.8	1335	±17.7
17	W-051408-8 121	850	8,422	0.0879	±0.0003	2.5310	±0.0322	0.2087	±0.0025	0.9621	1381	±3.3	1281	±4.6	1222	±6.7	1381	±3.3
18	W-051408-8 103	694	51,184	0.0883	±0.0003	3.2682	±0.0821	0.2684	±0.0067	0.9927	1390	±2.9	1474	±9.8	1532	±16.9	1390	±2.9
19	W-051408-8 80	385	51,332	0.0889	±0.0003	3.1174	±0.0888	0.2544	±0.0072	0.9922	1402	±3.4	1437	±10.9	1461	±18.4	1402	±3.4
20	W-051408-8 131	707	51,609	0.0890	±0.0004	2.7978	±0.0539	0.2279	±0.0043	0.9774	1405	±3.9	1355	±7.2	1323	±11.2	1405	±3.9
21	W-051408-8 52	188	51,536	0.0914	±0.0011	3.6514	±0.1027	0.2897	±0.0074	0.9107	1455	±11.0	1561	±11.2	1640	±18.5	1455	±11.0
22	W-051408-8 55	502	51,984	0.0924	±0.0005	3.2396	±0.0898	0.2543	±0.0069	0.9797	1476	±5.3	1467	±10.7	1461	±17.7	1476	±5.3
23	W-051408-8 67	374	52,329	0.0933	±0.0008	3.0189	±0.0836	0.2346	±0.0062	0.9541	1495	±7.8	1412	±10.6	1358	±16.1	1495	±7.8
24	W-051408-8 45	184	50,741	0.0944	±0.0007	3.6493	±0.0638	0.2804	±0.0044	0.9033	1516	±7.1	1560	±7.0	1593	±11.1	1516	±7.1
25	W-051408-8 113	253	49,650	0.0982	±0.0009	4.0695	±0.1821	0.3006	±0.0131	0.9765	1590	±9.0	1648	±18.2	1694	±32.5	1590	±9.0
26	W-051408-8 72	154	3,131	0.0993	±0.0019	4.2913	±0.4751	0.3133	±0.0327	0.9852	1612	±17.6	1692	±45.6	1757	±80.3	1612	±17.6
27	W-051408-8 98	77	51,175	0.1009	±0.0013	4.1998	±0.1665	0.3020	±0.0113	0.9459	1640	±11.9	1674	±16.3	1701	±28.0	1640	±11.9
28	W-051408-8 77	432	51,379	0.1015	±0.0006	3.7506	±0.0697	0.2681	±0.0047	0.9554	1651	±5.1	1582	±7.4	1531	±12.1	1651	±5.1
29	W-051408-8 20	162	54,929	0.1019	±0.0025	4.0492	±0.2276	0.2881	±0.0145	0.8962	1660	±23.1	1644	±22.9	1632	±36.2	1660	±23.1
30	W-051408-8 76	849	14,029	0.1031	±0.0004	4.4443	±0.4495	0.3126	±0.0313	0.9994	1681	±3.2	1721	±41.9	1753	±76.9	1681	±3.2
31	W-051408-8 42	572	51,495	0.1036	±0.0003	3.4585	±0.1171	0.2421	±0.0081	0.9951	1690	±3.1	1518	±13.3	1398	±21.1	1690	±3.1
32	W-051408-8 125	426	49,701	0.1038	±0.0007	3.8606	±0.0938	0.2698	±0.0063	0.9652	1693	±5.9	1605	±9.8	1540	±16.0	1693	±5.9
33	W-051408-8 93	124	959	0.1040	±0.0037	3.5326	±0.2216	0.2465	±0.0111	0.8176	1696	±32.8	1535	±24.8	1420	±28.8	1696	±32.8
34	W-051408-8 99	265	51,177	0.1042	±0.0004	4.0563	±0.0527	0.2823	±0.0035	0.9610	1701	±3.3	1646	±5.3	1603	±8.8	1701	±3.3
35	W-051408-8 41	1385	9,797	0.1043	±0.0010	3.4495	±0.1896	0.2399	±0.0128	0.9838	1701	±9.1	1516	±21.6	1386	±33.3	1701	±9.1
36	W-051408-8 130	643	51,291	0.1044	±0.0002	4.3941	±0.2215	0.3054	±0.0153	0.9990	1703	±2.1	1711	±20.8	1718	±37.9	1703	±2.1
37	W-051408-8 17	632	54,678	0.1048	±0.0003	4.8635	±0.1589	0.3367	±0.0109	0.9958	1710	±2.7	1796	±13.8	1871	±26.4	1710	±2.7
38	W-051408-8 65	268	4,048	0.1048	±0.0018	4.4905	±0.1890	0.3107	±0.0116	0.9151	1711	±15.6	1729	±17.5	1744	±28.5	1711	±15.6
39	W-051408-8 134	236	52,564	0.1053	±0.0008	3.5757	±0.0838	0.2464	±0.0055	0.9469	1719	±6.9	1544	±9.3	1420	±14.1	1719	±6.9
40	W-051408-8 127	548	50,337	0.1054	±0.0003	3.9533	±0.0893	0.2721	±0.0061	0.9909	1721	±2.8	1625	±9.2	1551	±15.4	1721	±2.8
41	W-051408-8 74	581	51,594	0.1054	±0.0003	4.6164	±0.1942	0.3175	±0.0133	0.9969	1722	±3.0	1752	±17.6	1778	±32.5	1722	±3.0
42	W-051408-8 81	310	51,316	0.1057	±0.0007	5.0277	±0.1014	0.3451	±0.0066	0.9472	1726	±5.9	1824	±8.5	1911	±15.8	1726	±5.9
43	W-051408-8 100	137	51,179	0.1062	±0.0020	4.4522	±0.1104	0.3040	±0.0048	0.6336	1735	±17.6	1722	±10.3	1711	±11.8	1735	±17.6
44	W-051408-8 119	211	48,495	0.1066	±0.0006	4.1388	±0.0754	0.2816	±0.0049	0.9533	1742	±5.0	1662	±7.4	1599	±12.3	1742	±5.0
45	W-051408-8 120	127	48,303	0.1072	±0.0012	4.2130	±0.0651	0.2851	±0.0030	0.6825	1752	±10.3	1677	±6.3	1617	±7.5	1752	±10.3
46	W-051408-8 105	226	51,188	0.1072	±0.0007	4.4415	±0.1635	0.3004	±0.0109	0.9852	1753	±5.8	1720	±15.3	1693	±26.9	1753	±5.8
47	W-051408-8 94	76	1,312	0.1087	±0.0019	4.8368	±0.1339	0.3228	±0.0063	0.7772	1778	±15.7	1791	±11.6	1803	±15.5	1778	±15.7
48	W-051408-8 22	432	55,096	0.1095	±0.0006	4.3493	±0.0702	0.2881	±0.0043	0.9364	1791	±5.2	1703	±6.7	1632	±10.9	1791	±5.2
49	W-051408-8 23	818	55,180	0.1101	±0.0004	5.1500	±0.1580	0.3392	±0.0103	0.9930	1801	±3.3	1844	±13.0	1883	±24.8	1801	±3.3
50	W-051408-8 106	230	23,333	0.1102	±0.0017	5.3995	±0.2219	0.3554	±0.0135	0.9305	1802	±13.7	1885	±17.6	1960	±32.2	1802	±13.7
51	W-051408-8 115	393	4,007	0.1103	±0.0009	4.1802	±0.0704	0.2749	±0.0039	0.8710	1804	±7.5	1670	±6.9	1566	±9.9	1804	±7.5
52	W-051408-8 15	953	11,030	0.1112	±0.0003	4.4606	±0.1617	0.2910	±0.0104	0.9973	1818	±2.4	1724	±15.0	1647	±26.0	1818	±2.4
53	W-051408-8 13	350	57,352	0.1179	±0.0016	6.1449	±0.2215	0.3782	±0.0126	0.9288	1924	±12.0	1997	±15.7	2068	±29.5	1924	±12.0
54	W-051408-8 38	205	52,500	0.1201	±0.0013	5.0996	±0.2903	0.3081	±0.0172	0.9817	1957	±9.7	1836	±24.2	1731	±42.3	1957	±9.7
55	W-051408-8 60	121	52,731	0.1237	±0.0014	5.5560	±0.0823	0.3258	±0.0032	0.6625	2010	±9.8	1909	±6.4	1818	±7.8	2010	±9.8
56	W-051408-8 5	490	61,357	0.1250	±0.0019	6.7548	±0.1997	0.3920	±0.0099	0.8586	2029	±13.4	2080	±13.1	2132	±23.0	2029	±13.4
57	W-051408-8 2	108	2,025	0.1295	±0.0065	7.2147	±0.4307	0.4042	±0.0123	0.5371	2091	±43.9	2138	±26.6	2188	±28.3	2091	±43.9
58	W-051408-8 50	597	51,237	0.1320	±0.0003	7.6133	±0.1546	0.4184	±0.0084	0.9916	2124	±2.3	2186	±9.1	2253	±19.1	2124	±2.3
59	W-051408-8 27	79	55,515	0.1345	±0.0037	7.6494	±0.2812	0.4126	±0.0101	0.6662	2157	±23.9	2191	±16.5	2227	±23.0	2157	±23.9
60	W-051408-8 26	115	55,431	0.1355	±0.0103	7.1503	±0.7850	0.3826	±0.0302	0.7200	2171	±66.4	2130	±48.9	2089	±70.4	2171	±66.4
61	W-051408-8 3	50	1,064	0.1551	±0.0234	9.5901	±1.6246	0.4486	±0.0305	0.4328	2402	±128.1	2396	±77.9	2389	±68.0	2402	±128.1
62	W-051408-8 25	24	55,348	0.1647	±0.0030	11.9284	±0.2710	0.5254	±0.0072	0.6027	2504	±15.2	2599	±10.6	2722	±15.2	2504	±15.2
63	W-051408-8 6	388	60,856	0.1734	±0.0074	10.9051	±0.6520	0.4561	±0.0190	0.6990	2591	±35.7	2515	±27.8	2422	±42.1	2591	±35.7
64	W-051408-8 18	194	54,761	0.1831	±0.0005	13.7073	±0.3954	0.5431	±0.0156	0.9946	2681	±2.5	2730	±13.6	2796	±32.5	2681	±2.5

Table C.7. Detrital zircon data table for GM-W-051508-3.

	Sample Name:	GM-W-051508-3	Isotopic Ratios									Apparent Ages (Ma)							
	Analysis	U	^{206}Pb	$^{207}Pb^*$	± 2 σ	$^{207}Pb^*$	± 2 σ	$^{206}Pb^*$	± 2 σ	Rho	$^{207}Pb^*$	± 1 σ	^{207}Pb	± 1 σ	$^{206}Pb^*$	± 1 σ	Best	± 1 σ
		ppm	^{204}Pb	$^{206}Pb^*$	abs	^{235}U	abs	^{238}U	abs		$^{206}Pb^*$	abs	^{235}U	abs	^{238}U	abs	Age	abs
1	W-051508-3 95	506	223	0.0558	±0.0062	0.0721	±0.0082	0.0094	±0.0003	0.2383	446	±123.1	71	±3.9	60	±0.8	60	±0.8
2	W-051508-3 65	1617	374	0.0677	±0.0149	0.1002	±0.0231	0.0107	±0.0008	0.3091	858	±228.0	97	±10.7	69	±2.4	69	±2.4
3	W-051508-3 121	522	206	0.0625	±0.0056	0.1106	±0.0105	0.0128	±0.0004	0.3109	690	±96.1	107	±4.8	82	±1.2	82	±1.2
4	W-051508-3 134	413	248	0.0515	±0.0045	0.0932	±0.0103	0.0131	±0.0009	0.5968	265	±101.3	91	±4.8	84	±2.7	84	±2.7
5	W-051508-3 23	768	90	0.0592	±0.0049	0.1089	±0.0113	0.0133	±0.0008	0.6054	573	±89.5	105	±5.2	85	±2.7	85	±2.7
6	W-051508-3 92	200	101	0.0718	±0.0130	0.1448	±0.0267	0.0146	±0.0005	0.1985	981	±183.9	137	±11.8	94	±1.7	94	±1.7
7	W-051508-3 17	958	361	0.0631	±0.0038	0.1307	±0.0106	0.0150	±0.0008	0.6766	710	±63.2	125	±4.7	96	±2.6	96	±2.6
8	W-051508-3 34	174	81	0.0624	±0.0075	0.1299	±0.0162	0.0151	±0.0005	0.2810	689	±127.4	124	±7.3	97	±1.7	97	±1.7
9	W-051508-3 75	266	109	0.0742	±0.0102	0.1619	±0.0232	0.0158	±0.0006	0.2863	1048	±138.4	152	±10.1	101	±2.1	101	±2.1
10	W-051508-3 126	732	261	0.0585	±0.0017	0.1335	±0.0063	0.0165	±0.0006	0.7770	550	±32.4	127	±2.8	106	±1.9	106	±1.9
11	W-051508-3 133	847	540	0.0527	±0.0026	0.1233	±0.0097	0.0170	±0.0011	0.7857	314	±55.6	118	±4.4	109	±3.3	109	±3.3
12	W-051508-3 130	181	118	0.0816	±0.0260	0.1968	±0.0638	0.0175	±0.0010	0.1819	1236	±312.6	182	±27.1	112	±3.3	112	±3.3
13	W-051508-3 53	262	68	0.0724	±0.0062	0.1749	±0.0162	0.0175	±0.0006	0.3714	998	±87.2	164	±7.0	112	±1.9	112	±1.9
14	W-051508-3 120	51	24	0.0601	±0.0429	0.1462	±0.1049	0.0176	±0.0014	0.1072	609	±770.9	139	±46.5	113	±4.3	113	±4.3
15	W-051508-3 39	585	229	0.0593	±0.0030	0.1458	±0.0088	0.0178	±0.0006	0.5635	579	±54.4	138	±3.9	114	±1.9	114	±1.9
16	W-051508-3 87	321	205	0.0691	±0.0158	0.1703	±0.0397	0.0179	±0.0008	0.1919	900	±235.9	160	±17.2	114	±2.5	114	±2.5
17	W-051508-3 122	282	190	0.0593	±0.0086	0.1467	±0.0219	0.0179	±0.0007	0.2478	578	±157.5	139	±9.7	115	±2.1	115	±2.1
18	W-051508-3 55	224	116	0.0530	±0.0051	0.1315	±0.0138	0.0180	±0.0008	0.4039	329	±109.2	125	±6.2	115	±2.4	115	±2.4
19	W-051508-3 115	86	80	0.0735	±0.0147	0.1964	±0.0411	0.0194	±0.0012	0.2907	1027	±202.6	182	±17.5	124	±3.7	124	±3.7
20	W-051508-3 69	541	329	0.0510	±0.0034	0.1368	±0.0103	0.0194	±0.0007	0.4873	243	±76.0	130	±4.6	124	±2.3	124	±2.3
21	W-051508-3 36	190	101	0.0575	±0.0066	0.1614	±0.0193	0.0204	±0.0007	0.2788	510	±126.6	152	±8.5	130	±2.1	130	±2.1
22	W-051508-3 119	122	97	0.0611	±0.0127	0.1746	±0.0368	0.0207	±0.0006	0.1417	641	±224.3	163	±15.9	132	±2.0	132	±2.0
23	W-051508-3 104	209	138	0.0616	±0.0078	0.1784	±0.0227	0.0210	±0.0004	0.1519	662	±134.7	167	±9.8	134	±1.3	134	±1.3
24	W-051508-3 58	42	27	0.0443	±0.0314	0.1335	±0.0948	0.0218	±0.0014	0.0931	0	±0.0	127	±42.5	139	±4.6	139	±4.6
25	W-051508-3 33	105	35	0.0635	±0.0154	0.1933	±0.0502	0.0221	±0.0021	0.3661	726	±256.2	179	±21.4	141	±6.6	141	±6.6
26	W-051508-3 112	512	352	0.0558	±0.0030	0.1697	±0.0101	0.0221	±0.0005	0.4106	443	±60.1	159	±4.4	141	±1.7	141	±1.7
27	W-051508-3 13	199	117	0.0629	±0.0088	0.1925	±0.0278	0.0222	±0.0008	0.2395	705	±148.9	179	±11.8	142	±2.4	142	±2.4
28	W-051508-3 20	237	101	0.0654	±0.0103	0.2040	±0.0324	0.0226	±0.0004	0.1049	786	±165.8	189	±13.7	144	±1.2	144	±1.2
29	W-051508-3 1	921	283	0.0554	±0.0026	0.1730	±0.0106	0.0226	±0.0009	0.6462	429	±52.3	162	±4.6	144	±2.8	144	±2.8
30	W-051508-3 37	148	69	0.0732	±0.0188	0.2411	±0.0633	0.0239	±0.0014	0.2166	1019	±259.5	219	±25.9	152	±4.3	152	±4.3
31	W-051508-3 32	1069	442	0.0506	±0.0012	0.1682	±0.0064	0.0241	±0.0007	0.7869	222	±27.1	158	±2.8	154	±2.3	154	±2.3
32	W-051508-3 71	194	94	0.0703	±0.0108	0.2385	±0.0377	0.0246	±0.0008	0.2143	938	±158.1	217	±15.4	157	±2.6	157	±2.6
33	W-051508-3 124	168	124	0.0636	±0.0126	0.2158	±0.0431	0.0246	±0.0006	0.1260	728	±210.1	198	±18.0	157	±1.9	157	±1.9
34	W-051508-3 88	230	128	0.0572	±0.0066	0.1983	±0.0246	0.0251	±0.0012	0.3767	500	±126.7	184	±10.4	160	±3.7	160	±3.7
35	W-051508-3 128	145	88	0.0958	±0.0155	0.3340	±0.0569	0.0253	±0.0014	0.3201	1544	±151.7	293	±21.7	161	±4.3	161	±4.3
36	W-051508-3 42	435	265	0.0588	±0.0031	0.2081	±0.0119	0.0257	±0.0006	0.3800	559	±57.5	192	±5.0	163	±1.7	163	±1.7
37	W-051508-3 129	460	436	0.0541	±0.0038	0.1995	±0.0147	0.0268	±0.0006	0.3200	374	±78.5	185	±6.2	170	±2.0	170	±2.0
38	W-051508-3 48	581	467	0.0548	±0.0027	0.2028	±0.0106	0.0268	±0.0004	0.3056	405	±55.7	187	±4.5	171	±1.3	171	±1.3
39	W-051508-3 66	344	295	0.0554	±0.0024	0.2071	±0.0103	0.0271	±0.0007	0.4857	428	±48.5	191	±4.3	172	±2.1	172	±2.1
40	W-051508-3 111	591	276	0.0573	±0.0022	0.2150	±0.0113	0.0272	±0.0009	0.6615	502	±43.2	198	±4.7	173	±3.0	173	±3.0
41	W-051508-3 26	1619	1,057	0.0503	±0.0012	0.1934	±0.0078	0.0279	±0.0009	0.8229	208	±26.5	180	±3.3	177	±2.9	177	±2.9
42	W-051508-3 135	257	376	0.0558	±0.0058	0.2262	±0.0238	0.0294	±0.0005	0.1467	446	±115.8	207	±9.9	187	±1.4	187	±1.4
43	W-051508-3 45	335	263	0.0545	±0.0040	0.2238	±0.0187	0.0298	±0.0012	0.4965	390	±81.5	205	±7.8	189	±3.9	189	±3.9
44	W-051508-3 74	316	312	0.0580	±0.0032	0.2478	±0.0169	0.0310	±0.0013	0.5947	530	±60.1	225	±6.9	197	±3.9	197	±3.9
45	W-051508-3 85	219	223	0.0592	±0.0050	0.2572	±0.0227	0.0315	±0.0009	0.3147	573	±91.2	232	±9.2	200	±2.7	200	±2.7
46	W-051508-3 29	267	177	0.0799	±0.0075	0.3478	±0.0354	0.0316	±0.0012	0.3840	1193	±92.7	303	±13.3	200	±3.9	200	±3.9
47	W-051508-3 24	76	36	0.0617	±0.0163	0.2693	±0.0722	0.0317	±0.0015	0.1801	664	±282.4	242	±28.9	201	±4.8	201	±4.8
48	W-051508-3 97	347	332	0.0514	±0.0033	0.2262	±0.0159	0.0319	±0.0009	0.3909	259	±74.2	207	±6.6	202	±2.7	202	±2.7
49	W-051508-3 116	76	59	0.0877	±0.0104	0.3992	±0.0547	0.0330	±0.0022	0.4942	1376	±114.6	341	±19.9	209	±7.0	209	±7.0
50	W-051508-3 108	282	209	0.0744	±0.0133	0.3498	±0.0643	0.0341	±0.0015	0.2341	1051	±180.1	305	±24.2	216	±4.6	216	±4.6
51	W-051508-3 3	73	45	0.0777	±0.0082	0.3725	±0.0420	0.0348	±0.0013	0.3416	1139	±105.4	322	±15.5	220	±4.2	220	±4.2
52	W-051508-3 132	291	319	0.0534	±0.0028	0.2623	±0.0202	0.0356	±0.0020	0.7365	348	±59.0	236	±8.1	225	±6.3	225	±6.3
53	W-051508-3 110	146	84	0.0651	±0.0054	0.3201	±0.0270	0.0356	±0.0006	0.2141	779	±86.6	282	±10.4	226	±2.0	226	±2.0
54	W-051508-3 28	563	615	0.0542	±0.0021	0.2790	±0.0196	0.0373	±0.0022	0.8368	380	±43.3	250	±7.8	236	±6.8	236	±6.8
55	W-051508-3 6	40	27	0.0872	±0.0219	0.4596	±0.1198	0.0382	±0.0027	0.2693	1366	±241.7	384	±41.7	242	±8.3	242	±8.3
56	W-051508-3 30	355	269	0.0531	±0.0021	0.2845	±0.0122	0.0389	±0.0007	0.4258	332	±43.9	254	±4.8	246	±2.2	246	±2.2
57	W-051508-3 54	487	473	0.0505	±0.0018	0.2735	±0.0149	0.0393	±0.0016	0.7645	220	±40.5	246	±5.9	248	±5.1	248	±5.1
58	W-051508-3 5	143	95	0.0683	±0.0075	0.3773	±0.0429	0.0401	±0.0011	0.2486	876	±114.0	325	±15.8	253	±3.5	253	±3.5
59	W-051508-3 70	205	186	0.0523	±0.0045	0.2935	±0.0265	0.0407	±0.0012	0.3150	297	±97.9	261	±10.4	257	±3.6	257	±3.6
60	W-051508-3 89	401	210	0.0578	±0.0027	0.3409	±0.0252	0.0428	±0.0024	0.7702	521	±51.8	298	±9.5	270	±7.5	270	±7.5
61	W-051508-3 103	66	72	0.0690	±0.0066	0.6886	±0.0743	0.0723	±0.0035	0.4532	900	±99.2	532	±22.3	450	±10.6	450	±10.6
62	W-051508-3 11	397	385	0.0803	±0.0065	1.0864	±0.1032	0.0981	±0.0049	0.5287	1205	±79.4	747	±25.1	603	±14.5	603	±14.5
63	W-051508-3 68	170	280	0.0580	±0.0018	0.7882	±0.0321	0.0985	±0.0026	0.6431	531	±34.2	590	±9.1	606	±7.6	606	±7.6
64	W-051508-3 38	492	635	0.0627	±0.0005	0.8687	±0.0237	0.1005	±0.0026	0.9473	698	±9.3	635	±6.4	617	±7.6	617	±7.6
65	W-051508-3 78	355	1,176	0.0592	±0.0008	0.9144	±0.0274	0.1120	±0.0030	0.8847	575	±15.2	659	±7.3	684	±8.6	684	±8.6
66	W-051508-3 49	102	334	0.0694	±0.0044	1.1777	±0.1331	0.1231	±0.0115	0.8290	911	±65.1	790	±31.0	748	±33.1	748	±33.1
67	W-051508-3 52	269	579	0.0643	±0.0037	1.1108	±0.0729	0.1254	±0.0041	0.4995	750	±60.0	759	±17.5	762	±11.8	762	±11.8
68	W-051508-3 2	18	42	0.0827	±0.0095	1.5400	±0.2628	0.1350	±0.0170	0.7379	1263	±112.5	946	±52.5	816	±48.3	816	±48.3
69	W-051508-3 106	182	1,128	0.0769	±0.0010	2.3159	±0.0689	0.2183	±0.0059	0.9013	1120	±12.9	1217	±10.6	1273	±15.5	1120	±12.9
70	W-051508-3 93	27	149	0.0783	±0.0065	1.7203	±0.1573	0.1593	±0.0062	0.4251	1155	±82.1	1016	±29.4	953	±17.2	1155	±82.1
71	W-051508-3 127	504	2,957	0.0803	±0.0011	2.3629	±0.1163	0.2133	±0.0101	0.9626	1205	±13.1	1231	±17.6	1246	±26.8	1205	±13.1
72	W-051508-3 86	131	1,180	0.0821	±0.0010	2.5366	±0.0424	0.2241	±0.0026	0.6889	1247	±11.9	1283	±6.1	1304	±6.8	1247	±11.9
73	W-051508-3 40	75	474	0.0838	±0.0016	2.7992	±0.0968	0.2421	±0.0069	0.8246	1289	±19.0	1355	±12.9	1398	±17.9	1289	±19.0
74	W-051508-3 99	161	1,406	0.0900	±0.0007	2.9724	±0.0374	0.2396	±0.0023	0.7684	1425	±7.7	1401	±4.8	1385	±6.0	1425	±7.7
75	W-051508-3 81	363	1,128	0.0937	±0.0004	2.7464	±0.0407	0.2127	±0.0030	0.9542	1501	±4.2	1341	±5.5	1243	±8.0	1501	±4.2
76	W-051508-3 22	249	1,811	0.0947	±0.0005	3.9075	±0.2130	0.2992	±0.0162	0.9958	1522	±4.7	1615	±22.0	1687	±40.3	1522	±4.7
77	W-051508-3 91	233	1,866	0.0958	±0.0005	3.5969	±0.2027	0.2722	±0.0153	0.9951	1544	±5.3	1549	±22.4	1552	±38.7	1544	±5.3
78	W-051508-3 90	152	1,365	0.1015	±0.0010	4.1595	±0.3095	0.2973	±0.0219	0.9916	1651	±8.9	1666	±30.5	1678	±54.5	1651	±8.9
79	W-051508-3 56	591	3,276	0.1035	±0.0003	3.5390	±0.0704	0.2479	±0.0049	0.9867	1688	±3.0	1536	±7.9	1428	±12.6	1688	±3.0
80	W-051508-3 100	163	2,012	0.1042	±0.0006	4.4177	±0.1003	0.3074	±0.0068	0.9725	1701	±4.9	1716	±9.4	1728	±16.7	1701	±4.9
81	W-051508-3 101	883	6,347	0.1046	±0.0005	4.0577	±0.1667	0.2814	±0.0115	0.9936	1707	±4.3	1646	±16.7	1598	±28.9	1707	±4.3
82	W-051508-3 44	785	6,134	0.1090	±0.0003	4.9544	±0.1016	0.3297	±0.0067	0.9909	1782	±2.5	1812	±8.7	1837	±16.2	1782	±2.5
83	W-051508-3 4	124	996	0.1104	±0.0006	5.0309	±0.0944	0.3304	±0.0059	0.9509	1806	±5.3	1825	±8.0	1840	±14.3	1806	±5.3
84	W-051508-3 10	97	577	0.1142	±0.0031	5.8841	±0.3049	0.3737	±0.0164	0.8475	1867	±24.8	1959	±22.5	2047	±38.5	1867	±24.8
85	W-051508-3 76	144	989	0.1232	±0.0027	5.9450	±0.2057	0.3500	±0.0094	0.7757	2003	±19.4	1968	±15.0	1935	±22.4	2003	±19.4
86	W-051508-3 80	52	236	0.1849	±0.0020	13.0866	±0.2835	0.5134	±0.0097	0.8729	2697	±8.7	2686	±10.2	2671	±20.7	2697	±8.7

Table C.8. Detrital zircon data table for GM-W-051608-4.

	Sample Name:	GM-W-051608-4	Isotopic Ratios								Apparent Ages (Ma)							
	Analysis	U ppm	$^{206}Pb/^{204}Pb$	$^{207}Pb^*/^{206}Pb^*$	± 2 σ abs	$^{207}Pb^*/^{235}U$	± 2 σ abs	$^{206}Pb^*/^{238}U$	± 2 σ abs	Rho	$^{207}Pb^*/^{206}Pb^*$	± 1 σ abs	$^{207}Pb^*/^{235}U$	± 1 σ abs	$^{206}Pb^*/^{238}U$	± 1 σ abs	Best Age	± 1 σ abs
1	W-051608-4 26	573	324	0.0529	±0.0032	0.1120	±0.0081	0.0153	±0.0006	0.5721	327	±67.6	108	±3.7	98	±2.0	98	±2.0
2	W-051608-4 106	164	194	0.0556	±0.0135	0.1186	±0.0296	0.0155	±0.0009	0.2369	437	±269.7	114	±13.4	99	±2.9	99	±2.9
3	W-051608-4 133	184	197	0.0538	±0.0062	0.1156	±0.0140	0.0156	±0.0006	0.2921	364	±130.5	111	±6.4	100	±1.7	100	±1.7
4	W-051608-4 128	236	255	0.0617	±0.0085	0.1337	±0.0194	0.0157	±0.0007	0.3186	664	±147.1	127	±8.7	101	±2.3	101	±2.3
5	W-051608-4 72	979	456	0.0546	±0.0018	0.1201	±0.0098	0.0160	±0.0012	0.9124	395	±37.4	115	±4.4	102	±3.8	102	±3.8
6	W-051608-4 90	58	66	0.0690	±0.0336	0.1524	±0.0750	0.0160	±0.0012	0.1488	899	±501.5	144	±33.0	102	±3.7	102	±3.7
7	W-051608-4 152	289	308	0.0551	±0.0182	0.1219	±0.0408	0.0161	±0.0009	0.1710	414	±368.5	117	±18.5	103	±2.9	103	±2.9
8	W-051608-4 109	408	282	0.0529	±0.0049	0.1227	±0.0119	0.0168	±0.0005	0.2837	323	±105.5	118	±5.4	108	±1.5	108	±1.5
9	W-051608-4 153	97	49,262	0.0732	±0.0192	0.1731	±0.0459	0.0171	±0.0007	0.1480	1021	±265.6	162	±19.9	110	±2.1	110	±2.1
10	W-051608-4 28	303	220	0.0531	±0.0089	0.1311	±0.0224	0.0179	±0.0005	0.1779	334	±190.9	125	±10.1	114	±1.7	114	±1.7
11	W-051608-4 130	164	260	0.0629	±0.0075	0.1564	±0.0234	0.0180	±0.0016	0.5996	706	±127.2	148	±10.3	115	±5.1	115	±5.1
12	W-051608-4 107	373	176	0.0779	±0.0060	0.1940	±0.0160	0.0181	±0.0005	0.3599	1145	±76.3	180	±6.8	115	±1.7	115	±1.7
13	W-051608-4 36	57	38	0.0786	±0.0235	0.2015	±0.0616	0.0186	±0.0011	0.2005	1162	±296.9	186	±26.0	119	±3.6	119	±3.6
14	W-051608-4 13	339	191	0.0483	±0.0077	0.1324	±0.0233	0.0199	±0.0015	0.4334	113	±187.4	126	±10.5	127	±4.8	127	±4.8
15	W-051608-4 52	64	49	0.0707	±0.0206	0.2013	±0.0653	0.0207	±0.0029	0.4405	948	±297.9	186	±27.6	132	±9.3	132	±9.3
16	W-051608-4 91	180	558	0.0653	±0.0107	0.1888	±0.0315	0.0210	±0.0007	0.2011	783	±171.9	176	±13.5	134	±2.2	134	±2.2
17	W-051608-4 41	81	67	0.0495	±0.0130	0.1434	±0.0383	0.0210	±0.0010	0.1841	173	±306.6	136	±17.0	134	±3.3	134	±3.3
18	W-051608-4 125	45	75	0.0894	±0.0330	0.2664	±0.1005	0.0216	±0.0016	0.2007	1413	±353.4	240	±40.3	138	±5.2	138	±5.2
19	W-051608-4 55	320	229	0.0562	±0.0043	0.1695	±0.0142	0.0219	±0.0007	0.4024	460	±84.8	159	±6.1	140	±2.3	140	±2.3
20	W-051608-4 70	403	324	0.0483	±0.0031	0.1530	±0.0120	0.0229	±0.0010	0.5803	116	±75.4	145	±5.3	146	±3.3	146	±3.3
21	W-051608-4 123	573	620	0.0517	±0.0026	0.1643	±0.0096	0.0231	±0.0007	0.5252	270	±57.1	154	±4.2	147	±2.2	147	±2.2
22	W-051608-4 39	129	125	0.0544	±0.0087	0.1754	±0.0289	0.0234	±0.0010	0.2587	388	±178.7	164	±12.5	149	±3.1	149	±3.1
23	W-051608-4 110	251	210	0.0703	±0.0046	0.2301	±0.0162	0.0237	±0.0007	0.3900	938	±66.6	210	±6.7	151	±2.1	151	±2.1
24	W-051608-4 157	95	128	0.0571	±0.0107	0.1955	±0.0377	0.0248	±0.0011	0.2359	497	±206.2	181	±16.0	158	±3.5	158	±3.5
25	W-051608-4 145	68	146	0.0711	±0.0280	0.2446	±0.0995	0.0250	±0.0025	0.2460	961	±402.5	222	±40.6	159	±7.8	159	±7.8
26	W-051608-4 143	309	49,290	0.0576	±0.0037	0.2128	±0.0141	0.0268	±0.0004	0.2511	514	±70.3	196	±5.9	171	±1.4	171	±1.4
27	W-051608-4 42	123	110	0.0534	±0.0264	0.2026	±0.1006	0.0275	±0.0014	0.0995	347	±558.8	187	±42.5	175	±4.3	175	±4.3
28	W-051608-4 44	273	331	0.0519	±0.0045	0.2003	±0.0177	0.0280	±0.0005	0.1906	282	±99.4	185	±7.5	178	±1.5	178	±1.5
29	W-051608-4 18	133	93	0.0653	±0.0075	0.2567	±0.0330	0.0285	±0.0017	0.4594	785	±119.9	232	±13.3	181	±5.3	181	±5.3
30	W-051608-4 81	132	218	0.0555	±0.0054	0.2317	±0.0240	0.0303	±0.0011	0.3381	434	±108.4	212	±9.9	192	±3.3	192	±3.3
31	W-051608-4 136	335	49,150	0.0660	±0.0040	0.2951	±0.0197	0.0325	±0.0008	0.3919	805	±64.1	263	±7.7	206	±2.6	206	±2.6
32	W-051608-4 142	353	1,087	0.0487	±0.0026	0.2189	±0.0137	0.0326	±0.0010	0.4956	133	±63.7	201	±5.7	207	±3.1	207	±3.1
33	W-051608-4 29	268	297	0.0525	±0.0022	0.2442	±0.0129	0.0337	±0.0010	0.5871	309	±48.7	222	±5.3	214	±3.3	214	±3.3
34	W-051608-4 139	202	420	0.0605	±0.0058	0.2985	±0.0314	0.0358	±0.0016	0.4165	621	±103.1	265	±12.3	227	±4.9	227	±4.9
35	W-051608-4 3	183	180	0.0598	±0.0057	0.2996	±0.0306	0.0364	±0.0014	0.3651	595	±103.1	266	±12.0	230	±4.2	230	±4.2
36	W-051608-4 35	438	492	0.0490	±0.0020	0.2561	±0.0124	0.0379	±0.0010	0.5492	148	±47.6	231	±5.0	240	±3.1	240	±3.1
37	W-051608-4 113	261	536	0.0549	±0.0022	0.3389	±0.0145	0.0448	±0.0007	0.3487	407	±44.8	296	±5.5	282	±2.1	282	±2.1
38	W-051608-4 168	116	282	0.0564	±0.0041	0.3540	±0.0265	0.0455	±0.0008	0.2273	468	±80.7	308	±9.9	287	±2.4	287	±2.4
39	W-051608-4 30	77	174	0.0493	±0.0109	0.3104	±0.0692	0.0457	±0.0011	0.1124	160	±259.2	274	±26.8	288	±3.5	288	±3.5
40	W-051608-4 165	131	292	0.0668	±0.0043	0.4303	±0.0287	0.0467	±0.0008	0.2620	832	±67.0	363	±10.2	294	±2.5	294	±2.5
41	W-051608-4 105	23	100	0.0951	±0.0195	0.6300	±0.1339	0.0481	±0.0027	0.2613	1530	±193.2	496	±41.7	303	±8.2	303	±8.2
42	W-051608-4 101	356	1,104	0.0533	±0.0010	0.3667	±0.0093	0.0499	±0.0008	0.6696	340	±21.3	317	±3.5	314	±2.6	314	±2.6
43	W-051608-4 132	234	1,513	0.0579	±0.0018	0.5745	±0.0207	0.0720	±0.0012	0.4649	524	±35.1	461	±6.7	448	±3.6	448	±3.6
44	W-051608-4 167	137	739	0.0597	±0.0030	0.6732	±0.0413	0.0818	±0.0028	0.5618	592	±55.0	523	±12.5	507	±8.4	507	±8.4
45	W-051608-4 94	11	90	0.0691	±0.0363	0.8909	±0.4887	0.0936	±0.0148	0.2887	900	±541.6	647	±131.2	577	±43.7	577	±43.7
46	W-051608-4 86	187	693	0.0677	±0.0018	0.9001	±0.0393	0.0965	±0.0033	0.7916	858	±27.7	652	±10.5	594	±9.8	594	±9.8
47	W-051608-4 17	85	245	0.0614	±0.0029	0.9566	±0.0494	0.1130	±0.0022	0.3805	654	±51.2	682	±12.8	690	±6.4	690	±6.4
48	W-051608-4 138	31	450	0.0879	±0.0099	1.6743	±0.1978	0.1381	±0.0047	0.2894	1381	±108.7	999	±37.6	834	±13.4	834	±13.4
49	W-051608-4 65	45	229	0.0680	±0.0024	1.7392	±0.0810	0.1854	±0.0056	0.6523	870	±36.6	1023	±15.0	1096	±15.3	870	±36.6
50	W-051608-4 67	108	748	0.0721	±0.0025	1.9684	±0.1198	0.1979	±0.0098	0.8172	990	±35.7	1105	±20.5	1164	±26.5	990	±35.7
51	W-051608-4 53	37	310	0.0807	±0.0027	2.3231	±0.0966	0.2087	±0.0052	0.5965	1215	±32.8	1219	±14.8	1222	±13.8	1215	±32.8
52	W-051608-4 22	254	1,820	0.0853	±0.0005	2.7691	±0.0576	0.2353	±0.0047	0.9662	1323	±5.2	1347	±7.8	1362	±12.3	1323	±5.2
53	W-051608-4 15	193	1,139	0.0866	±0.0008	3.1757	±0.0835	0.2660	±0.0066	0.9394	1352	±8.7	1451	±10.2	1520	±16.7	1352	±8.7
54	W-051608-4 16	136	921	0.0881	±0.0007	2.7749	±0.1099	0.2285	±0.0089	0.9818	1384	±7.2	1349	±14.8	1327	±23.3	1384	±7.2
55	W-051608-4 112	22	400	0.0902	±0.0057	3.3950	±0.2458	0.2728	±0.0096	0.4879	1431	±60.3	1503	±28.4	1555	±24.4	1431	±60.3
56	W-051608-4 24	274	1,441	0.0910	±0.0009	2.4972	±0.2848	0.1991	±0.0226	0.9963	1446	±9.3	1271	±41.3	1170	±60.8	1446	±9.3
57	W-051608-4 99	242	3,183	0.0914	±0.0004	3.5738	±0.1666	0.2834	±0.0131	0.9952	1456	±4.3	1544	±18.5	1609	±33.0	1456	±4.3
58	W-051608-4 127	314	2,587	0.0920	±0.0003	3.6660	±0.1448	0.2890	±0.0114	0.9965	1468	±3.1	1564	±15.8	1636	±28.4	1468	±3.1
59	W-051608-4 25	91	725	0.0936	±0.0026	3.6500	±0.1257	0.2828	±0.0057	0.5858	1500	±26.4	1561	±13.7	1606	±14.3	1500	±26.4
60	W-051608-4 88	85	836	0.0941	±0.0015	3.0674	±0.0960	0.2363	±0.0064	0.8666	1511	±14.7	1425	±12.0	1368	±16.7	1511	±14.7
61	W-051608-4 12	225	2,467	0.0959	±0.0006	3.9765	±0.1742	0.3006	±0.0131	0.9914	1547	±5.4	1629	±17.8	1694	±32.4	1547	±5.4
62	W-051608-4 154	107	2,223	0.0964	±0.0015	3.2480	±0.0928	0.2443	±0.0058	0.8277	1556	±15.1	1469	±11.1	1409	±15.0	1556	±15.1
63	W-051608-4 34	61	549	0.0968	±0.0091	3.1844	±0.8813	0.2387	±0.0621	0.9402	1563	±88.4	1453	±106.9	1380	±161.6	1563	±88.4
64	W-051608-4 4	122	569	0.0989	±0.0011	3.3608	±0.1936	0.2465	±0.0139	0.9807	1603	±10.5	1495	±22.5	1420	±36.0	1603	±10.5
65	W-051608-4 75	504	13,131	0.1002	±0.0003	4.2179	±0.0676	0.3054	±0.0048	0.9815	1627	±2.9	1678	±6.6	1718	±11.9	1627	±2.9
66	W-051608-4 60	264	2,140	0.1017	±0.0005	4.2467	±0.1584	0.3027	±0.0112	0.9905	1656	±4.7	1683	±15.3	1705	±27.7	1656	±4.7
67	W-051608-4 100	208	3,853	0.1018	±0.0006	4.6581	±0.1216	0.3320	±0.0085	0.9768	1656	±5.2	1760	±10.9	1848	±20.5	1656	±5.2
68	W-051608-4 140	1095	46,864	0.1032	±0.0002	4.0172	±0.0777	0.2823	±0.0054	0.9922	1683	±2.2	1638	±7.9	1603	±13.6	1683	±2.2
69	W-051608-4 129	685	11,303	0.1052	±0.0003	4.3840	±0.2678	0.3022	±0.0184	0.9991	1718	±2.4	1709	±25.2	1702	±45.6	1718	±2.4
70	W-051608-4 82	222	3,565	0.1059	±0.0012	5.0222	±0.1947	0.3438	±0.0128	0.9598	1731	±10.0	1823	±16.4	1905	±30.7	1731	±10.0
71	W-051608-4 97	237	4,132	0.1068	±0.0008	3.7308	±0.2456	0.2533	±0.0166	0.9936	1746	±6.8	1578	±26.4	1455	±42.6	1746	±6.8
72	W-051608-4 57	57	246	0.1102	±0.0083	5.4838	±0.6070	0.3610	±0.0294	0.7360	1802	±68.1	1898	±47.5	1987	±69.7	1802	±68.1
73	W-051608-4 2	334	3,279	0.1562	±0.0004	9.2847	±0.1574	0.4311	±0.0072	0.9864	2415	±2.4	2367	±7.8	2311	±16.2	2415	±2.4
74	W-051608-4 23	190	1,491	0.1653	±0.0014	9.9777	±0.7187	0.4377	±0.0313	0.9927	2511	±7.3	2433	±33.2	2340	±70.2	2511	±7.3

Table C.9. Detrital zircon data table for Urban 1.

	Sample Name:	Urban 1	Isotopic Ratios								Apparent Ages (Ma)							
	Analysis	U ppm	$^{206}Pb/^{204}Pb$	$^{207}Pb^{*}/^{206}Pb^{*}$	± 2 σ abs	$^{207}Pb^{*}/^{235}U$	± 2 σ abs	$^{206}Pb^{*}/^{238}U$	± 2 σ abs	Rho	$^{207}Pb^{*}/^{206}Pb^{*}$	± 1 σ abs	$^{207}Pb^{*}/^{235}U$	± 1 σ abs	$^{206}Pb^{*}/^{238}U$	± 1 σ abs	Best Age	± 1 σ abs
1	Urban-1 89	277	72	0.0755	±0.0098	0.1295	±0.0172	0.0124	±0.0003	0.2009	1081	±130.5	124	±7.7	80	±1.1	80	±1.1
2	Urban-1 95	329	93	0.0858	±0.0058	0.2329	±0.0212	0.0197	±0.0012	0.6725	1335	±65.0	213	±8.7	126	±3.8	126	±3.8
3	Urban-1 86	1637	238	0.0666	±0.0016	0.2182	±0.0069	0.0238	±0.0005	0.6450	824	±25.3	200	±2.9	151	±1.5	151	±1.5
4	Urban-1 83	328	103	0.0772	±0.0052	0.2847	±0.0202	0.0267	±0.0006	0.2919	1128	±67.5	254	±8.0	170	±1.7	170	±1.7
5	Urban-1 109	728	218	0.0725	±0.0037	0.2705	±0.0180	0.0271	±0.0012	0.6512	1000	±51.2	243	±7.2	172	±3.7	172	±3.7
6	Urban-1 3	848	39	0.0762	±0.0030	0.2875	±0.0129	0.0274	±0.0005	0.4463	1099	±40.1	257	±5.1	174	±1.7	174	±1.7
7	Urban-1 108	320	159	0.0639	±0.0039	0.2583	±0.0170	0.0293	±0.0007	0.3565	739	±65.1	233	±6.9	186	±2.2	186	±2.2
8	Urban-1 117	353	107	0.0861	±0.0026	0.4551	±0.0189	0.0383	±0.0011	0.6889	1340	±29.1	381	±6.6	243	±3.4	243	±3.4
9	Urban-1 67	234	86	0.1049	±0.0039	0.5762	±0.0322	0.0398	±0.0017	0.7534	1713	±33.8	462	±10.4	252	±5.2	252	±5.2
10	Urban-1 34	583	242	0.0844	±0.0066	0.4862	±0.0461	0.0418	±0.0022	0.5556	1302	±76.5	402	±15.7	264	±6.8	264	±6.8
11	Urban-1 14	311	35	0.1101	±0.0148	0.7083	±0.1034	0.0467	±0.0027	0.3905	1801	±122.2	544	±30.7	294	±8.2	294	±8.2
12	Urban-1 30	97	47	0.0991	±0.0080	0.7096	±0.0610	0.0519	±0.0015	0.3450	1607	±75.2	544	±18.1	326	±4.7	326	±4.7
13	Urban-1 142	531	331	0.0732	±0.0018	0.5249	±0.0247	0.0520	±0.0021	0.8453	1020	±25.5	428	±8.2	327	±6.3	327	±6.3
14	Urban-1 81	173	102	0.0751	±0.0023	0.6754	±0.0306	0.0652	±0.0022	0.7431	1071	±30.4	524	±9.3	407	±6.6	407	±6.6
15	Urban-1 110	275	544	0.0791	±0.0006	2.1000	±0.0426	0.1926	±0.0036	0.9293	1174	±7.4	1149	±7.0	1136	±9.8	1174	±7.4
16	Urban-1 41	179	255	0.0800	±0.0017	1.9258	±0.0555	0.1745	±0.0034	0.6781	1198	±20.9	1090	±9.6	1037	±9.4	1198	±20.9
17	Urban-1 94	360	487	0.0870	±0.0028	3.0169	±0.1154	0.2515	±0.0052	0.5370	1361	±31.1	1412	±14.6	1446	±13.3	1361	±31.1
18	Urban-1 36	86	177	0.0902	±0.0019	3.0217	±0.0912	0.2431	±0.0052	0.7047	1429	±20.4	1413	±11.5	1403	±13.4	1429	±20.4
19	Urban-1 93	107	271	0.0905	±0.0018	3.3029	±0.0839	0.2647	±0.0041	0.6085	1436	±19.2	1482	±9.9	1514	±10.4	1436	±19.2
20	Urban-1 39	137	368	0.0913	±0.0014	3.0894	±0.0923	0.2453	±0.0063	0.8549	1453	±14.8	1430	±11.5	1414	±16.2	1453	±14.8
21	Urban-1 16	214	370	0.0929	±0.0009	3.4681	±0.1293	0.2708	±0.0097	0.9629	1486	±9.5	1520	±14.7	1545	±24.6	1486	±9.5
22	Urban-1 150	80	360	0.0939	±0.0022	3.0868	±0.0818	0.2385	±0.0027	0.4283	1506	±22.6	1429	±10.2	1379	±7.0	1506	±22.6
23	Urban-1 126	101	289	0.0968	±0.0015	4.0825	±0.0953	0.3059	±0.0052	0.7309	1563	±14.9	1651	±9.5	1721	±12.9	1563	±14.9
24	Urban-1 98	140	464	0.1000	±0.0015	3.2241	±0.1175	0.2338	±0.0078	0.9106	1624	±14.0	1463	±14.1	1354	±20.3	1624	±14.0
25	Urban-1 125	152	200	0.1021	±0.0051	3.5568	±0.1928	0.2527	±0.0054	0.3970	1663	±46.1	1540	±21.5	1452	±14.0	1663	±46.1
26	Urban-1 119	83	203	0.1028	±0.0019	3.6284	±0.2701	0.2559	±0.0185	0.9701	1676	±16.7	1556	±29.6	1469	±47.4	1676	±16.7
27	Urban-1 59	255	1,404	0.1056	±0.0007	4.5873	±0.1087	0.3151	±0.0071	0.9550	1724	±6.5	1747	±9.9	1766	±17.5	1724	±6.5
28	Urban-1 13	884	90	0.1086	±0.0012	4.4844	±0.1279	0.2995	±0.0078	0.9169	1776	±10.4	1728	±11.8	1689	±19.4	1776	±10.4
29	Urban-1 84	234	720	0.1098	±0.0009	4.2541	±0.1229	0.2811	±0.0078	0.9608	1795	±7.3	1685	±11.9	1597	±19.6	1795	±7.3
30	Urban-1 71	268	533	0.1135	±0.0014	4.3147	±0.2608	0.2757	±0.0163	0.9800	1856	±10.9	1696	±24.9	1570	±41.3	1856	±10.9
31	Urban-1 137	178	610	0.1137	±0.0007	4.6689	±0.4183	0.2978	±0.0266	0.9974	1860	±5.8	1762	±37.5	1680	±66.1	1860	±5.8
32	Urban-1 106	152	463	0.1164	±0.0011	5.6761	±0.1787	0.3536	±0.0106	0.9535	1902	±8.5	1928	±13.6	1952	±25.3	1902	±8.5
33	Urban-1 123	242	446	0.1194	±0.0019	5.3957	±0.1951	0.3278	±0.0106	0.8942	1947	±14.5	1884	±15.5	1828	±25.7	1947	±14.5
34	Urban-1 43	77	196	0.1217	±0.0022	6.5334	±0.1932	0.3894	±0.0091	0.7919	1981	±16.1	2050	±13.0	2120	±21.2	1981	±16.1
35	Urban-1 8	421	128	0.1243	±0.0009	6.8834	±0.1916	0.4017	±0.0108	0.9676	2019	±6.2	2097	±12.3	2177	±24.9	2019	±6.2
36	Urban-1 100	90	227	0.1358	±0.0022	7.8438	±0.2457	0.4188	±0.0113	0.8614	2175	±13.9	2213	±14.1	2255	±25.7	2175	±13.9
37	Urban-1 103	147	219	0.1412	±0.0072	7.8132	±0.5522	0.4013	±0.0195	0.6874	2242	±44.4	2210	±31.8	2175	±44.8	2242	±44.4
38	Urban-1 120	224	518	0.1428	±0.0038	7.5521	±0.2681	0.3837	±0.0090	0.6626	2261	±22.9	2179	±15.9	2093	±21.0	2261	±22.9
39	Urban-1 139	58	109	0.1471	±0.0091	7.8068	±0.5802	0.3848	±0.0160	0.5578	2313	±52.9	2209	±33.4	2099	±37.1	2313	±52.9
40	Urban-1 116	347	607	0.1531	±0.0245	7.9668	±1.7305	0.3774	±0.0553	0.6751	2381	±136.5	2227	±98.0	2064	±129.5	2381	±136.5
41	Urban-1 128	115	294	0.1707	±0.0013	9.4563	±0.5025	0.4018	±0.0211	0.9894	2565	±6.4	2383	±24.4	2177	±48.6	2565	±6.4
42	Urban-1 141	175	1,065	0.1757	±0.0007	11.7336	±0.1808	0.4843	±0.0072	0.9658	2613	±3.3	2583	±7.2	2546	±15.6	2613	±3.3
43	Urban-1 96	134	232	0.1935	±0.0105	13.2151	±1.0945	0.4954	±0.0311	0.7576	2772	±44.3	2695	±39.1	2594	±67.0	2772	±44.3
44	Urban-1 65	94	156	0.2212	±0.0059	16.4718	±0.5244	0.5401	±0.0093	0.5394	2990	±21.6	2905	±15.2	2784	±19.4	2990	±21.6
45	Urban-1 91	94	59	0.2603	±0.0100	24.5110	±1.5361	0.6829	±0.0338	0.7894	3249	±30.3	3289	±30.6	3356	±64.7	3249	±30.3

Table C.10. Detrital zircon data table for Winch State 4.

	Sample Name:	Winch State 4				Isotopic Ratios						Apparent Ages (Ma)							
	Analysis	U	^{206}Pb / ^{204}Pb	$^{207}Pb^{*}$ / $^{206}Pb^{*}$	± 2 σ abs	$^{207}Pb^{*}$ / ^{235}U	± 2 σ abs	$^{206}Pb^{*}$ / ^{238}U	± 2 σ abs	Rho	$^{207}Pb^{*}$ / $^{206}Pb^{*}$	± 1 σ abs	$^{207}Pb^{*}$ / ^{235}U	± 1 σ abs	$^{206}Pb^{*}$ / ^{238}U	± 1 σ abs	Best Age	± 1 σ abs
		ppm																	
1	Winch St-4 135	280	79	0.0909	±0.0621	0.1989	±0.1398	0.0159	±0.0026	0.2362	1444	±650.7	184	±59.2	102	±8.4	102	±8.4
2	Winch St-4 78	78	43	0.0933	±0.0167	0.2376	±0.0457	0.0185	±0.0013	0.3648	1495	±169.4	216	±18.8	118	±4.1	118	±4.1
3	Winch St-4 145	310	132	0.0650	±0.0047	0.1687	±0.0129	0.0188	±0.0004	0.2957	775	±76.8	158	±5.6	120	±1.3	120	±1.3
4	Winch St-4 88	319	99	0.0929	±0.0077	0.2556	±0.0351	0.0200	±0.0022	0.7963	1486	±78.7	231	±14.2	127	±6.9	127	±6.9
5	Winch St-4 136	329	148	0.0572	±0.0052	0.1671	±0.0156	0.0212	±0.0004	0.2230	499	±100.4	157	±6.8	135	±1.4	135	±1.4
6	Winch St-4 54	392	152	0.0607	±0.0037	0.2085	±0.0139	0.0249	±0.0007	0.4134	629	±65.4	192	±5.8	159	±2.2	159	±2.2
7	Winch St-4 60	197	87	0.0694	±0.0053	0.2539	±0.0236	0.0265	±0.0014	0.5646	912	±78.9	230	±9.6	169	±4.4	169	±4.4
8	Winch St-4 91	217	108	0.0650	±0.0037	0.2796	±0.0172	0.0312	±0.0007	0.3705	775	±60.2	250	±6.8	198	±2.2	198	±2.2
9	Winch St-4 124	446	305	0.0548	±0.0012	0.2406	±0.0114	0.0318	±0.0013	0.8853	405	±24.7	219	±4.7	202	±4.2	202	±4.2
10	Winch St-4 89	41	44	0.0889	±0.0219	0.3915	±0.1132	0.0319	±0.0048	0.5239	1403	±235.8	335	±41.3	203	±15.1	203	±15.1
11	Winch St-4 55	286	220	0.0596	±0.0029	0.2778	±0.0150	0.0338	±0.0008	0.4132	589	±53.4	249	±6.0	214	±2.4	214	±2.4
12	Winch St-4 132	157	125	0.0538	±0.0034	0.2710	±0.0183	0.0365	±0.0009	0.3778	364	±70.3	244	±7.3	231	±2.9	231	±2.9
13	Winch St-4 118	228	285	0.0592	±0.0028	0.3789	±0.0202	0.0464	±0.0011	0.4618	575	±51.4	326	±7.4	292	±3.5	292	±3.5
14	Winch St-4 57	237	275	0.0573	±0.0015	0.4913	±0.0202	0.0622	±0.0020	0.7684	502	±28.9	406	±6.9	389	±6.0	389	±6.0
15	Winch St-4 4	129	142	0.0620	±0.0014	0.5866	±0.0209	0.0687	±0.0019	0.7666	673	±24.5	469	±6.7	428	±5.7	428	±5.7
16	Winch St-4 49	256	413	0.0566	±0.0013	0.6141	±0.0201	0.0787	±0.0019	0.7229	475	±25.0	486	±6.3	489	±5.6	489	±5.6
17	Winch St-4 8	80	126	0.0675	±0.0087	0.7592	±0.1023	0.0815	±0.0033	0.2964	854	±133.7	574	±29.5	505	±9.7	505	±9.7
18	Winch St-4 38	143	217	0.0750	±0.0046	0.8773	±0.0645	0.0848	±0.0034	0.5530	1068	±61.6	640	±17.4	525	±10.2	525	±10.2
19	Winch St-4 123	184	591	0.0739	±0.0008	1.5226	±0.0393	0.1495	±0.0035	0.8981	1038	±11.5	940	±7.9	898	±9.7	898	±9.7
20	Winch St-4 127	67	258	0.0978	±0.0045	2.0754	±0.1686	0.1539	±0.0103	0.8256	1583	±42.9	1141	±27.8	923	±28.8	923	±28.8
21	Winch St-4 47	64	178	0.0708	±0.0024	1.6140	±0.0627	0.1652	±0.0032	0.4966	953	±34.5	976	±12.2	986	±8.8	986	±8.8
22	Winch St-4 43	170	902	0.0781	±0.0005	2.2858	±0.1053	0.2122	±0.0097	0.9883	1150	±7.0	1208	±16.3	1240	±25.7	1150	±7.0
23	Winch St-4 70	125	575	0.0805	±0.0016	2.1599	±0.1592	0.1945	±0.0138	0.9641	1210	±19.3	1168	±25.6	1146	±37.3	1210	±19.3
24	Winch St-4 110	95	264	0.0881	±0.0082	3.1676	±0.3769	0.2609	±0.0193	0.6209	1384	±89.6	1449	±45.9	1494	±49.3	1384	±89.6
25	Winch St-4 143	60	198	0.0884	±0.0042	2.6946	±0.2008	0.2210	±0.0127	0.7735	1392	±45.3	1327	±27.6	1287	±33.6	1392	±45.3
26	Winch St-4 149	106	579	0.0890	±0.0018	3.4182	±0.0963	0.2787	±0.0053	0.6784	1403	±19.8	1509	±11.1	1585	±13.4	1403	±19.8
27	Winch St-4 56	405	1,523	0.0908	±0.0004	2.5436	±0.0729	0.2031	±0.0057	0.9873	1443	±4.3	1285	±10.4	1192	±15.4	1443	±4.3
28	Winch St-4 107	63	346	0.0915	±0.0016	3.2355	±0.2167	0.2563	±0.0166	0.9675	1458	±16.1	1466	±26.0	1471	±42.6	1458	±16.1
29	Winch St-4 46	158	966	0.0924	±0.0007	3.6537	±0.1283	0.2869	±0.0099	0.9787	1475	±6.8	1561	±14.0	1626	±24.7	1475	±6.8
30	Winch St-4 15	472	1,325	0.0939	±0.0048	3.5082	±0.4536	0.2709	±0.0321	0.9175	1507	±48.6	1529	±51.1	1545	±81.5	1507	±48.6
31	Winch St-4 105	366	1,302	0.0996	±0.0008	3.4052	±0.0839	0.2479	±0.0058	0.9420	1617	±7.7	1506	±9.7	1427	±14.9	1617	±7.7
32	Winch St-4 5	24	86	0.1004	±0.0110	3.2487	±0.8715	0.2347	±0.0575	0.9133	1631	±101.5	1469	±104.1	1359	±150.1	1631	±101.5
33	Winch St-4 26	132	723	0.1016	±0.0016	4.2720	±0.2825	0.3051	±0.0196	0.9704	1653	±14.8	1688	±27.2	1716	±48.4	1653	±14.8
34	Winch St-4 11	145	757	0.1022	±0.0012	4.2126	±0.2151	0.2991	±0.0149	0.9744	1664	±10.6	1676	±21.0	1687	±36.9	1664	±10.6
35	Winch St-4 101	192	1,167	0.1039	±0.0006	4.2943	±0.2666	0.2997	±0.0185	0.9958	1696	±5.3	1692	±25.6	1690	±45.9	1696	±5.3
36	Winch St-4 10	83	379	0.1047	±0.0023	4.4999	±0.6552	0.3119	±0.0449	0.9885	1708	±20.3	1731	±60.5	1750	±110.3	1708	±20.3
37	Winch St-4 30	234	1,358	0.1047	±0.0005	4.3921	±0.4164	0.3041	±0.0288	0.9987	1710	±4.5	1711	±39.2	1712	±71.2	1710	±4.5
38	Winch St-4 23	87	413	0.1055	±0.0144	4.9711	±0.7901	0.3416	±0.0281	0.5167	1724	±125.0	1814	±67.2	1894	±67.4	1724	±125.0
39	Winch St-4 22	195	1,418	0.1073	±0.0004	4.9210	±0.0747	0.3327	±0.0049	0.9691	1754	±3.4	1806	±6.4	1851	±11.8	1754	±3.4
40	Winch St-4 82	66	288	0.1083	±0.0027	5.1863	±0.2933	0.3474	±0.0177	0.8996	1771	±22.6	1850	±24.1	1922	±42.3	1771	±22.6
41	Winch St-4 18	27	106	0.1086	±0.0117	5.2257	±0.5861	0.3489	±0.0106	0.2701	1776	±98.5	1857	±47.8	1929	±25.3	1776	±98.5
42	Winch St-4 121	145	1,020	0.1088	±0.0009	5.2398	±0.2029	0.3493	±0.0132	0.9759	1779	±7.7	1859	±16.5	1931	±31.5	1779	±7.7
43	Winch St-4 44	48	388	0.1090	±0.0050	5.1134	±1.0646	0.3403	±0.0691	0.9750	1783	±42.2	1838	±88.4	1888	±166.1	1783	±42.2
44	Winch St-4 53	209	1,293	0.1107	±0.0006	5.4277	±0.1625	0.3556	±0.0105	0.9847	1811	±4.7	1889	±12.8	1961	±24.9	1811	±4.7
45	Winch St-4 137	718	685	0.1136	±0.0007	4.5843	±0.1391	0.2928	±0.0087	0.9815	1857	±5.2	1746	±12.6	1655	±21.7	1857	±5.2
46	Winch St-4 130	39	159	0.1146	±0.0203	5.3775	±1.0534	0.3404	±0.0285	0.4280	1873	±159.6	1881	±83.9	1888	±68.6	1873	±159.6
47	Winch St-4 32	741	5,129	0.1148	±0.0003	4.5017	±0.0501	0.2844	±0.0031	0.9789	1877	±2.0	1731	±4.6	1614	±7.8	1877	±2.0
48	Winch St-4 115	540	782	0.1172	±0.0026	5.5366	±0.1773	0.3427	±0.0080	0.7324	1914	±19.6	1906	±13.8	1900	±19.3	1914	±19.6
49	Winch St-4 68	182	373	0.1273	±0.0142	6.7343	±1.6166	0.3836	±0.0815	0.8856	2062	±98.3	2077	±106.1	2093	±190.0	2062	±98.3
50	Winch St-4 134	1282	1,114	0.1694	±0.0026	10.9436	±0.4171	0.4686	±0.0164	0.9166	2552	±12.8	2518	±17.7	2477	±35.9	2552	±12.8
51	Winch St-4 86	2	22	0.1842	±0.0479	13.1069	±5.0897	0.5160	±0.1489	0.7433	2691	±214.6	2687	±183.2	2682	±316.7	2691	±214.6
52	Winch St-4 104	1	15	0.2187	±0.0573	16.0091	±4.9075	0.5309	±0.0844	0.5187	2971	±211.2	2877	±146.5	2745	±177.7	2971	±211.2

Appendix D : Concordia Plots for Detrital Zircon Samples

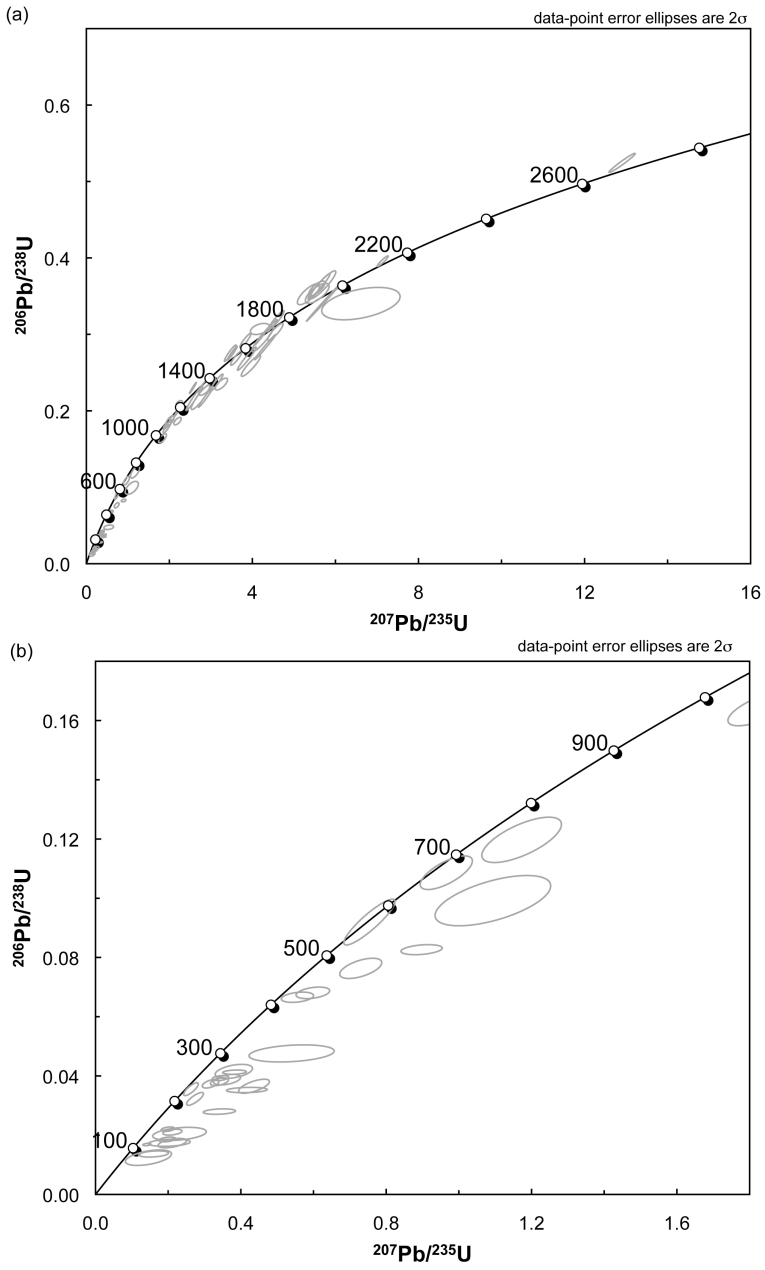

Figure D.1. Concordia plot of Bailey 1C. (a) All grain ages. (b) Grains younger than 1000 Ma.

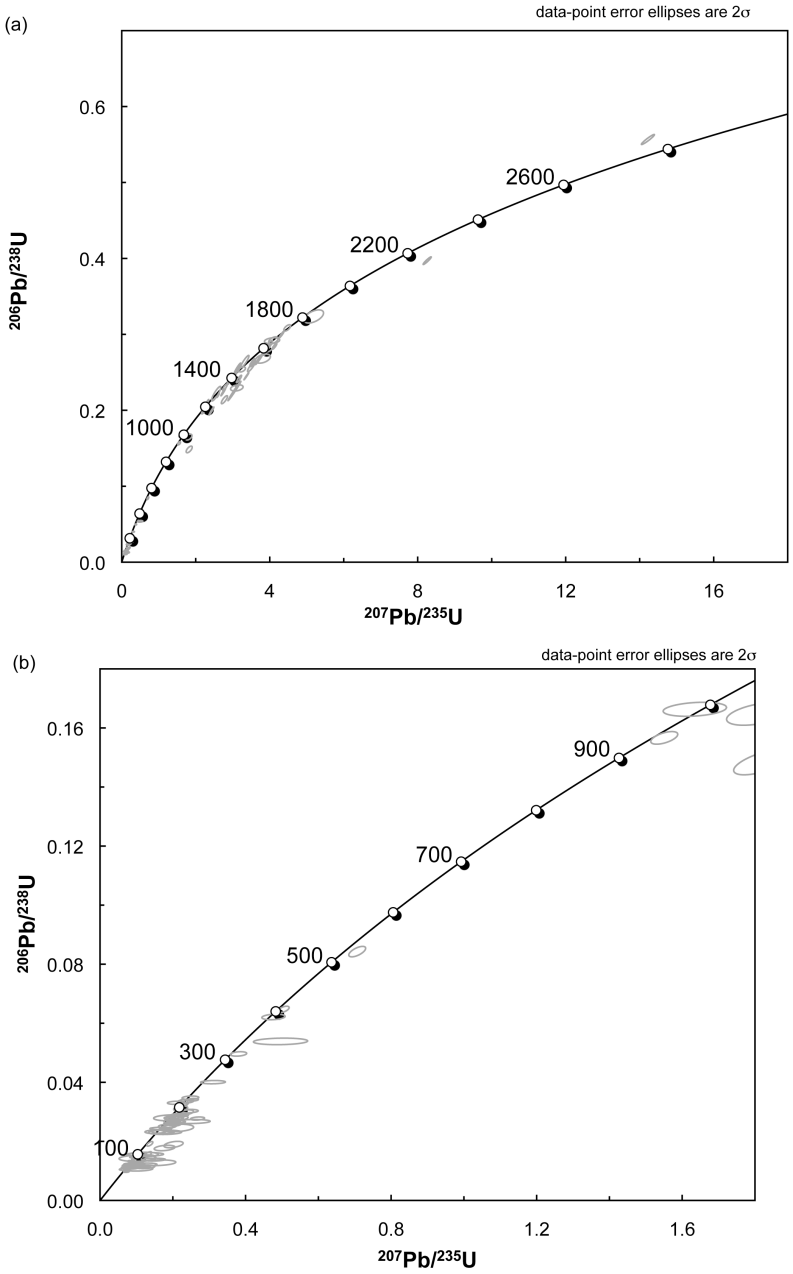

Figure D.2. Concordia plot of Burns 1. (a) All grain ages. (b) Grains younger than 1000 Ma.

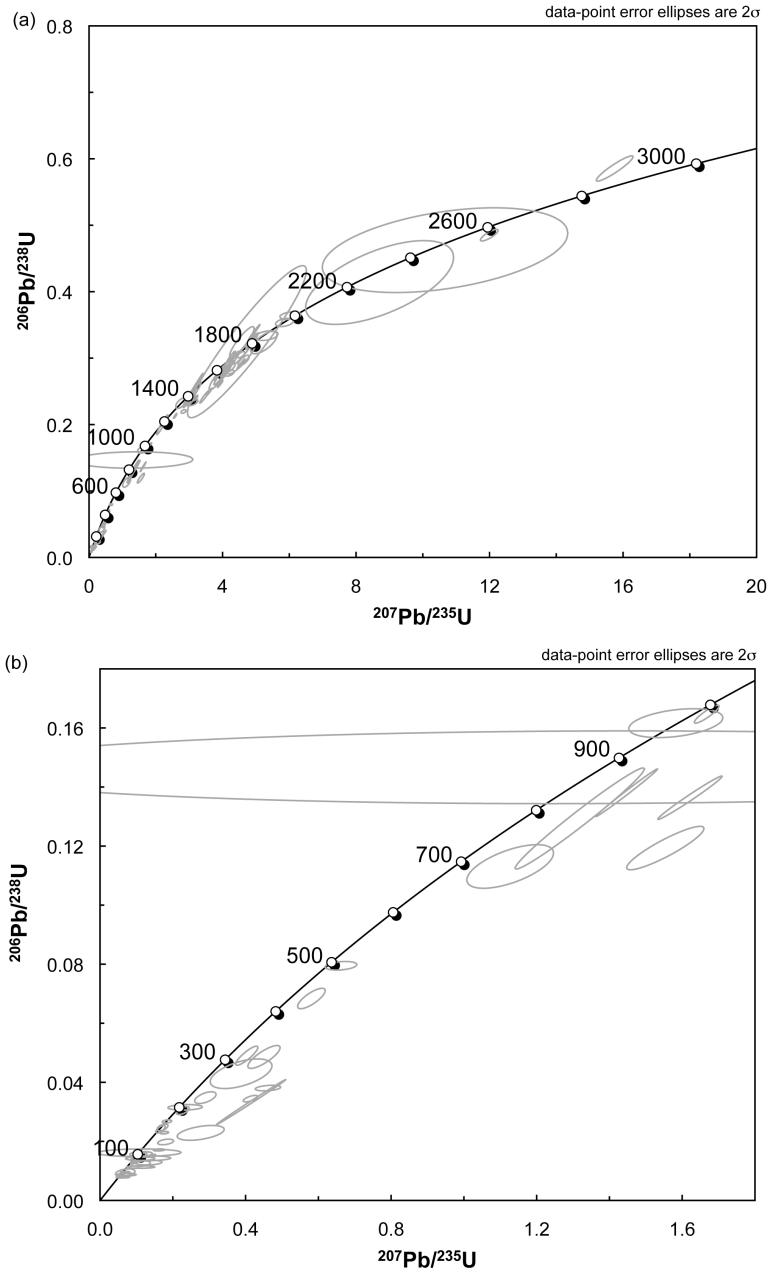

Figure D.3. Concordia plot of GM-C-051408-8. (a) All grain ages. (b) Grains younger than 1000 Ma.

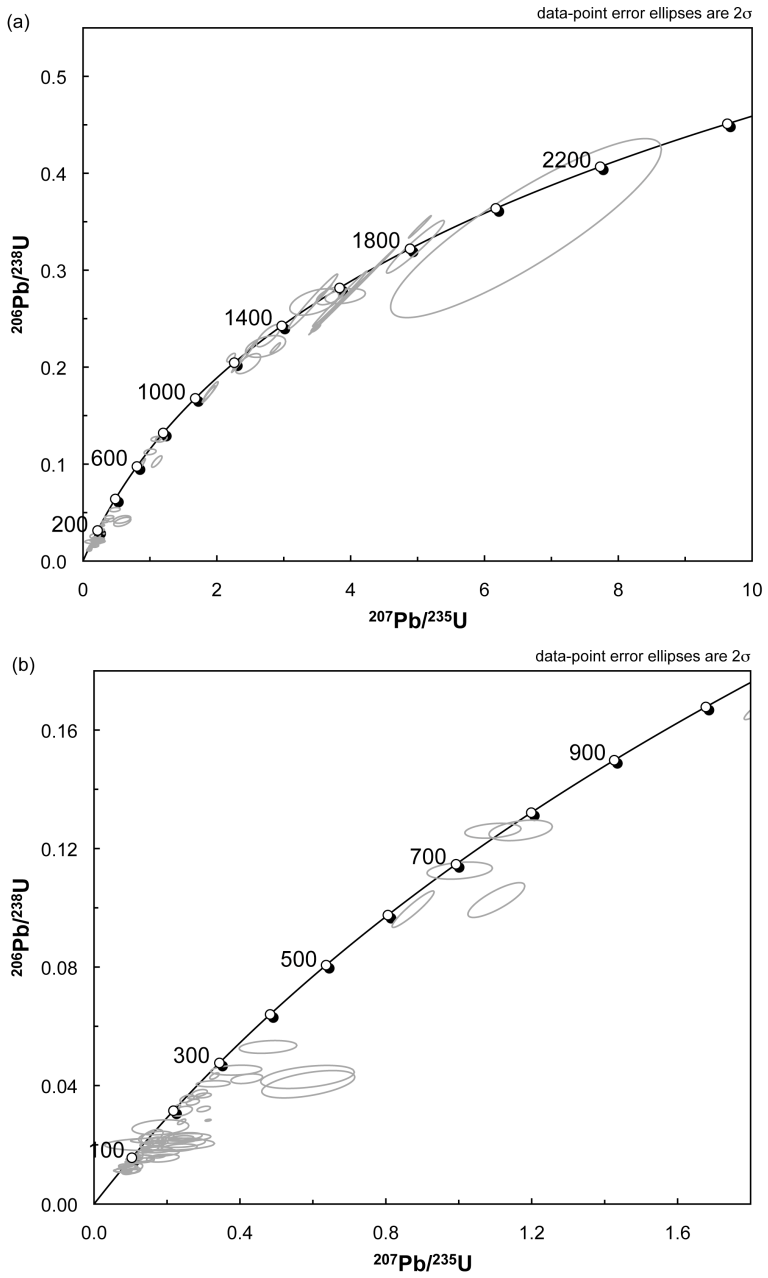

Figure D.4. Concordia plot of GM-C-051508-1. (a) All grain ages. (b) Grains younger than 1000 Ma.

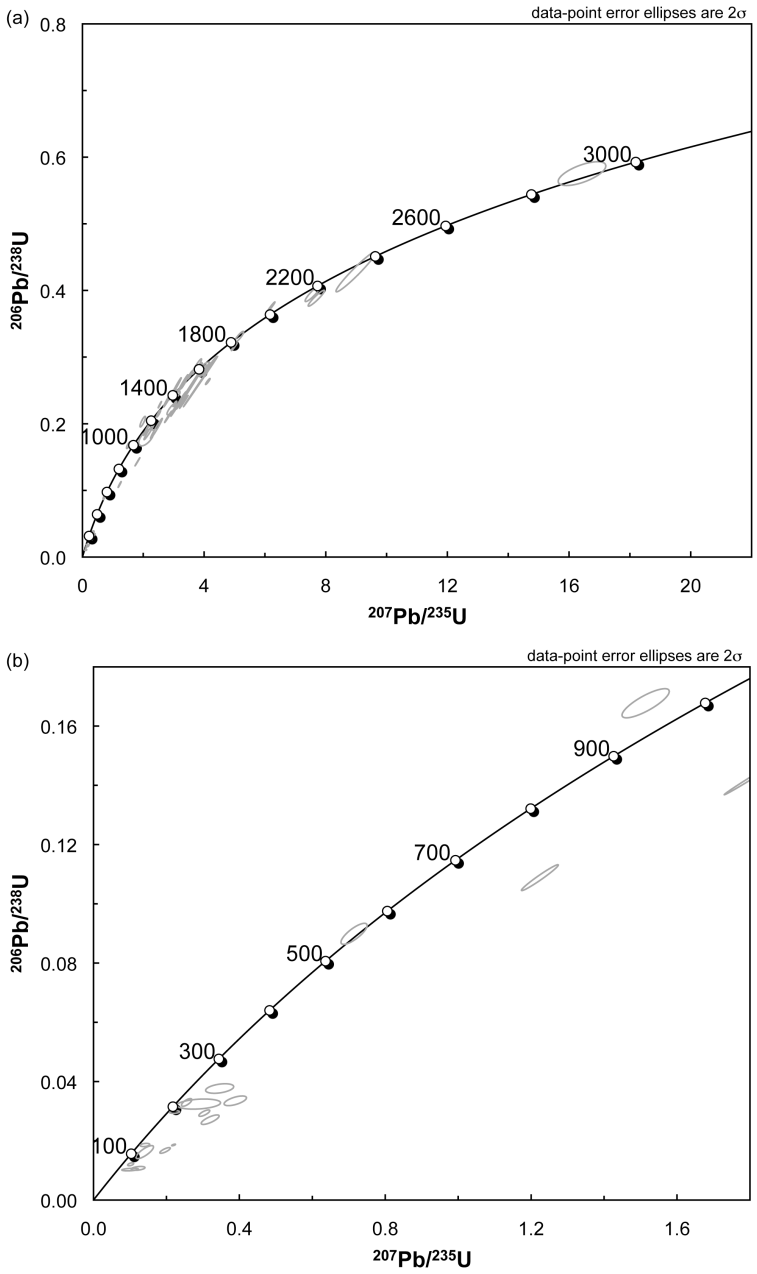

Figure D.5. Concordia plot of GM-C-051608-5. (a) All grain ages. (b) Grains younger than 1000 Ma.

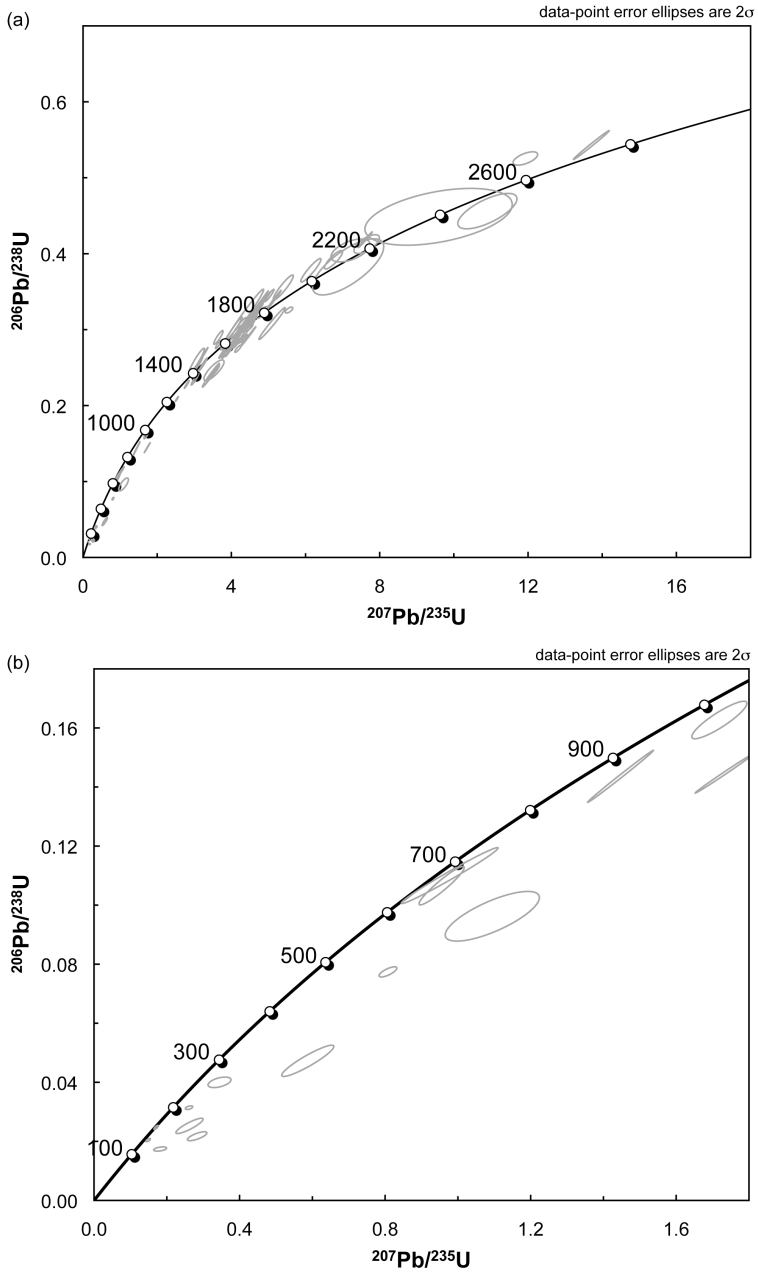

Figure D.6. Concordia plot of GM-W-051408-8. (a) All grain ages. (b) Grains younger than 1000 Ma.

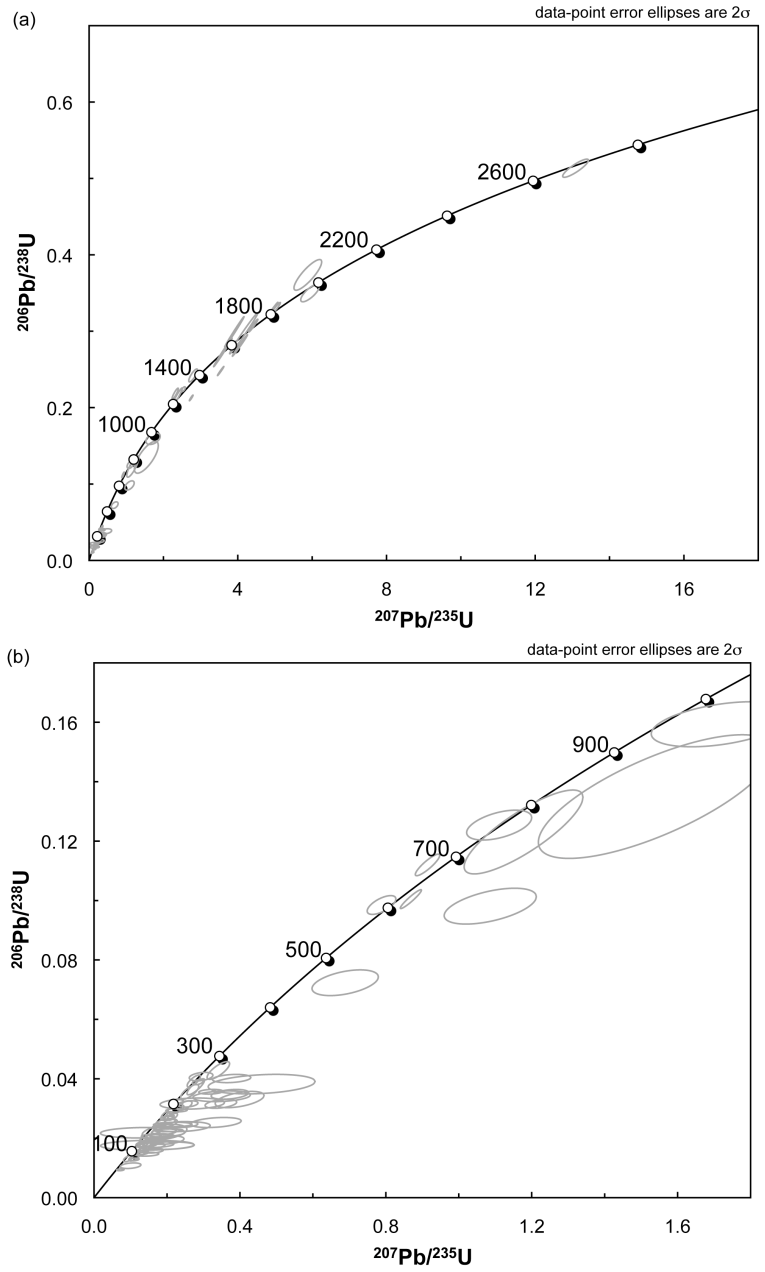

Figure D.7. Concordia plot of GM-W-051508-3. (a) All grain ages. (b) Grains younger than 1000 Ma.

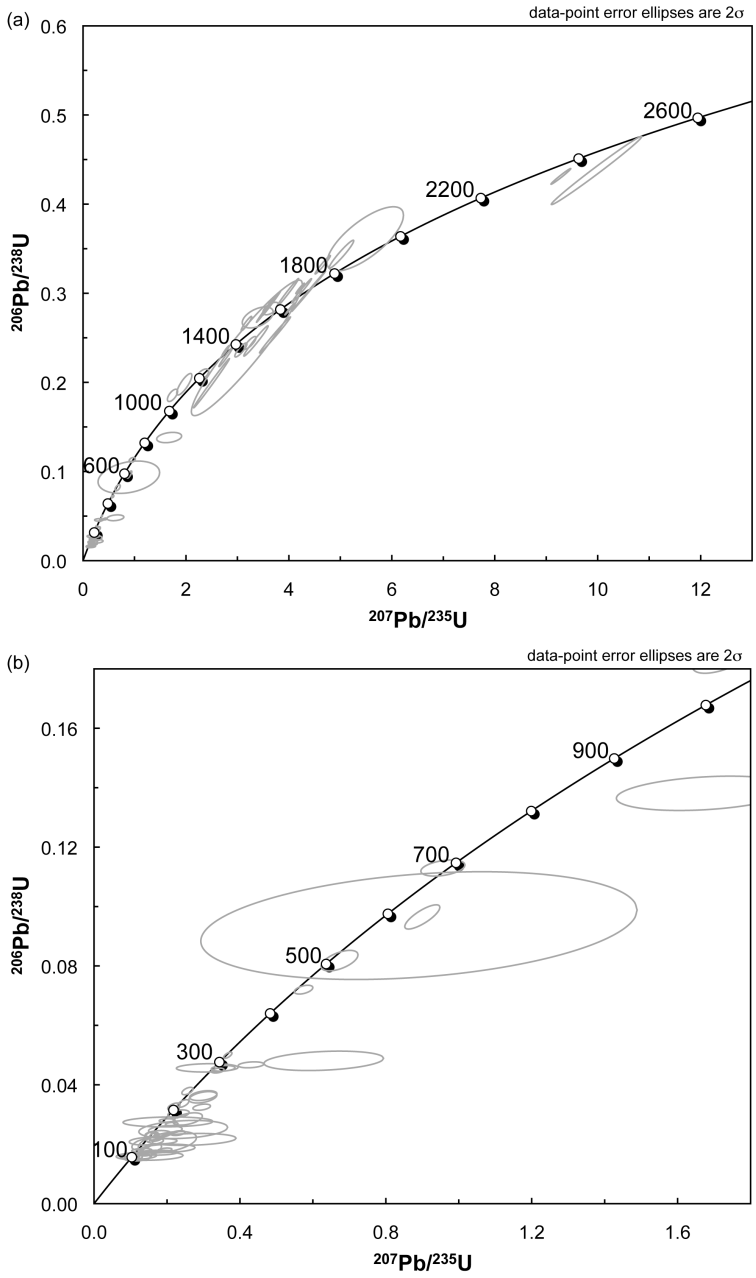

Figure D.8. Concordia plot of GM-W-051608-4. (a) All grain ages. (b) Grains younger than 1000 Ma.

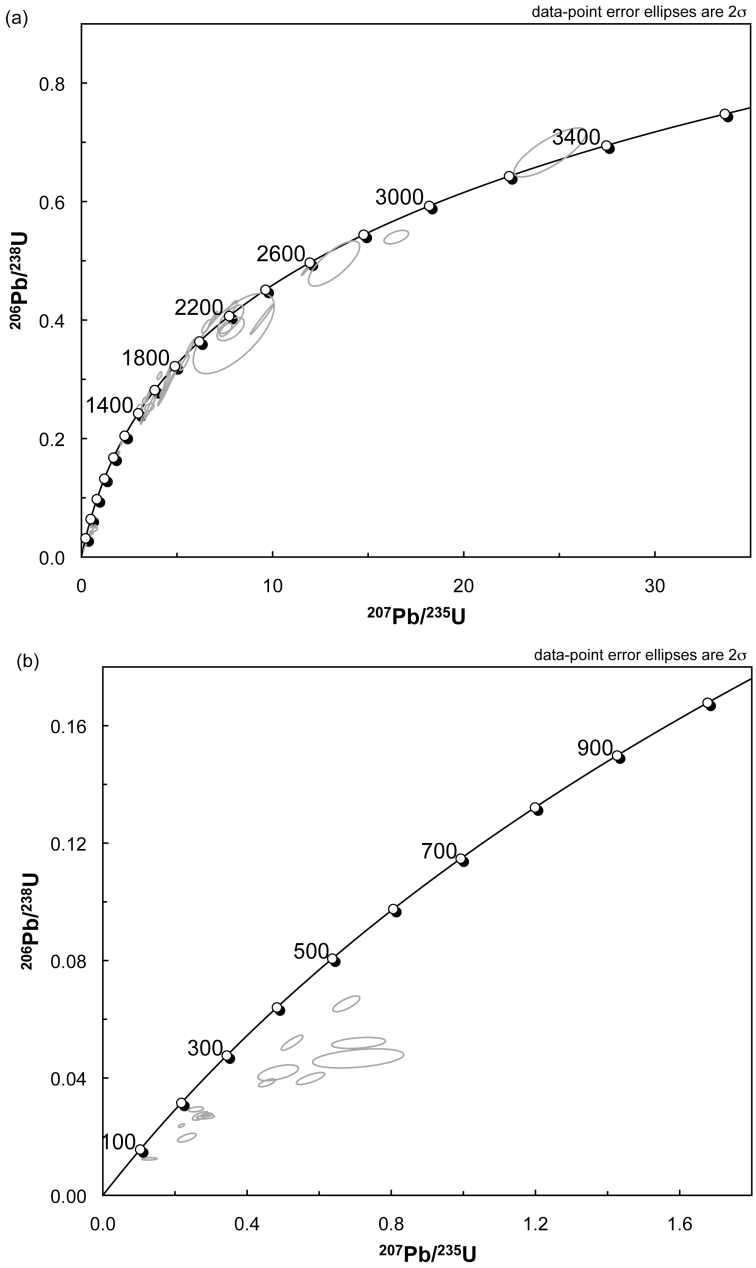

Figure D.9. Concordia plot of Urban 1. (a) All grain ages. (b) Grains younger than 1000 Ma.

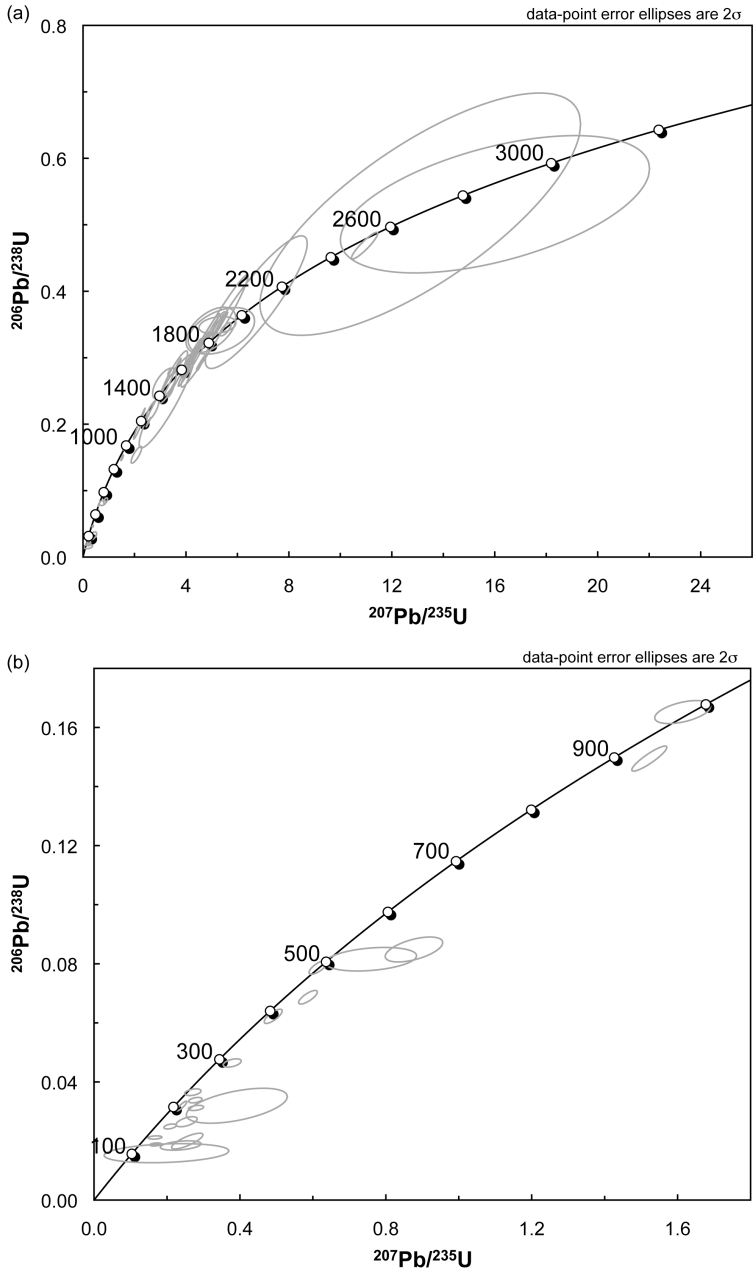

Figure D.10. Concordia plot of Winch State 4(a) All grain ages. (b) Grains younger than 1000 Ma.

Appendix E : Normalized Age Distribution Plots for Detrital Zircon Samples

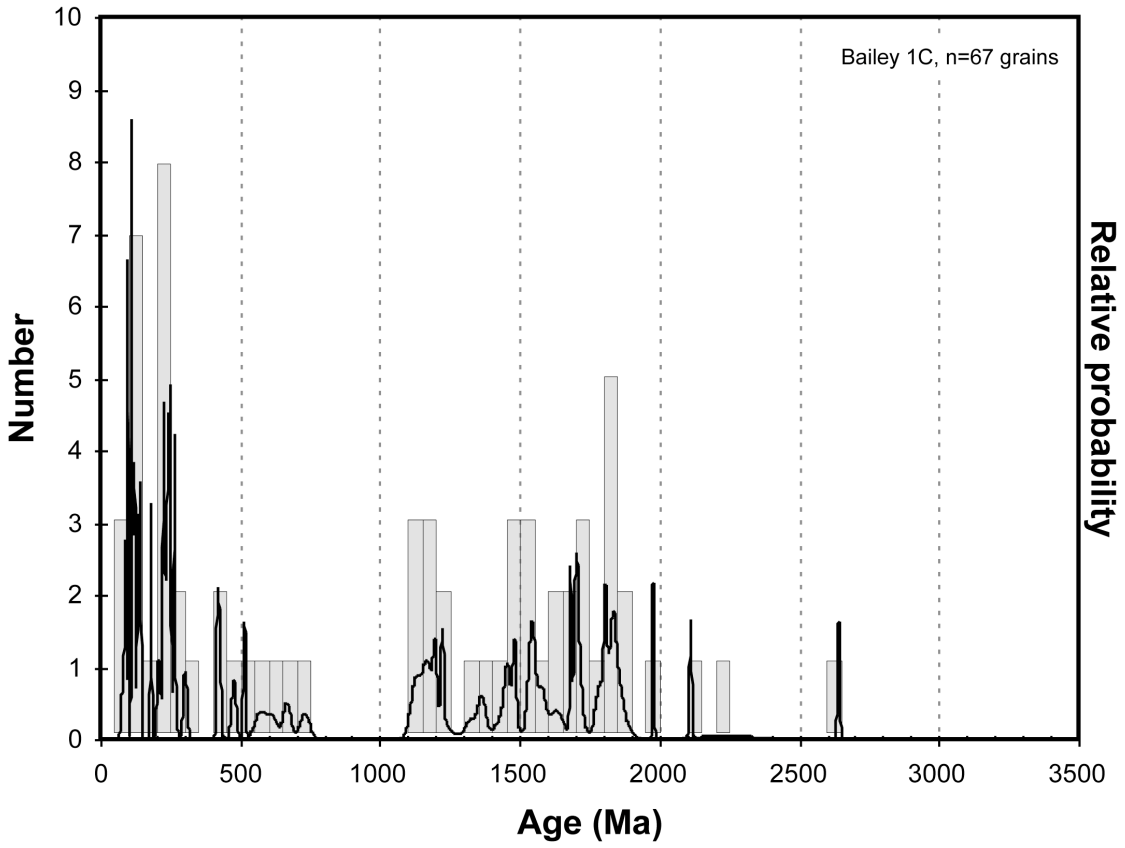

Figure E.1. Normalized age distribution plot of Bailey 1C.

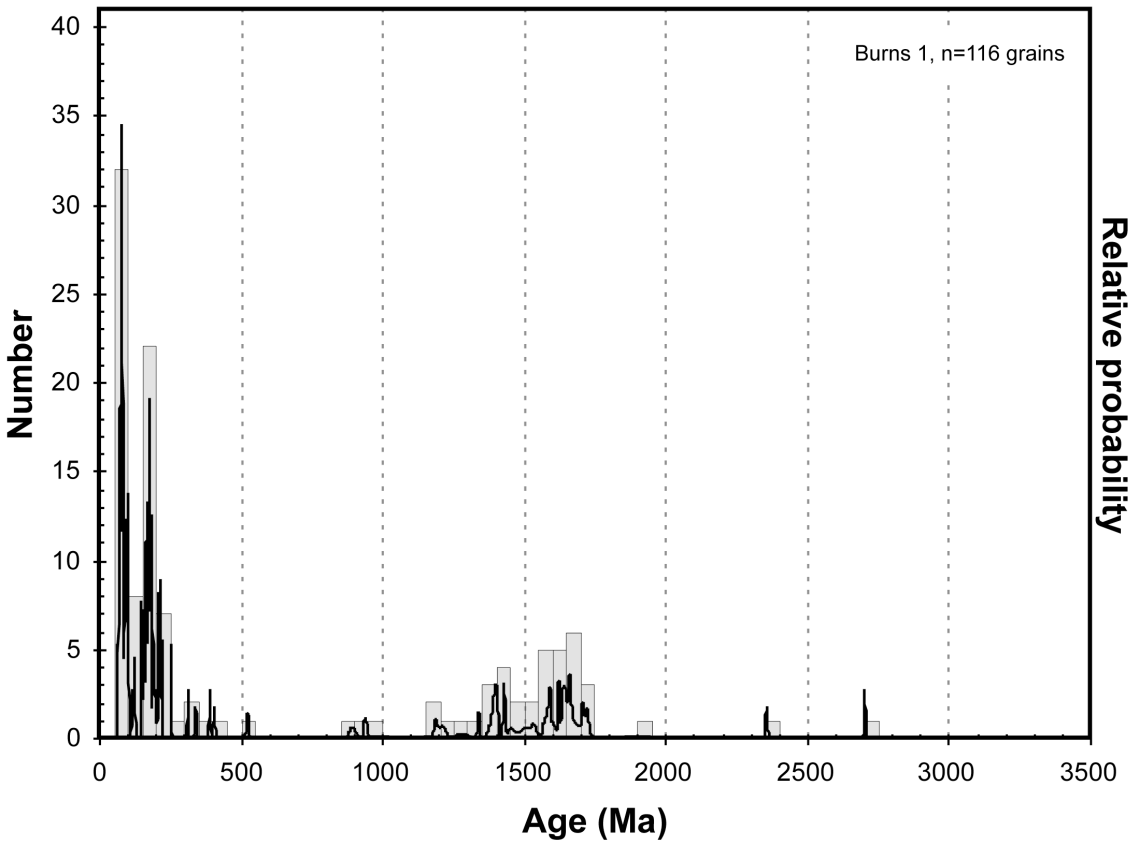

Figure E.2. Normalized age distribution plot of Burns 1.

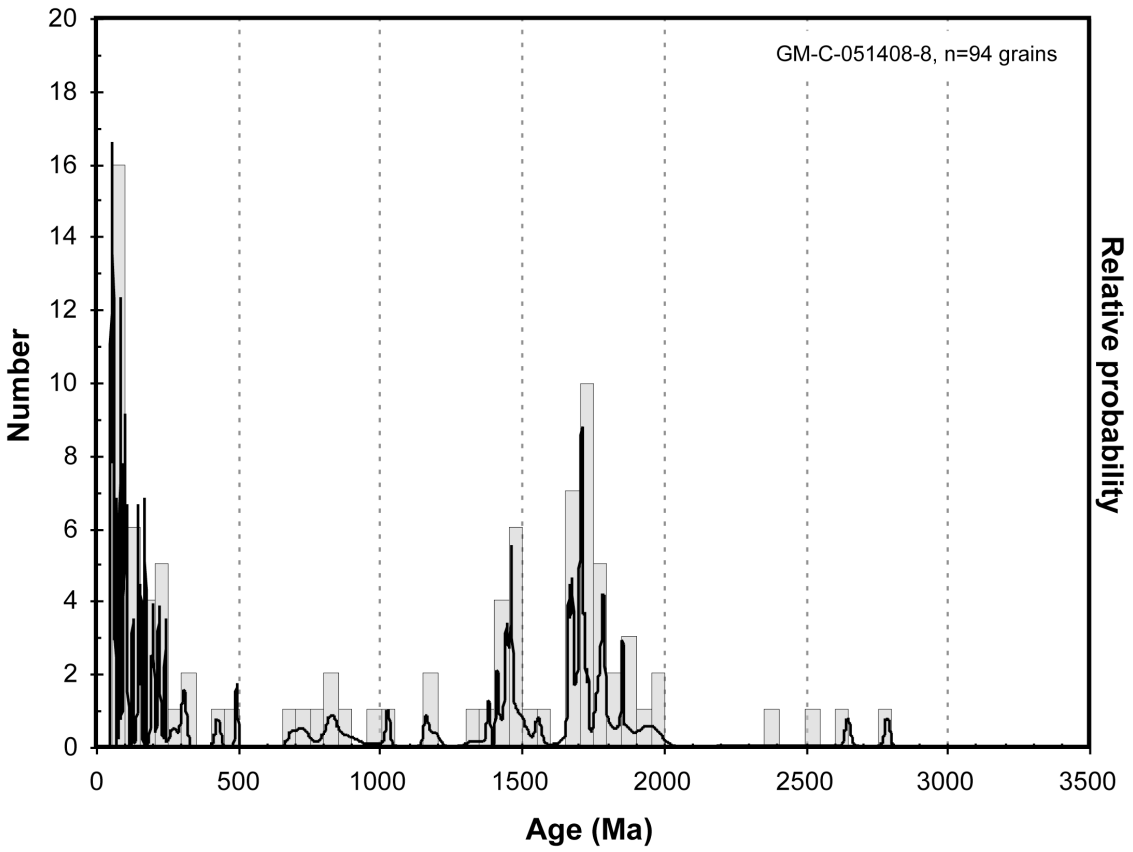

Figure E.3. Normalized age distribution plot of GM-C-051408-8.

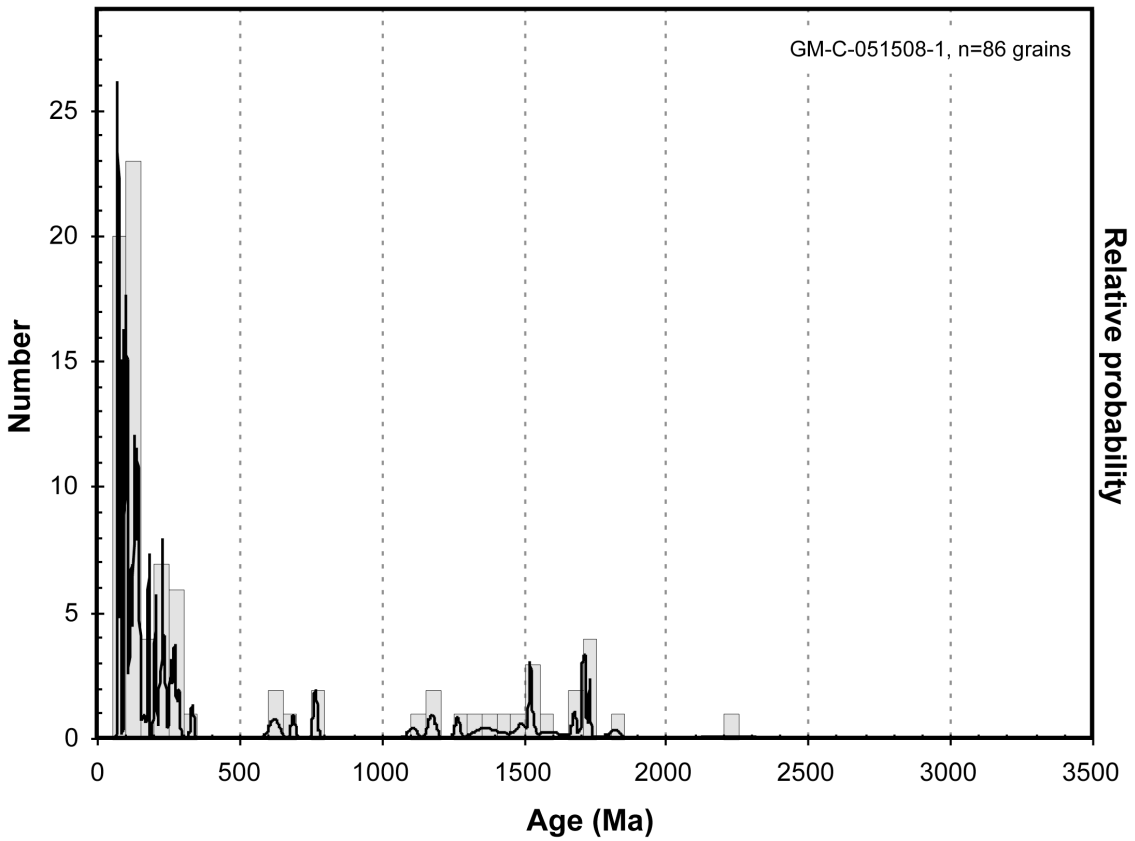

Figure E.4. Normalized age distribution plot of GM-C-051508-1.

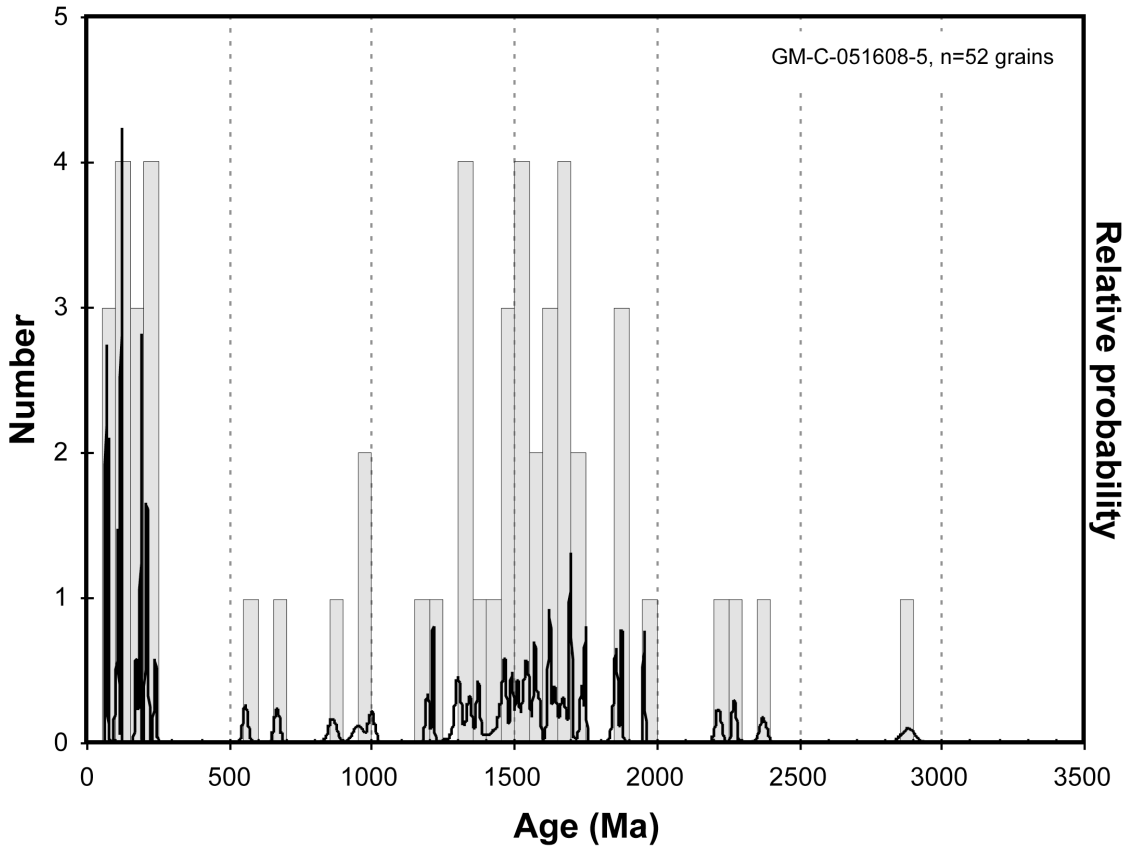

Figure E.5. Normalized age distribution plot of GM-C-051608-5.

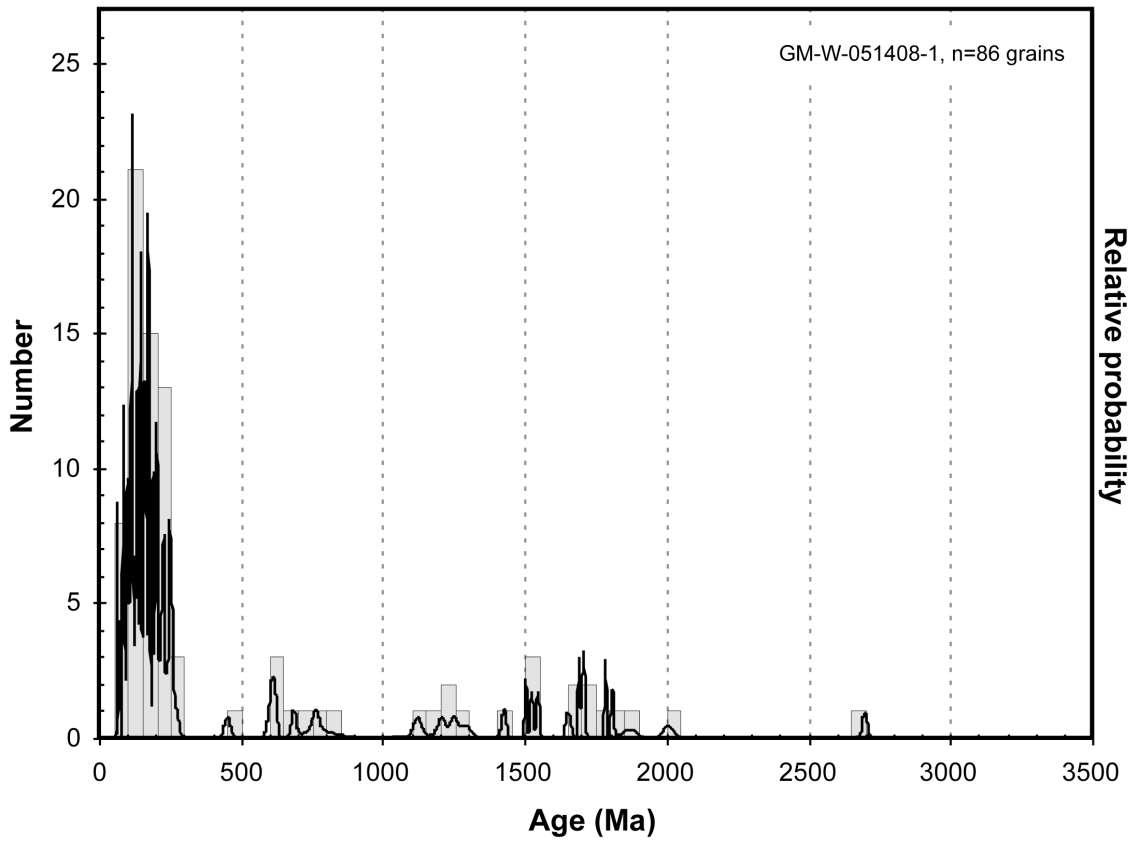

Figure E.6. Normalized age distribution plot of GM-W-051408-1.

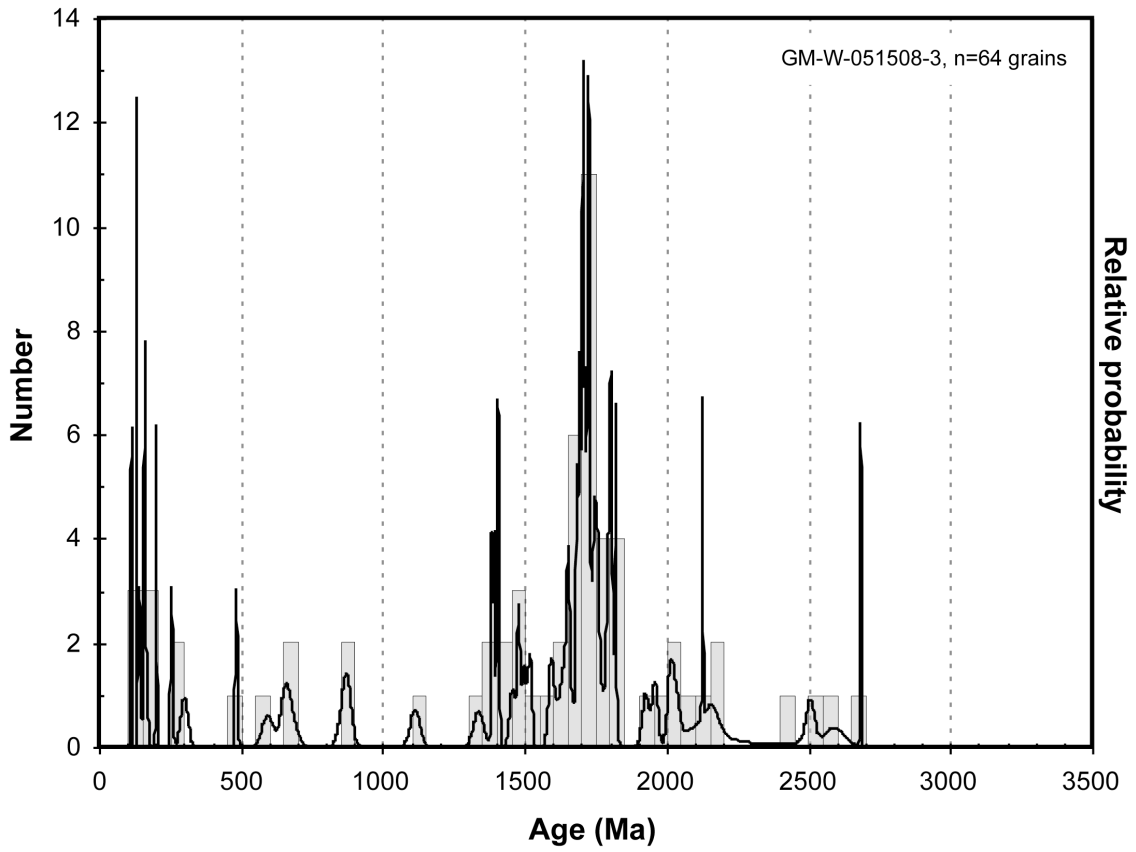

Figure E.7. Normalized age distribution plot of GM-W-051508-3.

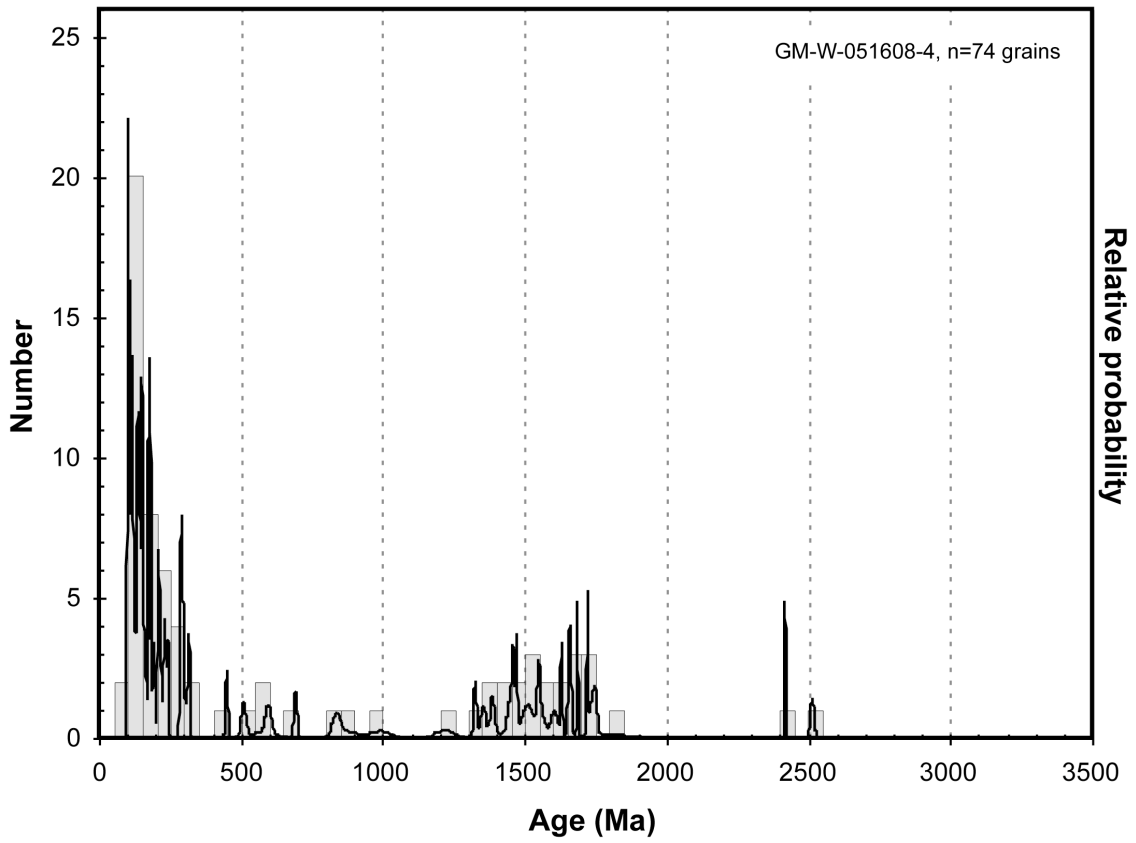

Figure E.8. Normalized age distribution plot of GM-W-051608-4.

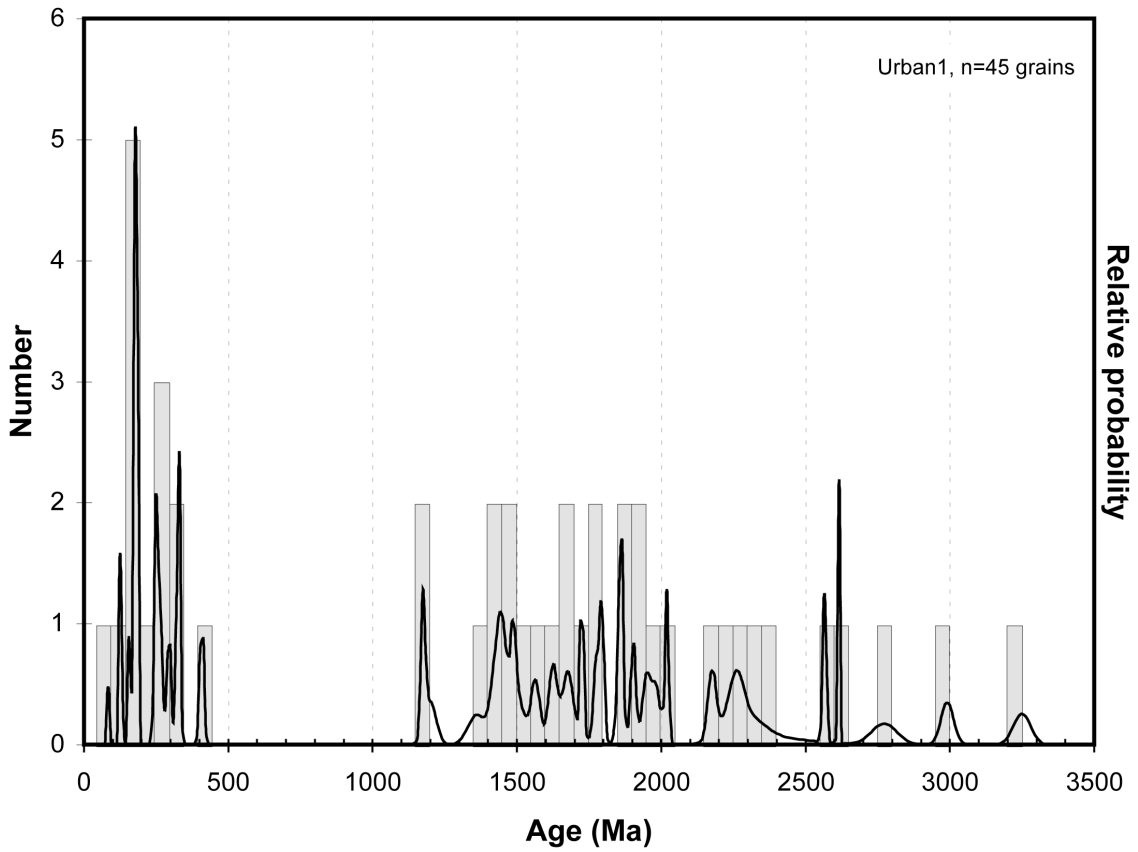

Figure E.9. Normalized age distribution plot of Urban1.

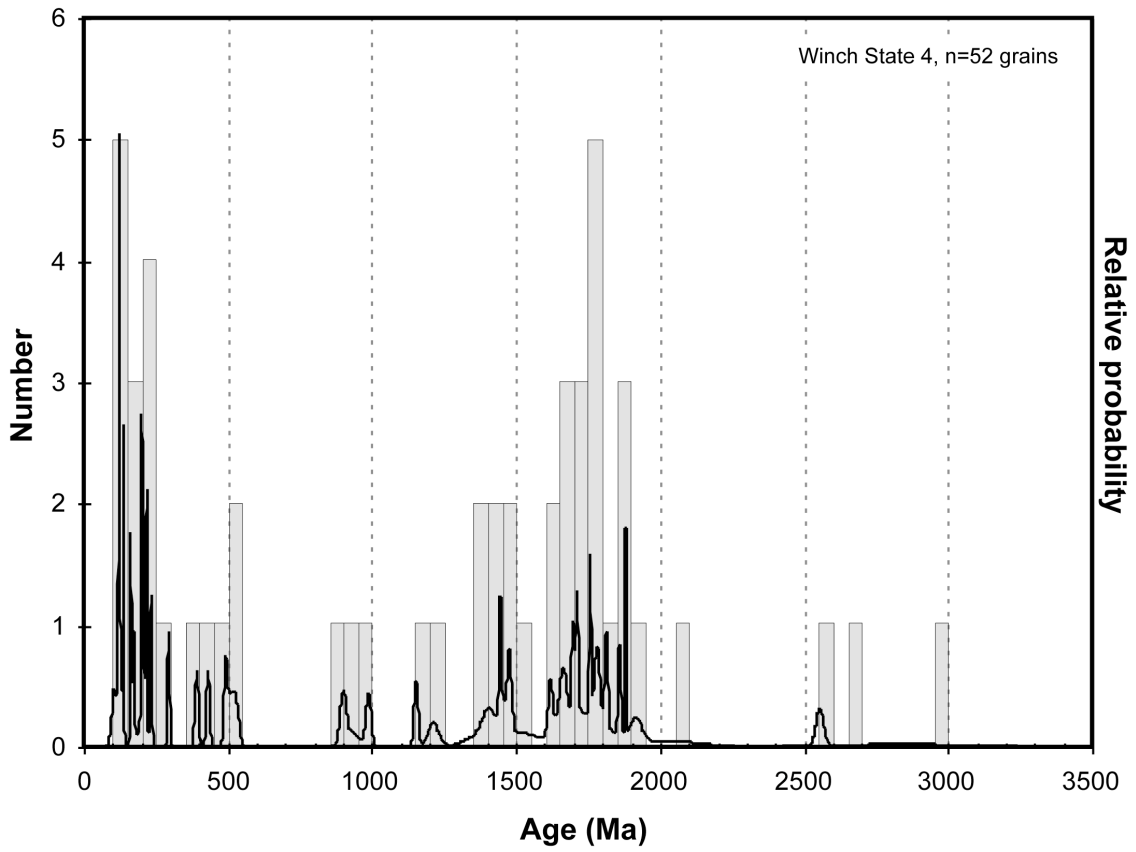

Figure E.10. Normalized age distribution plot of Winch State 4.

Appendix F : Zircon Population Ages with Relative Proportions of Each Population in Wilcox Group, Upper Wilcox, Lower Wilcox and Each Sample

Table F.1. Zircon Population Ages with Relative Proportions of Each Population in Wilcox Group, Upper Wilcox, Lower Wilcox and Each Sample.

	Min Age	Max Age	Winch State 4 [a]	GM-W-051608-4 [a]	GM-W-051508-3 [a]	GM-W-051408-1 [a]	Burns 1 [a]	GM-C-051608-5 [b]
E6	49	87	0.0%	0.0%	5.8%	0.0%	19.8%	5.7%
E5	87	105	1.9%	9.5%	4.7%	0.0%	9.5%	1.9%
E4	105	123	3.8%	8.1%	10.5%	1.6%	2.6%	5.7%
E3	123	167	5.8%	16.2%	20.9%	6.3%	7.8%	0.0%
E2	167	181	1.9%	5.4%	5.8%	0.0%	8.6%	1.9%
E1	181	339	11.5%	17.6%	22.1%	4.7%	13.8%	11.3%
D6	388	451	3.8%	1.4%	1.2%	0.0%	1.7%	0.0%
D5	473	526	5.8%	1.4%	0.0%	1.6%	0.9%	0.0%
D4	554	630	0.0%	2.7%	3.5%	1.6%	0.0%	1.9%
D3	652	691	0.0%	1.4%	1.2%	3.1%	0.0%	1.9%
D2	726	785	0.0%	0.0%	2.3%	0.0%	0.0%	0.0%
D1	815	923	3.8%	2.7%	1.2%	3.1%	0.9%	1.9%
C	937	1326	5.8%	4.1%	5.8%	1.6%	5.2%	13.2%
B3	1334	1500	11.5%	9.5%	1.2%	12.5%	8.6%	11.3%
B2	1500	1590	1.9%	5.4%	3.5%	3.1%	4.3%	11.3%
B1	1590	1819	26.9%	12.2%	7.0%	42.2%	13.8%	17.0%
B1a	1590	1754	17.3%	10.8%	4.7%	32.8%	13.8%	17.0%
B1b	1754	1819	9.6%	1.4%	2.3%	9.4%	0.0%	0.0%
A4	1829	1920	7.7%	0.0%	1.2%	0.0%	0.9%	5.7%
A3	1920	2062	1.9%	0.0%	1.2%	6.3%	0.0%	1.9%
A2	2090	2415	0.0%	1.4%	0.0%	7.8%	0.9%	5.7%
A1	2503	3250	5.8%	1.4%	1.2%	4.7%	0.9%	1.9%
Unassigned			0.0%	0.0%	0.0%	0.0%	0.0%	0.0%
E	49	339	25.0%	56.8%	69.8%	12.5%	62.1%	26.4%
D	388	923	13.5%	9.5%	9.3%	9.4%	3.4%	5.7%
C	937	1326	5.8%	4.1%	5.8%	1.6%	5.2%	13.2%
B	1334	1819	40.4%	27.0%	11.6%	57.8%	26.7%	39.6%
A	1829	3250	15.4%	2.7%	3.5%	18.8%	2.6%	15.1%
Total Grains:			52	74	86	64	116	53
Percent of total that represents 3 grains: [c]			5.8%	4.1%	3.5%	4.7%	2.6%	5.7%

[a] Lower Wilcox Samples

[b] Upper Wilcox Samples

[c] Grey squares mark populations with less than 3 grains

	Min Age	Max Age	GM-C-051508-1 [b]	GM-C-051408-1 [b]	Urban1 [b]	Whole Data Set	Lower Wilcox	Upper Wilcox
E6	49	87	14.0%	12.8%	2.2%	7.7%	7.1%	8.4%
E5	87	105	14.0%	6.4%	0.0%	6.0%	5.9%	6.1%
E4	105	123	5.8%	1.1%	0.0%	4.6%	5.4%	3.8%
E3	123	167	17.4%	5.3%	4.4%	9.6%	11.7%	7.2%
E2	167	181	2.3%	1.1%	6.7%	3.7%	4.8%	2.3%
E1	181	339	17.4%	9.6%	15.6%	14.4%	14.8%	13.9%
D6	388	451	0.0%	1.1%	2.2%	1.4%	1.5%	1.2%
D5	473	526	0.0%	1.1%	0.0%	1.2%	1.5%	0.9%
D4	554	630	2.3%	0.0%	0.0%	1.5%	1.5%	1.4%
D3	652	691	1.2%	1.1%	0.0%	1.1%	1.0%	1.2%
D2	726	785	2.3%	2.1%	0.0%	0.9%	0.5%	1.4%
D1	815	923	0.0%	3.2%	0.0%	1.6%	2.0%	1.2%
C	937	1326	4.7%	4.3%	4.4%	6.0%	4.6%	7.5%
B3	1334	1500	4.7%	12.8%	11.1%	8.7%	8.2%	9.3%
B2	1500	1590	4.7%	2.1%	4.4%	4.5%	3.8%	5.2%
B1	1590	1819	8.1%	25.5%	13.3%	17.5%	18.4%	16.5%
B1a	1590	1754	7.0%	18.1%	8.9%	13.7%	14.8%	12.5%
B1b	1754	1819	1.2%	7.4%	4.4%	3.8%	3.6%	4.1%
A4	1829	1920	0.0%	4.3%	6.7%	2.7%	1.5%	4.1%
A3	1920	2062	0.0%	2.1%	6.7%	1.8%	1.5%	2.0%
A2	2090	2415	1.2%	1.1%	11.1%	2.6%	1.8%	3.5%
A1	2503	3250	0.0%	3.2%	11.1%	2.6%	2.3%	2.9%
Unassigned			0.0%	0.0%	0.0%	0.0%	0.0%	0.0%
E	49	339	70.9%	36.2%	28.9%	46.0%	49.7%	41.7%
D	388	923	5.8%	8.5%	2.2%	7.7%	8.2%	7.2%
C	937	1326	4.7%	4.3%	4.4%	6.0%	4.6%	7.5%
B	1334	1819	17.4%	40.4%	28.9%	30.7%	30.4%	31.0%
A	1829	3250	1.2%	10.6%	35.6%	9.6%	7.1%	12.5%
Total Grains:			86	94	45	737	392	345
Percent of total that represents 3 grains: [c]			3.5%	3.2%	6.7%	0.4%	0.8%	0.9%

[a] Lower Wilcox Samples

[b] Upper Wilcox Samples

[c] Grey squares mark populations with less than 3 grains

Appendix G : Review of Zircon Characteristics and Literature

In recent years U-Pb detrital zircon geochronology by Laser Ablation-Inductively Coupled Plasma-Mass Spectrometry (LA-ICP-MS) has moved to the forefront of sedimentary provenance studies due to its ability to discriminate between potential sedimentary sources (e.g. Fedo et al., 2003). Zircons have long been used in geochronological studies because they typically contain 10-1000 ppm of U (Speer, 1980), but little initial Pb due to the size of their cation sites (Larsen et al., 1952), making them ideal for U-Pb geochronology. Zircons are suitable for sedimentary provenance studies because of their resistance to abrasion during transport (Larsen et al., 1952), chemical alteration during weathering and diagenesis (Milliken and Mack, 1990; Morton and Hallsworth, 1994), and minimal Pb-loss even at low-grade metamorphic temperatures unless they are metamict from age or high U content (Cherniak et al., 1991; Cherniak and Watson, 2001; Cherniak and Watson, 2003). Because of their high density (ρ=4.66 g/cm^3 (Finch et al., 2001)) compared to the major constituents of sedimentary rocks, quartz (ρ=2.65 g/cm^3) and feldspar (ρ=2.55-2.76 g/cm^3) (Nesse, 2000), zircons are included in the heavy mineral separate when the individual grains of a disaggregated sedimentary rock are separated using density sorting techniques, such as the Wilfley table or heavy organic liquids. The density difference also means that zircons are hydrodynamically equivalent to quartz grains one ϕ size larger (Komar et al., 2007). This is an important relationship to consider when sampling, as a very fine sandstone is likely to produce zircons that are to small to analyze with a LA-ICP-MS. Pure zircons are diamagnetic (Lewis and Senftle, 1966; see Sircombe and Stern (2002) for further discussion) and can easily be separated from the majority of the heavy minerals using a Frantz magnetic separator. Since there is a positive correlation between Pb-loss/discordance, U content and magnetic susceptibility (Silver, 1963), magnetic separation can also be used to remove discordant zircons, leaving only those that are likely to return acceptable data.

Improvements in LA-ICP-MS technology have reduced the cost and time involved in acquiring zircon age data of sufficient accuracy for provenance studies. This has resulted in the analysis of more grains from each sample, allowing quantitative studies, those which attempt to determine the proportions of different age populations, to be conducted instead of qualitative studies, which can only determine which ages are present (Fedo et al., 2003).

The detrital zircon technique has proved capable in examining a wide variety of geological problems, from confirming the long-distance drainage of ancient river systems (Rainbird et al., 1992) to determining whether an off-shore arc terrane developed near or far from the craton to which it is now accreted (Gehrels et al., 2000a). Such determinations cannot be made using sandstone petrography alone. However, combining detrital zircon geochronology data with sandstone petrography data makes provenance interpretations more robust by considering not only the age spectra of sediment sources, but also rock type and tectonic setting (e.g., Dickinson and Suczek, 1979; Dickinson, 1985). Comparison of sandstone modal compositions to detrital zircon age spectra can also help identify chemically mature, first-cycle quartz arenites that area a result of humid climate weathering (Avigad et al., 2005). Further, sandstone petrography can identify any potential sources (e.g., mafic source rocks) that may not produce zircons due to their bulk chemistry, and therefore may be overlooked in the age spectra (Fedo et al., 2003).

The resiliency of zircons to abrasion during sedimentary transport (Morton et al., 1996) and to chemical weathering and diagenesis (Milliken and Mack, 1990; Morton and Hallsworth, 1994) makes them suitable for identifying source areas, but is also a complicating factor in that they are subject to multiple stages of recycling. This process is well observed in the studies of Dickinson and Gehrels (2003, 2008a, 2009) where zircons derived from Grenville and Appalachian basement sources are present in great

quantities in Permian–Cretaceous strata of the western U.S., though in the case of Jurassic-Cretaceous strata these signatures come from recycling of older sediment and not directly from the basement itself. Sandstone petrography can help resolve such complexities by searching for indicators of whether the source of the sediment is principally sedimentary (i.e., sedimentary rock fragments, quartz grains with recycled quartz overgrowths) or igneous and metamorphic basement (i.e., metamorphic and plutonic rock fragments). Also, comparing the detrital zircon age spectrum of a sample to reference spectra for potential sedimentary sources (e.g., Gehrels and Dickinson, 1995; Gehrels et al., 1995; Gehrels and Stewart, 1998; Stewart et al., 2001) can help to determine if the proximate source of the sediment is the basement which the age spectrum suggests or if it has been recycled through a tectonically distinct sedimentary unit.

References

Aleinikoff, J. N., Burton, W. C., Lyttle, P. T., Nelson, A. E., and Southworth, C. S., 2000, U-Pb geochronology of zircon and monazite from Mesoproterozoic granitic gneisses of the northern Blue Ridge, Virginia and Maryland, USA: Precambrian Research, v. 99, p. 113-146.

Andersen, T., 2005, Detrital zircons as tracers of sedimentary provenance: limiting conditions from statistics and numerical simulation: Chemical Geology, v. 216, p. 249-270.

Andersen, T. H., and Silver, L. T., 1981, An Overview of Precambrian Rocks in Sonora: Universidad Autónoma de México Instituto de Geología Revista, v. 5, p. 131-139.

Anderson, J. L., 1983, Proterozoic anorogenic granite plutonism of North America, *in* Medaris, L. G., Byers, C. W., Mickelson, D. M., and Shank, W. C., eds., Proterozoic Geology: Selected papers from an international Proterozoic symposium: Geological Society of America Memoir 161, p. 133-154.

Armstrong, R. L., and Hills, F. A., 1967, Rb---Sr and K---Ar geochronologic studies of mantled gneiss domes, Albion Range, Southern Idaho, USA: Earth and Planetary Science Letters, v. 3, p. 114-124.

Avigad, D., Sandler, A., Kolodner, K., Stern, R. J., McWilliams, M., Miller, N., and Beyth, M., 2005, Mass-production of Cambro-Ordovician quartz-rich sandstone as a consequence of chemical weathering of Pan-African terranes: Environmental implications: Earth and Planetary Science Letters, v. 240, p. 818-826.

Ayers, W. B., Jr., and Lewis, A. H., 1985, The Wilcox Group and Carrizo sand depositional systems and deep-basin lignite: The University of Texas at Austin, Bureau of Economic Geology, 19 p.

Barnes, V. E., 1976, Crystal City-Eagle Pass Sheet: Bureau of Economic Geology, The University of Texas at Austin, scale 1:250,000.

Barnes, V. E., 1983, San Antonio Sheet: Bureau of Economic Geology, The University of Texas at Austin, scale 1:250,000.

Barth, A. P., and Wooden, J. L., 2006, Timing of Magmatism following Initial Convergence at a Passive Margin, Southwestern U.S. Cordillera, and Ages of Lower Crustal Magma Sources: The Journal of Geology, v. 114, p. 231-245.

Barth, A. P., Wooden, J. L., and Coleman, D. S., 2001, SHRIMP-RG U-Pb Zircon Geochronology of Mesoproterozoic Metamorphism and Plutonism in the Southwesternmost United States: The Journal of Geology, v. 109, p. 319-327.

Barth, A. P., Wooden, J. L., Coleman, D. S., and Fanning, C. M., 2000, Geochronology of the Proterozoic basement of southwesternmost North America, and the origin and evolution of the Mojave crustal province: Tectonics, v. 19, p. 616-629.

Barth, A. P., Wooden, J. L., Coleman, D. S., and Vogel, M. B., 2009, Assembling and Disassembling California: A Zircon and Monazite Geochronologic Framework for Proterozoic Crustal Evolution in Southern California: The Journal of Geology, v. 117, p. 221-239.

Beard, D. C., and Weyl, P. K., 1973, Influence of Texture on Porosity and Permeability of Unconsolidated Sand: AAPG Bulletin, v. 57, p. 349-369.

Befus, K. S., Hanson, R. E., Lehman, T. M., and Griffin, W. R., 2008, Cretaceous basaltic phreatomagmatic volcanism in West Texas: Maar complex at Peña Mountain, Big Bend National Park: Journal of Volcanology and Geothermal Research, v. 173, p. 245-264.

Brewton, J. L., 1970, Heavy mineral distribution in the Carrizo Formation (Eocene), East Texas [Master's Thesis]: Univeristy of Texas at Austin, 66 p.

Breyer, J. A., 1997, Sequence stratigraphy of Gulf Coast lignite, Wilcox Group (Paleogene), South Texas: Journal of Sedimentary Research, v. 67, p. 1018-1029.

Breyer, J. A., Busbey III, A. B., Hanson, R. E., Befus, K. E., Griffin, W. R., Hargrove, U. S., and Bergman, S. C., 2007, Evidence for Late Cretaceous Volcanism in Trans-Pecos Texas: The Journal of Geology, v. 115, p. 243-251.

Busby, C., 2004, Continental growth at convergent margins facing large ocean basins: a case study from Mesozoic convergent-margin basins of Baja California, Mexico: Tectonophysics, v. 392, p. 241-277.

Busby-Spera, C. J., 1988, Speculative tectonic model for the early Mesozoic arc of the southwest Cordilleran United States: Geology, v. 16, p. 1121-1125.

Callender, D. L., and Folk, R. L., 1958, Idiomorphic zircon, key to volcanism in the lower Tertiary sands of central Texas: American Journal of Science, v. 256, p. 257-269.

Cameron, K. L., and Blatt, H., 1971, Durabilities of sand size schist and 'volcanic' rock fragments during fluvial transport, Elk creek, Black Hills, South Dakota: Journal of Sedimentary Petrology, v. 41, p. 565-576.

Cameron, K. L., Lopez, R., Ortega-Gutierrez, F., Solari, L. A., Keppie, J. D., and Schulze, C., 2004, U-Pb geochronology and Pb isotopic compositions of leached feldspars: Constraints on the origin and evolution of Grenville rocks from eastern and southern Mexico, *in* Tollo, R. P., Corriveau, L., McLelland, J. M., and Bartholomew, M. J., eds., Proterozoic Tectonic Evolution of the Grenville Orogen in North America: Geological Society of America Memoir 197: Boulder, CO, Geological Society of America, p. 755-769.

Cather, S. M., 2004, The Laramide orogeny in central and northern New Mexico and southern Colorado, *in* Mack, G. H., and Giles, K. A., eds., The Geology of New Mexico, A Geologic History: New Mexico Geological Society Special Publication 11: Socorro, NM, New Mexico Geological Society, p. 203-248.

Cather, S. M., Karlstrom, K. E., Timmons, J. M., and Heizler, M. T., 2006, Palinspastic reconstruction of Proterozoic basement-related aeromagnetic features in north-central New Mexico: Implications for Mesoproterozoic to late Cenozoic tectonism: Geosphere, v. 2, p. 299-323.

Chamberlain, K. R., Frost, C. D., and Frost, B. R., 2003, Early Archean to Mesoproterozoic evolution of the Wyoming Province: Archean origins to modern lithospheric architecture: Canadian Journal of Earth Sciences, v. 40, p. 1357-1374.

Chapin, C. E., Wilks, M., and McIntosh, William C., 2004, Space--time patterns of Late Cretaceous to present magmatism in New Mexico-comparison with Andean volcanism and potential for future volcanism, *in* Chapin, Charles E., McIntosh, William C., and Kelley, S. A., eds., Tectonics, Geochronology, and Volcanism in the Southern Rocky Mountains and Rio Grande Rift, New Mexico Bureau of Geology & Mineral Resources, Bulletin 160: Socorro, NM, New Mexico Bureau of Geology & Mineral Resources, p. 13-40.

Cherniak, D. J., Lanford, W. A., and Ryerson, F. J., 1991, Lead diffusion in apatite and zircon using ion implantation and Rutherford Backscattering techniques: Geochimica et Cosmochimica Acta, v. 55, p. 1663-1673.

Cherniak, D. J., and Watson, E. B., 2001, Pb diffusion in zircon: Chemical Geology, v. 172, p. 5-24.

Cherniak, D. J., and Watson, E. B., 2003, Diffusion in Zircon: Reviews in Mineralogy and Geochemistry, v. 53, p. 113-143.

Condie, K. C., 1982, Plate-tectonics model for Proterozoic continental accretion in the southwestern United States: Geology, v. 10, p. 37-42.

Connelly, J. N., 2001, Degree of preservation of igneous zonation in zircon as a signpost for concordancy in U/Pb geochronology: Chemical Geology, v. 172, p. 25-39.

Corfu, F., Hanchar, J. M., Hoskin, P. W. O., and Kinny, P., 2003, Atlas of Zircon Textures: Reviews in Mineralogy and Geochemistry, v. 53, p. 469-500.

Cowan, D. S., and Bruhn, R. L., 1992, Late Jurassic to early Late Cretaceous geology of the U.S. Cordillera, *in* Burchfiel, B. C., Lipman, P. W., and Zoback, M. L., eds., The Cordilleran Orogen: Conterminous U.S.: The Geology of North America: Boulder, CO, Geological Society of America, p. 169-203.

Crabaugh, J. P., 2001, Nature and Growth of Nonmarine-to-Marine Clastic Wedges: Examples from the Upper Cretaceous Iles Formation, Western Interior (Colorado) and the Lower Paleogene Wilcox Group of the Gulf of Mexico Basin (Texas) [Ph.D. Dissertation]: University of Wyoming, 235 p.

Crabaugh, J. P., and Elsik, W. C., 2000, Calibration of the Texas Wilcox Group to the Revised Cenozoic Time Scale: Recognition of Four, Third-Order Clastic Wedges (2.7-3.3 m.y. in Duration): South Texas Geological Society Bulletin, v. 41, p. 10-17.

Cumella, S. P., 1983, Relation of Upper Cretaceous regressive sandstone units of the San Juan basin to source area tectonics, *in* Reynolds, M. W., and Dolly, E. D., eds., Mesozoic paleogeography of the west-central United States: Rocky Mountain Paleogeography Symposium 2, Rocky Mountain Section, SEPM (Society for Sedimentary Geology), p. 189-199.

Darby, B. J., Wyld, S. J., and Gehrels, G. E., 2000, Provenance and paleogeography of the Black Rock terrane, northwestern Nevada: Implications of U-Pb detrital zircon geochronology *in* Soreghan, M. J., and Gehrels, G. E., eds., Paleozoic and Triassic paleogeography and tectonics of western Nevada and northern California: Geological Society of America Special Paper 347: Bolder, CO, Geological Society of America, p. 77-87.

DeCelles, P. G., 2004, Late Jurassic to Eocene evolution of the Cordilleran thrust belt and foreland basin system, western U.S.A: American Journal of Science, v. 304, p. 105-168.

Denison, R. E., Kenny, G. S., Burke, W. H., Jr., and Hetherington, E. A., Jr., 1969, Isotopic Ages of Igneous and Metamorphic Boulders from the Haymond Formation (Pennsylvanian), Marathon Basin, Texas, and their Significance: Geological Society of America Bulletin, v. 80, p. 245-256.

Dickerson, P. W., Hamlin, H. S., Hentz, T. F., and Laubach, S. E., 1995, Regional Domains of the Wilcox Lobo Natural Gas Trend, South Texas: The University of Texas at Austin, Bureau of Economic Geology, 45 p.

Dickinson, W. R., 1985, Interpreting provenance relations from detrital modes of sandstones, *in* Zuffa, G. C., ed., Provenance of arenites: Hingham, MA, D. Reidel Publishing Company, p. 333-361.

Dickinson, W. R., 2008, Impact of differential zircon fertility of granitoid basement rocks in North America on age populations of detrital zircons and implications for granite petrogenesis: Earth and Planetary Science Letters, v. 275, p. 80-92.

Dickinson, W. R., and Gehrels, G. E., 2003, U-Pb ages of detrital zircons from Permian and Jurassic eolian sandstones of the Colorado Plateau, USA: paleogeographic implications: Sedimentary Geology, v. 163, p. 29-66.

Dickinson, W. R., and Gehrels, G. E., 2008a, Sediment delivery to the Cordilleran foreland basin: Insights from U-Pb ages of detrital zircons in Upper Jurassic and Cretaceous strata of the Colorado Plateau: American Journal of Science, v. 308, p. 1041-1082.

Dickinson, W. R., and Gehrels, G. E., 2008b, U-Pb Ages of Detrital Zircons in Relation to Paleogeography: Triassic Paleodrainage Networks and Sediment Dispersal Across Southwest Laurentia: Journal of Sedimentary Research, v. 78, p. 745-764.

Dickinson, W. R., and Gehrels, G. E., 2009, U-Pb ages of detrital zircons in Jurassic eolian and associated sandstones of the Colorado Plateau: Evidence for transcontinental dispersal and intraregional recycling of sediment: Geological Society of America Bulletin, v. 121, p. 408-433.

Dickinson, W. R., Klute, M. A., Hayes, M. J., Janecke, S. U., Lundin, E. R., McKittrick, M. A., and Olivares, M. D., 1988, Paleogeographic and paleotectonic setting of Laramide sedimentary basins in the central Rocky Mountain region: Geological Society of America Bulletin, v. 100, p. 1023-1039.

Dickinson, W. R., and Lawton, T. F., 2001, Carboniferous to Cretaceous assembly and fragmentation of Mexico: Geological Society of America Bulletin, v. 113, p. 1142-1160.

Dickinson, W. R., Lawton, T. F., and Gehrels, G. E., 2009, Recycling detrital zircons: A case study from the Cretaceous Bisbee Group of southern Arizona: Geology, v. 37, p. 503-506.

Dickinson, W. R., and Suczek, C. A., 1979, Plate tectonics and sandstone compositions: AAPG Bulletin, v. 63, p. 2164-2182.

Doughty, P. T., Price, R. A., and Parrish, R. R., 1998, Geology and U – Pb geochronology of Archean basement and Proterozoic cover in the Priest River complex, northwestern United States, and their implications for Cordilleran structure and Precambrian continent reconstructions: Canadian Journal of Earth Sciences, v. 35, p. 39-54.

Edwards, M. B., 1981, Upper Wilcox Rosita delta system of South Texas; growth-faulted shelf-edge deltas: AAPG Bulletin, v. 65, p. 54-73.

Eriksson, K. A., Campbell, I. H., Palin, J. M., and Allen, C. M., 2003, Predominance of Grenvillian Magmatism Recorded in Detrital Zircons from Modern Appalachian Rivers: The Journal of Geology, v. 111, p. 707-717.

Ewing, T. E., 2005, Phanerozoic Development of the Llano Uplift: South Texas Geological Society Bulletin, v. 45, p. 15-25.

Faure, G., and Mensing, T. M., 2005, Isotopes: Principles and Applications: Hoboken, NJ, John Wiley & Sons, 897 p.

Fedo, C. M., Sircombe, K. N., and Rainbird, R. H., 2003, Detrital Zircon Analysis of the Sedimentary Record: Reviews in Mineralogy and Geochemistry, v. 53, p. 277-303.

Ferrari, L., López-Martínez, M., Aguirre-Díaz, G., and Carrasco-Núñez, G., 1999, Space-time patterns of Cenozoic arc volcanism in central Mexico: From the Sierra Madre Occidental to the Mexican Volcanic Belt: Geology, v. 27, p. 303-306.

Ferrari, L., López-Martínez, M., and Rosas-Elguera, J., 2002, Ignimbrite flare-up and deformation in the southern Sierra Madre Occidental, western Mexico: Implications for the late subduction history of the Farallon plate: Tectonics, v. 21.

Finch, R. J., Hanchar, J. M., Hoskin, P. W. O., and Burns, P. C., 2001, Rare-earth elements in synthetic zircon: Part 2. A single-crystal X-ray study of xenotime substitution: American Mineralogist, v. 86, p. 681-689.

Fisher, R. S., 1982, Diagenetic history of Eocene Wilcox sandstones and associated formation waters, south-central Texas [Ph.D. Dissertation]: University of Texas at Austin, 185 p.

Fisher, W. L., and McGowen, J. H., 1967, Depositional Systems in the Wilcox Group of Texas and Their Relationship to Occurrence of Oil and Gas: Gulf Coast Association of Geological Societies Transactions, v. 17, p. 105-125.

Folk, R. L., 1980, Petrology of Sedimentary Rocks: Austin, TX, Hemphill Publishing Company, 184 p.

Galloway, W. E., 1989, Genetic stratigraphic sequences in basin analysis II: Application to Northwest Gulf of Mexico Cenozoic basin: AAPG Bulletin, v. 73, p. 143-154.

Galloway, W. E., 2001, Cenozoic evolution of sediment accumulation in deltaic and shore-zone depositional systems, Northern Gulf of Mexico Basin: Marine and Petroleum Geology, v. 18, p. 1031-1040.

Galloway, W. E., 2005, Gulf of Mexico basin depositional record of Cenozoic North American drainage basin evolution: International Association of Sedimentologists Special Publication, v. 35, p. 409-423.

Galloway, W. E., 2008, Depositional Evolution of the Gulf of Mexico Sedimentary Basin, *in* Miall, A. D., ed., Sedimentary Basins of the World: Amsterdam, The Netherlands, Elsevier, p. 505-549.

Galloway, W. E., Ganey-Curry, P. E., Li, X., and Buffler, R. T., 2000, Cenozoic Depositional History of the Gulf of Mexico Basin: AAPG Bulletin, v. 84, p. 1743-1774.

Galloway, W. E., Liu, X., Travis-Neuberger, D., and Xue, L., 1994, Reference high resolution correlation cross sections, Paleogene section, Texas coastal plain: The University of Texas at Austin, Bureau of Economic Geology, 19 p.

Galloway, W. E., and Williams, T. A., 1991, Sediment accumulation rates in time and space: Paleogene genetic stratigraphic sequences of the northwestern Gulf of Mexico basin: Geology, v. 19, p. 986-989.

Garzanti, E., and Vezzoli, G., 2003, A Classification of Metamorphic Grains in Sands Based on their Composition and Grade: Journal of Sedimentary Research, v. 73, p. 830-837.

Gehrels, G. E., and Dickinson, W. R., 1995, Detrital zircon provenance of Cambrian to Triassic miogeoclinal and eugeoclinal strata in Nevada: American Journal of Science, v. 295, p. 18-48.

Gehrels, G. E., and Dickinson, W. R., 2000, Detrital zircon geochronology of the Antler overlap and foreland basin assemblages, Nevada, *in* Soreghan, M. J., and Gehrels, G. E., eds., Paleozoic and Triassic paleogeography and tectonics of western Nevada and Northern California: Geological Society of America Special Paper 347: Bolder, CO, Geological Society of America, p. 57-63.

Gehrels, G. E., Dickinson, W. R., Darby, B. J., Harding, J. P., Manuszak, J. D., Riley, B. C. D., Spurlin, M. S., Finney, S. C., Girty, G. H., Harwood, D. S., Miller, M. M., Satterfield, J. I., Smith, M. T., Snyder, W. S., Wallin, E. T., and Wyld, S. J., 2000a, Tectonic implications of detrital zircon data from Paleozoic and Triassic strata in western Nevada and northern California, *in* Soreghan, M. J., and Gehrels, G. E., eds., Paleozoic and Triassic paleogeography and tectonics of western Nevada and northern California: Geological Society of America Special Paper 347: Bolder, CO, Geological Society of America, p. 133-150.

Gehrels, G. E., Dickinson, W. R., Riley, B. C. D., Finney, S. C., and Smith, M. T., 2000b, Detrital zircon geochronology of the Roberts Mountains allochthon, Nevada, *in* Soreghan, M. J., and Gehrels, G. E., eds., Paleozoic and Triassic paleogeography and tectonics of western Nevada and Northern California: Geological Society of America Special Paper 347: Bolder, CO, Geological Society of America, p. 19-42.

Gehrels, G. E., Dickinson, W. R., Ross, G. M., Stewart, J. H., and Howell, D. G., 1995, Detrital zircon reference for Cambrian to Triassic miogeoclinal strata of western North America: Geology, v. 23, p. 831-834.

Gehrels, G. E., and Miller, M. M., 2000, Detrital zircon geochronologic study of upper Paleozoic strata in the eastern Klamath terrane, northern California, *in* Soreghan, M. J., and Gehrels, G. E., eds., Paleozoic and Triassic paleogeography and tectonics of western Nevada and northern California: Geological Society of America Special Paper 347: Bolder, CO, Geological Society of America, p. 99-107.

Gehrels, G. E., and Stewart, J. H., 1998, Detrital zircon U-Pb geochronology of Cambrian to Triassic miogeoclinal and eugeoclinal strata of Sonora, Mexico: Journal of Geophysical Research, v. 103, p. 2471-2487.

Gehrels, G. E., Valencia, V., and Pullen, A., 2006, Detrital Zircon Geochronology by Laser-Ablation Multicollector ICPMS at the Arizona Laserchron Center, *in* Olszewski, T., ed., Geochronology: Emerging Opportunities, Paleontological Society Short Course, October 21, 2006: Philadelphia, PA, The Paleontological Society, p. 67-76.

Gleason, J. D., Gehrels, G. E., Dickinson, W. R., Patchett, P. J., and Kring, D. A., 2007, Laurentian Sources for Detrital Zircon Grains in Turbidite and Deltaic Sandstones of the Pennsylvanian Haymond Formation, Marathon Assemblage, West Texas, U.S.A: Journal of Sedimentary Research, v. 77, p. 888-900.

Graham, S. A., Ingersoll, R. V., and Dickinson, W. R., 1976, Common provenance for lithic grains in Carboniferous sandstones from Ouachita Mountains and Black Warrior Basin: Journal of Sedimentary Petrology, v. 46, p. 620-632.

Grambling, J. A., Williams, M. L., and Mawer, C. K., 1988, Proterozoic tectonic assembly of New Mexico: Geology, v. 16, p. 724-727.

Harding, J. P., Gehrels, G. E., Harwood, D. S., and Girty, G. H., 2000, Detrital zircon geochronology of the Shoo Fly Complex, northern Sierra terrane, northeastern California *in* Soreghan, M. J., and Gehrels, G. E., eds., Paleozoic and Triassic paleogeography and tectonics of western Nevada and northern California: Geological Society of America Special Paper 347: Bolder, CO, Geological Society of America, p. 43-55.

Hargis, R. N., 1985, Proposed Lithostratigraphic Classification of the Wilcox Group of South Texas: Gulf Coast Association of Geological Societies Transactions, v. 1985, p. 107-116.

Hargis, R. N., 1996, Major Transgressive Shales of the Wilcox, Northern Portion of South Texas: Gulf Coast Association of Geological Societies Transactions, v. 46, p. 465-467.

Hoffman, P. F., 1988, United Plates of America, The Birth of a Craton: Early Proterozoic Assembly and Growth of Laurentia: Annual Review of Earth and Planetary Sciences, v. 16, p. 543-603.

Hoffman, P. F., 1989, Speculations on Laurentia's first gigayear (2.0 to 1.0 Ga): Geology, v. 17, p. 135-138.

Hogan, J. P., and Gilbert, M. C., 1997, Timing of the final breakout of Laurentia: Geological Society of America Abstracts with Programs, v. 22, p. 327.

Hogan, J. P., and Gilbert, M. C., 1998, The Southern Oklahoma Aulacogen: a Cambrian analog for mid-Proterozoic AMCG (anorthosite–mangerite–charnockte–granite) complexes?, *in* Hogan, J. P., and Gilbert, M. C., eds., Central North America and Other Regions. Basement Tectonics 12: Dordrecht, The Netherlands, Kluwer Academic, p. 39-79.

Houghton, H. F., 1980, Refined techniques for staining plagioclase and alkali feldspars in thin section: Journal of Sedimentary Petrology, v. 50, p. 629-631.

Housh, T., 2009, Personal Communication: Austin, TX.

Iizuka, T., Hirata, T., Komiya, T., Rino, S., Katayama, I., Motoki, A., and Shigenori Maruyama, 2005, U-Pb and Lu-Hf isotope systematics of zircons from the Mississippi River sand; implications for reworking and growth of continental crust: Geology, v. 33, p. 485-488.

Imoto, N., and McBride, E. F., 1990, Volcanism recorded in the Tesnus Formation, Marathon uplift, Texas, *in* LaRoche, T. M., and Higgins, L., eds., Marathon Thrust Belt: Structure, Stratigraphy, and Hydrocarbon Potential: West Texas Geological Society and SEPM, Permian Basin Section, Field Seminar: Tulsa, OK, Society of Sedimentary Geology, p. 93-98.

Ingersoll, R. V., Fullard, T. F., Ford, R. L., Grimm, J. P., Pickle, J. D., and Sares, S. W., 1984, The effect of grain size on detrital modes; a test of the Gazzi-Dickinson point-counting method: Journal of Sedimentary Petrology, v. 54, p. 103-116.

Johnsson, M. J., 1990, Tectonic versus chemical-weathering controls on the composition of fluvial sands in tropical environments: Sedimentology, v. 37, p. 713-726.

Johnsson, M. J., and Meade, R. H., 1990, Chemical weathering of fluvial sediments during alluvial storage; the Macuapanim Island point bar, Solimoes River, Brazil: Journal of Sedimentary Petrology, v. 60, p. 827-842.

Johnsson, M. J., Stallard, R. F., and Meade, R. H., 1988, First-Cycle Quartz Arenites in the Orinoco River Basin, Venezuela and Colombia: The Journal of Geology, v. 96, p. 263-277.

Karlstrom, K. E., Amato, J. M., Williams, M. L., Heizler, M. T., Shaw, C. A., Read, A. S., and Bauer, P., 2004, Proterozoic Tectonic Evolution of the New Mexico Region: A Synthesis, *in* Mack, G. H., and Giles, K. A., eds., The Geology of New Mexico, A Geologic History: New Mexico Geological Society Special Publication 11: Socorro, NM, New Mexico Geological Society, p. 1-34.

Karlstrom, K. E., Dallmeyer, R. D., and Grambling, J. A., 1997, 40Ar/39Ar Evidence for 1.4 Ga Regional Metamorphism in New Mexico: Implications for Thermal Evolution of Lithosphere in the Southwestern USA: The Journal of Geology, v. 105, p. 205-224.

Keller, G. R., and Baldridge, W. S., 1995, The southern Oklahoma aulacogen, *in* Olsen, K. H., ed., Continental Rifts: Evolution, Structure, and Tectonics: International Lithosphere Program Publication 264: Amsterdam, The Netherlands, Elsevier, p. 427–436.

Kimbrough, D. L., Smith, D. P., Mahoney, J. B., Moore, T. E., Grove, M., Gastil, R. G., Ortega-Rivera, A., and Fanning, C. M., 2001, Forearc-basin sedimentary response to rapid Late Cretaceous batholith emplacement in the Peninsular Ranges of southern and Baja California: Geology, v. 29, p. 491-494.

Komar, P. D., Maria, A. M., and David, T. W., 2007, The Entrainment, Transport and Sorting of Heavy Minerals by Waves and Currents, Developments in Sedimentology: Amsterdam, The Netherlands, Elsevier, p. 3-48.

Košler, J., and Sylvester, P. J., 2003, Present Trends and the Future of Zircon in Geochronology: Laser Ablation ICPMS: Reviews in Mineralogy and Geochemistry, v. 53, p. 243-275.

Larsen, E. S., Jr., Keevil, N. B., and Harrison, H. C., 1952, Methods for determining the age of igneous rocks using the accessory minerals: Geological Society of America Bulletin, v. 63, p. 1045-1052.

Larsen, L. H., and Poldervaart, A., 1957, Measurement and distribution of zircons in some granitic rocks of magmatic origin: Mineralogical magazine, v. 31, p. 544-564.

Lawlor, P. J., Ortega-Gutierrez, F., Cameron, K. L., Ochoa-Camarillo, H., Lopez, R., and Sampson, D. E., 1999, U-Pb geochronology, geochemistry, and provenance of the Grenvillian Huiznopala Gneiss of Eastern Mexico: Precambrian Research, v. 94, p. 73-99.

Lawton, T. F., 2008, Laramide Sedimentary Basins, *in* Miall, A. D., ed., Sedimentary Basins of the World: Amsterdam, The Netherlands, Elsevier, p. 429-450.

Lawton, T. F., Bradford, I. A., Vega, F. J., Gehrels, G. E., and Amato, J. M., 2009, Provenance of Upper Cretaceous–Paleogene sandstones in the foreland basin system of the Sierra Madre Oriental, northeastern Mexico, and its bearing on fluvial dispersal systems of the Mexican Laramide Province: Geological Society of America Bulletin, v. 121, p. 820-836.

Lewis, R. R., and Senftle, F. E., 1966, The source of ferromagnetism in zircon: The American Mineralogist, v. 51, p. 1467-1475.

Lipman, P. W., 1992, Magmatism in the Cordilleran United States; Progress and problems, *in* Burchfiel, B. C., Lipman, P. W., and Zoback, M. L., eds., The Cordilleran Orogen: Conterminous U.S.: The Geology of North America: Boulder, CO, Geological Society of America, p. 481-514.

Lopez, R., 1997, High-Mg andesites from the Gila Bend Mountains, southwestern Arizona: Evidence for hydrous melting of lithosphere during Miocene extension. The pre-Jurassic geotectonic evolution of the Coahuila terrane, northwestern Mexico: Grenville basement, a late Paleozoic arc, Triassic plutonism, and the events south of the Ouachita suture [Ph.D. Dissertation]: University of California, Santa Cruz, 147 p.

Lopez, R., Cameron, K. L., and Jones, N. W., 2001, Evidence for Paleoproterozoic, Grenvillian, and Pan-African age Gondwanan crust beneath northeastern Mexico: Precambrian Research, v. 107, p. 195-214.

Loucks, R. G., Dodge, M. M., and Galloway, W. E., 1984, Regional Controls on Diagenesis and Reservoir Quality in Lower Tertiary Sandstone along the Texas Gulf Coast, *in* McDonald, D. A., and Surdam, R. C., eds., AAPG Memoir 37: Clastic Diagenesis: Tulsa, OK, American Association of Petroleum Geologists, p. 15-45.

Loucks, R. G., Dodge, M. M., and Galloway, W. E., 1986, Controls on porosity and permeability of hydrocarbon reservoirs in Lower Tertiary sandstones along the Texas Gulf Coast, Bureau of Economic Geology Report of Investigations No. 149: The University of Texas at Austin, Bureau of Economic Geology, 78 p.

Ludwig, K. R., 2003, Isoplot 3.2, A Geochronological Toolkit for Microsoft Excel, Berkeley Geochronology Center, Special Publication No. 4, p. 70.

Ludwig, K. R., 2008, Isoplot 3.7, A Geochronological Toolkit for Microsoft Excel, Berkeley Geochronology Center, Special Publication No. 4, p. 76.

Mack, G. H., 1981, Composition of modern stream sand in a humid climate derived from a low-grade metamorphic and sedimentary foreland fore-thrust belt of North Georgia: Journal of Sedimentary Petrology, v. 51, p. 1247-1258.

Mack, G. H., 1984, Exceptions to the relationship between plate tectonics and sandstone composition: Journal of Sedimentary Petrology, v. 54, p. 212-220.

Manuszak, J. D., Satterfield, J. I., and Gehrels, G. E., 2000, Detrital zircon geochronology of Upper Triassic strata in western Nevada, *in* Soreghan, M. J., and Gehrels, G. E., eds., Paleozoic and Triassic paleogeography and tectonics of western Nevada and northern California: Geological Society of America Special Paper 347: Bolder, CO, Geological Society of America, p. 109-118.

McBride, E. F., Diggs, T. N., and Wilson, J. C., 1991, Compaction of Wilcox and Carrizo sandstones (Paleocene-Eocene) to 4420 m, Texas Gulf Coast: Journal of Sedimentary Petrology, v. 61, p. 73-85.

McBride, E. F., Weidie, A. E., Wolleben, J. A., and Laudon, R. C., 1974, Stratigraphy and Structure of the Parras and La Popa Basins, Northeastern Mexico: Geological Society of America Bulletin, v. 85, p. 1603-1622.

McCarley, A. B., 1981, Metamorphic terrane favored over Rocky Mountains as source of Claiborne Group, Eocene, Texas coastal plain: Journal of Sedimentary Petrology, v. 51, p. 1267-1276.

McDowell, F. W., and Clabaugh, S. E., 1984, The igneous history of the Sierra Madre Occidental and its relation to the tectonic evolution of western Mexico: Universidad Autónoma de México Instituto de Geología Revista, v. 5, p. 195-206.

McDowell, F. W., and Keizer, R. P., 1977, Timing of mid-Tertiary volcanism in the Sierra Madre Occidental between Durango City and Mazatlan, Mexico: Geological Society of America Bulletin, v. 88, p. 1479-1487.

McDowell, F. W., and Mauger, R. L., 1994, K-Ar and U-Pb zircon chronology of Late Cretaceous and Tertiary magmatism in central Chihuahua State, Mexico: Geological Society of America Bulletin, v. 106, p. 118-132.

McDowell, F. W., Roldán-Quintana, J., and Connelly, J. N., 2001, Duration of Late Cretaceous–early Tertiary magmatism in east-central Sonora, Mexico: Geological Society of America Bulletin, v. 113, p. 521-531.

McKee, B. J., Jones, N. W., and Long, L. E., 1990, Stratigraphy and provenance of strata along the San Marcos fault, central Coahuila, Mexico: Geological Society of America Bulletin, v. 102, p. 593-614.

McMillan , N. J., and McLemore, V. T., 2004, Cambrian–Ordovician magmatism and extension in New Mexico and Colorado, *in* Cather, S. M., McIntosh, W. C., and Kelley, S. A., eds., Tectonics, geochronology, and volcanism in the Southern Rocky Mountains and Rio Grande rift, New Mexico Bureau of Geology & Mineral Resources, Bulletin 160: Socorro, NM, New Mexico Bureau of Geology & Mineral Resources, p. 1-12.

Miller, D. M., Nilsen, T. H., and Bilodeau, W. L., 1992, Late Cretaceous to early Eocene geological evolution of the U.S. Cordillera, *in* Burchfiel, B. C., Lipman, P. W., and Zoback, M. L., eds., The Cordilleran Orogen: Conterminous U.S.: The Geology of North America: Boulder, CO, Geological Society of America, p. 205-260.

Milliken, K. L., and Mack, L. E., 1990, Subsurface dissolution of heavy minerals, Frio Formation sandstones of the ancestral Rio Grande Province, South Texas: Sedimentary Geology, v. 68, p. 187-199.

Morton, A. C., Claoue-long, J. C., and Berge, C., 1996, SHRIMP constraints on sediment provenance and transport history in the Mesozoic Statfjord Formation, North Sea: Journal of the Geological Society, v. 153, p. 915-929.

Morton, A. C., and Hallsworth, C., 1994, Identifying provenance-specific features of detrital heavy mineral assemblages in sandstones: Sedimentary Geology, v. 90, p. 241-256.

Mosher, S., 1998, Tectonic evolution of the southern Laurentian Grenville orogenic belt: Geological Society of America Bulletin, v. 110, p. 1357-1375.

Mukhopadhyay, P. K., 1989, Organic petrography and organic geochemistry of Texas Tertiary coals in relation to depositional environment and hydrocarbon generation, Bureau of Economic Geology Report of Investigations No. 188: The University of Texas at Austin, Bureau of Economic Geology, 118 p.

Murray, G. E., 1955, Midway Stage, Saine Stage and WIlcox Group: AAPG Bulletin, v. 39, p. 671-696.

Nesse, W. D., 2000, Introduction to Mineralogy: New York, NY, Oxford University Press, 442 p.

Ortega-Gutierrez, F., Ruiz, J., and Centeno-Garcia, E., 1995, Oaxaquia, a Proterozoic microcontinent accreted to North America during the late Paleozoic: Geology, v. 23, p. 1127-1130.

Ortega-Rivera, A., 2003, Geochronological constraints on the tectonic history of the Peninsular Ranges Batholith of Alta and Baja California: Tectonic implications for western Mexico, *in* Johnson, S. E., Paterson, S. R., Fletcher, J. M., Girty, G. H., Kimbrough, D. L., and Martín-Barajas, A., eds., Tectonic evolution of northwestern México and the southwestern USA: Geological Society of America Special Paper 374: Bolder, CO, Geological Society of America, p. 297-335.

Paxton, S. T., Szabo, J. O., Ajdukiewicz, J. M., and Klimentidis, R. E., 2002, Construction of an Intergranular Volume Compaction Curve for Evaluating and Predicting Compaction and Porosity Loss in Rigid-Grain Sandstone Reservoirs: AAPG Bulletin, v. 86, p. 2047-2067.

Pedrick, J. N., Karlstrom, K. E., and Bowring, S. A., 1998, Reconciliation of conflicting tectonic models for Proterozoic rocks of northern New Mexico: Journal of Metamorphic Geology, v. 16, p. 687-707.

Potter, P. E., 1978, Petrology and Chemistry of Modern Big River Sands: The Journal of Geology, v. 86, p. 423-449.

Pryor, W. A., 1973, Permeability-Porosity Patterns and Variations in Some Holocene Sand Bodies: AAPG Bulletin, v. 57, p. 162-189.

Rainbird, R. H., Heaman, L. M., and Young, G. M., 1992, Sampling Laurentia; detrital zircon geochronology offers evidence for an extensive Neoproterozoic river system originating from the Grenville Orogen: Geology, v. 20, p. 351-354.

Reed, W. P., 1992, Certificate of Analysis, Standards Reference Materials, 610, 611: Gaithersburg, Maryland, National Institute of Standards and Technology.

Riley, B. C. D., Snyder, W. S., and Gehrels, G. E., 2000, U-Pb detrital zircon geochronology of the Golconda allochthon, Nevada, *in* Soreghan, M. J., and Gehrels, G. E., eds., Paleozoic and Triassic paleogeography and tectonics of western Nevada and Northern California: Geological Society of America Special Paper 347: Boulder, CO, Geological Society of America, p. 65-75.

Ross, C. P., Andrews, D. A., and Witkind, I. J., 1955, Geological Map of Montana: U.S. Geological Survey, scale 1:500,000.

Saleeby, J. B., and Busby-Spera, C. J., 1992, Early Mesozoic tectonic evolution of the western U.S. Crodillera, *in* Burchfiel, B. C., Lipman, P. W., and Zoback, M. L., eds., The Cordilleran Orogen: Conterminous U.S.: The Geology of North America: Boulder, CO, Geological Society of America, p. 107-168.

Silver, L. T., 1963, The relation between radioactivity and discordance in zircons, National Research Council Publication 1075, National Academy of Sciences, p. 34-52.

Sircombe, K. N., and Stern, R. A., 2002, An investigation of artificial biasing in detrital zircon U-Pb geochronology due to magnetic separation in sample preparation: Geochimica et Cosmochimica Acta, v. 66, p. 2379-2397.

Sláma, J., Košler, J., Condon, D. J., Crowley, J. L., Gerdes, A., Hanchar, J. M., Horstwood, M. S. A., Morris, G. A., Nasdala, L., Norberg, N., Schaltegger, U., Schoene, B., Tubrett, M. N., and Whitehouse, M. J., 2008, Plešovice zircon -- A new natural reference material for U-Pb and Hf isotopic microanalysis: Chemical Geology, v. 249, p. 1-35.

Smith, D. R., Noblett, J., Wobus, R. A., Unruh, D., Douglass, J., Beane, R., Davis, C., Goldman, S., Kay, G., Gustavson, B., Saltoun, B., and Stewart, J., 1999, Petrology and geochemistry of late-stage intrusions of the A-type, mid-Proterozoic Pikes Peak batholith (Central Colorado, USA): implications for petrogenetic models: Precambrian Research, v. 98, p. 271-305.

Smyth, H. R., Hall, R., and Nichols, G. J., 2008, Significant Volcanic Contribution to Some Quartz-Rich Sandstones, East Java, Indonesia: Journal of Sedimentary Research, v. 78, p. 335-356.

Speer, J. A., 1980, Zircon: Reviews in Mineralogy and Geochemistry, v. 5, p. 67-112.

Spurlin, M. S., Gehrels, G. E., and Harwood, D. S., 2000, Detrital zircon geochronology of upper Paleozoic and lower Mesozoic strata of the northern Sierra terrane, northeastern California, *in* Soreghan, M. J., and Gehrels, G. E., eds., Paleozoic and Triassic paleogeography and tectonics of western Nevada and northern California: Geological Society of America Special Paper 347: Bolder, CO, Geological Society of America, p. 89-98.

Stacey, J. S., and Kramers, J. D., 1975, Approximation of terrestrial lead isotope evolution by a two-stage model: Earth and Planetary Science Letters, v. 26, p. 207-221.

Stewart, J. H., Anderson, T. H., Haxel, G. B., Silver, L. T., and Wright, J. E., 1986, Late Triassic paleogeography of the southern Cordillera: The problem of a source for voluminous volcanic detritus in the Chinle Formation of the Colorado Plateau region: Geology, v. 14, p. 567-570.

Stewart, J. H., Blodgett, R. B., Boucot, A. J., Carter, J. L., and López, R., 1999, Exotic Paleozoic strata of Gondwanan provenance near Ciudad Victoria, Tamaulipas, México, *in* Ramos, V. A., and Keppie, J. D., eds., Laurentia-Gondwana connections before Pangea: Geological Society of America Special Paper 336: Bolder, CO, Geological Society of America, p. 227-252.

Stewart, J. H., Gehrels, G. E., Barth, A. P., Link, P. K., Christie-Blick, N., and Wrucke, C. T., 2001, Detrital zircon provenance of Mesoproterozoic to Cambrian arenites in the western United States and northwestern Mexico: Geological Society of America Bulletin, v. 113, p. 1343-1356.

Stoeser, D. B., Shock, N., Green, G. N., Dumonceaux, G. M., and Heran, W. D., 2005, Geologic Map Database of Texas: U.S. Geological Survey, scale 1:500,000.

Storm, L. W., 1945, Resume of Facts and Opinions on Sedimentation in the Gulf Coast Region ot Texas and Louisana: AAPG Bulletin, v. 29, p. 1304-1335.

Suttner, L. J., Basu, A., and Mack, G. H., 1981, Climate and the origin of quartz arenites: Journal of Sedimentary Petrology, v. 51, p. 1235-1246.

Thorkildsen, D., and Price, R. D., 1991, Ground-water resources of the Carrizo-Wilcox aquifer in the Central Texas region: Texas Water Development Board Report 332, 46 p.

Todd, T. W., and Folk, R. L., 1957, Basal Claiborne of Texas, record of Appalachian tectonism during Eocene: AAPG Bulletin, v. 41, p. 2545-2566.

Torres, R., Ruiz, J., Patchett, P. J., and Grajales, J. M., 1999, Permo-Triassic continental arc in eastern Mexico: Tectonic implications for reconstructions of southern North America, Mesozoic sedimentary and tectonic history of north-central Mexico: Geological Society of America Special Paper 340: Boulder, CO, Geological Society of America, p. 191-196.

Vermeesch, P., 2004, How many grains are needed for a provenance study?: Earth and Planetary Science Letters, v. 224, p. 441-451.

Wallin, E. T., Noto , R. C., and Gehrels, G. E., 2000, Provenance of the Antelope Mountain Quartzite, Yreka terrane, California: Evidence for large-scale late Paleozoic sinistral displacement along the North American Cordilleran margin and implications for the mid-Paleozoic fringing-arc model *in* Soreghan, M. J., and Gehrels, G. E., eds., Paleozoic and Triassic paleogeography and tectonics of western Nevada and Northern California: Geological Society of America Special Paper 347: Bolder, CO, Geological Society of America, p. 119-134.

Wetmore, P. H., Herzig, C., Alsleben, H., Sutherland, M., Schmidt, K. L., Schultz, P. W., and Paterson, S. R., 2003, Mesozoic tectonic evolution of the Peninsular Ranges of southern and Baja California, *in* Johnson, S. E., Paterson, S. R., Fletcher, J. M., Girty, G. H., Kimbrough, D. L., and Martín-Barajas, A., eds., Tectonic evolution of northwestern México and the southwestern USA: Geological Society of America Special Paper 374: Bolder, CO, Geological Society of America, p. 93-116.

Winker, C. D., 1982, Cenozoic Shelf Margins, Nowrthwestern Gulf of Mexico: Gulf Coast Association of Geological Societies Transactions, v. 32, p. 427-448.

Xue, L., and Galloway, W. E., 1993, Sequence stratigraphic and depositional framework of the Paleocene lower Wilcox strata, northwest Gulf of Mexico Basin: Gulf Coast Association of Geological Societies Transactions, v. 43, p. 453–464.

Xue, L., and Galloway, W. E., 1995, High-resolution depositional framework of the Paleocene middle Wilcox strata, Texas coastal plain: AAPG Bulletin, v. 79, p. 205-230.

Young, S. W., 1976, Petrographic textures of detrital polycrystalline quartz as an aid to interpreting crystalline source rocks: Journal of Sedimentary Petrology, v. 46, p. 595-603.

Vita

Glen Nelson Mackey, III was born in Roanoke, VA on May 14, 1981, the son of Nelson and Jean Mackey. After graduating from North Cross High School, Roanoke, VA in 1999, he entered the Johns Hopkins University in Baltimore, MD. He received the degrees of Bachelor of Arts in 1999. Upon graduating from Johns Hopkins University he served in the U.S. Army from 2003 until 2007. In August 2007, he began graduate studies at the University of Texas at Austin.

Permanent address: 1910 Greenwood Road, Roanoke, VA, 24015

This thesis was typed by the author.